Advances
in Clinical and Experimental Medicine

WROCLAW
MEDICAL UNIVERSITY

Advances
in Clinical and Experimental Medicine

Editorial Policy

Contents

Investigating gender dynamics in forensic toxicology:
The role of masculinity and femininity in alcohol and drug abuse

Arianna Giorgetti[1,A,D,F], Rafael Boscolo-Berto[2,A,D,F]

[1] Unit of Legal Medicine, Department of Medical and Surgical Sciences, University of Bologna, Italy

[2] Institute of Human Anatomy, Department of Neurosciences, University of Padova, Italy

A – research concept and design; B – collection and/or assembly of data; C – data analysis and interpretation;
D – writing the article; E – critical revision of the article; F – final approval of the article

Address for correspondence
Rafael Boscolo-Berto
E-mail: rafael.boscoloberto@unipd.it

Abstract

The concept of "gender" refers to the socially constructed characteristics that define feminine or masculine behavior, which are constantly changing and can influence access to healthcare and patterns of help-seeking. These factors significantly impact forensic toxicology, a key area within the medicolegal landscape, forcing the adoption of a gender-sensitive approach to better understand the differing impacts of substances on men and women. Research indicates significant disparities in drug use between genders; men are more likely to abuse alcohol and illicit drugs, while women tend to use prescription medications. Although men typically show higher rates of driving under influence (DUI) related to alcohol, significant alcohol-related DUI cases also exist among women. In postmortem toxicology, gender affects drug pharmacokinetics and pharmacodynamics, with a pressing need for more research focused on women's specific toxic and fatal ranges. The rise of new psychoactive substances (NPS) presents additional challenges; while most users are male, the gender gap appears to be narrowing. Further investigation into the gender differences in drug usage and effects, particularly regarding NPS, is essential for improving justice system responses and healthcare delivery. A gender-based approach in forensic toxicology is vital for addressing these issues effectively.

Key words: gender, forensic toxicology, new psychoactive substances, drugs of abuse

Introduction

The term "gender" encompasses the socially constructed characteristics and attributes that define what it means to be a woman or a man in society; this concept is constantly shifting. These characteristics include distinct behaviors, societal roles and expectations, all of which can significantly impact individuals' access to healthcare services and inform their patterns of seeking assistance when needed.[1–3] These factors play a role in the medicolegal landscape. Over the years, forensic medicine has expanded to include various subdisciplines, each contributing uniquely to the overall understanding of scientific principles applicable in legal contexts.[4] This growth has particularly boosted advancements in forensic toxicology, a field that focuses on the effects of drugs and toxins in biological systems and their implications in legal cases.[5] In developed countries, there has been a marked increase in the integration of scientific research with forensic practices, leading to more informed investigations and reliable evidence in courtrooms.[6] This enhanced scientific collaboration underscores the importance of forensic toxicology as a vital tool in the pursuit of justice and the resolution of legal matters.

Forensic toxicology plays an essential role in the justice system. It provides critical insights that can inform legal cases and public health policies. A gender-sensitive approach in this field is crucial, as it helps illuminate the diverse and potentially differing impacts of substances on men and women. Understanding these distinctions can lead to more effective interventions and a fairer administration of justice.[2,7]

Integrating gender perspectives in traditional drugs

Numerous studies have indicated a disparity in the prevalence of drug abuse between men and women, influenced by biological, psychological and sociocultural factors.[8] Historically, men are considered approx. 2–3 times more likely to consume alcohol and use illicit drugs, while women are more inclined to use prescription medications. Substance use is typically perceived as risky behavior, which is less acceptable for women, particularly in societies characterized by larger gender gap, so the narrowing of the gap might also lead to higher engagement of women in harmful behaviors.[9] This is particularly relevant for some developing countries, which, due to poor resources, might face additional challenges in implementing gender-sensitive forensic toxicology, while witnessing the closure of the gender gap and an increase in women drug-related issues. This issue is of global significance. The United Nations Sustainable Development Goals were unanimously adopted by member states in 2015.[10] Among these goals, the need to reduce inequalities between nations and to transfer resources, knowledge, technology, and capabilities

to the Global South is emphasized. This transfer is essential for socio-economic development and enhancing global influence worldwide. To continue advancing forensic science as an international endeavor, it is crucial to narrow the inequalities between jurisdictions in alignment with the United Nations Sustainable Development Goals. Conversely, the evolution of jurisdictions cannot be separated from the development of forensic sciences.[11] In terms of driving under the influence (DUI), men typically demonstrate a higher rate of alcohol positivity, especially in road traffic incidents. Nevertheless, the prevalence of alcohol-related DUI among women is also significant and has been accompanied by an increase in related arrests.[12] Additionally, research has found no notable gender gap in DUI cases involving opioids and prescription drugs.[13]

Prevalence data can often be heterogeneous and difficult to compare, as recently pointed out in systematic reviews and meta-analyses by Pelletti et al.[12,13] In this context, hair analysis might provide a reliable tool to retrospectively assess drug use for gender-sensitive research.[14] Nevertheless, gender is a factor that can influence decision-making in post-mortem forensic toxicology, including requests for toxicological analyses. This challenge has also been identified based on other contextual information, such as age and ethnicity.[15] Conversely, in instances involving recently prescribed medications in women who have succumbed to opioid intoxication, such data may provide opportunities for preventing future fatalities.[16]

In the realm of postmortem investigations, it is crucial to acknowledge that gender plays a significant role in the pharmacokinetics and pharmacodynamics of drugs.[16,17] Traditionally, gender impact on toxicity has been mainly attributed to differences in body weight and fat, but additional gender-specific characteristics, such as expression of drug-metabolizing enzymes, drug-transporters and hormonal effects on drug targets and receptors, could provide additional molecular explanation for differential adverse drug reactions.[18] As an example, estrogens have been reported as one of the possible factors explaining the greater vulnerability of women to the reinforcing (rewarding) effects of stimulants.[19]

It is known that, despite equivalent consumption of alcohol, women achieve higher blood alcohol levels than men. They are also reportedly more sensible to adverse drug reactions, including misused prescription and illicit drugs, but the pharmacokinetic research is focused on therapeutic drugs.[20] Some studies have found no notable differences in clinical states and treatments in the setting of acute recreational drug toxicity or in drug levels between genders considering poisoning suicides.[21,22]

Nevertheless, toxic and lethal ranges are predominantly derived from male intoxication cases. More research should be devoted to understand how gender-related differences in pharmacokinetics and pharmacodynamics can

impact adverse outcomes secondary to drug use, including fatal intoxications.[20]

Moreover, for drugs that are also produced endogenously, such as γ-hydroxybutyric acid (GHB), gender may influence baseline or normal levels.[23] The existing literature on this topic is limited, suggesting that each instance of suspected fatal intoxication should be assessed on a case-by-case basis.[8] On this point, there is a pressing need for more research focused on toxic and fatal ranges specific to women.

Implementing a gender-sensitive strategy for addressing new psychoactive substances

The global rise of new psychoactive substances (NPS) has posed additional challenges for forensic toxicology. These substances typically exhibit heightened potency and health risks compared to traditional drugs, along with a wide range of chemical diversity.[24] Recent evidence suggests that the majority of NPS users are male, as supported by a case study of patients with substance use disorders analyzed by hair testing.[25,26] However, the gender gap seems to be narrowing, particularly for self-reported use of synthetic cannabinoids among 12–34-year olds.[27] Considering acute intoxications by synthetic cannabinoids, similar rates of psychosis for women (79%) and men (80%) were seen, while women appeared more severely agitated.[21] A recent study suggests that the gender gap in NPS-related deaths is also narrowing.[28] Indeed, the NPS death risk for men was 1.897 times higher than for women, but this did not reflect the difference between male and female drug-related mortality (approx. 4:1) over the same period. Also, women using NPS are more likely than men to additionally be positive for antidepressant or sedating drugs.[22]

However, it has to be highlighted that this trend is not universally observed in all research.[29,30] There is a clear need for further investigation to understand these trends, especially when distinguishing between various classes of NPS involved.

Current research on NPS has not sufficiently explored gender differences in NPS usage patterns and their effects on humans. For instance, studies related to psychomotor performance, particularly in the context of driving,[31] have overlooked this important factor. Nevertheless, some evidence of gender-based differences does emerge from animal studies.[27]

Conclusions

As forensic toxicology advances, it is essential for future research to emphasize a thorough analysis of gender-specific responses to drugs, particularly NPS. Implementing a gender-based approach in forensic toxicology establishes a crucial framework for deepening our understanding of its implications in the justice system and for improving the appropriateness and personalization of healthcare delivery.

ORCID iDs

Arianna Giorgetti ⓘ https://orcid.org/0000-0002-0441-9787
Rafael Boscolo-Berto ⓘ https://orcid.org/0000-0001-7556-1943

References

1. World Health Organization (WHO). Gender and health. World Health Organization Overview. Geneva, Switzerland: World Health Organization (WHO); 2024. https://www.who.int/health-topics/gender#tab=tab_1. Accessed December 5, 2024.
2. Marinelli S, Basile G, Manfredini R, Zaami S. Sex- and gender-specific drug abuse dynamics: The need for tailored therapeutic approaches. *J Pers Med.* 2023;13(6):965. doi:10.3390/jpm13060965
3. Yıldız M, Batun KD, Şahinoğlu H, et al. Suicide among doctors in Turkey: Differences across gender, medical specialty and the method of suicide. *Adv Clin Exp Med.* 2023;32(9):977–986. doi:10.17219/acem/159423
4. Ferrara SD, Bajanowski T, Cecchi R, Boscolo-Berto R, Viel G. Bio-medicolegal scientific research in Europe: A comprehensive bibliometric overview. *Int J Legal Med.* 2011;125(3):393–402. doi:10.1007/s00414-010-0538-1
5. Boscolo-Berto R, Viel G, Cecchi R, et al. Journals publishing bio-medicolegal research in Europe. *Int J Legal Med.* 2012;126(1):129–137. doi:10.1007/s00414-011-0620-3
6. Viel G, Boscolo-Berto R, Cecchi R, Bajanowski T, Vieira ND, Ferrara SD. Bio-medicolegal scientific research in Europe: A country-based analysis. *Int J Legal Med.* 2011;125(5):717–725. doi:10.1007/s00414-011-0576-3
7. Sablone S, Campobasso C, Tettamanti C, et al. Gender-based approach: An essential tool in patient safety management and forensic medicine practice. *J Sex Gender Specif Med.* 2024;10(3):167–168. doi:10.1723/4343.43288
8. Buccelli C, Della Casa E, Paternoster M, Niola M, Pieri M. Gender differences in drug abuse in the forensic toxicological approach. *Forensic Sci Int.* 2016;265:89–95. doi:10.1016/j.forsciint.2016.01.014
9. Cosma A, Elgar FJ, De Looze M, et al. Structural gender inequality and gender differences in adolescent substance use: A multilevel study from 45 countries. *SSM Popul Health.* 2022;19:101208. doi:10.1016/j.ssmph.2022.101208
10. Lee BX, Kjaerulf F, Turner S, et al. Transforming Our World: Implementing the 2030 Agenda through sustainable development goal indicators. *J Public Health Pol.* 2016;37(Suppl 1):13–31. doi:10.1057/s41271-016-0002-7
11. Bouzin JT, Lópes T, Heavey AL, Parrish J, Sauzier G, Lewis SW. Mind the gap: The challenges of sustainable forensic science service provision. *Forensic Sci Int Synerg.* 2023;6:100318. doi:10.1016/j.fsisyn.2023.100318
12. Pelletti G, Boscolo-Berto R, Anniballi L, et al. Prevalence of alcohol-impaired driving: A systematic review with a gender-driven approach and meta-analysis of gender differences. *Int J Legal Med.* 2024;138(6):2523–2540. doi:10.1007/s00414-024-03291-3
13. Pelletti G, Boscolo-Berto R, Barone R, et al. Gender differences in driving under the influence of psychoactive drugs: Evidence mapping of real case studies and meta-analysis. *Forensic Sci Int.* 2022;341:111479. doi:10.1016/j.forsciint.2022.111479
14. Giorgetti A, Pascali JP, Pelletti G, et al. Optimizing screening cutoffs for drugs of abuse in hair using immunoassay for forensic applications [published online as ahead of print on February 27, 2024]. *Adv Clin Exp Med.* 2024. doi:10.17219/acem/183124
15. Hamnett HJ, Dror IE. The effect of contextual information on decision-making in forensic toxicology. *Forensic Sci Int Synerg.* 2020;2:339–348. doi:10.1016/j.fsisyn.2020.06.003
16. Wightman RS, Perrone J, Scagos R, et al. Toxicological and pharmacologic sex differences in unintentional or undetermined opioid overdose death. *Drug Alcohol Depend.* 2021;227:108994. doi:10.1016/j.drugalcdep.2021.108994
17. Drummer OH. Emerging trends in forensic toxicology. *Aust J Forensic Sci.* 2003;35(1):141–148. doi:10.1080/00450610309410573

18. Soldin OP, Mattison DR. Sex differences in pharmacokinetics and pharmacodynamics. *Clin Pharmacokinet*. 2009;48(3):143–157. doi:10.2165/00003088-200948030-00001

19. National Institute od Drug Abuse (NIDA). Sex and Gender Differences in Substance Use. Bethesda, USA: National Institutes of Health (NIH); 2020. https://nida.nih.gov/publications/research-reports/substance-use-in-women/sex-gender-differences-in-substance-use. Accessed December 14, 2024.

20. Choo EK, Beauchamp G, Beaudoin FL, et al. A research agenda for gender and substance use disorders in the emergency department. *Acad Emerg Med*. 2014;21(12):1438–1446. doi:10.1111/acem.12534

21. Jones AW, Holmgren A, Ahlner J. Toxicology findings in suicides: Concentrations of ethanol and other drugs in femoral blood in victims of hanging and poisoning in relation to age and gender of the deceased. *J Forensic Leg Med*. 2013;20(7):842–847. doi:10.1016/j.jflm.2013.06.027

22. Syse VL, Brekke M, Grimsrud MM, et al. Gender differences in acute recreational drug toxicity: A case series from Oslo, Norway. *BMC Emerg Med*. 2019;19(1):29. doi:10.1186/s12873-019-0244-3

23. Vaiano F, Serpelloni G, Furlanetto S, et al. Determination of endogenous concentration of γ-hydroxybutyric acid (GHB) in hair through an ad hoc GC–MS analysis: A study on a wide population and influence of gender and age. *J Pharm Biomed Anal*. 2016;118:161–166. doi:10.1016/j.jpba.2015.10.036

24. Boscolo-Berto R. Challenges and future trends of forensic toxicology to keep a cut above the rest. *Adv Clin Exp Med*. 2024;33(5):423–425. doi:10.17219/acem/185730

25. Calvetti C, Salomone A, Verzeletti A, Di Nardo F, Begni PMG, Vezzoli S. Are the NPS commonly used? An extensive investigation in Northern Italy based on hair analysis. *J Anal Toxicol*. 2023;47(7):574–579. doi:10.1093/jat/bkad040

26. Giorgetti A, Mohamed S, Pirani F, et al. Prevalence of new psychoactive substances and drugs of abuse in the hair of individuals diagnosed with substance use disorder: Polydrug and emerging pattern of consumption [published online as ahead of print on December 10, 2024]. *J Forensic Sci*. 2024. doi:10.1111/1556-4029.15683

27. Fattore L, Marti M, Mostallino R, Castelli MP. Sex and gender differences in the effects of novel psychoactive substances. *Brain Sci*. 2020;10(9):606. doi:10.3390/brainsci10090606

28. Webb L, Shi X, Goodair C, Cheeta S. Trends in mortality from novel psychoactive substances as "legal highs": Gender differences in manner of death and implications for risk differences for women. *Front Psychiatry*. 2022;13:890840. doi:10.3389/fpsyt.2022.890840

29. Giorgetti A, Busardò FP, Tittarelli R, Auwärter V, Giorgetti R. Post-mortem toxicology: A systematic review of death cases involving synthetic cannabinoid receptor agonists. *Front Psychiatry*. 2020;11:464. doi:10.3389/fpsyt.2020.00464

30. Giorgetti A, Große Perdekamp M, Franchetti G, et al. Intoxications involving methoxyacetylfentanyl and U-47700: A study of 3 polydrug fatalities. *Int J Legal Med*. 2024;138(5):1801–1811. doi:10.1007/s00414-024-03263-7

31. Orazietti V, Basile G, Giorgetti R, Giorgetti A. Effects of synthetic cannabinoids on psychomotor, sensory and cognitive functions relevant for safe driving. *Front Psychiatry*. 2022;13:998828. doi:10.3389/fpsyt.2022.998828

Survival benefits of gastrectomy in patients with metastatic gastric cancer: A meta-analysis

Lifan Chen[1,A,D–F], Yu Chen[2,A–C,F]

[1] Medical Department, Shantou Central Hospital, Guangdong, China

[2] Department of Cardiology, Longgang District People's Hospital of Shenzhen, Guangdong, China

A – research concept and design; B – collection and/or assembly of data; C – data analysis and interpretation;
D – writing the article; E – critical revision of the article; F – final approval of the article

Address for correspondence
Yu Chen
E-mail: yuchenlgdr@outlook.com

Abstract

Background. Individuals with metastatic gastric cancer (MGC) are incurable and have a poor prognosis. To date, surgical resection with curative intent is the only treatment providing hope for a cure, but the role of surgical resection is still controversial.

Objectives. To assess the effects of gastrectomy compared to non-resection on MGC patient survival.

Materials and methods. PubMed, Embase, Cochrane Library, and Web of Science databases were searched up to October 10, 2023. Primary outcomes were 1-, 2-, 3-, and 5-year overall survival (OS), OS, and OS time.

Results. Forty-six studies with 7,152 MGC patients were included. Compared to MGC patients receiving no resection, MGC patients with gastrectomy had significantly improved 1-year OS (pooled relative risk (RR):1.90, 95% confidence intervals (95% CIs): 1.50, 2.41), 2-year OS (pooled RR: 2.23, 95% CI: 1.40, 3.53), 3-year OS (pooled RR: 6.09, 95% CI: 3.12, 11.87), 5-year OS (pooled RR: 4.30, 95% CI: 1.35, 13.74), and reduced risk of death (pooled hazard ratio (HR): 0.49, 95% CI: 0.37, 0.65). Gastrectomy combined with metastasectomy or not also revealed similar results regarding OS and risk of death. Additionally, OS time was significantly longer in patients receiving gastrectomy than patients not receiving resection (pooled weighted mean difference (WMD): 6.06, 95% CI: 1.36, 10.760). No significant difference in postoperative morbidity was detected between the patients receiving gastrectomy and patients not receiving resection (pooled RR: 2.54, 95% CI: 0.13, 51.39).

Conclusions. Gastrectomy, with or metastasectomy, may provide MGC patients with survival benefits.

Key words: survival, meta-analysis, gastrectomy, metastatic gastric cancer

Introduction

Gastric cancer (GC) is the 5th most prevalent cancer and the 4th most common cause of cancer-related death worldwide. Since GC is often diagnosed at an advanced stage, it leads to high mortality, with 769,000 deaths globally in 2020.[1,2] Over half of GC patients in the USA have regional or distant metastases at the time of diagnosis.[3] Individuals with metastatic GC (MGC) are incurable and have a poor prognosis, with a median overall survival (OS) of less than 1 year.[4–6] Currently, MGC remains a primary global health problem, and timely and effective therapies are of great significance.

Chemotherapy is the gold standard MGC treatment.[7,8] At present, trastuzumab is the only molecularly targeted drug accepted in first-line treatment, combined with cisplatin and fluoropyrimidine, for patients with MGC with human epidermal growth factor receptor 2 (HER2) overexpression who have not received anti-cancer therapy.[9] However, only around 20% of MGC patients have overexpressed HER2.[10]

The National Comprehensive Cancer Network (NCCN) guidelines indicate gastrectomy for the relief of GC-related symptoms, such as bleeding or obstruction, in patients with incurable diseases.[11] The Japanese Gastric Cancer Association (JGCA) guidelines recommend that patients with MGC but no substantial symptoms can receive gastrectomy.[12] Dittmar et al.[13] showed that primary non-curative gastrectomy could lower the incidence of serious tumor-related complications and extend OS in patients with advanced GC, as confirmed by Kulig et al.[14] in multicenter settings. In contrast, the REGATTA trial in 2016 showed that advanced GC patients with a single incurable factor did not obtain survival benefit from gastrectomy followed by chemotherapy compared with those undergoing chemotherapy alone.[15] Moreover, selected patients with MGC who underwent surgical resection for therapeutic purposes were shown to have a relatively poor prognosis,[16] and MGC patient prognosis was only moderately improved after palliative gastrectomy based on Surveillance, Epidemiology, and End Results (SEER).[17] Due to these debatable findings, the effect of gastrectomy in patients with MGC requires clarification.

Objectives

This meta-analysis systematically evaluated the influence of gastrectomy on MGC patient survival and included subgroup analysis of metastatic sites.

Methods

Study search and selection

PubMed, Embase, Cochrane Library, and Web of Science databases were comprehensively searched for studies on gastrectomy in MGC patients up to October 10, 2023, using the following terms: "gastric neoplasms" OR "gastric neoplasm" OR "neoplasm, gastric" OR "neoplasms" OR "gastric" OR "gastric cancer" OR "cancer, gastric" OR "cancers, gastric" OR "gastric cancers" AND "neoplasm metastasis" OR "neoplasm metastases" OR "metastases, neoplasm" OR "metastasis, neoplasm" OR "metastases" OR "metastasis" OR "metastatic" AND "gastrectomy" OR "gastrectomies" OR "metastasectomy" OR "metastasectomies" OR "surgery" OR "surgical resection." As an example, Supplementary Table 1 outlines the search strategy for PubMed. The full texts and their references were also thoroughly reviewed for eligible studies. Afterward, Endnote X9 (Clarivate Analytics, London, UK) was used to remove duplicates. The search was completed by 2 reviewers independently, and the study followed the Preferred Reporting Items for Systematic Reviews and Meta-Analyses (PRISMA) guidelines (Supplementary Table 2).

Eligibility criteria

Inclusion criteria (PICOS) were: 1) population (P): patients who suffered from MGC; 2) intervention (I): patients in the intervention group who underwent gastrectomy, comparator (C): patients in the control group who did not receive resection for MGC treatment; 3) outcome (O): at least 1 of the following outcomes were included: 1-, 2-, 3-, and 5-year OS, OS, OS time, postoperative morbidity, perioperative mortality, and hospital stay; and 4) study design (S): studies were cohort in design.

Exclusion criteria were: 1) studies on animals; 2) studies with incomplete or invalid data; 3) reviews, meta-analyses, case reports, conference reports, editorial materials, letters, errata, notes, and protocols; 4) studies with data from public databases, such as the SEER and National Cancer Database (NCDB); 5) non-English literature; and 6) studies without available full texts.

Outcome measures

Primary outcomes were 1-, 2-, 3-, and 5-year OS, OS, and OS time. Secondary outcomes were postoperative morbidity, perioperative mortality and hospital stay. Postoperative morbidity mainly included bleeding, intestinal obstruction, anastomotic leakage, and wound infection. Perioperative mortality was defined as death within 30 days after surgery or during postoperative hospitalization.

Data extraction and quality assessment

Two independent authors extracted the data from the eligible studies, including first author, year of publication, country, study design, group, surgery, number of patients (n), sex (male/female), age [years], chemotherapy, Eastern Cooperative Oncology Group Performance Status (ECOG PS), histology, timing of metastases, T-grade, N-grade,

tumor location, metastatic site, follow-up time [months], median survival time [months], and outcomes.

The Newcastle–Ottawa scale (NOS)[18] evaluated the quality of cohort studies, with a maximum score of 9 points indicating low (0–3), medium (4–6) or high (7–9) quality. Two reviewers conducted the assessments independently and settled disagreements through discussion.

Statistical analyses

Statistical analyses employed Stata v. 15.1 (StataCorp, College Station, USA), with relative risk (RR) values used for enumeration data, hazard ratio (HR) for survival data and weighted mean difference (WMD) for measurement data (all included 95% confidence intervals (95 CIs)). The effect size of each outcome was tested for heterogeneity, with funnel plots used to present the results. A random-effects model was selected for use a priori, with a random-effects meta-analysis conducted to assess the effects of gastrectomy compared to non-resection treatment in MGC. When the heterogeneity statistic (I^2) was greater than 50% and the difference was statistically significant ($p < 0.05$), subgroup analysis was performed based on metastatic sites (liver, peritoneum, lymph node, and mixed sites), and meta-regression analysis was used to explore the source of the heterogeneity. Forest plots were drawn, and sensitivity analysis was carried out for outcomes when analyzing more than 2 studies. For outcomes with more than 2 studies, other outcomes were subject to sensitivity analysis by deleting a single study at a time and comprehensively analyzing the remaining studies, and each paper underwent deletion.

Begg's test was employed to assess publication bias. For publication bias assessment, meta-analyses should include at least 10 studies for the outcome evaluated.[19,20] The trim-and-fill method was performed using the funnel plot, which formalized the qualitative approach. In brief, the asymmetric outer part was trimmed after estimating the number of studies in the asymmetric part of the funnel, and the symmetric residual was used to assess the real center of the funnel and replace the trimmed studies and their missing equivalents around the center. The filled funnel plot was then used to calculate the true mean and its variance.[21] Differences were statistically significant when $p < 0.05$.

Results

Study characteristics

After searching the 4 databases, 24,998 studies were retrieved, of which 11,379 were removed due to duplication. The flowchart for study screening is shown in Fig. 1. Finally, 46 studies[22–67] with 7,152 MGC patients were included according to the eligibility criteria. The publication year of the studies ranged from 2000 to 2023. Supplementary Table 3 exhibits the baseline characteristics of the included

Fig. 1. Flowchart for study screening

24,998 records identified
PubMed (n = 6,845)
Embase (n = 9,202)
Web of Science (n = 7,954)
Cochrane Library (n = 997)

13,619 records after duplicates removed

13,455 records excluded
  Subjects not meeting the requirements (n = 7,087)
  Non-English articles (n = 2,249)
  Abstracts (n = 1,884)
  Case reports (n = 1,258)
  Reviews or meta-analyses (n = 808)
  Animal experiments (n = 90)
  Editorial materials, letters, errata, notes (n = 60)
  Unable to obtain full texts (n = 19)

164 full-text articles screened for eligibility

118 Full-text articles excluded
  Groups not meeting the requirements (n = 52)
  Data not available (n = 42)
  Public databases (n = 23)
  Unqualified studies design (n = 1)

46 studies included in quantitative synthesis

studies. In the current study, patients who received gastrectomy were grouped into the gastrectomy group, gastrectomy + metastasectomy group or gastrectomy ± metastasectomy group, and patients who did not receive resection were classified into the non-resection group. In this regard, 16 studies[23,28,30,32,37,40,42,44,50,51,53,55,59,61,63,64] made comparisons between the gastrectomy group and the non-resection group, 8 studies[22,25,34,41,43,54,60,66] compared the gastrectomy + metastasectomy group with the non-resection group, and 22 studies[24,26,27,29,31,33,35,36,38,39,45–47,48,49,52,56–58,62,65,67] compared the gastrectomy ± metastasectomy group with the non-resection group. Of 46 cohort studies, 30 were of medium quality and 16 had high quality.

Primary outcomes

One-year overall survival

Gastrectomy vs non-resection

Five studies[27,28,30,41,42] of 552 patients provided data on the 1-year OS rate of the gastrectomy and non-resection groups. The overall analysis demonstrated that the 1-year OS rate was significantly higher after gastrectomy than after non-resection treatment (pooled RR: 1.90, 95% CI: 1.50, 2.41, p < 0.001) (Table 1, Fig. 2A, Supplementary Fig. 1A).

Gastrectomy + metastasectomy vs non-resection

Comparison of the 1-year OS rate between gastrectomy + metastasectomy and non-resection was presented in 3 studies[25,41,54] with 156 subjects. Metastatic gastric cancer patients undergoing gastrectomy and metastasectomy had significantly greater 1-year OS than those receiving no resection (pooled RR: 1.63, 95% CI: 1.18, 2.26, p = 0.003) (Table 1, Fig. 2B, Supplementary Fig. 1B).

Gastrectomy ± metastasectomy vs non-resection

Twelve studies,[24,27,29,31,35,38,39,45,46,52,58,65] including 2,475 individuals, compared the 1-year OS rate of the gastrectomy ± metastasectomy and non-resection groups. After the combined analysis, the gastrectomy ± metastasectomy group was found to have a significantly increased 1-year OS rate than the non-resection group (pooled RR: 2.65, 95% CI: 1.95, 3.61, p < 0.001) (Fig. 2C, Supplementary Fig. 1C). Since the heterogeneity was non-negligible (I^2 = 78.0%, p < 0.05), subgroup analysis based on metastatic sites was carried out. When the metastatic site was the liver (pooled RR: 2.54, 95% CI: 1.73, 3.74, p < 0.001), the peritoneum (pooled RR: 4.15, 95% CI: 2.94, 5.85, p < 0.001) or lymph node (pooled RR: 3.50, 95% CI: 1.79, 6.83, p < 0.001), the 1-year OS rate of the gastrectomy ± metastasectomy group was significantly higher than non-resection (Table 1). To explore the source of heterogeneity, meta-regression analysis

was performed with metastatic sites, and the results suggested that metastatic sites had nothing to do with inter-study heterogeneity (p > 0.05) (Supplementary Table 5).

Two-year overall survival

Gastrectomy vs non-resection

Information on the 2-year OS rate of the gastrectomy and non-resection groups was reported in 5 studies[28,30,32,42,61] with 726 patients. The pooled analysis revealed that the gastrectomy group had a significantly higher 2-year OS rate than the non-resection group (pooled RR: 2.23, 95% CI: 1.40, 3.53, p = 0.001) (Table 1, Fig. 3A, Supplementary Fig. 1D).

Gastrectomy + metastasectomy vs non-resection

Two studies[25,54] investigated the 2-year OS rate in 119 subjects undergoing gastrectomy plus metastasectomy or no resection. Patients undergoing gastrectomy and metastasectomy had a significantly elevated 2-year OS rate compared to those not treated with resection (pooled RR: 2.48, 95% CI: 1.23, 5.00, p = 0.011) (Table 1, Fig. 3B, Supplementary Fig. 1E).

Gastrectomy ± metastasectomy vs non-resection

Data on the 2-year OS rate for 1,877 patients were given in 12 studies.[24,29,31,35,38,39,45,46,48,52,56,65] A significantly higher 2-year OS rate was observed through combined analysis in the gastrectomy ± metastasectomy group in contrast to the corresponding rate in the non-resection group (pooled RR: 4.77, 95% CI: 3.12, 7.27, p < 0.001) (Table 1, Fig. 3C, Supplementary Fig. 1F).

Three-year overall survival

Gastrectomy vs non-resection

Seven studies[22,23,28,34,40,41,43] with 625 patients included a 3-year OS analysis of the gastrectomy and non-resection groups. The gastrectomy group had a significantly greater 3-year OS rate than the non-resection group (pooled RR: 6.09, 95% CI: 3.12, 11.87, p < 0.001) (Table 1, Fig. 4A, Supplementary Fig. 1G).

Gastrectomy + metastasectomy vs non-resection

Three-year OS was compared between gastrectomy + metastasectomy and non-resection in 420 patients across 5 studies.[22,34,41,43,54] Overall analysis illustrated that the 3-year OS rate of patients with gastrectomy and metastasectomy was significantly higher than that of patients without resection (pooled RR: 11.40, 95% CI: 5.73, 22.66, p < 0.001) (Table 1, Fig. 4B, Supplementary Fig. 1H).

Table 1. Overall analysis for the impact of gastrectomy on different outcomes in MGC patients

Outcome	Indicators	Group	Studies	RR/HR/WMD (95% CI) random-effects model	p-value	I^2
1-year OS	G vs 0	overall	5	1.90 (1.50, 2.41)	<0.001	3.4
	G + M vs 0	overall	3	1.63 (1.18, 2.26)	0.003	0.0
	G ± M vs 0	overall	12	2.65 (1.95, 3.61)	<0.001	78.0
	metastatic sites	liver	5	2.54 (1.73, 3.74)	<0.001	42.1
		peritoneum	3	4.15 (2.94, 5.85)	<0.001	0.0
		lymph node	1	3.50 (1.79, 6.83)	<0.001	N/A
		mixed	5	2.53 (1.35, 4.72)	0.004	90.3
2-year OS	G vs 0	overall	5	2.23 (1.40, 3.53)	0.001	24.3
	G + M vs 0	overall	2	2.48 (1.23, 5.00)	0.011	0.0
	G ± M vs 0	overall	12	4.77 (3.12, 7.27)	<0.001	32.6
3-year OS	G vs 0	overall	7	6.09 (3.12, 11.87)	<0.001	0.0
	G + M vs 0	overall	5	11.40 (5.73, 22.66)	<0.001	0.0
	G ± M vs 0	overall	8	4.95 (2.49, 9.85)	<0.001	43.2
5-year OS	G vs 0	overall	3	4.30 (1.35, 13.74)	0.014	0.0
	G + M vs 0	overall	3	7.68 (1.50, 39.15)	0.014	0.0
	G ± M vs 0	overall	9	4.20 (2.20, 8.01)	<0.001	0.0
OS	G vs 0	overall	8	0.49 (0.37, 0.65)	<0.001	75.5
	metastatic sites	peritoneum	5	0.48 (0.32, 0.71)	<0.001	76.4
		mixed	3	0.49 (0.30, 0.81)	0.005	80.8
	G + M vs 0	overall	3	0.31 (0.24, 0.40)	<0.001	0.0
	G ± M vs 0	overall	2	0.46 (0.34, 0.64)	<0.001	0.0
OS time	G vs 0	overall	2	6.06 (1.36, 10.76)	0.012	96.1
Postoperative morbidity	G vs 0	overall	2	2.54 (0.13, 51.39)	0.544	86.9
	G ± M vs 0	overall	3	1.35 (0.72, 2.54)	0.356	51.5
Perioperative mortality	G ± M vs 0	overall	5	0.63 (0.33, 1.19)	0.153	0.0
Hospital stay	G ± M vs 0	overall	2	1.04 (−0.25, 2.33)	0.114	0.0

MGC – metastatic gastric cancer; RR – relative risk; HR – hazard ratio; WMD – weighted mean difference; 95% CI – 95% confidence interval; OS – overall survival; G – gastrectomy; M – metastasectomy; 0 – non-resection; N/A – not applicable.

Gastrectomy ± metastasectomy vs non-resection

The 3-year OS rate was assessed by 8 studies[26,31,35,39,46,49,52,62] with 1,707 subjects in the gastrectomy ± metastasectomy and non-resection groups. Compared to patients receiving gastrectomy ± metastasectomy, those not treated with resection had a significantly elevated 3-year OS rate (pooled RR: 4.95, 95% CI: 2.49, 9.85, p < 0.001) (Table 1, Fig. 4C, Supplementary Fig. 1I).

Five-year overall survival

Gastrectomy vs non-resection

Three studies[37,41,67] containing 366 patients evaluated 5-year OS in the gastrectomy and non-resection groups. Pooled analysis indicated that the 5-year OS rate of patients receiving gastrectomy was significantly higher than that of patients not receiving resection (pooled RR: 4.30, 95% CI: 1.35, 13.74, p = 0.014) (Table 1, Fig. 5A, Supplementary Fig. 1J).

Gastrectomy + metastasectomy vs non-resection

The 5-year OS rate of the gastrectomy + metastasectomy and non-resection groups were compared in 3 studies[25,41,54] of 156 patients. The gastrectomy + metastasectomy group had a significantly increased 5-year OS rate relative to the non-resection group (pooled RR: 7.68, 95% CI: 1.50, 39.15, p = 0.014) (Table 1, Fig. 5B, Supplementary Fig. 1K).

Gastrectomy ± metastasectomy vs non-resection

Nine studies[24,31,36,39,45,46,48,52,67] presented data on 5-year OS in 1,680 patients of the gastrectomy ± metastasectomy and non-resection groups. The 5-year OS rate was significantly greater in patients treated with

Fig. 2. Forest plot for 1-year OS in MGC patients. A. Gastrectomy vs non-resection; B. Gastrectomy + metastasectomy vs non-resection; C. Gastrectomy ± metastasectomy vs non-resection

MGC – metastatic gastric cancer; OS – overall survival; RR – relative risk; 95% CI – 95% confidence interval.

A

B

C

Fig. 3. Forest plot for 2-year OS in MGC patients. A. Gastrectomy vs non-resection; B. Gastrectomy + metastasectomy vs non-resection; C. Gastrectomy ± metastasectomy vs non-resection

MGC – metastatic gastric cancer; OS – overall survival; RR – relative risk; 95% CI – 95% confidence interval.

Fig. 4. Forest plot for 3-year OS in MGC patients. A. Gastrectomy vs non-resection; B. Gastrectomy + metastasectomy vs non-resection; C. Gastrectomy ± metastasectomy vs non-resection

MGC – metastatic gastric cancer; OS – overall survival; RR – relative risk; 95% CI – 95% confidence interval.

A

B

C

Fig. 5. Forest plot for 5-year OS in MGC patients. A. Gastrectomy vs non-resection; B. Gastrectomy + metastasectomy vs non-resection; C. Gastrectomy ± metastasectomy vs non-resection

MGC – metastatic gastric cancer; OS – overall survival; RR – relative risk; 95% CI – 95% confidence interval.

gastrectomy ± metastasectomy than in patients not undergoing resection (pooled RR: 4.20, 95% CI: 2.20, 8.01, p < 0.001) (Table 1, Fig. 5C, Supplementary Fig. 1L).

Overall survival

Gastrectomy vs non-resection

Regarding OS, 8 studies[23,30,34,44,50,55,61,63] made comparisons between gastrectomy and non-resection. The overall analysis demonstrated that patients undergoing gastrectomy had a significantly lower risk of death than those not receiving resection (pooled HR: 0.49, 95% CI: 0.37, 0.65, p < 0.001) (Fig. 6A, Supplementary Fig. 1M). Due to relatively large heterogeneity (I^2 = 75.5%, p < 0.05), subgroup analysis of metastatic sites was conducted. As the tumor metastasized to the peritoneum, the OS of the gastrectomy group was significantly better than that of the non-resection group (pooled HR: 0.48, 95% CI: 0.32, 0.71, p < 0.001) (Table 1). Furthermore, metastatic sites were not the source of the heterogeneity between studies, as found through meta-regression analysis (p > 0.05) (Supplementary Table 6).

Gastrectomy + metastasectomy vs non-resection

Three studies[34,60,66] evaluated OS in patients undergoing gastrectomy plus metastasectomy and not receiving resection. In comparison with the non-resection group, the gastrectomy + metastasectomy group had a significantly reduced risk of death (pooled HR: 0.31, 95% CI: 0.24, 0.40, p < 0.001) (Table 1, Fig. 6B, Supplementary Fig. 1N).

Gastrectomy ± metastasectomy vs non-resection

The OS of the gastrectomy ± metastasectomy and non-resection groups was explored in 2 studies.[33,47] The pooled results showed that the risk of death in patients with gastrectomy ± metastasectomy was significantly decreased by 53.6% compared to those without resection (pooled HR: 0.46, 95% CI: 0.34, 0.64, p < 0.001) (Table 1, Fig. 6C, Supplementary Fig. 1O).

Overall survival time

Gastrectomy vs non-resection

Overall survival time for patients who received gastrectomy and no resection was reported in 2 studies.[51,53] The OS time of the gastrectomy group was significantly longer than that of the non-resection group (pooled WMD: 6.06, 95% CI: 1.36, 10.76, p = 0.012) (Table 1, Fig. 7, Supplementary Fig. 1P).

Secondary outcomes

Postoperative morbidity

Gastrectomy vs non-resection

Two studies[44,59] with 382 subjects assessed the postoperative morbidity of gastrectomy and non-resection groups. The gastrectomy group had comparable postoperative morbidity to the non-resection group (pooled RR: 2.54, 95% CI: 0.13, 51.39, p = 0.544) (Table 1).

Gastrectomy ± metastasectomy vs non-resection

Postoperative morbidity in the gastrectomy ± metastasectomy and non-resection groups was compared in 3 studies[47,52,57] of 574 patients. The postoperative morbidity of subjects receiving gastrectomy and metastasectomy did not significantly differ from that of those without resection (pooled RR: 1.35, 95% CI: 0.72, 2.54, p = 0.36) (Table 1).

Perioperative mortality

Gastrectomy ± metastasectomy vs non-resection

Five studies[36,47,48,56,57] compared perioperative mortality between 304 patients undergoing gastrectomy ± metastasectomy and 296 not undergoing resection. No significant difference was detected between the gastrectomy ± metastasectomy and non-resection groups in perioperative mortality (pooled RR: 0.63, 95% CI: 0.33, 1.19, p = 0.153; Table 1).

Hospital stay

Gastrectomy ± metastasectomy vs non-resection

The hospital stays of 395 patients in the gastrectomy ± metastasectomy and non-resection groups were analyzed in 2 studies.[45,57] The gastrectomy ± metastasectomy group and the non-resection group had equivalent hospital stays according to overall analysis (pooled WMD: 1.04, 95% CI: −0.25, 2.33, p = 0.114) (Table 1).

Publication bias

Begg's test evaluated publication bias in 1- and 2-year OS outcomes. Other outcomes did not meet the requirement for publication bias assessment, and at least 10 studies were included in the outcome evaluation. The results suggested that publication bias existed when the 2-year OS (Z = 2.54, p = 0.011) rather than the 1-year OS (Z = 0.75, p = 0.451) was the outcome. Using the trim-and-fill method, the point estimate for 2-year OS was adjusted slightly from 5.570 (95% CI: 3.966, 6.966) to 5.492 (95% CI: 5.205, 5.779),

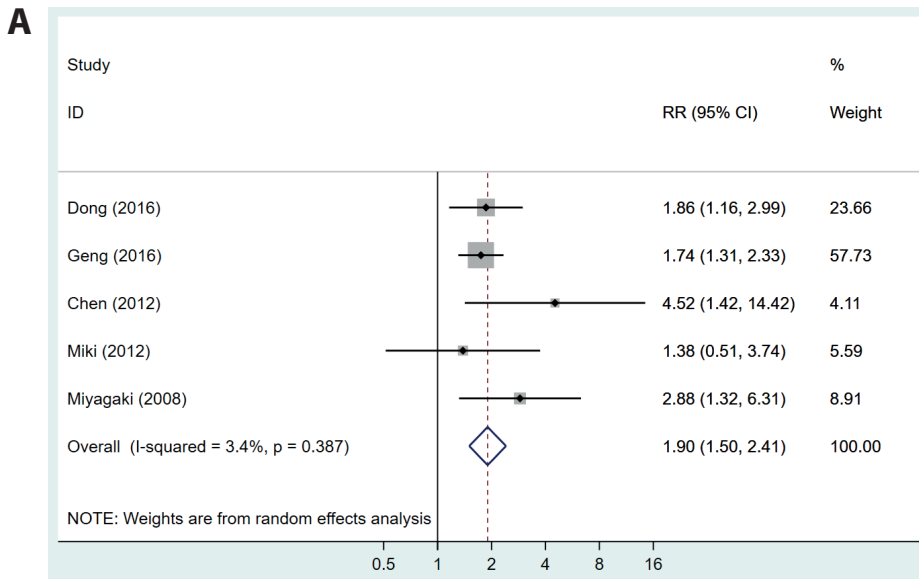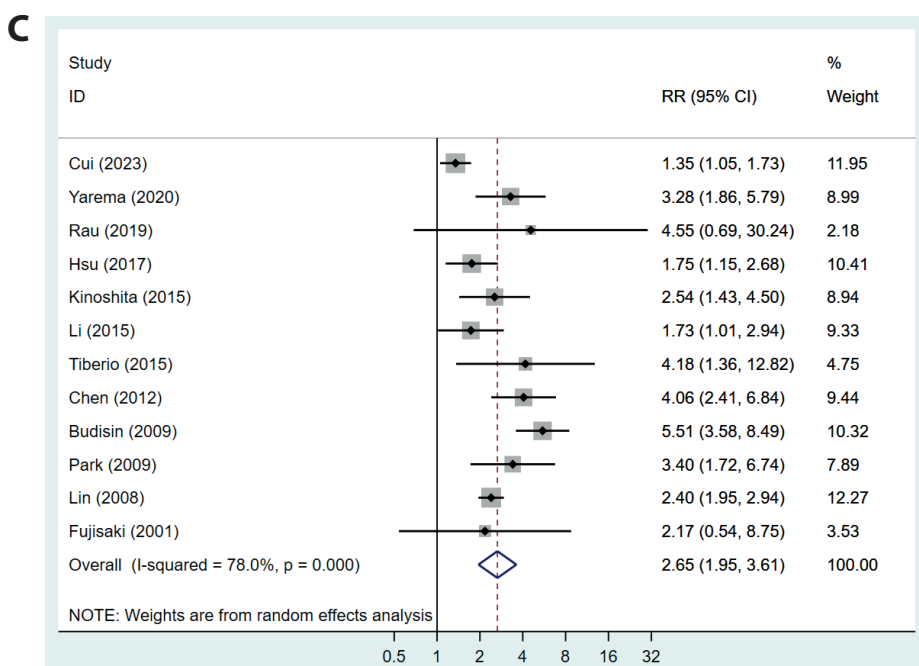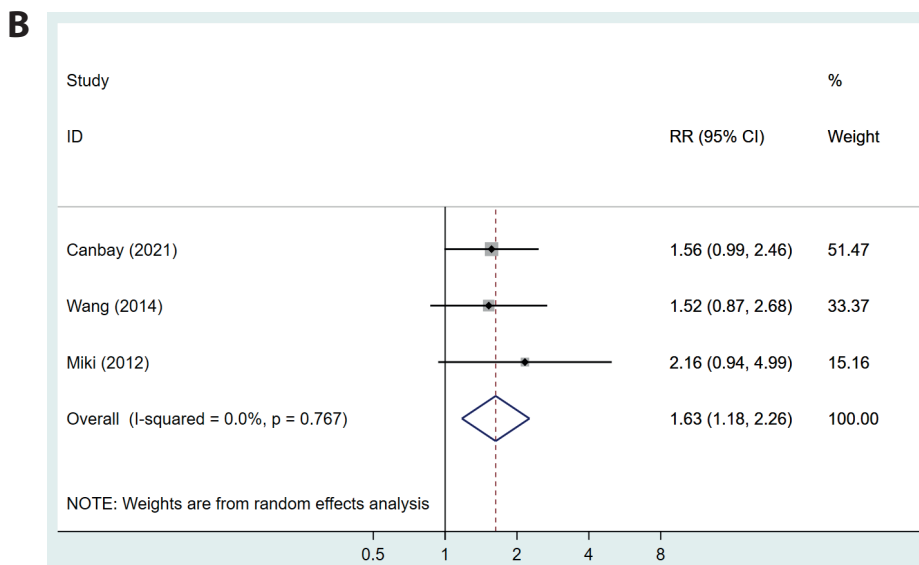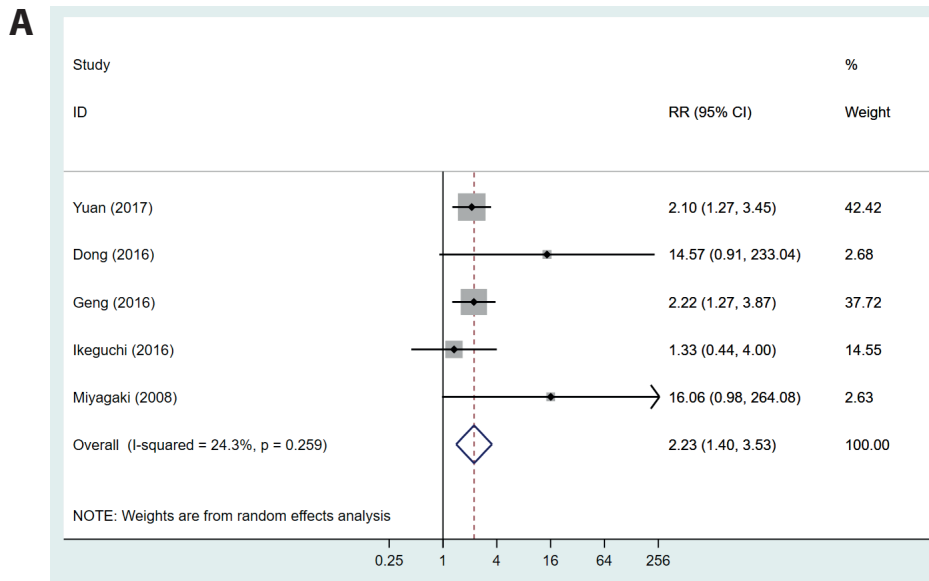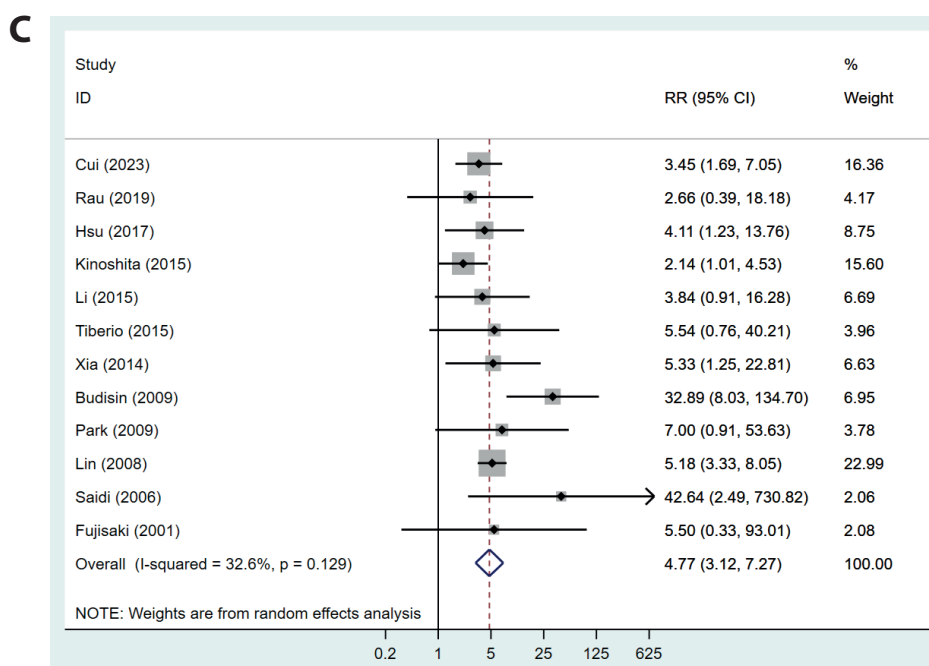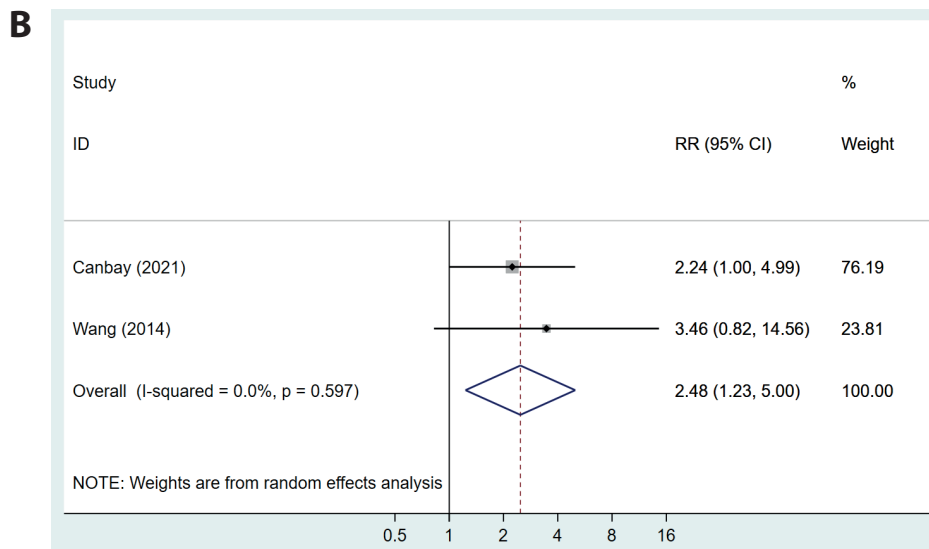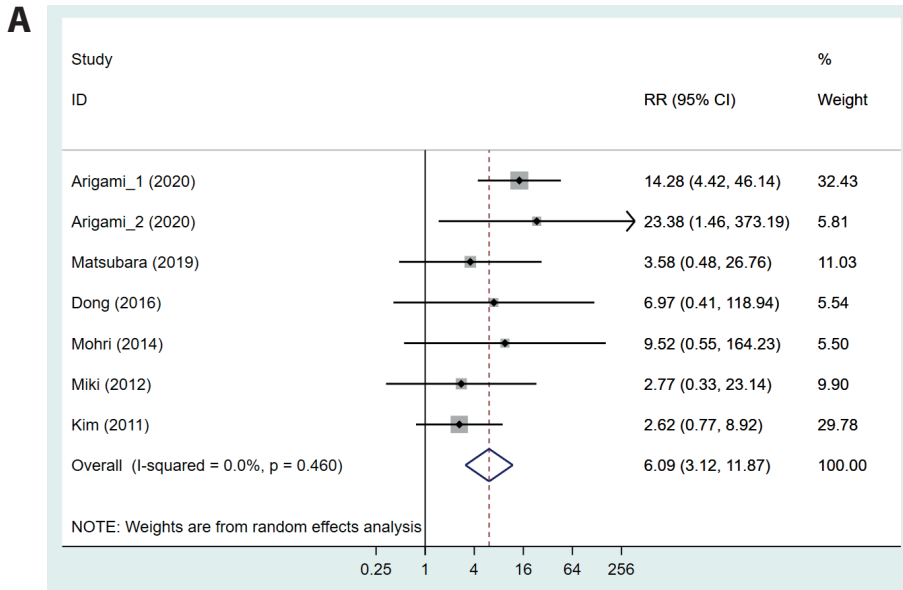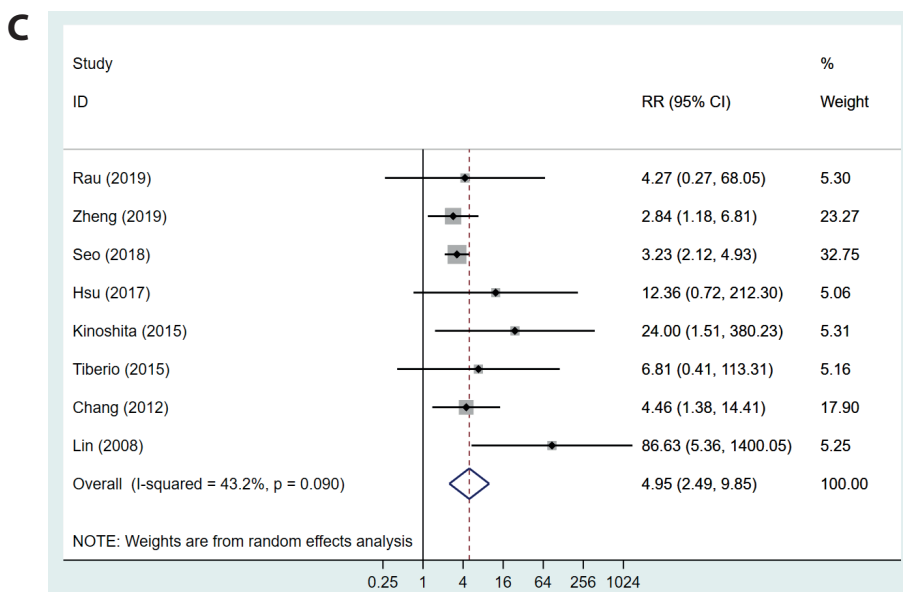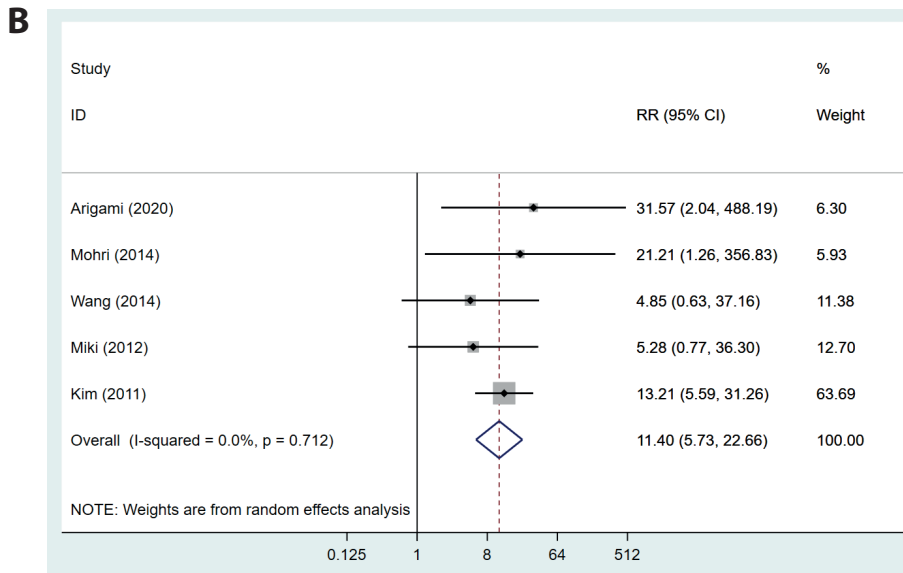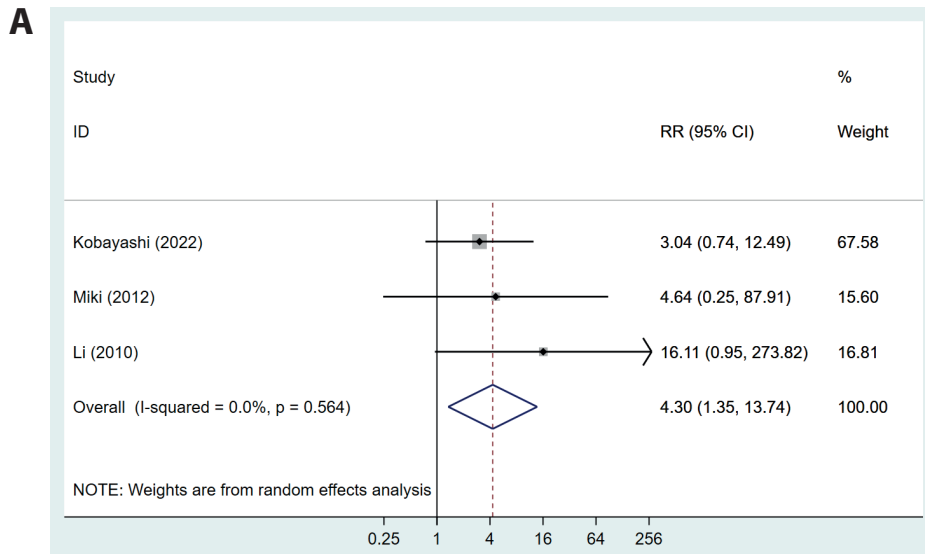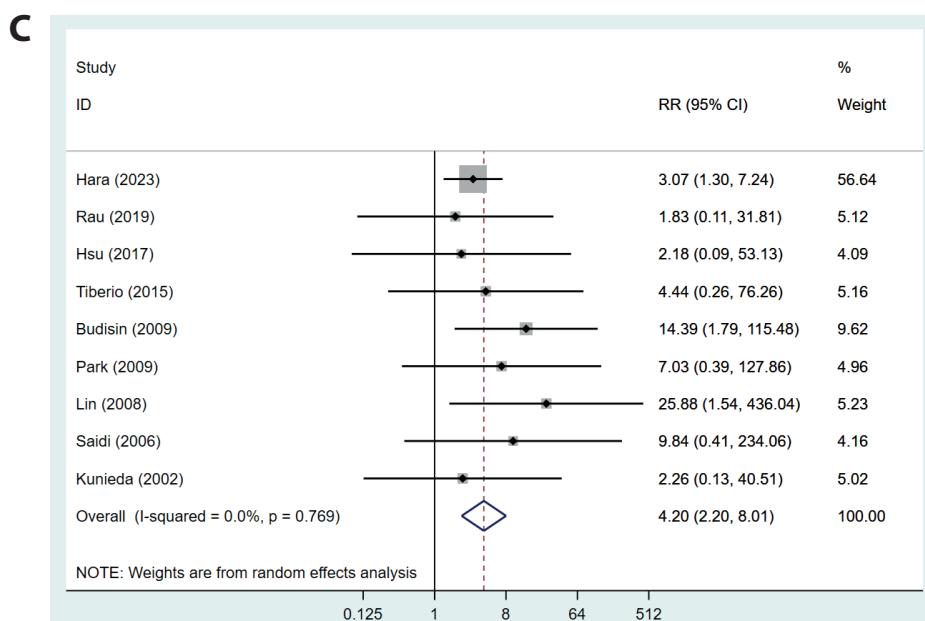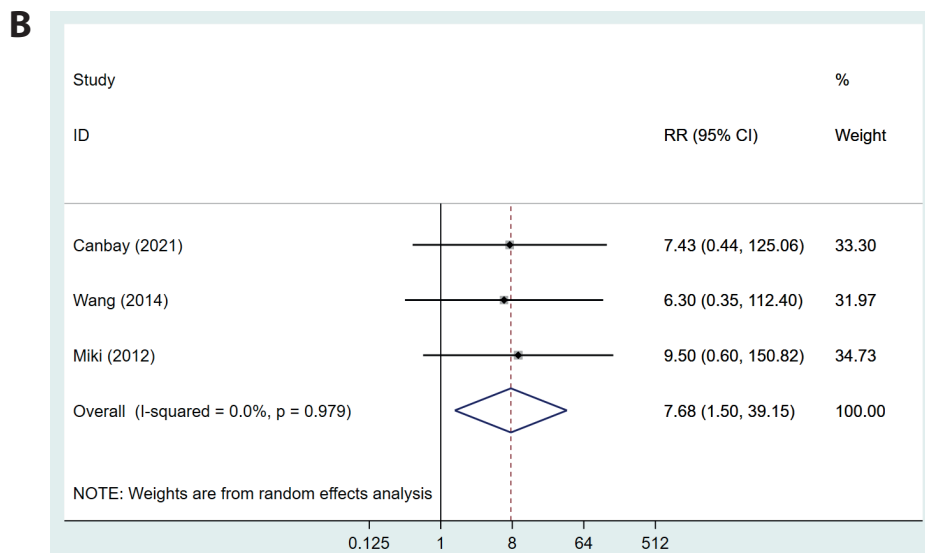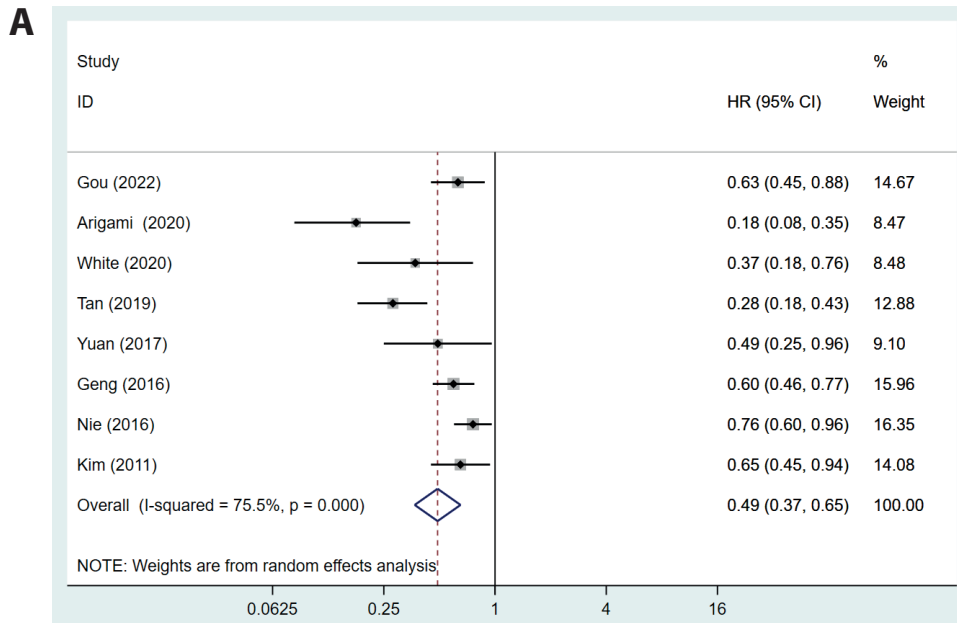**Fig. 6.** Forest plot for OS in MGC patients. A. Gastrectomy vs non-resection; B. Gastrectomy + metastasectomy vs non-resection; C. Gastrectomy ± metastasectomy vs non-resection

MGC – metastatic gastric cancer; OS – overall survival; HR – hazard ratio; 95% CI – 95% confidence interval.

20

L. Chen, Y. Chen. Survival benefit of gastrectomy for MGC
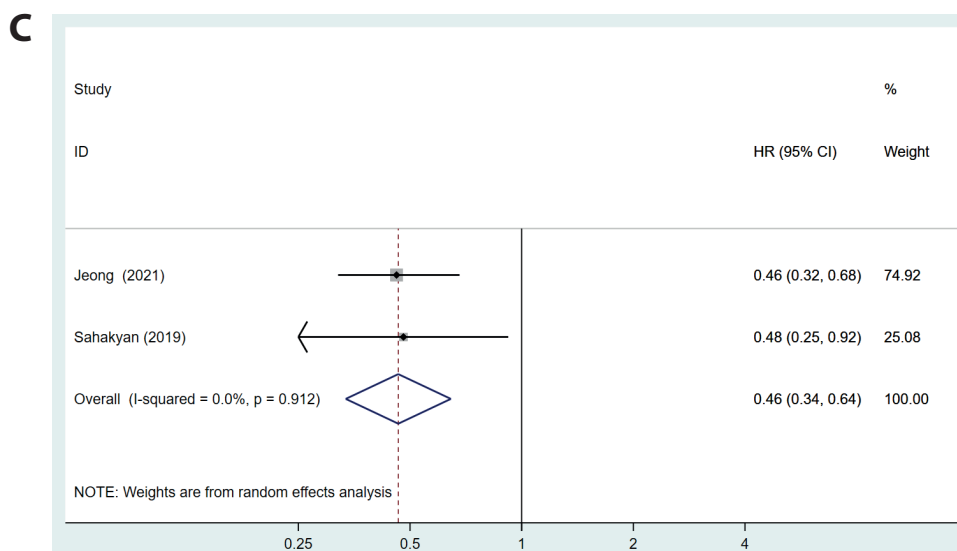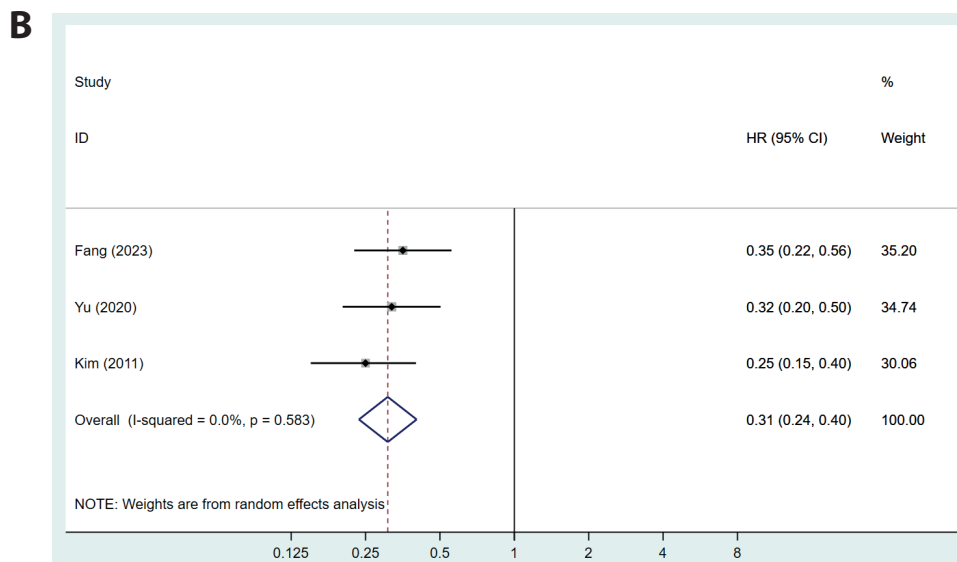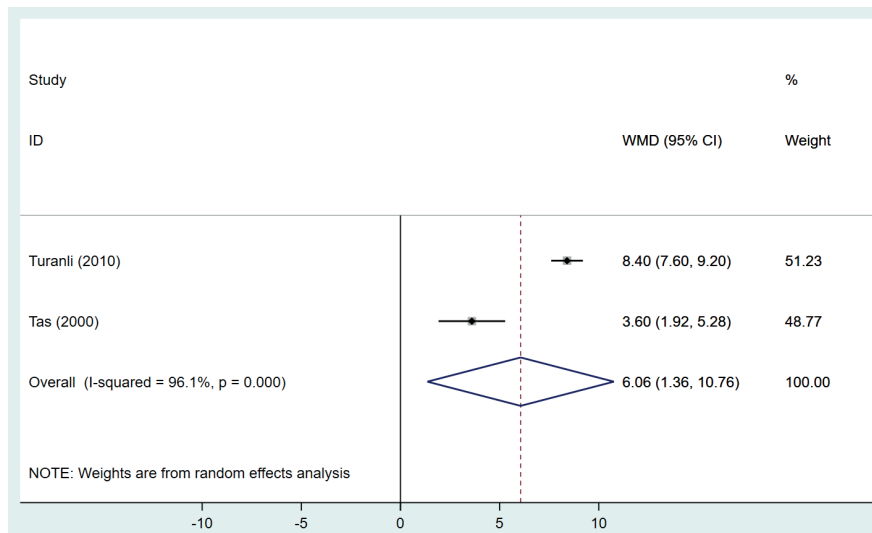
Fig. 7. Forest plot for OS time in gastrectomy vs non-resection

MGC – metastatic gastric cancer; OS – overall survival; WMD – weighted mean difference; 95% CI – 95% confidence interval.

indicating that publication bias did not exert a significant influence on the results for 2-year OS outcome, and the results were relatively robust.

Sensitivity analysis

The results of sensitivity analysis revealed that 1-study removal did not significantly impact the combined results, suggesting that the corresponding findings were stable and robust (Supplementary Table 7, Supplementary Fig. 2A–M).

Discussion

To date, surgical resection with curative intent has been the only treatment providing hope for cure,[68] but, for MGC, palliative chemotherapy with best supportive care is the best current standard,[4,69] and the role of surgical resection is still controversial. Hence, this study undertook a meta-analysis to quantitatively and synthetically analyze the survival effect of gastrectomy among MGC patients. Using 46 studies on 7,152 MGC patients, we revealed that gastrectomy, with or without metastasectomy, was beneficial to 1-, 2-, 3-, 4-, and 5-year OS and OS compared to no resection treatment. Moreover, patients undergoing gastrectomy may have longer OS time than those receiving no resection.

Lasithiotakis et al.[70] conducted a systematic review and meta-analysis to evaluate the impact of gastrectomy for patients with stage IV GC on 1- and 2-year OS, postoperative mortality and morbidity, palliation, and quality of life, though the meta-analysis was only done for 1-year OS. The above evaluation focused on GC patients in stage IV (any T, any N and metastatic (M1) gastric carcinoma), while our analysis paid attention to patients with MGC, including GC with distant metastasis, lymph node metastasis or both. The current study also assessed the role of gastrectomy in 3-year OS, 5-year OS, OS, OS time, postoperative

morbidity, perioperative mortality, and hospital stay, and subgroup analysis by stratification of metastatic sites further explored the effect of gastrectomy. Consequently, gastrectomy provided survival benefits for individuals with MGC, with greater 1-, 2-, 3-, and 5-year OS, better OS, and possibly longer OS time. This may be primarily due to the progress in technology and surgical equipment, advances in anesthesia and nutritional support, effective postoperative care, and timely resolution of medical problems.

As supported by the findings of Li et al.,[71] palliative gastrectomy was related to improved survival of MGC patients. Prominent survival benefits were achieved by non-curative gastrectomy for patients with MGC.[14] Consistently, primary tumor resection combined with chemotherapy was shown to bring better OS and 2-year OS than chemotherapy alone for MGC patients.[72] Fornaro et al.[73] put forward that gastrectomy was a predictor of prolonged OS in asymptomatic metastatic esophagogastric cancer. Thus, gastrectomy may be a promising treatment for improving OS in patients undergoing MGC. Furthermore, mortality risk in MGC patients was comparable following gastrectomy and non-resection treatment. Since MGC is a heterogeneous disease with specific complications and therapeutic outcomes at different metastatic sites, more studies are required to seek the most suitable strategies to treat patient subgroups with distinct metastatic sites.

Of note, the present study also revealed the survival advantage of gastrectomy plus metastasectomy compared with non-resection therapy. Similarly, a study applying the SEER database demonstrated that gastrectomy combined with metastasectomy had better OS than no surgery.[74] Choi et al.[75] reported a case of a 53-year-old man suffering from GC with synchronous bone metastasis and concluded that gastrectomy combined with metastasectomy might improve quality of life and OS. Berger et al.[76] and Choi et al.[77] believed in the OS benefit of this therapy. On this front, our revelations cast light on the therapeutic role of combined treatment of gastrectomy. As a multi-modality, gastrectomy

plus metastasectomy could be taken into consideration and have a favorable prognosis.

Nevertheless, some researchers have proposed contrasting results. Kokkola et al.[78] reported that non-curative gastrectomy did not enhance OS for MGC patients, and prophylactic, palliative gastrectomy was not required if no bleeding or obstruction occurred before surgery. A relatively poor prognosis was found after resection among patients with MGC noted before the resection.[16] The discrepancies may be attributed to different study designs, analysis methods, target populations, and sample sizes. Future well-designed studies can help verify our findings and advance clinical decisions in MGC treatment.

The strengths of this study were that it included 7,152 patients with MGC, including distant metastasis, lymph node metastasis or both, and quantitatively analyzed more outcomes, covering a broader range. Furthermore, sensitivity analysis showed most findings were robust and reliable.

Limitations

Some limitations should be considered in the interpretation of results. All studies were retrospective cohort in design, and more prospective studies and randomized controlled trials are needed for analysis. Metastatic gastric cancer grades and gastrectomy types were not analyzed in subgroups, and only articles in English were included.

This meta-analysis assessed the effects of gastrectomy compared to non-resection treatment on the OS of patients with MGC but did not involve comparisons between gastrectomy with different extents of resection or between a range of interventions (e.g., gastrectomy, metastasectomy and non-resection treatment), which can be investigated in future research. Additionally, sensitivity analysis was not conducted for the outcomes with only 2 studies, such as gastrectomy plus metastasectomy compared to non-resection for 2-year OS. The limited number of studies may affect the stability of these results. More studies are needed for validation.

Conclusions

This up-to-date meta-analysis suggests that gastrectomy, with or without metastasectomy, could provide MGC patients with survival benefits, and may be adopted to improve OS among the MGC population. Properly designed prospective research is required to validate our findings.

Supplementary data

The Supplementary materials are available at https://zenodo.org/uploads/10609032. The package includes the following files:

Supplementary Table 1. The search strategy for PubMed database.

Supplementary Table 2. The Preferred Reporting Items for Systematic Reviews and Meta-Analyses (PRISMA) checklist.

Supplementary Table 3. The baseline characteristics of the included studies.

Supplementary Table 4. The quality assessment of the included studies.

Supplementary Table 5. Meta-regression analysis on metastatic sites for 1-year OS in gastrectomy ± metastasectomy vs non-resection groups.

Supplementary Table 6. Meta-regression analysis on metastatic sites for OS in gastrectomy vs non-resection groups.

Supplementary Table 7. Sensitivity analysis for the outcomes with over two studies included.

Supplementary Fig. 1. Funnel plot for presenting result heterogeneity in different outcomes. 1A. 1-year OS in gastrectomy vs non-resection groups; 1B. 1-year OS in gastrectomy + metastasectomy vs. non-resection groups; 1C. 1-year OS in gastrectomy ± metastasectomy vs non-resection groups; 1D. 2-year OS in gastrectomy vs non-resection groups; 1E. 2-year OS in gastrectomy + metastasectomy vs. non-resection groups; 1F. 2-year OS in gastrectomy ± metastasectomy vs. non-resection groups; 1G. 3-year OS in gastrectomy vs non-resection groups; 1H. 3-year OS in gastrectomy + metastasectomy vs non-resection groups; 1I. 3-year OS in gastrectomy ± metastasectomy vs non-resection groups; 1J. 5-year OS in gastrectomy vs non-resection groups; 1K. 5-year OS in gastrectomy + metastasectomy vs non-resection groups; 1L. 5-year OS in gastrectomy ± metastasectomy vs non-resection groups; 1M. OS in gastrectomy vs non-resection groups; 1N. OS in gastrectomy + metastasectomy vs non-resection groups; 1O. OS in gastrectomy ± metastasectomy vs non-resection groups; 1P. OS time in gastrectomy vs non-resection groups.

Supplementary Fig. 2. Sensitivity analysis for the outcomes with over two studies included. 2A. 1-year OS in gastrectomy vs non-resection groups; 2B. 1-year OS in gastrectomy + metastasectomy vs non-resection groups; 2C. 1-year OS in gastrectomy ± metastasectomy vs non-resection groups; 2D. 2-year OS in gastrectomy vs non-resection groups; 2E. 2-year OS in gastrectomy ± metastasectomy vs non-resection groups; 2F. 3-year OS in gastrectomy vs non-resection groups; 2G. 3-year OS in gastrectomy + metastasectomy vs non-resection groups; 2H. 3-year OS in gastrectomy ± metastasectomy vs non-resection groups; 2I. 5-year OS in gastrectomy vs non-resection groups; 2J. 5-year OS in gastrectomy + metastasectomy vs non-resection groups; 2K. 5-year OS in gastrectomy ± metastasectomy vs non-resection groups; 2L. OS in gastrectomy vs non-resection groups; 2M. OS in gastrectomy + metastasectomy vs non-resection groups.

Supplementary File 1. The reference lists of the included studies for analysis.

Data availability

The datasets generated and/or analyzed during the current study are available from the corresponding author on reasonable request.

Consent for publication

Not applicable.

ORCID iDs

Lifan Chen https://orcid.org/0000-0002-2271-4448
Yu Chen https://orcid.org/0000-0002-2353-668X

References

1. Jaroenlapnopparat A, Bhatia K, Coban S. Inflammation and gastric cancer. *Diseases*. 2022;10(3):35. doi:10.3390/diseases10030035

2. Sung H, Ferlay J, Siegel RL, et al. Global Cancer Statistics 2020: GLOBOCAN estimates of incidence and mortality worldwide for 36 cancers in 185 countries. *CA Cancer J Clin*. 2021;71(3):209–249. doi:10.3322/caac.21660

3. Chidambaram S, Guiral DC, Markar SR. Novel multi-modal therapies and their prognostic potential in gastric cancer. *Cancers (Basel)*. 2023;15(12):3113. doi:10.3390/cancers15123113

4. Patel TH, Cecchini M. Targeted therapies in advanced gastric cancer. *Curr Treat Options Oncol*. 2020;21(9):70. doi:10.1007/s11864-020-00774-4

5. Ajani JA, D'Amico TA, Bentrem DJ, et al. Gastric Cancer, Version 2.2022, NCCN Clinical Practice Guidelines in Oncology. *J Natl Compr Canc Netw*. 2022;20(2):167–192. doi:10.6004/jnccn.2022.0008

6. Liang X, Zhu J, Li Y, et al. Treatment strategies for metastatic gastric cancer: Chemotherapy, palliative surgery or radiotherapy? *Future Oncol*. 2020;16(5):91–102. doi:10.2217/fon-2019-0495

7. Catenacci DVT, Chung HC, Shen L, et al. Safety and efficacy of HER2 blockade by trastuzumab-based chemotherapy-containing combination strategies in HER2+ gastroesophageal adenocarcinoma. *ESMO Open*. 2022;7(1):100360. doi:10.1016/j.esmoop.2021.100360

8. Smyth EC, Verheij M, Allum W, Cunningham D, Cervantes A, Arnold D. Gastric cancer: ESMO Clinical Practice Guidelines for diagnosis, treatment and follow-up. *Ann Oncol*. 2016;27:v38–v49. doi:10.1093/annonc/mdw350

9. Pellino A, Riello E, Nappo F, et al. Targeted therapies in metastatic gastric cancer: Current knowledge and future perspectives. *World J Gastroenterol*. 2019;25(38):5773–5788. doi:10.3748/wjg.v25.i38.5773

10. Janjigian YY, Kawazoe A, Yañez P, et al. The KEYNOTE-811 trial of dual PD-1 and HER2 blockade in HER2-positive gastric cancer. *Nature*. 2021;600(7890):727–730. doi:10.1038/s41586-021-04161-3

11. Ajani JA, Bentrem DJ, Besh S, et al. Gastric Cancer, Version 2.2013. *J Natl Compr Canc Netw*. 2013;11(5):531–546. doi:10.6004/jnccn.2013.0070

12. Japanese Gastric Cancer Association. Japanese Classification of Gastric Carcinoma: 2nd English Edition. *Gastric Cancer*. 1998;1(1):10–24. doi:10.1007/s101209800016

13. Dittmar Y, Rauchfuss F, Goetz M, et al. Non-curative gastric resection for patients with stage 4 gastric cancer: A single center experience and current review of literature. *Langenbecks Arch Surg*. 2012;397(5):745–753. doi:10.1007/s00423-012-0902-3

14. Kulig P, Sierzega M, Kowalczyk T, Kolodziejczyk P, Kulig J. Non-curative gastrectomy for metastatic gastric cancer: Rationale and long-term outcome in multicenter settings. *Eur J Surg Oncol*. 2012;38(6):490–496. doi:10.1016/j.ejso.2012.01.013

15. Fujitani K, Yang HK, Mizusawa J, et al. Gastrectomy plus chemotherapy versus chemotherapy alone for advanced gastric cancer with a single non-curable factor (REGATTA): A phase 3, randomised controlled trial. *Lancet Oncol*. 2016;17(3):309–318. doi:10.1016/S1470-2045(15)00553-7

16. Gold JS, Jaques DP, Bentrem DJ, et al. Outcome of patients with known metastatic gastric cancer undergoing resection with therapeutic intent. *Ann Surg Oncol*. 2007;14(2):365–372. doi:10.1245/s10434-006-9059-z

17. Ebinger SM, Warschkow R, Tarantino I, Schmied BM, Güller U, Schiesser M. Modest overall survival improvements from 1998 to 2009 in metastatic gastric cancer patients: A population-based SEER analysis. *Gastric Cancer*. 2016;19(3):723–734. doi:10.1007/s10120-015-0541-9

18. Stang A. Critical evaluation of the Newcastle–Ottawa scale for the assessment of the quality of nonrandomized studies in meta-analyses. *Eur J Epidemiol*. 2010;25(9):603–605. doi:10.1007/s10654-010-9491-z

19. Kicinski M, Springate DA, Kontopantelis E. Publication bias in meta-analyses from the Cochrane Database of Systematic Reviews. *Stat Med*. 2015;34(20):2781–2793. doi:10.1002/sim.6525

20. Sterne JAC, Sutton AJ, Ioannidis JPA, et al. Recommendations for examining and interpreting funnel plot asymmetry in meta-analyses of randomised controlled trials. *BMJ*. 2011;343:d4002. doi:10.1136/bmj.d4002

21. Duval S, Tweedie R. Trim and fill: A simple funnel-plot–based method of testing and adjusting for publication bias in meta-analysis. *Biometrics*. 2000;56(2):455–463. doi:10.1111/j.0006-341X.2000.00455.x

22. Arigami T, Matsushita D, Okubo K, et al. Indication and prognostic significance of conversion surgery in patients with liver metastasis from gastric cancer. *Oncology*. 2020;98(5):273–279. doi:10.1159/000505555

23. Arigami T, Matsushita D, Okubo K, et al. Clinical significance of conversion surgery for gastric cancer with peritoneal dissemination: A retrospective study. *Oncology*. 2020;98(11):798–806. doi:10.1159/000509530

24. Budisin NI, Majdevac IZ, Budisin ES, Manic D, Patrnogic A, Radovanovic Z. Surgery for patients with gastric cancer in the terminal stage of the illness: TNM stage IV. *J BUON*. 2009;14(4):593–603. PMID:20148448.

25. Canbay E, Canbay Torun B, Cosarcan K, et al. Surgery with hyperthermic intraperitoneal chemotherapy after response to induction chemotherapy in patients with peritoneal metastasis of gastric cancer. *J Gastrointest Oncol*. 2021;12(Suppl 1):S47–S56. doi:10.21037/jgo-20-121

26. Chang YR, Han DS, Kong SH, et al. The value of palliative gastrectomy in gastric cancer with distant metastasis. *Ann Surg Oncol*. 2012;19(4):1231–1239. doi:10.1245/s10434-011-2056-x

27. Chen S, Li Y, Feng X, Zhou Z, Yuan X, Chen Y. Significance of palliative gastrectomy for late-stage gastric cancer patients. *J Surg Oncol*. 2012;106(7):862–871. doi:10.1002/jso.23158

28. Dong Y, Ma S, Yang S, Luo F, Wang Z, Guo F. Non-curative surgery for patients with gastric cancer with local peritoneal metastasis: A retrospective cohort study. *Medicine (Baltimore)*. 2016;95(49):e5607. doi:10.1097/MD.0000000000005607

29. Fujisaki S, Tomita R, Nezu T, Kimizuka K, Park E, Fukuzawa M. Prognostic studies on gastric cancer with concomitant liver metastases. *Hepatogastroenterology*. 2001;48(39):892–894. PMID:11462950.

30. Geng X, Liu H, Lin T, et al. Survival benefit of gastrectomy for gastric cancer with peritoneal carcinomatosis: A propensity score-matched analysis. *Cancer Med*. 2016;5(10):2781–2791. doi:10.1002/cam4.877

31. Hsu JT, Liao JA, Chuang HC, et al. Palliative gastrectomy is beneficial in selected cases of metastatic gastric cancer. *BMC Palliat Care*. 2017;16(1):19. doi:10.1186/s12904-017-0192-1

32. Ikeguchi M, Miyatani K, Takaya S, et al. Role of surgery in the management for gastric cancer with synchronous distant metastases. *Indian J Surg Oncol*. 2016;7(1):32–36. doi:10.1007/s13193-015-0428-6

33. Jeong O, Jung MR, Kang JH. Treatment modality based survival in gastric carcinoma patients with stand-alone peritoneal metastasis: A case-control study. *J Gastric Cancer*. 2021;21(2):122. doi:10.5230/jgc.2021.21.e12

34. Kim KH, Lee KW, Baek SK, et al. Survival benefit of gastrectomy ± metastasectomy in patients with metastatic gastric cancer receiving chemotherapy. *Gastric Cancer*. 2011;14(2):130–138. doi:10.1007/s10120-011-0015-7

35. Kinoshita J, Fushida S, Tsukada T, et al. Efficacy of conversion gastrectomy following docetaxel, cisplatin, and S-1 therapy in potentially resectable stage IV gastric cancer. *Eur J Surg Oncol*. 2015;41(10):1354–1360. doi:10.1016/j.ejso.2015.04.021

36. Kunieda K, Saji S, Sugiyama Y, et al. Evaluation of treatment for synchronous hepatic metastases from gastric cancer with special reference to long-term survivors. *Surg Today*. 2002;32(7):587–593. doi:10.1007/s005950200106

37. Li C, Yan M, Chen J, et al. Survival benefit of non-curative gastrectomy for gastric cancer patients with synchronous distant metastasis. *J Gastrointest Surg*. 2010;14(2):282–288. doi:10.1007/s11605-009-1095-0

38. Li Z, Fan B, Shan F, et al. Gastrectomy in comprehensive treatment of advanced gastric cancer with synchronous liver metastasis: A prospectively comparative study. *World J Surg Onc*. 2015;13(1):212. doi:10.1186/s12957-015-0627-1

39. Lin SZ, Tong HF, You T, et al. Palliative gastrectomy and chemotherapy for stage IV gastric cancer. *J Cancer Res Clin Oncol*. 2007;134(2): 187–192. doi:10.1007/s00432-007-0268-z

40. Matsubara D, Konishi H, Kubota T, et al. Comparison of clinical outcomes of gastrojejunal bypass and gastrectomy in patients with metastatic gastric cancer. *Anticancer Res*. 2019;39(5):2545–2551. doi:10.21873/anticanres.13376

41. Miki Y, Fujitani K, Hirao M, et al. Significance of surgical treatment of liver metastases from gastric cancer. *Anticancer Res*. 2012;32(2): 665–670. PMID:22287760.

42. Miyagaki H, Fujitani K, Tsujinaka T, et al. The significance of gastrectomy in advanced gastric cancer patients with non-curative factors. *Anticancer Res*. 2008;28(4C):2379–2384. PMID:18751422.

43. Mohri Y, Tanaka K, Ohi M, et al. Identification of prognostic factors and surgical indications for metastatic gastric cancer. *BMC Cancer*. 2014;14(1):409. doi:10.1186/1471-2407-14-409

44. Nie RC, Chen S, Yuan SQ, et al. Significant role of palliative gastrectomy in selective gastric cancer patients with peritoneal dissemination: A propensity score matching analysis. *Ann Surg Oncol*. 2016; 23(12):3956–3963. doi:10.1245/s10434-016-5223-2

45. Park S, Kim J, Park J, et al. Value of nonpalliative resection as a therapeutic and pre-emptive operation for metastatic gastric cancer. *World J Surg*. 2009;33(2):303–311. doi:10.1007/s00268-008-9829-9

46. Rau B, Brandl A, Thuss-Patience P, et al. The efficacy of treatment options for patients with gastric cancer and peritoneal metastasis. *Gastric Cancer*. 2019;22(6):1226–1237. doi:10.1007/s10120-019-00969-1

47. Sahakyan MA, Gabrielyan A, Aghayan DL, et al. Gastrectomy for metastatic gastric cancer: A 15-year experience from a developing country. *Indian J Surg Oncol*. 2019;10(3):527–534. doi:10.1007/s13193-019-00943-4

48. Saidi RF, ReMine SG, Dudrick PS, Hanna NN. Is there a role for palliative gastrectomy in patients with stage IV gastric cancer? *World J Surg*. 2006;30(1):21–27. doi:10.1007/s00268-005-0129-3

49. Seo HS, Song KY, Jung YJ, et al. Radical gastrectomy after chemotherapy may prolong survival in stage IV gastric cancer: A Korean multi-institutional analysis. *World J Surg*. 2018;42(10):3286–3293. doi:10.1007/s00268-018-4635-5

50. Tan HL, Chia CS, Tan GHC, et al. Metastatic gastric cancer: Does the site of metastasis make a difference? *Asia Pac J Clin Oncol*. 2019;15(1): 10–17. doi:10.1111/ajco.13025

51. Tas F, Aykan NF, Aydiner A, et al. The roles of chemotherapy and surgery in gastric carcinoma and the influence of prognostic factors on survival. *Am J Clin Oncol*. 2000;23(1):53–57. doi:10.1097/00000421-200002000-00015

52. Tiberio GAM, Baiocchi GL, Morgagni P, et al. Gastric cancer and synchronous hepatic metastases: Is it possible to recognize candidates to R0 resection? *Ann Surg Oncol*. 2015;22(2):589–596. doi:10.1245/s10434-014-4018-6

53. Turanli S. The value of resection of primary tumor in gastric cancer patients with liver metastasis. *Indian J Surg*. 2010;72(3):200–205. doi:10.1007/s12262-010-0053-0

54. Wang W, Liang H, Zhang H, Wang X, Xue Q, Zhang R. Prognostic significance of radical surgical treatment for gastric cancer patients with synchronous liver metastases. *Med Oncol*. 2014;31(11):258. doi:10.1007/s12032-014-0258-3

55. White MG, Kothari A, Ikoma N, et al. Factors associated with resection and survival after laparoscopic HIPEC for peritoneal gastric cancer metastasis. *Ann Surg Oncol*. 2020;27(13):4963–4969. doi:10.1245/s10434-020-08842-7

56. Xia X, Li C, Yan M, Liu B, Yao X, Zhu Z. Who will benefit from noncurative resection in patients with gastric cancer with single peritoneal metastasis? *Am Surg*. 2014;80(2):124–130. doi:10.1177/000313481408000219

57. Yang K, Liu K, Zhang WH, et al. The value of palliative gastrectomy for gastric cancer patients with intraoperatively proven peritoneal seeding. *Medicine (Baltimore)*. 2015;94(27):e1051. doi:10.1097/MD.0000000000001051

58. Yarema R, Ohorchak M, Hyrya P, et al. Gastric cancer with peritoneal metastases: Efficiency of standard treatment methods. *World J Gastrointest Oncol*. 2020;12(5):569–581. doi:10.4251/wjgo.v12.i5.569

59. Yoshikawa T, Kanari M, Tsuburaya A, et al. Should gastric cancer with peritoneal metastasis be treated surgically? *Hepatogastroenterology*. 2003;50(53):1712–1715. PMID:14571824.

60. Yu P, Zhang Y, Ye Z, et al. Treatment of synchronous liver metastases from gastric cancer: A single-center study. *Cancer Manag Res*. 2020;12:7905–7911. doi:10.2147/CMAR.S261353

61. Yuan SQ, Nie RC, Chen S, et al. Selective gastric cancer patients with peritoneal seeding benefit from gastrectomy after palliative chemotherapy: A propensity score matching analysis. *J Cancer*. 2017; 8(12):2231–2237. doi:10.7150/jca.18932

62. Zheng XH, Zhang W, Yang L, et al. Role of D2 gastrectomy in gastric cancer with clinical para-aortic lymph node metastasis. *World J Gastroenterol*. 2019;25(19):2338–2353. doi:10.3748/wjg.v25.i19.2338

63. Gou M, Qian N, Zhang Y, et al. Construction of a nomogram to predict the survival of metastatic gastric cancer patients that received immunotherapy. *Front Immunol*. 2022;13:950868. doi:10.3389/fimmu.2022.950868

64. Kobayashi H, Honda M, Kawamura H, et al. Clinical impact of gastrectomy for gastric cancer patients with positive lavage cytology without gross peritoneal dissemination. *J Surg Oncol*. 2022;125(4): 615–620. doi:10.1002/jso.26770

65. Cui Y, Yu Y, Zheng S, et al. Does resection after neoadjuvant chemotherapy of docetaxel, oxaliplatin, and S-1 (DOS regimen) benefit for gastric cancer patients with single non-curable factor? A multicenter, prospective cohort study (Neo-REGATTA). *BMC Cancer*. 2023; 23(1):308. doi:10.1186/s12885-023-10773-x

66. Fang J, Huang X, Chen X, et al. Efficacy of chemotherapy combined with surgical resection for gastric cancer with synchronous ovarian metastasis: A propensity score matching analysis. *Cancer Med*. 2023;12(16):17126–17138. doi:10.1002/cam4.6362

67. Hara K, Cho H, Onodera A, et al. Long-term treatment outcomes in gastric cancer with oligometastasis. *Ann Gastroenterol Surg*. 2024; 8(1):60–70. doi:10.1002/ags3.12733

68. Santoro R. Subtotal gastrectomy for gastric cancer. *World J Gastroenterol*. 2014;20(38):13667. doi:10.3748/wjg.v20.i38.13667

69. Choi JH, Choi YW, Kang SY, et al. Combination versus single-agent as palliative chemotherapy for gastric cancer. *BMC Cancer*. 2020; 20(1):167. doi:10.1186/s12885-020-6666-1

70. Lasithiotakis K, Antoniou SA, Antoniou GA, Kaklamanos I, Zoras O. Gastrectomy for stage IV gastric cancer: A systematic review and meta-analysis. *Anticancer Res*. 2014;34(5):2079–2085. PMID:24778009.

71. Li Q, Zou J, Jia M, et al. Palliative gastrectomy and survival in patients with metastatic gastric cancer: A propensity score-matched analysis of a large population-based study. *Clin Transl Gastroenterol*. 2019; 10(5):e00048. doi:10.14309/ctg.0000000000000048

72. Warschkow R, Baechtold M, Leung K, et al. Selective survival advantage associated with primary tumor resection for metastatic gastric cancer in a Western population. *Gastric Cancer*. 2018;21(2):324–337. doi:10.1007/s10120-017-0742-5

73. Fornaro L, Fanotto V, Musettini G, et al. Selecting patients for gastrectomy in metastatic esophago-gastric cancer: Clinics and pathology are not enough. *Future Oncol*. 2017;13(25):2265–2275. doi:10.2217/fon-2017-0246

74. Yang LP, Wang ZX, He MM, et al. The survival benefit of palliative gastrectomy and/or metastasectomy in gastric cancer patients with synchronous metastasis: A population-based study using propensity score matching and coarsened exact matching. *J Cancer*. 2019; 10(3):602–610. doi:10.7150/jca.28842

75. Choi YJ, Kim DH, Han HS, et al. Long-term survival after gastrectomy and metastasectomy for gastric cancer with synchronous bone metastasis. *World J Gastroenterol*. 2018;24(1):150–156. doi:10.3748/wjg.v24.i1.150

76. Berger Y, Giurcanu M, Vining CC, et al. Cytoreductive surgery for selected patients whose metastatic gastric cancer was treated with systemic chemotherapy. *Ann Surg Oncol*. 2021;28(8):4433–4443. doi:10.1245/s10434-020-09475-6

77. Choi YW, Ahn MS, Jeong GS, et al. The role of surgical resection before palliative chemotherapy in advanced gastric cancer. *Sci Rep*. 2019; 9(1):4136. doi:10.1038/s41598-019-39432-7

78. Kokkola A, Louhimo J, Puolakkainen P. Does non-curative gastrectomy improve survival in patients with metastatic gastric cancer? *J Surg Oncol*. 2012;106(2):193–196. doi:10.1002/jso.23066

Polycythemia vera and essential thrombocythemia of intermediate-age: A real-life, multicenter analysis of first-line treatment approach

Patryk Sobieralski[1,A–D], Maria Bieniaszewska[1,A,C,E,F], Łukasz Bołkun[2,B,E,F], Tomasz Sacha[3,B,E,F], Magdalena Muzalewska-Wolska[4,B,E,F], Wojciech Homenda [4,B,E,F], Łucja K. Bartkowiak[5,B,E,F], Justyna Smith[5,B,E,F], Marcin Rymko[5,B,E,F], Anna Jachalska[6,B,E,F], Andrzej R. Mital[1,B,E,F], Witold Prejzner[1,B,E,F], Jan Zaucha[1,B,E,F]

[1] Department of Hematology and Transplantology, Medical University of Gdańsk, Poland

[2] Department of Hematology, Medical University of Bialystok, Poland

[3] Department of Hematology, Jagiellonian University Hospital, Cracow, Poland

[4] Department of Hematology and Bone Marrow Transplantation, Pomeranian University, Słupsk, Poland

[5] Department of Hematology and Bone Marrow Transplantation, Copernicus Hospital, Toruń, Poland

[6] Department of Hematology, Collegium Medicum in Bydgoszcz, Nicolaus Copernicus University in Toruń, Bydgoszcz, Poland

A – research concept and design; B – collection and/or assembly of data; C – data analysis and interpretation;
D – writing the article; E – critical revision of the article; F – final approval of the article

Abstract

Background. The treatment of patients with polycythemia vera (PV) and essential thrombocythemia (ET) is conducted according to well-defined risk stratification systems. We hypothesized that adherence to the guidelines, namely the decision to refrain from introducing cytoreduction in non-high-risk patients, is particularly difficult in patients diagnosed when they are between 40 and 59 years of age (intermediate-age group).

Objectives. To evaluate the group of intermediate-age PV and ET patients, focusing on a first-line treatment approach adapted at diagnosis.

Materials and methods. The study group consisted of 308 PV and ET patients recruited from 6 Polish Adult Leukemia Group (PALG) Centers. Patients were analyzed with respect to disease phenotype, risk group, treatment approach, cardiovascular (CV) risk factors, and occurrence of bleeding or thrombosis.

Results. Overall, 74% of patients in the study group were started on cytoreduction at diagnosis, including 70% of the low-risk PV patients and 85–89% of the non-high-risk ET patients. Factors influencing the decision to start the treatment included higher hemoglobin (Hb) concentration (in PV) as well as higher platelet (PLT) count, and the presence of CV risk factors (in ET). Introducing cytoreduction at diagnosis had no impact on thrombotic events. Patients harboring CV risk factors experienced a higher incidence of complications both at diagnosis and follow-up, independently of the treatment strategy.

Conclusions. We underline the low adherence to recommendations in the treatment of intermediate-age PV and ET patients. Moreover, we emphasize the importance of CV risk factors and stress their impact on disease phenotype in this patient population.

Key words: cardiovascular risk, essential thrombocythemia, cytoreduction, polycythemia vera

Background

Polycythemia vera (PV) and essential thrombocythemia (ET) are myeloproliferative neoplasms (MPN) in which the treatment is aimed at preventing disease-specific complications and reducing the risk of progression. During the course of the disease, with respect to the general population, patients with PV and ET are exposed to an increased rate of thrombotic and bleeding events, and, as a consequence, the treatment recommendations are designed to help mitigate the risk of those complications.[1,2] Additionally, a small proportion of patients will manifest progressive disease and experience the transformation of phenotype to secondary myelofibrosis or acute leukemia, which directly translates into a dismal prognosis.[3,4] To date, numerous treatment approaches have become available for patients with PV and ET, and these range from observation only, through phlebotomy and antiplatelet therapy, to a variety of cytoreductive agents. Before establishing the treatment plan in newly diagnosed patients, several factors, including age, cardiovascular (CV) risk, history of thrombosis, and mutational profile, must be considered in order to attribute patients to the specific risk group. Nevertheless, the greatest dilemma concerns the time at which cytoreduction should be started. There are well-defined guidelines supporting the decision to start cytoreductive treatment (CTR) in ET or PV patients above 60 years of age.[1] However, in patients below 40 years of age, cytoreduction is performed more rigorously due to the expected marginal risk of thrombosis along with the possible long-term consequences associated with prolonged exposure to cytoreductive agents, including, but not limited to, secondary neoplasms.[5] However, considering both the literature as well as their own observations, physicians often struggle with the decision regarding the most appropriate treatment strategy in patients aged 40–59 years, i.e., the intermediate-age group. Patients from the intermediate-age group are still considered low-risk if they had no prior thrombotic event. On the other hand, data from population-based studies suggest an accumulation of CV risk factors in this patient population, along with an impact on overall survival (OS), which may stimulate the decision to introduce cytoreduction.[6] It remains unclear whether the earlier introduction of cytoreductive therapy in the intermediate-age group results in a lower rate of complications, slower disease progression and better OS.

Objectives

In the current study, we aim to analyze the intermediate-age patients diagnosed with PV or ET and demonstrate real-life based observations regarding adherence to the guidelines and treatment approaches adapted at diagnosis.

Materials and methods

Data source

This retrospective study was performed on behalf of the Polish Adult Leukemia Group (PALG). Six PALG Centers in Poland were invited to participate in the study. Study participants were selected on the basis of a study-specific data questionnaire received from the participating Centers.

Study population and variables of interest

Adult patients diagnosed with PV or ET between 2000 and 2022, in whom the diagnosis was established between 40 and 59 years of age, were identified as potential candidates for inclusion in the study group. Only patients alive at the study time, with available full clinical data regarding investigated variables and meeting the myeloproliferative neoplasms (MPN) World Health Organization (WHO) 2016 criteria for PV or ET, apart from triple-negative ET patients (n = 20), were considered.[7]

The study focused on the treatment approach used at diagnosis, specifically whether the patient underwent cytoreduction or not. Additional variables included demographic data, laboratory values at diagnosis, molecular profile, presence of CV risk factors, and thrombotic complications recorded at diagnosis or follow-up. Extreme thrombocytosis was defined as platelet (PLT) count >1000 G/L (ExT1000) or >1500 G/L (ExT1500). The molecular profile was established by screening for the presence of *JAK2V617F*, *JAK2* exon 12, *CALR*, and *MPL* mutations.[8–10] Patients in whom none of those mutations had been detected were labeled as *JAK2*-negative or triple negative (TN) for PV and ET patients, respectively. Cardiovascular risk factors included arterial hypertension, hypercholesterolemia, diabetes mellitus, obesity, and smoking. Thrombotic events included myocardial infarction (MI), ischemic stroke (IS), deep vein thrombosis (DVT), splanchnic vein thrombosis (SVT), central nervous system (CNS), and arterial thrombosis (AT).

Risk group

The collected data were used to assign patients to the risk groups in accordance with current European Leukemia Network (ELN) recommendations: PV patients were evaluated with a conventional prognostic system, whereas ET patients with the use of the IPSET-thrombosis (IPSET-T) system and the revised IPSET-thrombosis (rIPSET-T) criteria proposed by Barbui et al. in 2015.[1,11,12] The collected data were used to characterize the study population and to further characterize patients with and without cytoreduction.

Statistical analyses

Statistical analysis was performed to screen for significant differences between groups. Calculations were done

using Statistica v. 13.3 (StatSoft, Tulsa, USA). Data were statistically described in terms of median and range. Since none of the analyzed variables showed normal distribution, a comparison between the 2 groups was performed using the Mann–Whitney U (MWU) test for continuous variables and the χ^2 test for categorical variables.

Univariable and multivariable logistic regression models were built to test associations between the introduction of CTR and independent variables of interest for PV and ET group separately. Collected data were analyzed to search for factors possibly influencing the decision to introduce CTR. Sex, presence of CV risk factors, ExT1000, mutational status, and presence of thrombosis (as qualitative variables) followed by age, hemoglobin (Hb) concentration, PLT, and white blood cells (WBC) count (as qualitative variables) were considered for the inclusion in the model. Given that we revealed that CTR is introduced independently of the risk group, variables used to calculate the risk – presence of thrombosis and mutational status – were not included in the model. Moreover, since all PV patients with ExT1000 were started with cytoreduction, ExT1000 was not used in the PV group. In summary, sex, presence of CV, ExT1000, age, Hb concentration, PLT, and WBC count were retained in the model. Only variables showing statistical significance in univariable analysis were analyzed in multivariable analysis. Linear relationships of dependent variables with quantitative variables included in the regression model were checked. P-values in the likelihood ratio test were >0.05 for all quantitative variables (Hb in PV and PLT in ET). Multicollinearity was statistically significant for WBC and PLT count in the ET group (p < 0.05) and Hb and WBC count in the PV group (p < 0.05). Only PLT count in the ET group was retained in the multivariable regression model. Since Hb concentration was the only variable showing statistical significance in the PV group, no multivariable model was created. In ET, the multivariable regression model was built using a backward stepwise approach with cross-validation. The analysis ended at the 4th step. Out of 3 previously statistically significant variables, PLT count has been eliminated from the model, with only CV and ExT1000 being retained as independent variables. Pseudo R^2 for each logistic regression model and multivariable model was calculated using the Cox–Snell formula. P-values were considered significant when p < 0.05.

Results

The final study group consisted of 308 representative patients diagnosed with PV or ET in the intermediate-age bracket. The median time from the diagnosis to this analysis was 11 years (range 0–22 years).

Cytoreductive treatment was introduced at diagnosis in 227 (74%) patients (Table 1). The most frequently used cytoreductive agent was hydroxyurea (HU) (n = 211), followed by anagrelide (n = 8) and busulfan (n = 8). No patients

received interferon as the first-line therapy. The high-risk group constituted of 24 (20.2%) PV patients and 71 (37.6%) and 37 (19.6%) ET patients when IPSET-T and rIPSET-T were used, respectively (Table 2). In PV, all patients from the high-risk group, along with 67 (70%) patients from the low-risk group, received cytoreduction at diagnosis. In ET, cytoreduction was started in 60 (85%) and 33 (89%)

Table 1. General characteristics of the study group

Diagnosis	PV	ET
n	119	189
Age, median (range) [years]	52 (40–59)	52 (40–59)
Sex, F/M	56/63	125/64
Parameters at diagnosis, median (range)		
Hb [g/dL]	17.8 (14.8–23.1)	14 (10.6–16.4)
Hct [%]	53.7 (45.9–72.0)	42 (28.6–48.5)
PLT [G/L]	421 (130–1630)	835 (455–2638)
WBC [G/L]	9.6 (4.92–21.12)	8.6 (3.0–25.9)
LDH [U/L]	230 (134–426)	219 (59–651)
EPO [mU/mL]	2.2 (0.6–40)	6.8 (1–120)
Mutational status, n (%)		
JAK2V617F	97 (81.6)	119 (63)
CALR	N/A	33 (17.4)
MPL	N/A	6 (3.2)
TN	N/A	20 (10.6)
Ex12	0 (0)	N/A
JAK2-negative	22 (18.4)	11 (5.8)
ExT1000 (%)	5 (4.2)	62 (32.8)
ExT1500 (%)	1 (0.8)	9 (4.8)
Hb >20 g/dL (%)	23 (19.3)	0
Hct >55% (%)	47 (40)	0
WBC >15 G/L (%)	12 (10)	5 (2.6)
CV risk factors (%)	63 (52.9)	97 (51.3)
Treatment		
Cytoreduction (%)	91 (76.5)	136 (72)
Phlebotomy (%)	60 (50.4)	N/A
Antiplatelet/anticoagulant (%)	85 (71.4)	159 (84.1)
Complications at diagnosis, n (%)	24 (20.2)	37 (19.6)
MI	5 (4.2)	9 (4.8)
IS	12 (10)	9 (4.8)
DVT	6 (5)	13 (6.9)
SVT	1 (1)	1 (0.5)
CNS	0	3 (1.6)
AT	0	1 (0.5)
Complications at follow-up, n (%)	10 (8.5)	22 (11.6)
MI	1 (0.8)	6 (3.2)
IS	7 (5.9)	4 (2.1)
DVT	1 (0.8)	6 (3.2)
SVT	0	3 (1.6)
CNS	1 (0.8)	0
AT	0	1 (0.5)

n – number; F – female; M – male; CV – cardiovascular risk; ExT1000 – PLT>1000 G/L; ExT1500 – PLT>1500 G/L; MI – myocardial infarction; IS – ischemic stroke; DVT – deep vein thrombosis; SVT – splanchnic vein thrombosis; CNS – central nervous system thrombosis; AT – arterial thrombosis; PV – polycythemia vera; ET – essential thrombocythemia; Hb – hemoglobin; Hct – hematocrit; PLT – platelet count; WBC – white blood cell count; LDH – lactate dehydrogenase; EPO – erythropoietin. Extreme thrombocytosis was defined as platelet (PLT) count >1000 G/L (ExT1000) or >1500 G/L (ExT1500).

Table 2. Risk stratification of the study group

Risk	Very low	Low	Intermediate	High
PV	N/A	95 (79.8)	N/A	24 (20.2)
ET (IPSET-T)	N/A	64 (33.8)	54 (28.6)	71 (37.6)
JAK2V617F	N/A	0	51 (42.9)	68 (57.1)
CALR	N/A	30 (91)	2 (6)	1 (3)
ET (IPSET-T revised)	60 (31.7)	92 (48.7)	0	37 (19.6)
JAK2V617F	0	88 (74)	0	31 (26)
CALR	30 (91)	0	0	3 (9)

PV – polycythemia vera; ET – essential thrombocythemia.

Table 3. Results of logistic regression model identifying variables contributing to the introduction of CTR in the study group

Covariate		Univariable analysis				Multivariable analysis			
		OR	95% CI	p-value	pseudo R^2	OR	95% CI	p-value	pseudo R^2
PV	age	1.041	0.97–1.12	0.2645	0.010	–	–	–	–
	female sex	1.017	0.67–1.55	0.9391	0.000	–	–	–	–
	presence of CV	1.186	0.78–1.81	0.4308	0.005	–	–	–	–
	Hb	1.438	1.07–1.92	0.0146	0.058	–	–	–	–
	PLT	1.001	0.99–1.00	0.1599	0.019	–	–	–	–
	WBC	1.133	0.99–1.30	0.0779	0.030	–	–	–	–
ET	age	1.028	0.98–1.08	0.3138	0.005	–	–	–	
	male sex	1.846	0.90–3.78	0.0931	0.016	–	–	–	
	presence of CV	3.406	1.73–6.72	0.0004	0.069	5.025	2.38–10.63	<0.0001	
	Hb	0.891	0.68–1.18	0.4172	0.003	–	–	–	0.25
	PLT	1.004	1.00–1.00	<0.0001	0.133	–	–	–	
	WBC	1.089	0.97–1.22	0.1485	0.012	–	–	–	
	ExT1000	12.771	3.78–42.97	<0.0001	0.147	18.001	5.14–63.06	<0.0001	

PV – polycythemia vera; ET – essential thrombocythemia; CV – cardiovascular risk; OR – odds ratio; 95% CI – 95% confidence interval; Hb – hemoglobin; PLT – platelet count; WBC – white blood cell count; CRT – cytoreductive treatment. Extreme thrombocytosis was defined as platelet (PLT) count >1000 G/L (ExT1000) or >1500 G/L (ExT1500).

high-risk patients but also in 76 (64%) and 103 (68%) patients from the non-high-risk group according to IPSET-T or rIPSET-T, respectively (Fig. 1).

Covariables with possible influence on the tendency to start cytoreduction were investigated in the logistic regression model created independently for the PV and ET groups. In the univariable analysis, only a higher Hb concentration was identified as a factor contributing to the introduction of CTR in PV patients (p = 0.015). For ET patients, the presence of CV risk factors (p = 0.001), ExT1000 (p < 0.001) and higher PLT count (p < 0.001) were identified as factors contributing to the introduction of CTR. In the multivariable analysis, ExT1000 and CV risk retained their significance. The results of this analysis are presented in Table 3.

To further investigate patients who were started with cytoreduction, despite being in the non-high-risk group, an additional comparative analysis, employing the variables indicated in the regression model, was performed in the non-high-risk patients only. Here, low-risk PV patients who started with CTR had a higher Hb concentration with respect to patients without cytoreduction

(median 18.2 g/dL compared to 17.5 g/dL; p = 0.027; MWU; U = 667). Non-high-risk ET patients receiving cytoreduction had a higher PLT count (median 980 G/L compared to 720 G/L; p < 0.001; MWU; U = 1178.5) and more frequently had ExT1000 (47.6% compared to 6%; p < 0.001; χ^2) or CV risk factors (49.5% compared to 26.5%; p = 0.007; χ^2) than patients not started with CTR. Those findings further underline that the decision to start cytoreduction was independent of the risk group.

Subsequently, patients with and without thrombotic complications at follow-up were compared regarding the variables identified as contributing to introducing cytoreduction in order to examine whether starting the treatment early translates to outcomes. The incidence of thrombosis at follow-up was 6/91 (7%) and 18/136 (13%) in patients with cytoreduction and 4/28 (14%) and 4/53 (8%) in patients without cytoreduction in the PV (p = 0.372; χ^2) and ET (p = 0.399; χ^2) groups, respectively. There were no differences in the baseline median PLT count (872 G/L compared to 828 G/L; p = 0.270; MWU; U = 1570.5 for ET and 581 G/L compared to 414 G/L; p = 0.294; MWU; U = 435 for PV) and median Hb concentration (14.2 g/dL compared to 14.0 g/dL,
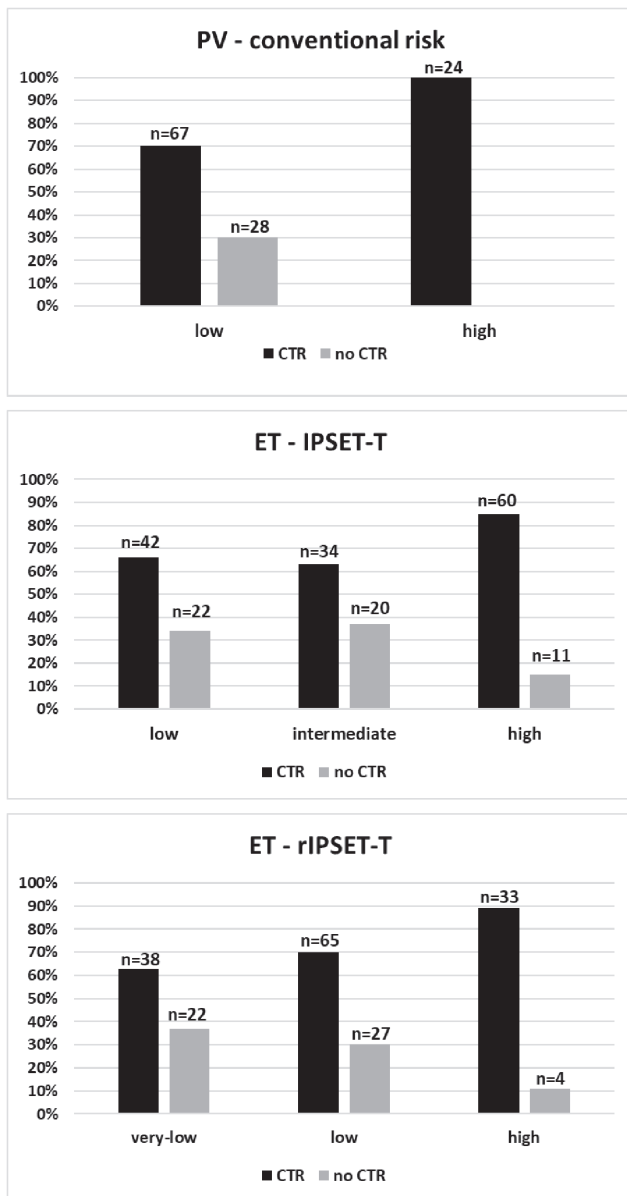
Fig. 1. The number of patients who received CTR among the risk groups

PV – polycythemia vera; ET – essential thrombocythemia;
CTR – cytoreductive treatment.

p = 0.932, MWU; U = 1816 for ET and 17.9 g/dL compared to 17.8 g/dL; p = 0.807; MWU; U = 519 for PV) in patients experiencing thrombosis as compared to patients without complications, respectively. Similarly, the distribution of CV risk factors was comparable among patients with (12/22; 54%) and without (85/167; 51%) thrombosis in the ET group (p = 0.748; χ^2). In the PV group, CV risk factors were present in 10/10 (100%) patients who developed complications and only in 53/109 (48%) patients without complications (p = 0.005; χ^2). However, those findings must be considered with caution given that the study group did not compriseconsecutive patients and only the data regarding the first-line therapy were collected.

As an exploratory objective, we investigated the relationship between the presence of CV risk (evaluated at diagnosis) and the incidence of thrombosis (at diagnosis). In PV, 20/24 (83%) patients who had experienced complications at diagnosis had already harbored CV risk factors, compared to only 43/95 (45%) patients without complications at diagnosis (p = 0.002; χ^2). Similarly, in ET, 33/37 (89%) patients who had experienced complications at diagnosis had had CV risk factors, compared to 64/152 (42%) patients without complications at diagnosis (p < 0.001; χ^2).

Discussion

In this study we performed a retrospective evaluation of the real-world trends in the treatment of 308 Polish patients diagnosed with ET and PV in the age range of 40–59 years (intermediate-age group). The study revealed a higher-than-expected willingness to adopt the approach of introducing cytoreductive therapy at diagnosis in the evaluated patients. According to the Philadelphia-negative MPN management recommendations provided by the ELN, patients with PV should be stratified into risk groups depending on age and presence of prior thrombosis, whereas risk stratification in patients diagnosed with ET should be based on the IPSET-T or rIPSET-T system.[1,11–14] Recently, novel stratification systems incorporating genomic data were developed for PV and ET (MIPSS-PV and MIPSS-ET) to better assess the risk of progression to AML or MF.[15] While it is indisputable that, in the future, every patient should be evaluated from a cytogenetic and molecular standpoint, those assessments are inaccessible in everyday clinical practice in the majority of centers worldwide. Nevertheless, regardless of the diagnosis and stratification system, cytoreduction is recommended only for high-risk patients. In the analyzed population, the majority of patients were assigned to the non-high-risk group and nevertheless started with cytoreduction at diagnosis. These findings raise a question about the adherence to and usefulness of the aforementioned recommendations. When physicians easily recognized high-risk patients, refraining from starting treatment in the non-high-risk group appeared to be a challenge and trends of overtreatment could also be found among other studies. In a study evaluating a young ET group (age 18–39 years), among 192 patients (12% in the high-risk group), as many as 107 (55%) received CTR.[16] Similar results were obtained from the analysis of an entire population of young low-risk ET patients (age 18–59 years), where cytoreduction was started in 170 (51%) of patients.[17] In a recent real-world study focused on young patients with a diagnosis of MPN, a total of 444 patients (median age of diagnosis 20.4 years, range 2–25 years) from multiple European centers were evaluated.[18] During a median follow-up of 9.7 years, cytoreduction was introduced in 301 (67.8%) of evaluated patients. However, the authors underline that only 21.4% of patients were strictly eligible to receive cytoreduction according to guidelines. In light of this, it is important

to determine what, if not the recommendations, is a driving factor for introducing CTR in our intermediate-age group. Through the construction of a logistic regression model, we revealed that a higher Hb concentration in PV and the presence of CV risk factors and ExT1000 in ET patients were variables contributing to the introduction of CTR. The confirmation of those findings was limited to the non-high-risk group. The results suggest that extreme laboratory values and comorbidities may be perceived as indicators for initiating therapy.

In regard to PV, the decision to introduce cytoreduction may be more understandable than in ET. Even young patients with PV are exposed to a higher risk of thromboembolic complications with respect to ET.[19] Additionally, a recent publication showed that the cumulation of CV risk factors in PV patients, independent of age, has a negative impact on OS.[20] Treatment recommendations underline that all patients with PV, regardless of age, should receive phlebotomy to reduce hematocrit (Hct) below 45%, based on the results of the CYTO-PV trial.[21] However, the risk of symptomatic iron deficiency and logistic problems in real-life settings encourages the physician to introduce cytoreduction, even in low-risk patients, as a more reliable approach to managing Hct and minimizing the possibility of complications. Therapeutic dilemma in low-risk PV is debated.[22,23] On the other hand, the justification for introducing cytoreduction in ET patients is not as understandable. Findings similar to those presented in this study have been observed for young patients with ET, with 1 study highlighting that cytoreduction is given willingly in patients with ExT1000, despite a comparable distribution of CV risk factors and lower incidence of AT.[16]

Recently, Abu-Zeinah et al. presented a database analysis of 40,333 MPN patients followed between 2001–2017. The authors confirmed higher mortality in young PV and ET patients in comparison to the healthy population of the same age. Furthermore, the study revealed a significantly higher excess of all-cause mortality in young (<60 years of age) MPN patients with respect to the older (≥60 years of age) population of MPN patients.[24] The authors indicate that this excess mortality may be the result of undertreatment within the group of young and potentially low-risk patients with MPNs. However, those observations are based on a database analysis that does not include the data regarding treatment, with the assumption that patients are treated strictly according to the guidelines. If findings from our study could be extrapolated to worldwide practice, and similar trends shown in numerous studies suggest that they could, this higher excess mortality may not be a result of undertreatment but rather overtreatment or improper treatment. In both our study groups and in the literature, HU is the most frequently used cytoreductive agent.[16,17,20] There is an abundance of warnings regarding the use of HU in younger patients, resulting mainly from uncertainty concerning its leukemogenicity and the possibility of the development of a second malignancy.[5,25] This threat

was further acknowledged by Abu-Zeinah et al. in their study of excess mortality, where the authors reported an unacceptably high degree of cancer death in young patients with MPNs.[24] Nonetheless, each patient should be evaluated individually, and if the physician qualifies for cytoreduction, the use of different agents needs to be considered. Anagrelide is a potent cytoreductive agent available as a second-line treatment for patients with ET.[26] However, reports of inducing bone marrow fibrosis should be taken into consideration.[27] Alternatively, ruxolitinib is an attractive therapeutic option for symptomatic patients with PV. However, its use is limited to patients with confirmed refractoriness to HU.[28,29] Finally, peg-IFN and ropeg-IFN represent the best alternatives for PV and ET patients, allowing them to limit the hazards of extended cytoreduction, avoid exposure to iron deficiency, achieve molecular remissions, and possibly prolong OS.[30–36] Nevertheless, due to limited accessibility, none of our patients were treated with the use of this agent as the first-line therapy.

We revealed that the occurrence of thrombotic complications was independent of introducing CTR, Hb concentration and PLT count at diagnosis in both the ET and PV groups. These findings suggest that the rationale for an early start of cytoreduction, based on extreme laboratory values, might not modify the disease course. On the other hand, the study conducted on the European general population highlighted that, starting from the age of 40, there is an increasing impact of CV risk factors on survival.[6] In our study group, patients with CV risk factors constituted 52% of the study population. When compared to young ET patients, where only 26% harbored CV risk, it is apparent that CV burden increases exponentially within intermediate-age group.[16] An exploratory finding from our study showed that almost all patients who had experienced complications at diagnosis presented CV risk factors (83% of PV and 89% of ET patients), while all PV patients who developed complications post diagnosis also harbored CV risk factors at diagnosis. In the aforementioned study by Abu-Zeinah et al., excess mortality from CV events was significantly higher only in PV patients.[24] Considering those observations, the importance of evaluating CV risk should be emphasized and may indicate treatment introduction in the intermediate-age group.

Limitations

The study's main limitation is its retrospective nature. However, it was conducted in a multicenter setting and included a relatively large patient population. The study focuses on the data regarding the first-line treatment approach and does not evaluate follow-up treatment.

The study group consists of patients who were alive at the time the study was conducted, hence does not include patients who were deceased as a result of thrombosis, bleeding or disease evolution. This exclusion does not affect the study's findings.

Conclusions

In this study, we revealed that cytoreduction is used in excess when confronted with the guidelines in intermediate-age patients diagnosed with ET and PV. Based on our findings, it remains to be seen whether starting cytoreduction in young patients is reasonable, given that it does not translate into a reduced incidence of disease-specific complications. Patients with ET and PV, regardless of age, are a heterogenous group. Therefore, multiple factors, possibly yet undiscovered, contribute to disease phenotype. Moreover, we underlined that the presence of CV risk factors also plays a significant role in patients below 60 years of age, emphasizing the idea of pursuing individualized treatment approaches.

Data availability

The datasets generated and/or analyzed during the current study are available from the corresponding author on reasonable request.

Consent for publication

Not applicable.

ORCID iDs

Patryk Sobieralski https://orcid.org/0000-0001-9112-5017
Maria Bieniaszewska https://orcid.org/0000-0002-5704-0244
Tomasz Sacha https://orcid.org/0000-0002-7207-6595
Wojciech Homenda https://orcid.org/0000-0002-4721-0916
Łucja K. Bartkowiak https://orcid.org/0000-0001-6828-815X
Marcin Rymko https://orcid.org/0000-0002-6830-0240
Anna Jachalska https://orcid.org/0000-0002-4389-1152
Andrzej R. Mital https://orcid.org/0000-0003-0854-3096
Witold Prejzner https://orcid.org/0000-0002-4537-2372
Jan Zaucha https://orcid.org/0000-0002-0986-8936

References

1. Barbui T, Tefferi A, Vannucchi AM, et al. Philadelphia chromosome-negative classical myeloproliferative neoplasms: Revised management recommendations from European LeukemiaNet. *Leukemia*. 2018;32(5):1057–1069. doi:10.1038/s41375-018-0077-1
2. Tefferi A. Primary myelofibrosis: 2021 update on diagnosis, risk-stratification and management. *Am J Hematol*. 2021;96(1):145–162. doi:10.1002/ajh.26050
3. Tefferi A, Guglielmelli P, Larson DR, et al. Long-term survival and blast transformation in molecularly annotated essential thrombocythemia, polycythemia vera, and myelofibrosis. *Blood*. 2014;124(16):2507–2513. doi:10.1182/blood-2014-05-579136
4. Barosi G, Mesa RA, Thiele J, et al. Proposed criteria for the diagnosis of post-polycythemia vera and post-essential thrombocythemia myelofibrosis: A consensus statement from the international working group for myelofibrosis research and treatment. *Leukemia*. 2008;22(2):437–438. doi:10.1038/sj.leu.2404914
5. Tefferi A, Rumi E, Finazzi G, et al. Survival and prognosis among 1545 patients with contemporary polycythemia vera: An international study. *Leukemia*. 2013;27(9):1874–1881. doi:10.1038/leu.2013.163
6. Hageman S, Pennells L, Ojeda F, et al; SCORE2 working group and ESC Cardiovascular risk collaboration. SCORE2 risk prediction algorithms: New models to estimate 10-year risk of cardiovascular disease in Europe. *Eur Heart J*. 2021;42(25):2439–2454. doi:10.1093/eurheartj/ehab309
7. Arber DA, Orazi A, Hasserjian R, et al. The 2016 revision to the World Health Organization classification of myeloid neoplasms and acute leukemia. *Blood*. 2016;127(20):2391–2405. doi:10.1182/blood-2016-03-643544
8. Wojtaszewska M, Iwoła M, Lewandowski K. Frequency and molecular characteristics of calreticulin gene *(CALR)* mutations in patients with *JAK2*-negative myeloproliferative neoplasms. *Acta Haematol*. 2015;133(2):193–198. doi:10.1159/000366263
9. Pancrazzi A, Guglielmelli P, Ponziani V, et al. A Sensitive detection method for MPLW515L or MPLW515K mutation in chronic myeloproliferative disorders with locked nucleic acid-modified probes and real-time polymerase chain reaction. *J Mol Diagn*. 2008;10(5):435–441. doi:10.2353/jmoldx.2008.080015
10. Jones AV. Widespread occurrence of the JAK2 V617F mutation in chronic myeloproliferative disorders. *Blood*. 2005;106(6):2162–2168. doi:10.1182/blood-2005-03-1320
11. Barbui T, Finazzi G, Carobbio A, et al. Development and validation of an International Prognostic Score of thrombosis in World Health Organization – essential thrombocythemia (IPSET-thrombosis). *Blood*. 2012;120(26):5128–5133. doi:10.1182/blood-2012-07-444067
12. Barbui T, Vannucchi AM, Buxhofer-Ausch V, et al. Practice-relevant revision of IPSET-thrombosis based on 1019 patients with WHO-defined essential thrombocythemia. *Blood Cancer J*. 2015;5(11):e369–e369. doi:10.1038/bcj.2015.94
13. Tefferi A, Barbui T. Polycythemia vera and essential thrombocythemia: 2017 update on diagnosis, risk-stratification, and management. *Am J Hematol*. 2017;92(1):94–108. doi:10.1002/ajh.24607
14. Tefferi A, Barbui T. Polycythemia vera and essential thrombocythemia: 2021 update on diagnosis, risk-stratification and management. *Am J Hematol*. 2020;95(12):1599–1613. doi:10.1002/ajh.26008
15. Tefferi A, Guglielmelli P, Lasho TL, et al. Mutation-enhanced international prognostic systems for essential thrombocythaemia and polycythaemia vera. *Br J Haematol*. 2020;189(2):291–302. doi:10.1111/bjh.16380
16. Gangat N, Szuber N, Jawaid T, Hanson CA, Pardanani A, Tefferi A. Young platelet millionaires with essential thrombocythemia. *Am J Hematol*. 2021;96(4):E93–E95. doi:10.1002/ajh.26114
17. Tefferi A, Szuber N, Pardanani A, et al. Extreme thrombocytosis in low-risk essential thrombocythemia: Retrospective review of vascular events and treatment strategies. *Am J Hematol*. 2021;96(6):E182–E184. doi:10.1002/ajh.26137
18. Sobas M, Kiladjian JJ, Beauverd Y, et al. Real-world study of children and young adults with myeloproliferative neoplasms: Identifying risks and unmet needs. *Blood Adv*. 2022;6(17):5171–5183. doi:10.1182/bloodadvances.2022007201
19. Choi HS, Hong J, Hwang SM, et al. Evaluation of the need for cytoreduction and its potential carcinogenicity in children and young adults with myeloproliferative neoplasms. *Ann Hematol*. 2021;100(10):2567–2574. doi:10.1007/s00277-021-04527-7
20. Mancuso S, Santoro M, Accurso V, et al. Cardiovascular risk in polycythemia vera: Thrombotic risk and survival. Can cytoreductive therapy be useful in patients with low-risk polycythemia vera with cardiovascular risk factors? *Oncol Res Treat*. 2020;43(10):526–530. doi:10.1159/000509376
21. Marchioli R, Finazzi G, Specchia G, et al. Cardiovascular events and intensity of treatment in polycythemia vera. *N Engl J Med*. 2013;368(1):22–33. doi:10.1056/NEJMoa1208500
22. Sankar K, Stein BL. Do all patients with polycythemia vera or essential thrombocythemia need cytoreduction? *J Natl Compr Canc Netw*. 2018;16(12):1539–1545. doi:10.6004/jnccn.2018.7073
23. How J, Hobbs G. Management issues and controversies in low-risk patients with essential thrombocythemia and polycythemia vera. *Curr Hematol Malig Rep*. 2021;16(5):473–482. doi:10.1007/s11899-021-00649-x
24. Abu-Zeinah K, Saadeh K, Silver RT, Scandura JM, Abu-Zeinah G. Excess mortality in younger patients with myeloproliferative neoplasms. *Leuk Lymphoma*. 2023;64(3):725–729. doi:10.1080/10428194.2022.2070914
25. Marchetti M, Ghirardi A, Masciulli A, et al. Second cancers in MPN: Survival analysis from an international study. *Am J Hematol*. 2020;95(3):295–301. doi:10.1002/ajh.25700

26. Birgegård G, Besses C, Griesshammer M, et al. Treatment of essential thrombocythemia in Europe: A prospective long-term observational study of 3649 high-risk patients in the Evaluation of Anagrelide Efficacy and Long-term Safety study. *Haematologica*. 2018;103(1):51–60. doi:10.3324/haematol.2017.174672

27. Barbui T, Thiele J, Passamonti F, et al. Survival and disease progression in essential thrombocythemia are significantly influenced by accurate morphologic diagnosis: An international study. *J Clin Oncol*. 2011; 29(23):3179–3184. doi:10.1200/JCO.2010.34.5298

28. Vannucchi AM, Kiladjian JJ, Griesshammer M, et al. Ruxolitinib versus standard therapy for the treatment of polycythemia vera. *N Engl J Med*. 2015;372(5):426–435. doi:10.1056/NEJMoa1409002

29. Passamonti F, Griesshammer M, Palandri F, et al. Ruxolitinib for the treatment of inadequately controlled polycythaemia vera without splenomegaly (RESPONSE-2): A randomised, open-label, phase 3b study. *Lancet Oncol*. 2017;18(1):88–99. doi:10.1016/S1470-2045(16)30558-7

30. Gowin K, Jain T, Kosiorek H, et al. Pegylated interferon alpha-2a is clinically effective and tolerable in myeloproliferative neoplasm patients treated off clinical trial. *Leuk Res*. 2017;54:73–77. doi:10.1016/j.leukres.2017.01.006

31. Kiladjian JJ, Barbui T. From leeches to interferon: Should cytoreduction be prescribed for all patients with polycythemia vera? *Leukemia*. 2020;34(11):2837–2839. doi:10.1038/s41375-020-0984-9

32. Quintás-Cardama A, Abdel-Wahab O, Manshouri T, et al. Molecular analysis of patients with polycythemia vera or essential thrombocythemia receiving pegylated interferon α-2a. *Blood*. 2013;122(6): 893–901. doi:10.1182/blood-2012-07-442012

33. Mascarenhas J, Kosiorek HE, Prchal JT, et al. A randomized phase 3 trial of interferon-α vs hydroxyurea in polycythemia vera and essential thrombocythemia. *Blood*. 2022;139(19):2931–2941. doi:10.1182/blood.2021012743

34. Kiladjian JJ, Klade C, Georgiev P, et al. Long-term outcomes of polycythemia vera patients treated with ropeginterferon alfa-2b. *Leukemia*. 2022;36(5):1408–1411. doi:10.1038/s41375-022-01528-x

35. Abu-Zeinah G, Silver RT, Abu-Zeinah K, Scandura JM. Normal life expectancy for polycythemia vera (PV) patients is possible. *Leukemia*. 2022;36(2):569–572. doi:10.1038/s41375-021-01447-3

36. Barbui T, Vannucchi AM, De Stefano V, et al. Ropeginterferon alfa-2b versus phlebotomy in low-risk patients with polycythaemia vera (Low-PV study): A multicentre, randomised phase 2 trial. *Lancet Haematol*. 2021;8(3):e175–e184. doi:10.1016/S2352-3026(20)30373-2

Safety and efficacy of Yaobitong capsules for lumbar disc herniation: A multicenter, randomized, double-blinded, parallel, positive-controlled clinical trial

*Ye Zhao[1,A,B], Shi Rong Huang[1,C,D], *Yu Jie Zhang[1,B,D], Yong Qiang Chen[2,A,B,D], Wen Gang Liu[3,B,C], Fu Shun Gu[4,A,B], Hui Wen[5,C,E], Xi Lin Xu[6,C,E], Jiu Yi Chen[7,B,C], Da Xiang Jin[8,B,E], Hong Yin[9,E,F], Zhong Dong[10,C,F], Wei An Yuan[11,A,E,F], Hong Sheng Zhan[1,E,F]

[1] Department of Traditional Chinese Medicine Orthopedics & Traumatology, Shuguang Hospital Affiliated to Shanghai University of Traditional Chinese Medicine, China

[2] Department of Traditional Chinese Medicine Orthopedics & Traumatology, Shanghai Hospital of Traditional Chinese Medicine, China

[3] Department of Traditional Chinese Medicine Orthopedics & Traumatology, Guangdong Second Hospital of Traditional Chinese Medicine, Guangzhou, China

[4] Department of Orthopedics, The Second Affiliated Hospital of Tianjin University of Traditional Chinese Medicine, China

[5] Department of Traditional Chinese Medicine Orthopedics & Traumatology, The Hospital Affiliated to Changchun University of Traditional Chinese Medicine, China

[6] Department of Traditional Chinese Medicine Orthopedics & Traumatology, The Second Affiliated Hospital of Heilongjiang University of Traditional Chinese Medicine, Harbin, China

[7] Department of Traditional Chinese Medicine Orthopedics & Traumatology, The First Affiliated Hospital of Guiyang College of Traditional Chinese Medicine, China

[8] Department of Orthopedics, The First Affiliated Hospital of Guangzhou University of Traditional Chinese Medicine, China

[9] Department of Traditional Chinese Medicine Orthopedics & Traumatology, Nanjing Hospital of Traditional Chinese Medicine, China

[10] Department of Traditional Chinese Medicine Orthopedics & Traumatology, Fujian Institute of Traditional Chinese Medicine, Fuzhou, China

[11] Clinical Research Center, Shuguang Hospital Affiliated to Shanghai University of Traditional Chinese Medicine, Shanghai, China

A – research concept and design; B – collection and/or assembly of data; C – data analysis and interpretation;
D – writing the article; E – critical revision of the article; F – final approval of the article

Address for correspondence
Wei An Yuan
E-mail: weian_1980@sina.com

Abstract

Background. Lumbar disc herniation (LDH) is one of the most common diseases and is a global medical and socioeconomic problem characterized by leg or back pain, weakness in the lower extremities and paresthesia.

Objectives. A multicenter, randomized, double-blinded, parallel, positive-controlled clinical trial was conducted to evaluate the efficacy and safety of Yaobitong capsules (YBT) for LDH.

Materials and methods. Patients (n = 479) were recruited and randomized into YBT and Jingyaokang capsule (JYK) groups (the positive control), and received YBT or JYK at a dose of 3 capsules 3 times per day after a meal for 30 days. The primary efficacy outcome was the Oswestry Disability Index (ODI), with the visual analogue scale (VAS) used as the secondary efficacy outcome. The adverse events and adverse reactions were also evaluated.

Results. There was no significant difference in baseline characteristics between YBT (n = 358) and JYK groups (n = 120), and no difference was observed between groups for mean ODI score at day 0 (p = 0.064) or day 7 (p = 0.196), but there were differences at days 14, 21 and 30 (p < 0.001). The YBT showed more decline from baseline, and the decreased ODI score was substantially different from JYK (p < 0.001). The differences in decreased VAS scores between YBT and JYK were also significant at each time point (days 7, 14, 21, and 30), with better scores in the YBT group than in the JYK group (p < 0.001). In terms of safety, there was no obvious disparity in adverse events or adverse reactions between the 2 groups (p > 0.05).

Conclusions. Yaobitong was better than JYK for LDH treatment, with no significant difference in safety. The study suggests that YBT is a promising and effective treatment for LDH.

Key words: lumbar disc herniation (LDH), clinical trial, Jingyaokang, Yaobitong

Background

Lumbar disc herniation (LDH) is one of the most common diseases and is a global medical and socioeconomic problem characterized by leg or back pain, weakness in the lower extremities and paresthesia.[1,2] One epidemiological investigation showed LDH incidence at approx. 5 per 1000 adults each year worldwide.[3] In addition, lower back pain is the primary cause of worldwide productivity loss per year in 195 countries and the top cause of disability in 126.[4] In China, relevant epidemiological investigations show that LDH incidence is as high as 14.3%, and with changes in lifestyle and the aging population, LDH incidence has increased significantly, particularly in younger persons.[5] The most common LDH treatment options are surgical options and conservative treatments.[6] Only 10% of LDH cases are candidates for immediate surgery, and 8–40% of patients still feel pain after surgery.[7,8] Physical therapy, complementary treatments, alternative medicine (acupotomy, acupuncture, Chinese herbal medicine, and Chinese massage), pharmacotherapy (including non-steroidal anti-inflammatory drugs (NSAIDs), systemic steroids, steroid injections, and muscle relaxants), and an active lifestyle are routinely used as effective conservative treatments for LDH.[9] Most LDH patients gradually prefer continued conservative management due to its unique advantages in mid-term and long-term follow-up.[10]

At present, conservative LDH treatments are numerous, though a single satisfactory treatment method is still lacking. Traditional Chinese medicine (TCM), as an important component of complementary and alternative medicine, has developed for over 1000 years and has shown to be effective for the treatment of a variety of disorders, particularly musculoskeletal diseases, in Asian countries, especially China.[11,12] For instance, Yaobitong capsules (YBT) are a new Chinese patented medicine for LDH treatment, originating from the clinical experience in Chinese herbal compounds by Shuchun Sun, a famous TCM physician.[13] Our preclinical animal experiments have indicated that YBT has significant therapeutic effects on rat lumbar radiculopathy, with a positive analgesic effect on physical and chemical pain stimulation. However, the lack of a large sample and the need for high-quality clinical trials call for more evidence on the efficacy of YBT in treating LDH. The Jingyaokang capsule (JYK) is considered an effective drug for LDH in China and is approved by the China Food and Drug Administration.

Objectives

The objective of this trial was to compare the efficacy of YBT with JYK in the treatment of LDH patients, to understand the performance of YBT in relieving patient symptoms and improving quality of life, and to evaluate its safety.

Materials and methods

Study design

This multicenter, randomized, double-blinded, parallel positive-controlled clinical trial used a computer-generated list of random numbers in Microsoft Excel 2013 (Microsoft Corp. Armonk, USA), with patients randomly allocated into YBT and JYK groups in a 3:1 ratio. The randomized assignments sealed in opaque envelopes were prepared by a nurse who was blinded to the study design. The nurse opened the envelopes for each participating patient and then submitted them to the clinical trial unit and sponsor for safekeeping. The researchers were blinded to the medication management throughout the whole process, and the participants were given similar vials with YBT or JYK by the pharmacy.

All researchers received protocol training before the beginning of this trial, with the full-time Clinical Research Coordinator (CRC) staffed to schedule the treatment procedure in each center. A supervisor sent to all centers monitored the study to ensure data integrity and quality. The entire trial complied with Good Clinical Practice (GCP), which was ensured by 2 independent quality audits.

The Institutional Review Board of Shuguang Hospital affiliated with the Shanghai University of Traditional Chinese Medicine (batch No. 2014-352-48-01), approved the trial (approval No. 2014-352-48-01), and it was registered at the Chinese Clinical Trial Registry (No. ChiCTR2200057819). All patients gave written informed consent.

Participants

From June 2015 to February 2016, 479 LDH patients were recruited from 10 Chinese centers. The inclusion criteria were: 1) LDH patients meeting the standard of Western and TCM diagnostic criteria (patients have local pain and tenderness in the lower back and legs,

flexion or extension negative, purple tongue with ecchymosis, thin and white coating, as well as Wiry and tense pulse or uneven pulse)[14,15]; 2) aged 18–60 years (including 18 and 60 years), male or female; 3) Oswestry Disability Index between 30% and 80%; 4) visual analogue scale (VAS) between 30 mm and 80 mm; 5) not taking NSAIDs or other medications for LDH within 1 week before visit; and 6) who gave informed consent. The exclusion criteria included: 1) pregnant or breastfeeding women; 2) allergic constitution or an allergy to YBT or JYK; 3) recurrent LDH after surgery; 4) asymptomatic LDH or non-discogenic low back and leg pain; 5) LDH complicated with cauda equina syndrome or conus medullaris syndrome; 6) LDH complicated with lumbar tumor or tuberculosis, lumbar spondylolisthesis above 0, lumbar spinal stenosis, ankylosing spondylitis, or severe osteoporosis; 7) LDH complicated with severe hypertension, heart disease, or other serious primary organ system or psychiatric diseases; 8) other acute and chronic pain, such as migraines and joint pain affecting how patients describe pain; 9) recently receiving epidural steroid injection or various interventional and surgery treatments; 10) allergy to meloxicam; 11) serious primary diseases of the heart, liver and kidney, including alanine transaminase (ALT), aspartate aminotransferase (AST) ≥normal upper limit, creatinine (Cr) >normal upper limit, hematopoietic system and endocrine system, psychosis, and epilepsy; 12) taking part in another study within 3 months; and 13) those judged inappropriate for the study by the researchers.

Intervention

The drugs used in the YBT group were YBT and JYK simulation agents, whose main ingredient was placebo starch. The main ingredients of YBT are San Qi (Notoginseng Radix), Du Huo (Angelicae Pubescentis Radix), Chuan Xiong (Chuanxiong Rhizoma), Bai Shao (Paeoniae Radix Alba), Niu Xi (Cyathulae Radix), Gou Ji (Cibotii Rhizoma), Shu Da Huang (Rhei Radix et Rhizoma), and Yan Hu Suo (Corydalis Rhizoma). The drugs used in the JYK group were JYK and YBT simulation agents whose main ingredient was placebo starch. The main ingredients of JYK are Ma Qian Zi (Strychni Semen), Shen Jin Cao (Lycopodii Herba), Hong Hua (Carthami Flos), Xiang Jia Pi (Periplocae Cortex), Ru Xiang (Olibanum), Di Long (Pheretima), Gu Cui Bu (Drynariae Rhizoma), Fang Ji (Stephaniae Tetrandrae Radix), Niu Xi (Cyathulae Radix), and Mo Yao (Myrrha). Jiangsu Kangyuan Pharmaceutical Co. Ltd. (Lianyungang, China) provided JYK (specification: 0.33 g/capsule, batch No. 140438), YBT (specification: 0.42 g/capsule, batch No. 140438) and simulation agent (batch No. 140701 and No. 140702) for this study. All drugs were stored at room temperature. Patients in both groups were given 3 drug capsules 3 times per day after meals for 30 days.

Outcome measurements

Symptom burden and quality of life, including pain intensity, personal care, lifting, walking, sitting, standing, sleeping, social life, and travelling, were assessed as primary outcomes using the ODI (ranging from 0 to 45 points), which has been validated in the LDH population.[16] Patients answered the questions to evaluate the severity of their symptoms through a numerical rating scale of 0–5 over the previous 24 h, with 0 meaning the absence of symptom and 5 meaning the worst symptom. The ODI dysfunction index is the percentage of the sum score of 9 items to the highest score (45 points), with a higher percentage equating to more severe dysfunction.[17]

The VAS (ranging from 0 to 100 points) score was included as the secondary efficacy outcome of LDH. Visual analogue scale was a 10 cm horizontal line drawn on paper, with 0 marked at one end and 10 at the other. The line was equally divided into 10 segments. A 0 VAS score indicated no pain and a 10 score signified the most severe pain.[18] Patients were asked to mark on the line to express their degree of self-reported pain within 48 h. The ODI and the VAS were evaluated at baseline (0 days) and at 7, 14, 21, and 30 days. Before using the scale, all patients received an illustration and practice on using the scale by professionals. Professional statisticians collected and analyzed the data.

Treatment safety was evaluated using 1) serum biochemicals, including ALT, AST, total bilirubin (TBIL), gamma-glutamyl transpeptidase (γ-GT), alkaline phosphatase (AKP), blood urea nitrogen (BUN), and Cr; 2) routine blood and urine examinations (e.g., urine protein, red blood cell and white blood cell count); 3) routine stool and occult blood; 4) electrocardiogram; and 5) adverse events and adverse reactions.

Sample size

The sample size was calculated using the superiority test and estimated on account of the rate of decline from the baseline ODI score, the primary efficacy measure of this study. It was assumed that the therapeutic effect of YBT on LDH was better than JYK. We assumed an α = 0.05 and a power = 80% for YBT:JYK, according to a 3:1 design. The difference in the reduction rate of ODI score from baseline between the YBT group and the JYK group was estimated to be 15%, and the combined variance was 40%, with an estimated number of 228 patients in the YBT group and of 76 in the JYK group. Considering the possible loss of follow-up (20%), the number of cases in the clinical trial was 360 in the YBT group and 120 in the JYK group, according to the requirements of national regulations in China.

36

Y. Zhao et al. Efficacy and safety of Yaobitong capsule

Statistical analyses

All data were analyzed using Statistical Analysis System (SAS) v. 9.2 (SAS Institute, Cary, USA) and R v. 4.1.3 (R Foundation for Statistical Computing, Vienna, Austria). Data management adopted epidata v. 3.0 using double independent input, and statistical analysis was carried out after assessment. Kolmogorov–Smirnov tests and Q–Q plots evaluated data distribution, while Bartlett's or Levene's test checked for homogeneity of variances. The results of these tests can be found in the Supplementary materials.

The equilibrium analysis of basic values adopted t-tests, Wilcoxon tests or χ^2 test/Fisher exact tests to compare demographic data and other indicators of balance between the 2 groups. Effectiveness analysis employed repeated-measures linear mixed models (R package: lmerTest) to assess the effect of treatment on LDH. The models included outcome data collected at every follow-up visit, with fixed effects for the treatment, time point as a categorical variable, baseline of ODI, sex, age, center, with and without the interaction between treatment and time point, and random intercepts for participants accounted for the dependence of repeated measures, with the same models used to estimate VAS score. The last observation carried forward (LOCF) was used to fill missing primary outcome data. Robust mixed analysis of variance (ANOVA) (R package: WRS2) was used for sensitivity analysis of primary endpoint and different terms of ODI score;[19] 20% trimmed means were used to fit between-within-subjects ANOVA, with post hoc comparisons on single effects performed with modified one-step estimators (MOM). Safety analysis mainly used descriptive statistical analysis, with adverse events described on a list. If necessary, Fisher's exact probability method was used to compare the incidence of adverse events between the 2 groups. The laboratory test results described the normal conditions before the test but abnormal conditions after treatment, as well as the relationship between abnormal changes and the test drug. A 2-sided test was used for all hypotheses testing, and $p \leq 0.05$ was considered statistically significant. The reliability of all confidence intervals was assumed as 95% (95% CI).
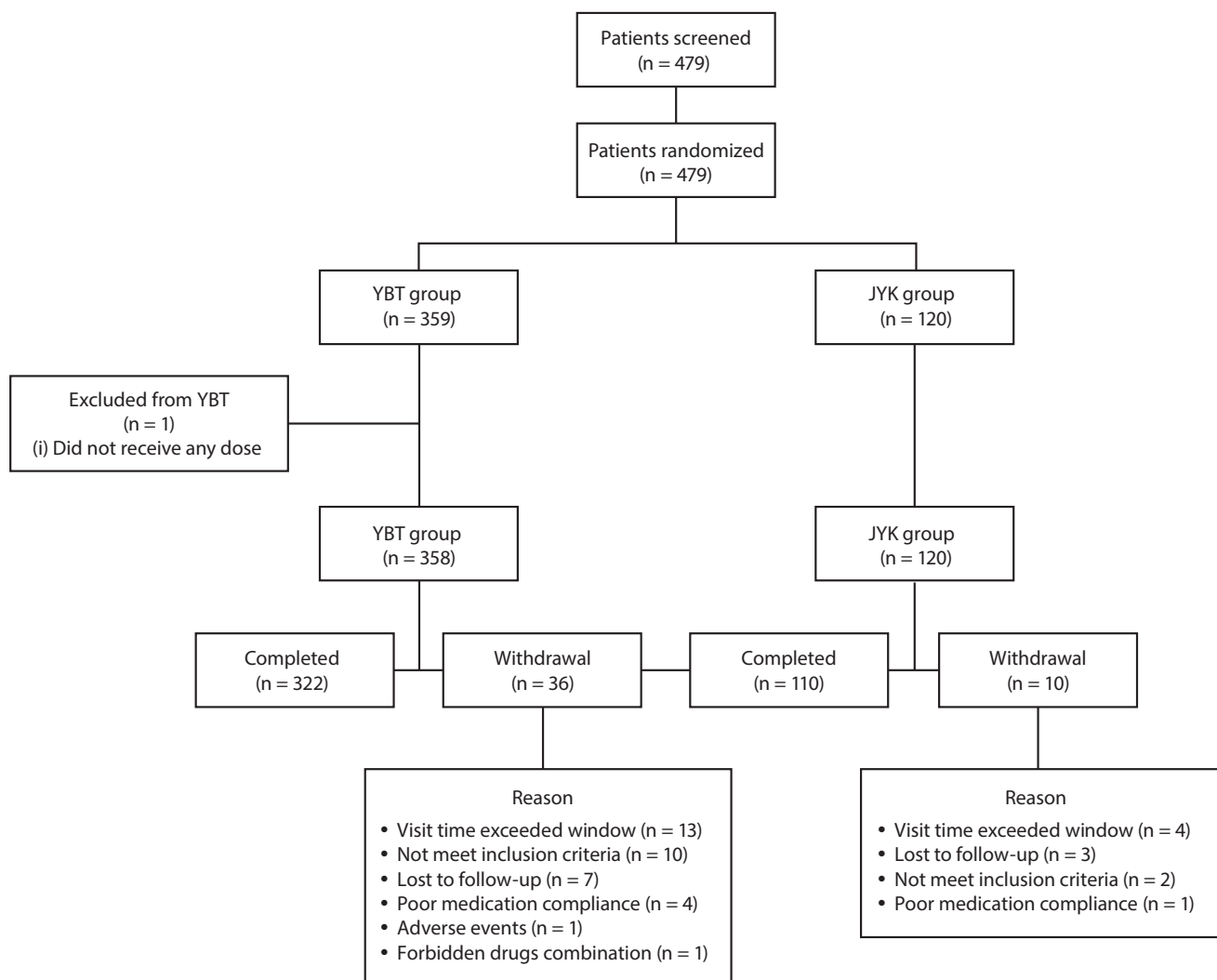
Fig. 1. Screening flowchart

YBT – Yaobitong capsules, JYK – Jingyaokang capsule.

Table 1. Comparison of baseline characteristics

Variable	Variable	YBT (n = 358)	JYK (n = 120)	Test value	p-value
Gender, n (%)	male	125 (34.92)	44 (36.67)	–	0.742*
	female	233 (65.08)	76 (63.33)		
Age [years], mean +SD		47.36 ±10.34	48.13 ±10.30	t = 0.72	0.472
Ethnicity, n (%)	Han nationality	353 (98.60)	118 (98.33)	–	1.000*
	other	5 (1.40)	2 (1.67)		
Weight [kg], mean +SD		63.36 ±10.21	63.46 ±9.59	t = 0.10	0.923
Height [cm], mean +SD		164.17 ±7.35	164.66 ±7.62	t = 0.62	0.533
Heart rate [bpm], mean +SD		69.72 ±8.13	70.55 ±8.91	t = 0.94	0.347
Respiratory rate [bpm], mean +SD		18.61 ±1.96	18.68 ±1.89	t = 0.35	0.727
SBP [mm Hg], mean +SD		123.66 ±9.79	125.18 ±11.49	t = 1.30	0.196
DBP [mm Hg], mean +SD		73.89 ±7.17	74.58 ±8.79	t = 0.77	0.442
Duration of LBP [months], mean +SD		12.00 ±23.00	12.00 ±40.00	t = 0.77	0.141
Baseline of ODI, mean ±SD	total index	43.53 ±8.00	41.94 ±8.30	t = 1.86	0.064
	pain intensity	2.55 ±0.65	2.46 ±0.59	Z = 1.35	0.176#
	personal care	2.13 ±0.58	2.08 ±0.60	Z = 1.13	0.257#
	lifting	2.23 ±0.72	2.18 ±0.66	Z = 0.84	0.399#
	walking	1.21 ±0.68	1.31 ±0.73	Z = 1.39	0.164#
	sitting	2.40 ±0.68	2.19 ±0.74	Z = 3.11	0.002#
	standing	2.30 ±0.67	2.17 ±0.74	Z = 2.00	0.045#
	sleeping	1.70 ±0.76	1.68 ±0.76	Z = 0.30	0.766#
	social life	2.51 ±0.71	2.41 ±0.68	Z = 1.38	0.168#
	travelling	2.56 ±0.85	2.42 ±0.88	Z = 1.73	0.084#
Baseline of VAS, mean ±SD		61.82 ±10.61	61.29 ±11.77	t = 0.46	0.647
History of treatment, n (%)					
TCM treatment	no	301 (84.08)	99 (82.50)	–	0.671*
	yes	57 (15.92)	21 (17.50)		
Drug treatment	no	317 (88.55)	103 (85.83)	–	0.423*
	yes	41 (11.45)	17 (14.17)		
History of allergy, n (%)	no	351 (98.04)	119 (99.17)	–	0.686*
	yes	7 (1.96)	1 (0.83)		
Other diseases combined, n (%)	no	313 (87.43)	104 (86.67)	–	0.875*
	yes	45 (12.57)	16 (13.33)		

*Fisher's exact probability method was used to compare gender, ethnicity, history of treatment, and other diseases combined between the 2 groups. #Wilcoxon test was used to compare each term of ODI at baseline, and t-test was used to compare other items between the 2 groups. YBT – Yaobitong capsule; JYK – Jingyaokang capsule; ODI – Oswestry Disability Index; VAS – visual analogue scale; SD – standard deviation; SBP – systolic blood pressure; DBP – diastolic blood pressure; TCM – traditional Chinese medicine; LBP – low back pain.

Results

Baseline characteristics of patients

Between June 2015 and February 2016, 479 patients fulfilled the screening process and were recruited for the trial (Fig. 1). One patient withdrew from the YBT group. A total of 478 patients entered the full analysis set and safety analysis set (YBT group n = 358; JYK group n = 120). An intention-to-treat analysis was used in this trial. As shown in Table 1, there was no significant difference in demographic data or vital signs between the 2 groups (p > 0.05).

Among disease conditions, there was no obvious correlation between groups (p = 0.875). In addition, each baseline ODI and VAS score had no statistical difference between the groups, indicating comparability (p > 0.05).

Efficacy results

After adjusting for baseline ODI, center, age, and sex, the linear mixed models showed that the YBT provided a significant benefit over JYK. As shown in Table 2 (model 1), the mean ODI in the YBT group decreased by 5.25 points more than in the JYK group (95%

Table 2. Linear mixed model results for ODI and VAS. Linear mixed model adjust center, age, sex and baseline of ODI or VAS, model 2 and model 4 also add interaction term in the model

Variable	ODI			VAS		
	estimate (95% CI)	t-value	p-value	estimate (95% CI)	t-value	p-value
	Model 1			Model 3		
group	−5.25 (−6.09, −4.41)	−12.10	<0.001	−5.06 (−6.10, −4.01)	−9.35	<0.001
time_7D	−5.98 (−6.59,−5.36)	−19.02	<0.001	−9.65 (−10.49, −8.82)	−22.60	<0.001
time_14D	−14.83 (−15.45,−14.21)	−47.19	<0.001	−21.47 (−22.31, −20.63)	−50.26	<0.001
time_21D	−23.15 (−23.77, −22.54)	−73.67	<0.001	−32.89 (−33.72, −32.05)	−76.99	<0.001
time_30D	−29.09 (−29.71, −28.48)	−92.58	<0.001	−43.38 (−44.22, −42.54)	−101.48	<0.001
	Model 2			Model 4		
group	0.37 (−0.80, 1.55)	0.62	0.535	0.10 (−1.45, 1.66)	0.13	0.900
time_7D	−3.96 (−5.08, −2.84)	−6.91	<0.001	−8.00 (−9.60, −6.41)	−9.81	<0.001
time_14D	−10.78 (−11.9, −9.66)	−18.80	<0.001	−17.85 (−19.45, −16.25)	−21.88	<0.001
time_21D	−16.81 (−17.94, −15.69)	−29.33	<0.001	−27.10 (−28.69, −25.50)	−33.22	<0.001
time_30D	−20.44 (−21.57, −19.32)	−35.66	<0.001	−34.90 (−36.50, −33.31)	−42.78	<0.001
time_7D:YBT	−2.69 (−3.99,−1.4)	−4.06	<0.001	−2.20 (−4.05, −0.36)	−2.34	0.020
time_14D:YBT	−5.41 (−6.71, −4.11)	−8.17	<0.001	−4.83 (−6.68, −2.99)	−5.13	<0.001
time_21D:YBT	−8.46 (−9.76, −7.17)	−12.77	<0.001	−7.73 (−9.57, −5.88)	−8.20	<0.001
time_30D:YBT	−11.55 (−12.84, −10.25)	−17.43	<0.001	−11.32 (−13.16, −9.47)	−12.01	<0.001

ODI – Oswestry Disability Index; VAS – visual analogue scale; 95% CI – 95% confidence interval.

Table 3. Comparison of ODI total index and VAS score between 2 groups before and after intervention

Variable	Time	Decreased value from baseline in the group, mean ±SD		M-estimators (YBT-JYK)	Average M-estimators	p-value
		YBT (n = 358)	JYK (n = 120)			
ODI total score	7 D	−6.65 ±4.91	−3.96 ±4.87	−2.54	−7.76#	<0.001
	14 D	−16.19 ±6.62	−10.78 ±5.91	−5.12		
	21 D	−25.28 ±7.56	−16.82 ±6.30	−9.59		
	30 D	−32.00 ±8.13	−20.45 ±7.13	−13.80		
VAS score	7 D	−10.22 ±6.68	−7.93 ±6.71	−2.58	−7.62#	<0.001
	14 D	−22.70 ±8.61	−17.78 ±9.64	−6.93		
	21 D	−34.84 ±10.12	−27.03 ±11.31	−8.90		
	30 D	−46.23 ±10.99	−34.83 ±13.12	−12.06		

Comparison between YBT group and JYK group was done using robust mixed ANOVA. # average across measurement; YBT – Yaobitong capsule; JYK – Jingyaokang capsule; ODI – Oswestry Disability Index; VAS – visual analogue scale; ANOVA – analysis of variance.

CI: −6.09 to −4.41). Compared to baseline, the ODI on 7, 14, 21, and 30 days all decreased significantly, with scores of −5.98 (−6.59 to −5.36), −14.83 (−15.45 to −14.21), −23.15 (−23.77 to −22.54), and −29.09 (−29.71 to −28.48), respectively. Considering the interaction between treatment and time point, model 2 showed that, compared to JYK, the ODI in YBT group decreased more visibly at days 7, 14, 21, and 30, with significantly lower scores of −2.69 (−3.99 to −1.4), −5.41 (−6.71 to −4.11), −8.46 (−9.76 to −7.17), and −11.55 (−12.84 to −10.25), respectively.

The same models were applied to the total VAS score, with model 3 showing a mean YBT decrease of 5.06 more than in the JYK group (95% CI: −6.10 to 4.01). Compared to baseline, the VAS of 7, 14, 21, and 30 days all decreased significantly, with scores of −9.65 (−10.49 to −8.82), −21.47

(−22.31 to −20.63), −32.89 (−33.72 to −32.05), and −43.38 (−44.22 to −42.54). Considering the interaction between treatment and time point, model 4 showed that, compared to JYK, the VAS in the YBT group decreased more at days 7, 14, 21, and 30, with statistically significant decreased scores of −2.20 (−4.05 to −0.36), −4.83 (−6.68 to −2.99), −7.73 (−9.57 to −5.88), and −11.32 (−13.16 to −9.47), respectively.

As shown in Fig. 2 and Table 2,3, both YBT and JYK groups showed a tendency of a decreased total ODI score, with no statistically significant difference observed between groups on days 0 (p = 0.064) and 7 (p = 0.196), but with significant differences at 14, 21 and 30 days (p < 0.001). The decreased ODI improved gradually over time in both groups (p < 0.001), though the YBT group showed more

Table 4. Comparison of decreased ODI score from baseline

Variable	Time	Decreased value from baseline in the group, mean ±SD		M-estimators (YBT-JYK)	Average M-estimators	Average M-estimators p-value	p-value
		YBT (n = 358)	JYK (n = 120)				
Pain intensity	7 D	−0.35 ±0.53	−0.14 ±0.40	0.00	−0.35#	<0.001	<0.001
	14 D	−0.87 ±0.63	−0.60 ±0.63	−0.40			
	21 D	−1.39 ±0.69	−1.04 ±0.61	0.00			
	30 D	−1.78 ±0.78	−1.31 ±0.67	−1.00			
Personal care	7 D	−0.30 ±0.50	−0.20 ±0.46	0.00	−0.25#	<0.001	<0.001
	14 D	−0.83 ±0.59	−0.61 ±0.66	0.00			
	21 D	−1.36 ±0.68	−0.88 ±0.58	0.00			
	30 D	−1.72 ±0.65	−1.11 ±0.67	−1.00			
Lifting	7 D	−0.29 ±0.52	−0.17 ±0.51	0.00	−0.38#	<0.001	0.030
	14 D	−0.76 ±0.68	−0.44 ±0.63	−1.00			
	21 D	−1.18 ±0.74	−0.79 ±0.61	0.00			
	30 D	1.52 ±0.80	−0.99 ±0.60	−0.52			
Walking	7 D	−0.12 ±0.41	−0.13 ±0.48	0.00	−0.11#	0.204	0.416
	14 D	−0.53 ±0.54	−0.35 ±0.54	0.00			
	21 D	−0.91 ±0.51	−0.64 ±0.62	−0.44			
	30 D	−1.09 ±0.53	−0.83 ±0.64	0.00			
Sitting	7 D	−0.36 ±0.51	−0.13 ±0.49	0.00	−0.58#	<0.001	<0.001
	14 D	−0.87 ±0.66	−0.43 ±0.65	−1.00			
	21 D	−1.32 ±0.74	−0.76 ±0.70	−0.30			
	30 D	−1.73 ±0.76	−0.91 ±0.71	−1.00			
Standing	7 D	−0.39 ±0.53	−0.24 ±0.47	0.00	−0.25#	0.026	0.18
	14 D	−0.84 ±0.64	−0.57 ±0.62	0.00			
	21 D	−1.30 ±0.68	−0.84 ±0.71	0.00			
	30 D	−1.72 ±0.78	−0.95 ±0.71	−1.00			
Sleeping	7 D	−0.49 ±0.59	−0.38 ±0.55	0.00	−0.10#	0.088	0.134
	14 D	−0.87 ±0.70	−0.67 ±0.57	0.00			
	21 D	−1.24 ±0.75	−0.93 ±0.60	0.00			
	30 D	−1.45 ±0.76	−1.05 ±0.63	−0.41			
Social life	7 D	−0.37 ±0.61	−0.15 ±0.53	0.00	−0.42#	<0.001	<0.001
	14 D	−0.90 ±0.72	−0.63 ±0.65	−0.38			
	21 D	−1.43 ±0.76	−0.89 ±0.66	−0.42			
	30 D	−1.88 ±0.84	−1.08 ±0.75	−0.88			
Travelling	7 D	−0.38 ±0.57	−0.29 ±0.54	0.00	−0.37#	<0.001	<0.001
	14 D	−0.93 ±0.74	−0.66 ±0.72	−0.36			
	21 D	−1.41 ±0.76	−0.92 ±0.75	−0.40			
	30 D	−1.72 ±0.84	−1.13 ±0.75	−0.71			

Comparison between YBT group and JYK group was done using robust mixed ANOVA. # average across measurement; YBT – Yaobitong capsule; JYK – Jingyaokang capsule; ODI – Oswestry Disability Index; VAS – visual analogue scale; ANOVA – analysis of variance.

decline compared to baseline, and the ODI decreases were significantly different from the JYK group ($p < 0.001$).

For the between-within-subject ANOVA on the 20% trimmed means, the main effects and interaction of the ODI total score, VAS score and different terms of the ODI score were all significant, with single effects of intervention as the main focus, as shown in Table 3,4. There was no significant difference between YBT and JYK groups after 7 days of treatment in terms of lifting, walking and sleeping, and within the pairwise group comparisons of standing (not average) ($p > 0.05$). However, statistically significant differences were found between the groups in other ODI scores at each time point, as shown in Table 4 ($p < 0.05$).

As shown in Fig. 2, the mean VAS score of both groups decreased gradually, and no comparable difference in VAS score was found between the groups on days 0 and 7
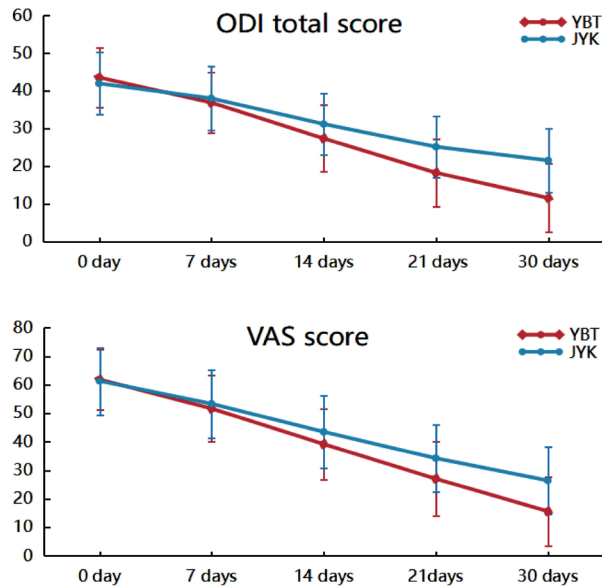
Fig. 2. Mean change of the Oswestry Disability Index (ODI) (A) and visual analogue scale (VAS) score (B). The means of outcomes are shown for the Yaobitong capsule (YBT) group (diamond) and the Jingyaokang capsule (JYK) group (circle). Measurements were observed at baseline and at 7, 14, 21, and 30 days after intervention. ODI total score ranged from 0 to 45 points and VAS scores ranged from 0 to 100 points

($p > 0.05$). As shown in Table 2,3, the differences in decreased VAS score between YBT and JYK were statistically significant at each time point, and YBT group showed more decline than JYK group ($p < 0.001$).

Safety results

As shown in Table 5, 38 adverse events were reported (YBT group, n = 31 (8.66%); JYK group, n = 7 (5.83%)), as were 11 adverse reactions, with 9 (2.51%) in the YBT group and 2 (1.67%) in the JYK group. In the incidence of adverse events and adverse reactions, no significant difference was found between the 2 groups ($p = 0.435$). Meanwhile, no serious adverse event occurred in any group. Among the 11 cases of adverse reactions, 6 cases exhibited ALT and AST elevation, including 5 (1.40%) cases in the YBT group and 1 (0.83%) in the JYK group. Three (0.84%) cases occurred with γ-GT abnormalities in the YBT group. One (0.28%) case each of BUN elevation, dyspepsia, nausea, and stomach discomfort occurred in the YBT group, and 1 (0.83%) case of tongue numbness was found in the JYK group. Overall, there was no significant difference between the YBT and JYK groups for adverse reactions ($p = 0.738$).

During the study, 59 patients, including 44 (12.29%) in the YBT group and 15 (12.50%) in the JYK group, used drug combinations, and there was no clear difference between the 2 groups ($p = 1.000$) in this regard. After treatment, no statistically significant differences in routine blood, blood biochemical values, urine, stool, occult blood, and electrocardiogram were found compared to those at baseline ($p > 0.05$).

Discussion

Lumbar disc herniation is a major contributor to low back pain and physical dysfunction.[20] Based on TCM theory, LDH is mainly induced by blood stasis and qi (the normal flow of vital energy) stagnation, blocked veins caused by strain, wind-cold dampness, and trauma.[21] In clinical practice, blood stasis, qi stagnation and blocked vein syndrome are the most common syndromes in LDH patients.[22] It is crucial to treat inflammation, improve blood circulation and remove stasis.[23] Yaobitong is a new Chinese patented medicine with the effects of promoting circulation, removing stasis, dispelling wind, clearing collaterals, promoting qi, and relieving pain.

Many studies have developed experimental animal models to verify the efficacy and mechanisms of YBT on LDH. In addition, YBT alleviates LDH symptoms and radiculopathy and increases inflammatory factor serum levels in rats.[24] The LDH mechanism relates to endocrine and immune state regulation and the release of inflammatory factors. A network analysis identified 56 components as active YBT capsule ingredients, including ginsenoside Rg1, ginsenoside Rb1, senkyunolide H, and tetrahydropalmatine. These active ingredients regulate 29 pathways via 87 direct target genes, including MAPK, Ras, PI3K-Akt, and NF-kappa B. These active compounds have been demonstrated to inhibit excessive inflammatory reactions, thereby reducing nerve sensitivity and pain. This, in turn, has been shown to relieve LDH.[25] All theoretical and preliminary experiments provide objective evidence for the effectiveness of YBT in treating LDH.

Our main findings indicate that YBT shows more efficacy in LDH patients than the JYK control drug. In this study, JYK was used as a positive control drug because it is a Chinese patented medicine widely used for cervical spondylosis and LDH, and its significant analgesic, anti-inflammatory and detumescence pharmacological effects are similar to YBT.[26,27] Yaobitong significantly decreased the ODI and

Table 5. Comparison of adverse events and adverse reactions

Item	YBT (n = 358)		JYK (n = 120)		p-value
	frequency	case [%]	frequency	case [%]	
Adverse events	31	8.66	7	5.83	0.435
Adverse reactions	9	2.51	2	1.67	0.738

Comparison between YBT group and JYK group done using the Fisher's exact probability method. YBT – Yaobitong capsule; JYK – Jingyaokang capsule.

VAS scores, which may demonstrate that it could improve low back and leg dysfunction and pain. In addition, the curative effect of YBT was better than that of JYK, particularly in the degree of pain, as well as in enhancing daily self-care ability, sitting, standing, and social life in general.

Safety analysis showed that YBT was as safe as JYK. The adverse reactions of YBT manifested as elevated ALT/AST, abnormal γ-GT, elevated BUN, dyspepsia, nausea, and stomach discomfort, indicating YBT may cause liver and kidney dysfunction and gastrointestinal reactions in clinical use. Thus, although few cases were observed, close attention should be given when using YBT in the clinic.

Although NSAIDs are still widely used for pain relief in LDH, taking them regularly should be reduced due to adverse gastrointestinal reactions and the risk of drug dependence.[28] Yaobitong was used in combination with the NSAID celecoxib as routine drugs in some clinical trials.[29] Clinical evidence also shows that YBT, combined with other therapies such as acupuncture, massage and functional exercise is more effective for LDH patients and can be generally used as a reliable and safe option.[30,31]

Limitations

The current study had several limitations, with the 30-day follow-up intervention period being insufficient to confirm the long-term effects of YBT. Second, a dose-dependent YBT design, which could enhance clinical evidence, was not included in this study. Third, manually measuring the VAS score may result in systematic error; an electronic scale is the currently preferred option. Fourth, the study lacked a comparison of YBT and JYK with traditional painkillers and NSAIDs. However, despite these limitations, this trial provides objective and clinically beneficial outcomes for comparing the effects of YBT and JYK.

Conclusions

This multicenter, randomized, double-blinded, parallel, positive-controlled clinical trial conducted in China to assess the efficacy and safety of YBT for LDH patients showed that the curative effect of YBT was significantly better than the JYK control drug, which has been widely used in the market, particularly for alleviating pain and enhancing physical function, which are the most affected aspects in LDH patients. Taken together, YBT appears to be a safe and effective treatment option for LDH patients who do not wish or cannot receive surgical treatment.

Supplementary data

The Supplementary materials are available at https://doi.org/10.5281/zenodo.10671690. The package includes the following files:

Supplementary Table 1. Kolmogorov–Smirnov test of ODI and VAS score relative to baseline.

Supplementary Table 2. Bartlett's test of ODI and VAS score relative to baseline.

Supplementary Table 3. Levene's test of ODI and VAS score relative to baseline.

Supplementary Fig. 1. QQ plot of rate of decline from baseline in ODI score (ODI1_0: 7D-0D, ODI2_0: 14D-0D, ODI3_1: 21D_0D, ODI4_1: 30D_0D).

Supplementary Fig. 2. QQ plot of decline from baseline in VAS score (VAS1_0: 7D-0D, VAS2_0: 14D-0D, VAS3_0: 21D-0D, VAS4_0: 30D-0D).

Data availability

The datasets generated and/or analyzed during the current study are available from the corresponding author on reasonable request.

Consent for publication

Not applicable.

ORCID iDs

Ye Zhao https://orcid.org/0000-0002-9561-6435
Shi Rong Huang https://orcid.org/0009-0009-3212-6082
Yu Jie Zhang https://orcid.org/0000-0003-1588-8842
Yong Qiang Chen https://orcid.org/0009-0003-5800-0935
Wen Gang Liu https://orcid.org/0009-0003-1043-7337
Fu Shun Gu https://orcid.org/0009-0005-5794-9051
Hui Wen https://orcid.org/0009-0009-7533-1641
Xi Lin Xu https://orcid.org/0009-0008-7276-6933
Jiu Yi Chen https://orcid.org/0009-0000-8081-4634
Da Xiang Jin https://orcid.org/0009-0005-5159-4173
Hong Yin https://orcid.org/0009-0003-0540-0556
Zhong Dong https://orcid.org/0009-0005-0594-710X
Hong Sheng Zhan https://orcid.org/0000-0002-6442-7244
Wei An Yuan https://orcid.org/0000-0003-1025-2319

References

1. Liu K, Huo H, Jia W, et al. *RAB40C* gene polymorphisms rs62030917 and rs2269556 are associated with an increased risk of lumbar disc herniation development in the Chinese Han population. *J Gene Med*. 2021;23(4):e3252. doi:10.1002/jgm.3252
2. Zhang L, Chang T, Xu Y, Jing Q, Zhao X, Li C. Epidural anesthesia with low concentration ropivacaine and sufentanil for percutaneous transforaminal endoscopic discectomy: A randomized controlled trial. *Front Med (Lausanne)*. 2020;7:362. doi:10.3389/fmed.2020.00362
3. Buchmann N, Preuß A, Gempt J, et al. Outcome after surgical treatment for late recurrent lumbar disc herniations in standard open microsurgery. *World Neurosurg*. 2016;89:382–386. doi:10.1016/j.wneu.2016.02.028
4. James SL, Abate D, Abate KH, et al. Global, regional, and national incidence, prevalence, and years lived with disability for 354 diseases and injuries for 195 countries and territories, 1990–2017: A systematic analysis for the Global Burden of Disease Study 2017. *Lancet*. 2018;392(10159):1789–1858. doi:10.1016/S0140-6736(18)32279-7
5. Yuan P, Shi X, Wei X, Wang Z, Mu J, Zhang H. Development process and clinical application of collagenase chemonucleolysis in the treatment of lumbar disc herniation: A narrative review in China. *Postgrad Med J*. 2023;99(1172):529–534. doi:10.1136/postgradmedj-2021-141208

42

Y. Zhao et al. Efficacy and safety of Yaobitong capsule

6. Xu Z, Wu S, Li X, Liu C, Fan S, Ma C. Ultrasound-guided transforaminal injections of platelet-rich plasma compared with steroid in lumbar disc herniation: A prospective, randomized, controlled study. *Neural Plast*. 2021;2021:5558138. doi:10.1155/2021/5558138

7. Ozer AF, Keskin F, Oktenoglu T, et al. A novel approach to the surgical treatment of lumbar disc herniations: Indications of simple discectomy and posterior transpedicular dynamic stabilization based on Carragee classification. *Adv Orthop*. 2013;2013:270565. doi:10.1155/2013/270565

8. Pereira P, Avelino A, Monteiro P, Vaz R, Castro-Lopes JM. New insights from immunohistochemistry for the characterization of epidural scar tissue. *Pain Physician*. 2014;17(5):465–474. PMID:25247903.

9. Zhang B, Xu H, Wang J, Liu B, Sun G. A narrative review of non-operative treatment, especially traditional Chinese medicine therapy, for lumbar intervertebral disc herniation. *Biosci Trends*. 2017;11(4):406–417. doi:10.5582/bst.2017.01199

10. Schoenfeld A, Weiner B. Treatment of lumbar disc herniation: Evidence-based practice. *Int J Gen Med*. 2010;3:209–214. doi:10.2147/IJGM.S12270

11. Kavadar G, Eroğlu Demï RS, Aytekï N E, Akbal Y. Use of traditional and complementary medicine for musculoskeletal diseases. *Turk J Med Sci*. 2019;49(3):809–814. doi:10.3906/sag-1509-71

12. Luo Y, Huang J, Xu L, Zhao W, Hao J, Hu Z. Efficacy of Chinese herbal medicine for lumbar disc herniation: A systematic review of randomized controlled trials. *J Tradit Chin Med*. 2013;33(6):721–726. doi:10.1016/S0254-6272(14)60003-0

13. Zhang X, Yang K, Wang S, et al. Efficacy and safety of Yaobitong capsule for acute lumbar disc herniation: A protocol for a multi-center randomized controlled trial. *Medicine (Baltimore)*. 2022;101(47):e31533. doi:10.1097/MD.0000000000031533

14. Hu Y. *Lumbar Disc Herniation* [in Chinese]. 3rd ed. Beijing, China: People's Medical Publishing House; 2004. ISBN:978-7-5067-3729-6.

15. Liang B, Zhang F, Xiao T, Yang Y, Zhang W. Application of big data digitization in the study of functional exercises system under expert database diagnostic technology. Paper presented at the 2021 IEEE International Conference on Data Science and Computer Application (ICDSCA), October 29, 2021; Dalian, China; 2021:477–481. doi:10.1109/ICDSCA53499.2021.9650188

16. Brodke DS, Goz V, Voss MW, Lawrence BD, Spiker WR, Hung M. PROMIS PF CAT outperforms the ODI and SF-36 physical function domain in spine patients. *Spine (Phila Pa 1976)*. 2017;42(12):921–929. doi:10.1097/BRS.0000000000001965

17. Melloh M, Elfering A, Salathé CR, et al. Predictors of sickness absence in patients with a new episode of low back pain in primary care. *Ind Health*. 2012;50(4):288–298. doi:10.2486/indhealth.MS1335

18. Boonstra AM, Schiphorst Preuper HR, Balk GA, Stewart RE. Cut-off points for mild, moderate, and severe pain on the visual analogue scale for pain in patients with chronic musculoskeletal pain. *Pain*. 2014;155(12):2545–2550. doi:10.1016/j.pain.2014.09.014

19. Mair P, Wilcox R. Robust statistical methods in R using the WRS2 package. *Behav Res*. 2020;52(2):464–488. doi:10.3758/s13428-019-01246-w

20. Cunha C, Silva AJ, Pereira P, Vaz R, Gonçalves RM, Barbosa MA. The inflammatory response in the regression of lumbar disc herniation. *Arthritis Res Ther*. 2018;20(1):251. doi:10.1186/s13075-018-1743-4

21. Shi Q. *Clinical Research on Orthopedics and Traumatology of Chinese Medicine* [in Chinese]. Beijing, China: People's Medical Publishing House; 2009. ISBN:978-7-117-11161-4.

22. Guo R. Randomized parallel controlled study of warming acupuncture combined with Yaotong Ning for treating lumbar disc herniation [In Chinese]. *Journal of Pratical Traditional Chinese Internal Medicine*. 2018;32(11):43–45. doi:10.13729/j.issn.1671-7813.Z20180146

23. Li C, Zhang X, Li H, et al. Brain edema after intracerebral hemorrhage in rats: The role of inflammation. *Neurol India*. 2006;54(4):402. doi:10.4103/0028-3886.28115

24. Tang CH, Cao L, Ding G, Wang Z, Xiao W. Efficiency and influence of inflammatory cytokines by Yaobitong capsule in rat lumbar disc herniation [in Chinese]. *Chinese Journal of Experimental Traditional Medical Formula*. 2015;21(5):155–158. doi:10.13422/j.cnki.syfjx.2015050155

25. Deng Y, Gao X, Feng T, et al. Systematically characterized mechanism of treatment for lumbar disc herniation based on Yaobitong capsule ingredient analysis in rat plasma and its network pharmacology strategy by UPLC-MS/MS. *J Ethnopharmacol*. 2020;260:113097. doi:10.1016/j.jep.2020.113097

26. Xu J, Jiang WY, Wang YL. Study on anti-inflammatory and detumescent pharmacodynamic material basis of Jingyaokang capsule [in Chinese]. *China Pharmacy*. 2018;4:478–483.

27. Zhong T, Qui BC, Xiang QS. Clinical study on Jingyaokang capsules combined with diclofenac sodium in treatment of lumbar disc herniation [in Chinese]. *Drugs and Clinic*. 2019;34(12):3712–3715. https://www.tiprpress.com/xdywlc/article/abstract/20191247. Accessed July 15, 2023.

28. Zhang SY, Li B, Xiang QS. "Yaobitong capsule" for prolapsed lumbar intervertebral discs in 65 cases [in Chinese]. *Shanghai Journal of Traditional Chinese Medicine*. 2004;3:33–34. doi:10.16305/j.1007-1334.2004.03.015

29. Li H, Ge D, Liu S, et al. Baduanjin exercise for low back pain: A systematic review and meta-analysis. *Complement Ther Med*. 2019;43:109–116. doi:10.1016/j.ctim.2019.01.021

30. Zhang C, Li X, Peng W, Jia H, Cai L. Treating lumbar disc herniation of blood stasis type with Chinese herbs, acupuncture, moxibustion, and massage: A Bayesian network meta-analysis [in Chinese]. *Chinese Journal of Tissue Engineering Research*. 2021;25(17):2781–2788. doi:10.3969/j.issn.2095-4344.3170

31. Li Y, Jin H, Liu X, Yu H. Clinical observation on 120 cases of lumbar disc herniation treated with Yaotongning capsule. *Pak J Pharm Sci*. 2020;33(1(Special)):433–436. PMID:32173639.

Expression of CD226 on γδ T cells is lower in advanced chronic lymphocytic leukemia and correlates with IgA, IgG and LDH levels

Michał K. Zarobkiewicz[1,A–D], Natalia Lehman[1,B,F], Wioleta Kowalska[1,B,E,F], Izabela Dąbrowska[2,B,E,F], Agnieszka Bojarska-Junak[1,A,D–F]

[1] Department of Clinical Immunology, Medical University of Lublin, Poland

[2] Department of Interventional Radiology and Neuroradiology, Medical University of Lublin, Poland

A – research concept and design; B – collection and/or assembly of data; C – data analysis and interpretation;
D – writing the article; E – critical revision of the article; F – final approval of the article

Address for correspondence
Michał K. Zarobkiewicz
E-mail: michal.zarobkiewicz@umlub.pl

Abstract

Background. Gamma-delta (γδ) T cells comprise an important subset of human T cells, responding to viral and bacterial infections, and are significant for cancer immunosurveillance. Human γδ T cells are divided into 5 major subsets, namely Vδ1–Vδ5, of which the latter 3 have limited available literature. At present, Vδ2 is the most studied subpopulation.

Objectives. In the current paper, we focused on non-Vδ2 cells in chronic lymphocytic leukemia (CLL). We assessed the expression of co-inhibitory checkpoint receptors (CTLA-4, PD-1 and TIGIT) and co-stimulatory (CD226 and NKp30) molecules separately on Vδ1 and Vδ3–Vδ5 cells.

Materials and methods. We assessed γδ T cells for their expression of both cytotoxicity-related (NKp30, CD226) and co-inhibitory (PD-1, TIGIT) molecules with flow cytometry in CLL patients. Moreover, we evaluated the expression of TIGIT and CD226 ligand (PVR , CD155) in neoplastic B cells in CLL patients with quantitative real-time polymerase chain reaction (qPCR).

Results. A significant accumulation of Vδ1 T cells was noted, while no difference was observed in the total percentage of Vδ2 cells. Contrary to our initial hypothesis, the impact of CLL burden on CD226 and TIGIT expression was lower than anticipated. The former tends to be lower in more advanced disease. Finally, a strong upregulation of CD155 (PVR) was noted on CLL-derived B cells when compared to healthy B cells.

Conclusions. Chronic lymphocytic leukemia regulates the expression of the CD155-CD226/TIGIT axis. Contrary to expectations, the ligand is significantly more affected than the receptors. Nevertheless, the relatively high expression of CD155 and TIGIT makes CLL an interesting target for anti-TIGIT immunotherapy.

Key words: CLL, Vδ1, chronic lymphocytic leukemia, Vδ3–Vδ5, γδ T

Background

Chronic lymphocytic leukemia (CLL) is an indolent leukemia derived from mature B cells.[1] It is mainly diagnosed in older adults and is the most common adult leukemia.[2,3] However, despite significant progress, it remains incurable.[4] Thus, patients are commonly observed, and treatment is initiated only after certain conditions are fulfilled.[4] Furthermore, CLL is associated with a high tumor burden as neoplastic B cells can easily comprise >90% of the total peripheral blood mononuclear cells.[5] This leads to the creation of a significant immunosuppressive environment and pushes T cells towards exhaustion.[6,7] Exhausted T cells show alterations in their cytokine secretion profiles, low proliferative rates and, most importantly, overexpression of multiple inhibitory receptors on their surfaces (e.g., PD-1, Lag-3, Tim-3, or TIGIT).[8] Notably, T cell exhaustion is comprehensively described for αβ T lymphocytes and the Vδ2 subset of human γδ T cells.[9]

Gamma-delta T cells constitute a major subset of unconventional T cells and are characterized by the expression of TCR γ and δ chains instead of α and β chains. Murine γδ T cells are usually split up into subsets by their Vγ fragment, while human γδ T cells can be divided based on Vδ fragment into Vδ1–Vδ5.[10,11] Vδ2 cells comprise the major subset of circulating γδ T cells and can be easily expanded in vitro with aminobisphosphonates. Therefore, the majority of γδ T cell research is oriented towards the Vδ2 subtype.[12,13] Vδ1 cells constitute the 2nd largest portion of γδ T cells in peripheral blood, but due to more complicated protocols for their expansion, they are far less understood.[14] Vδ3, Vδ4 and Vδ5 are virtually unstudied, mostly due to the lack of appropriate monoclonal antibodies that enable easy immunophenotyping or sorting.

Gamma-delta T cells are severely affected by the CLL disease burden.[13] However, current data suggest that this applies unequally to different subsets. While Vδ2 cells show signs of exhaustion and are usually almost unresponsive, Vδ1 cells remain highly active in a large portion of CLL patients.[9,15] Indeed, expansion and domination of Vδ1

may have an important positive influence on the course of CLL.[13,15] While the clinical-grade large-scale expansion of autologous Vδ2 lymphocytes currently seems unreachable, there are such attempts with Vδ1 cells.[14] Nevertheless, successful immunotherapy with Vδ1 cells requires a better understanding of the impact that CLL has on both γδ T cells as a whole and their non-Vδ2 compartment.

Objectives

The current paper presents the results of immunophenotyping of human non-Vδ2 cells in CLL patients. The study was based on the hypothesis that the immunosuppressive CLL environment would upregulate the expression of co-inhibitory molecules while downregulating the co-stimulatory potential. Finally, we demonstrated that non-Vδ2 cells seem to be mildly affected by CLL, at least in terms of co-inhibitory and co-stimulatory molecule expression.

Materials and methods

Patients and material

A total of 37 treatment-naïve patients diagnosed with CLL were recruited from the Department of Hematooncology and Bone Marrow Transplantation at the Medical University of Lublin (Poland). Disease staging was performed according to the Rai classification.[4,16] An age- and sex-matched control group was recruited from the Department of Interventional Radiology and Neuroradiology at the Medical University of Lublin and consisted of 20 individuals. Peripheral blood mononuclear cells (PBMCs) were obtained by gradient centrifugation in LSM 1077 (PromoCell, Heidelberg, Germany). Clinically important data were obtained from hospital records, including gene deletions in *ATM* (11q22.3 locus) and *TP53* (17p13.1 locus). Table 1 summarizes the basic characteristics of patients and controls.

Table 1. Characteristics of patients and controls

Characteristics	Patients	Controls
Number of patients	37	20
Percentage of men	53.38%	61.11%
Age, mean (±SD)	64.46 (±10.73)	65 (±10.58)
Percentage of ZAP-70-positive patients*	23.68%	–
Percentage of CD38+	26.32%	–
Percentage of patients with del(17p13.1) or del(11q22.3)	21.62%	–
Percentage of patients with Rai stage 0 (low-risk)	18.91%	–
Percentage of patients with Rai stages I–II (intermediate-risk)	43.24%	–
Percentage of patients with Rai stages III–IV (high-risk)	37.84%	–

* Leukemic B cells (CD5+/CD19+) were considered positive for ZAP-70 or CD38 expression with a cutoff point of ≥20%. SD – standard deviation.

Immunophenotyping

Peripheral blood mononuclear cells were incubated with a mix of monoclonal antibodies consisting of anti-CD3 APC (BioLegend, San Diego, USA; cat. No. 300439, clone: UCHT1), anti-TCRγδ BV421 (BD Biosciences, Warsaw, Poland; cat. No. 744870, clone: 11F2), anti-Vδ1 FITC (ThermoFisher, Warsaw, Poland; cat. No. TCR2730, clone: TS8.2), anti-Vδ2 PE (BioLegend; cat. No. 331408, clone: B6), anti-CTLA-4 APC-Fire750 (BioLegend; cat. No. 349930, clone: L3D10), anti-PD-1 PE-Cy7 (BD Biosciences, Franklin Lakes, USA; cat. No. 561272, clone: EH12.1), anti-TIGIT BV650 (BD Biosciences; cat. No. 747840, clone: 741182), anti-NKp30 BV785 (BioLegend; cat No. 325230, clone: P30-15), and anti-CD226 BV605 (BD Biosciences; cat. No. 742495, clone: DX11). Fluorescence minus one (FMO) controls were used to set the correct gates for each fluorophore. Samples were acquired on a Cytoflex LX (Beckman Coulter, Warsaw, Poland) and analyzed with FlowJo 10 (BD Biosciences). The percentage of positive cells was a standard measure for each of the markers except for CD226, where mean fluorescence intensity (MFI) was additionally provided due to its high overall expression.

Bioinformatics

Available RNAseq datasets were used to assess the expression of CD226/TIGIT ligands on the surface of neoplastic B cells. The Chronic Lymphocytic Leukemia (Broad, Nature 2015) dataset was queried on cBioPortal.[17–19] The expression of *PVR, NECTIN2* and *NECTIN3* was assessed in a subset of 157 CLL patients with mRNA expression data. Expression in transcripts-per-million (TPM) was extracted.

qPCR

B cells were isolated magnetically from healthy donors and CLL patients with anti-CD19 microbeads and LS columns (Miltenyi Biotec, Bergisch Gladbach, Germany). Total RNA was isolated with a Blood RNA Mini kit (Qiagen, Hilden, Germany) and reverse transcription was performed with QuantiTect Reverse Transcription Kit (Qiagen). Finally, quantitative real-time polymerase chain reaction (qPCR) was performed with qPCR Master Mix (Promega, Madison, USA) and primers for *PVR* and *GAPDH*. Reactions were run with the Applied Biosystems 7300 Real-Time PCR System (Applied Biosystems, Austin, USA). Gene expression was normalized to *GAPDH* and is presented as $2^{-\Delta CT}$. Primer sequences:

PVR for.: 5' GGATATCTGGCTCCGAGTGC 3'
PVR rev.: 5' CTCCACCTTGCAGGTCACAT 3'
GAPDH for.: 5' ATCACCATCTTCCAGGAGCG 3'
GAPDH rev.: 5' TGGACTCCACGACGTACTCA 3'

Statistical analyses

Results were analyzed with GraphPad Prism v. 9 (GraphPad Software, San Diego, USA) and JASP 0.16.3 (Department of Psychological Methods, University of Amsterdam, Netherlands). A Shapiro–Wilk test was used for data distribution analysis. The p-values were calculated with Mann–Whitney U tests, and differences were considered significant when $p < 0.05$. Data are presented as the median and interquartile range (IQR). Correlations were assessed with a Spearman's test. In the statistical analysis, we employed an exploratory approach, not including a correction for families of hypotheses, which leads to an increased risk of type 1 error. Thus, the results must be interpreted with caution. The study might serve as a starting point for further research in the field. Detailed p-values for each comparison are presented in Supplementary Table 1.

Results

Vδ1 cells are expanded in CLL patients

First, we assessed the percentage of Vδ1 and Vδ2 T cells. While the percentage of Vδ2 cells seemed unaffected by CLL, Vδ1 lymphocytes were significantly expanded (0.33% in healthy volunteers (HV) compared to 0.98% in the CLL group) (Fig. 1A). Vδ3–Vδ5 subset was gated among Vδ1- and Vδ2-negative cells (Fig. 1B). Next, we assessed the expression of NKp30 and CD226 on each subset, again without any significant differences (Fig. 2,3). Finally, we assessed the expression of checkpoint molecules on Vδ1 and Vδ3–Vδ5 subsets. No significant differences were noted, except for the downregulation of CTLA-4 on Vδ1 (2.99% in HV compared to 1.67% in CLL) (Fig. 4)

CD226 expression is higher in ZAP-70 negative cases

Next, we checked whether CD38 and ZAP-70 status significantly affected the immune parameters we tested. Out of all the markers, only CD226 MFI increased significantly between ZAP-70 positive and negative cases (19,041 compared to 15,058) (Fig. 5A). No differences were noted for the remaining parameters (TIGIT, PD-1, CTLA-4, NKp30) (data not shown).

Patients with known deletions have lower CD226 expression on Vδ2 cells

Out of the total group, 8 patients had some identified deletions, being mostly *TP53* deletions. Thus, we divided patients into those with and without known deletions. Then, we compared the immunological parameters between those 2 groups. Patients with identified deletions
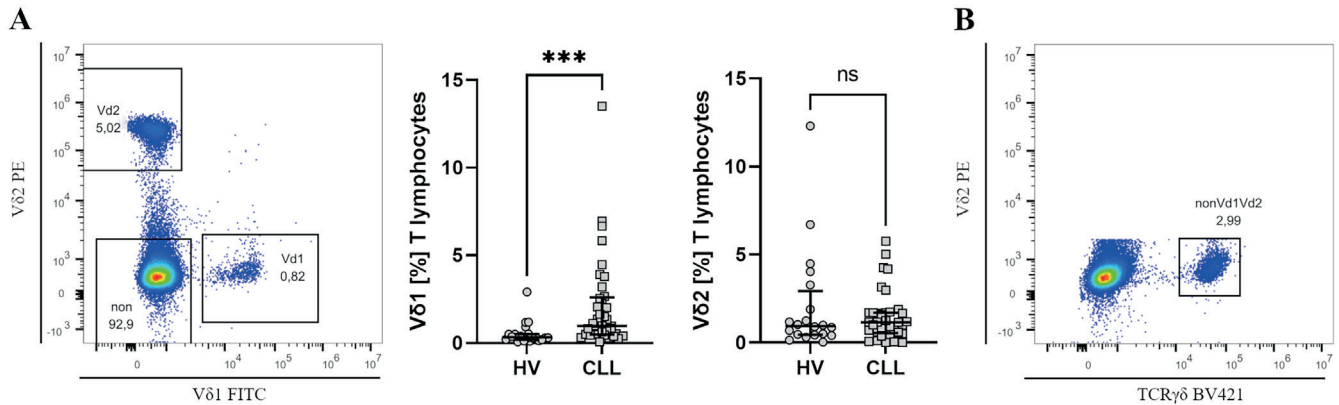
Fig. 1. The identification of γδ T subsets along with CD226 and NKp30 expression. Vδ1 and Vδ2 cells were gated among CD3+ lymphocytes (A), while non-Vδ1–Vδ2 were gated from the negative population (non in A) and then gated as TCRγδ+ HV (healthy volunteers) (B)

* p ≤ 0.05; ** p ≤ 0.01; *** p ≤ 0.001; **** p ≤ 0.0001.
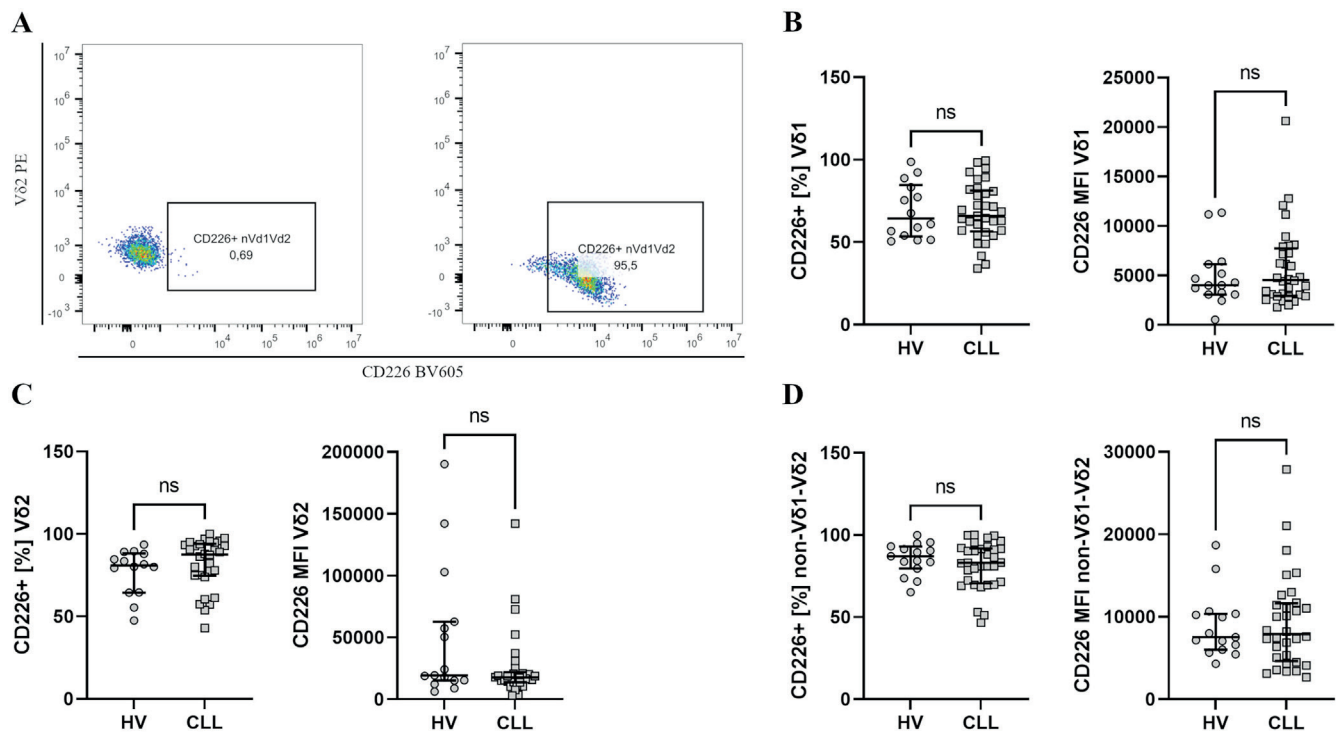
Fig. 2. CD226 expression on γδ T cells. The gating for CD226 was controlled with FMO (fluorescence minus one) controls (A); results are presented separately for each subset – Vδ1 (B), Vδ2 (C) and non-Vδ1–Vδ2 (D)

HV – healthy volunteers; * p ≤ 0.05; ** p ≤ 0.01; *** p ≤ 0.001; **** p ≤ 0.0001.

exhibited significantly lower expression of CD226 on Vδ2 cells compared to those without deletions (77.50% compared to 91.60%). (Fig. 5A).

The percentage of Vδ1 drops with the disease stage, but the expression of CD226 thereon increases

Rai classification is commonly used for the clinical staging of CLL. Thus, we divided patients into 3 groups: stage 0, stages I–II and stages III–IV. The percentage of Vδ1 trended down with an increase in the disease stage, although this

was not significant (Fig. 5B). Interestingly, we noted a significant increase in the expression of CD226 on Vδ1 cells (Fig. 5B). In contrast, CD226 expression on Vδ2 cells decreased with stage progression (Fig. 5B).

CD226/TIGIT ligands expression varies between IGVH mutated and unmutated subjects

Using a publicly available dataset, we assessed the expression of CD226/TIGIT ligands on neoplastic B cells in CLL. Only *PVR (CD155)* had a notable expression,
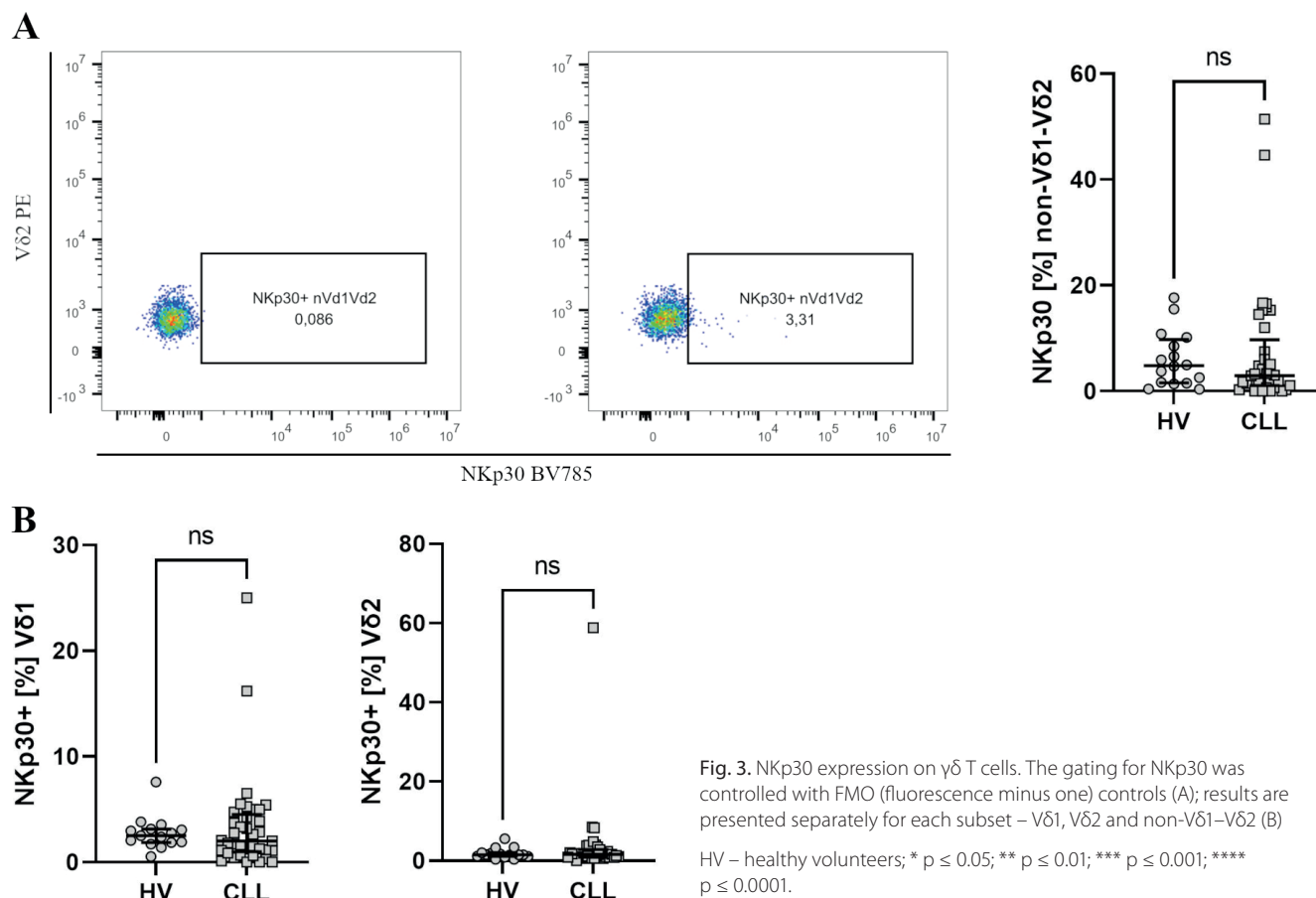
Fig. 3. NKp30 expression on γδ T cells. The gating for NKp30 was controlled with FMO (fluorescence minus one) controls (A); results are presented separately for each subset – Vδ1, Vδ2 and non-Vδ1–Vδ2 (B)

HV – healthy volunteers; * p ≤ 0.05; ** p ≤ 0.01; *** p ≤ 0.001; **** p ≤ 0.0001.

and both *NECTIN2 (CD112)* and *NECTIN3 (CD113)* had negligible expression levels (Fig. 6A). PVR expression was also significantly higher in IGVH unmutated subjects, and no differences were observed for the other 2 ligands (Fig. 6A). The overexpression of *PVR* was also confirmed with qPCR in isolated B cells from CLL patients and HV (Fig. 6B).

CD226 expression on Vδ2 correlates positively with IgA and IgG levels and negatively with LDH

A moderate positive correlation between CD226 (ρ = 0.63) expression on Vδ1 and Vδ3–Vδ5 was noted, and a similar correlation was observed for PD-1 (ρ = 0.727). CD226 expression on Vδ2 cells correlated moderately with lactate dehydrogenase (LDH) levels (ρ = −0.637), immunoglobulin A (IgA) (ρ = 0.608) and IgG (ρ = 0.573) serum concentrations. Moreover, IgG correlated with NKp30+ Vδ1 (ρ = −0.529), while similarly IgA correlated with TIGIT+ Vδ1 (ρ = 0.6) (Fig. 7). For the remaining correlations, the monotonic component of the relationship was not detected, and they are presented in the full matrix of correlations for immunological, hematological and clinical parameters (Supplementary Fig. 1,3).

Discussion

Chronic lymphocytic leukemia, especially a relatively advanced disease, is characterized by an accumulation of highly immunosuppressive cells, e.g., monocytic myeloid-derived suppressor cells (MDSCs) or B regulatory cells (Bregs).[20,21] Such an immunosuppressive environment is believed to promote co-inhibitory checkpoint molecule expression.[22] The expression of co-inhibitory and co-stimulatory molecules, e.g., PD-1, on Vδ2 was previously studied in CLL with some significant differences noted.[23,24] Thus, we focused on non-Vδ2 cells, which are currently lacking investigations. Most importantly, we did not observe any significant upregulation of CTLA-4, PD-1 or TIGIT in either Vδ1 or Vδ3–Vδ5 subsets. This suggests that Vδ1 cells may be less affected by the highly immunosuppressive environment of peripheral blood from CLL patients. Indeed, previous observations, e.g., good response to autologous neoplastic B cells, high cytotoxic potential or good in vitro proliferation, seem to confirm this.[9,14,15] This is in sharp contrast to Vδ2 cells, which tend to be exhausted and dysfunctional in CLL. Moreover, even Vδ2 cells obtained from healthy individuals provide significantly weaker responses to neoplastic B cells.[13,23–25]

CD226, also known as DNAM-1, is an activating receptor important for cytotoxicity of NK and γδ T cells. It competes
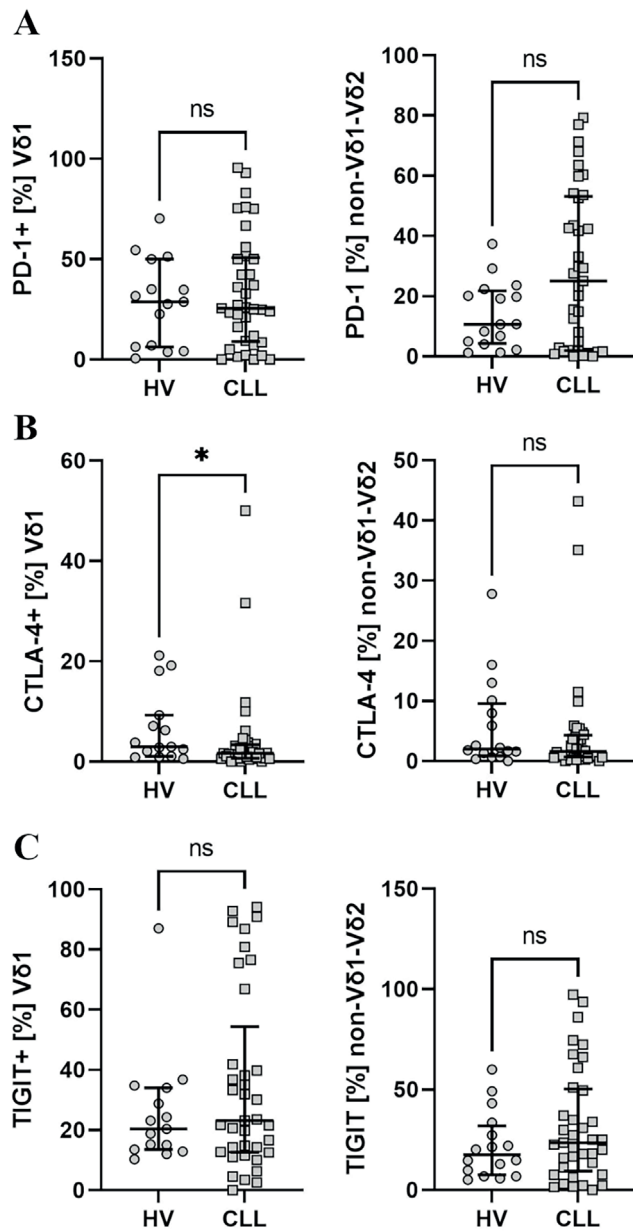
Fig. 4. Expression of checkpoint molecules: PD-1 (A), CTLA-4 (B) and TIGIT (C) was assessed using flow cytometry. Gating was set according to the FMO (fluorescence minus one) controls (presented in Supplementary Fig. 1)

HV – healthy volunteers; * p ≤ 0.05; ** p ≤ 0.01; *** p ≤ 0.001; **** p ≤ 0.0001.

with TIGIT for its ligands, namely PVR (CD155), CD112 and CD113.[26,27] Reduced expression of CD226 on γδ T cells results in decreased cytotoxic potential in neuroblastoma.[8] No differences in CD226 expression were noted for any of the subsets in the current study. This is similar to the observation of CD226 expression on NK cells in CLL.[28] While Veuillen et al. argued that CD226 ligands are rarely expressed by neoplastic B cells in CLL,[29] contrary results were obtained from RNAseq data analysis, namely, a significantly upregulated expression of *PVR (CD155)* was

noted. TIGIT is a novel checkpoint molecule that was discovered in 2009.[30] TIGIT competes with CD226 for their ligands, and studies with blocking antibodies against TIGIT demonstrated that it comprises mostly the Th1-related and cytotoxic response.[31] In this study, we noted an insignificant increase in TIGIT expression on non-Vδ2 cells. This is partly comparable to the situation in acute myeloid leukemia (AML) where, on the one hand, TIGIT expression is increased and, on the other, CD226 is decreased.[32]

Similar to Bartkowiak et al., we observed a significant expansion of Vδ1 in CLL patients,[33] whereas we noted only a small and statistically insignificant expansion of Vδ2 cells, which is in line with de Weerdt et al., who also noted an insignificant accumulation of Vδ2.[23] Interestingly, despite the drop in Vδ1 percentage in patients with more advanced disease, we observed an increase in CD226 expression on Vδ1. This may suggest that Vδ1 retains at least some of its activity and, hopefully, some of its cytotoxic potential. Almeida et al. proposed an optimized protocol for clinical-grade expansion of Vδ1 cells from CLL patients for further use in in vitro immunotherapy.[14] The results of the current study suggest that Vδ1 cells are less affected by the CLL burden than Vδ2 ones, and with such a feasible clinical-grade expansion, they show a real potential for CLL immunotherapy. Vδ1 cells exhibit significant cytotoxicity against leukemic cells and have been observed to persist in the circulation for longer periods than Vδ2 cells.[34] Moreover, Vδ1, both from healthy donors and from CLL patients, are significantly more cytotoxic against CLL cells.[13,15]

ZAP-70 and CD38 are important prognostic factors in CLL.[35] The standard cutoff (as in our study) for positive/negative ZAP-70/CD38 is 20% of positive B cells.[35] After such division, we noted a significantly lower expression of CD226 on Vδ2 cells from ZAP-70-positive patients. Moreover, we have also noted a decreasing trend in CD226 expression on Vδ2 in patients with more advanced disease. This suggests that Vδ2 may be more affected by the immunosuppressive environment of CLL than Vδ1. Lactate dehydrogenase level is commonly considered to be a marker of disease burden with an important prognostic value; the higher the LDH level, the more advanced the disease.[36,37] Similarly, both IgA and IgG have prognostic value, and their low serum level is usually associated with an advanced and progressive disease.[38,39] Thus, correlations of LDH, IgA and IgG on one side and CD226 expression on Vδ2 on the other seem to be a reflection of similar changes related to tumor burden and progressing dysfunction of Vδ2 cells. The presence of PVR overexpression, a known CD226/TIGIT-ligand, on neoplastic B cells suggests that the CD226/TIGIT–PVR axis may be a significant target for therapeutic modulations. In addition, since Vδ1 cells appear to be much less susceptible to CLL-induced immunosuppression, Vδ1 immunotherapy could be used together with CD226/TIGIT PVR modulators.

A

B
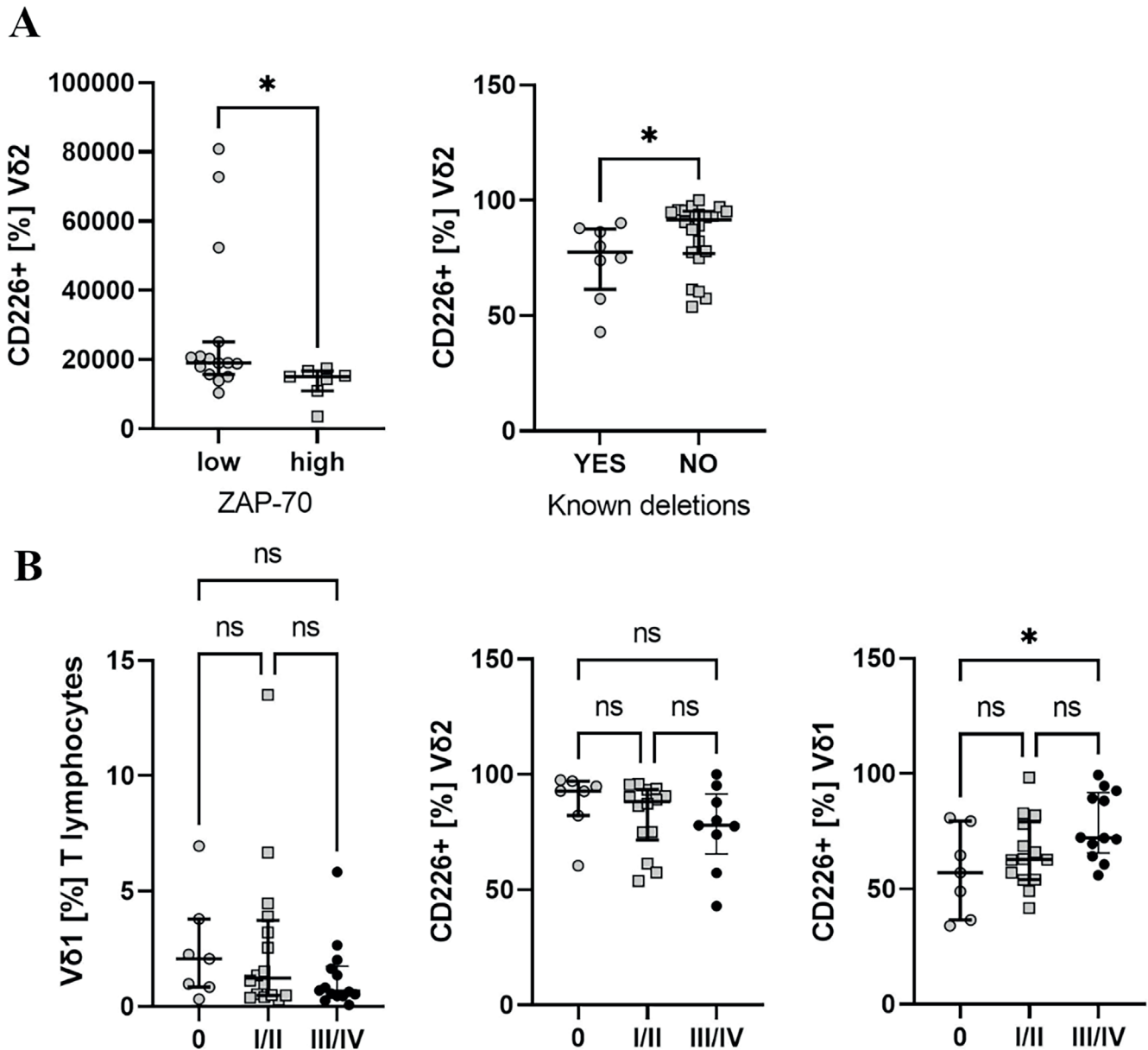
Fig. 5. Differences in immunological parameters in patients in high/low risk groups (cutoff point: 20% positive B cells). Each patient was screened for *TP53* and *ATM* deletions; no known deletions means that neither of those genes was affected (A); different stages of disease (B)

* $p \leq 0.05$; ** $p \leq 0.01$; *** $p \leq 0.001$; **** $p \leq 0.0001$.

Limitations

The current study has some important limitations. First, the Vδ3–Vδ5 cells were analyzed as a whole due to the lack of appropriate monoclonal antibodies. Specifically, there are no anti-Vδ3, anti-Vδ4 or anti-Vδ5 antibodies available on the market. Moreover, the current study lacks any functional analyses. Due to COVID-19, we were experiencing a decrease in the number of patient samples and patients at more advanced stages of the disease reported to the clinic. Most samples did not allow for cell cultures and functional studies. Finally, as the inter-group comparisons and Spearman's correlation analysis were pre-planned, we decided to employ no post hoc correction for p-value calculations which may have increased the risk of type I error.

Conclusions

Gamma-delta T cells are a heterogeneous group of T cells. The current study suggests that the non-Vδ2 subset of γδ T cells is less affected by the immunosuppressive environment of CLL than the Vδ2 population. This is further corroborated by previously published results regarding cytotoxicity and activation triggered by CLL-derived B cells.
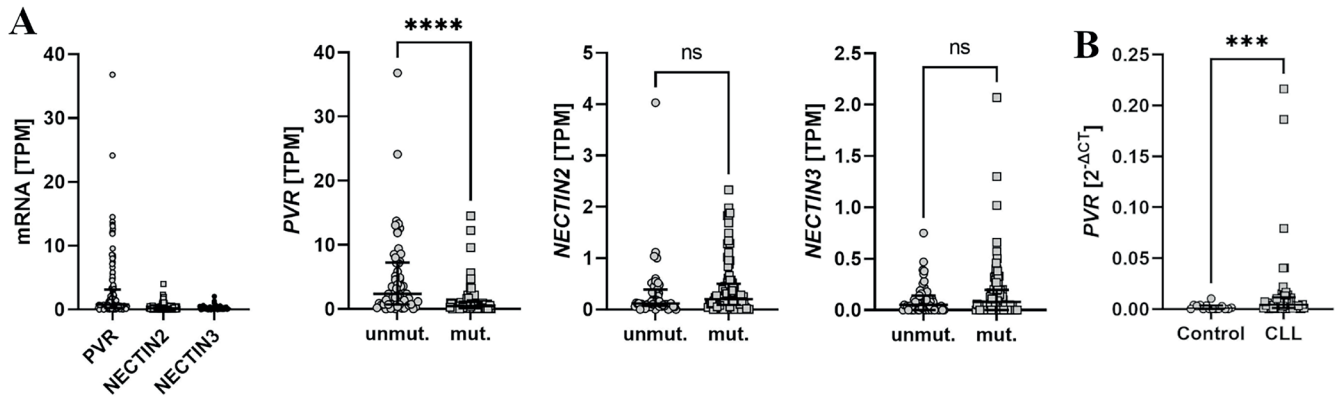
Fig. 6. Expression of CD226/TIGIT ligands on chronic lymphocytic leukemia (CLL) B cells was assessed in publicly available RNAseq datasets (A). *PVR* expression was assessed using real-time quantitative polymerase chain reaction (qPCR) in isolated B cells from CLL patients and healthy volunteers (B). Gene expression was normalized against *GAPDH*

unmut – unmutated IGVH; mut – mutated IGVH; * $p \leq 0.05$; ** $p \leq 0.01$; *** $p \leq 0.001$; **** $p \leq 0.0001$.
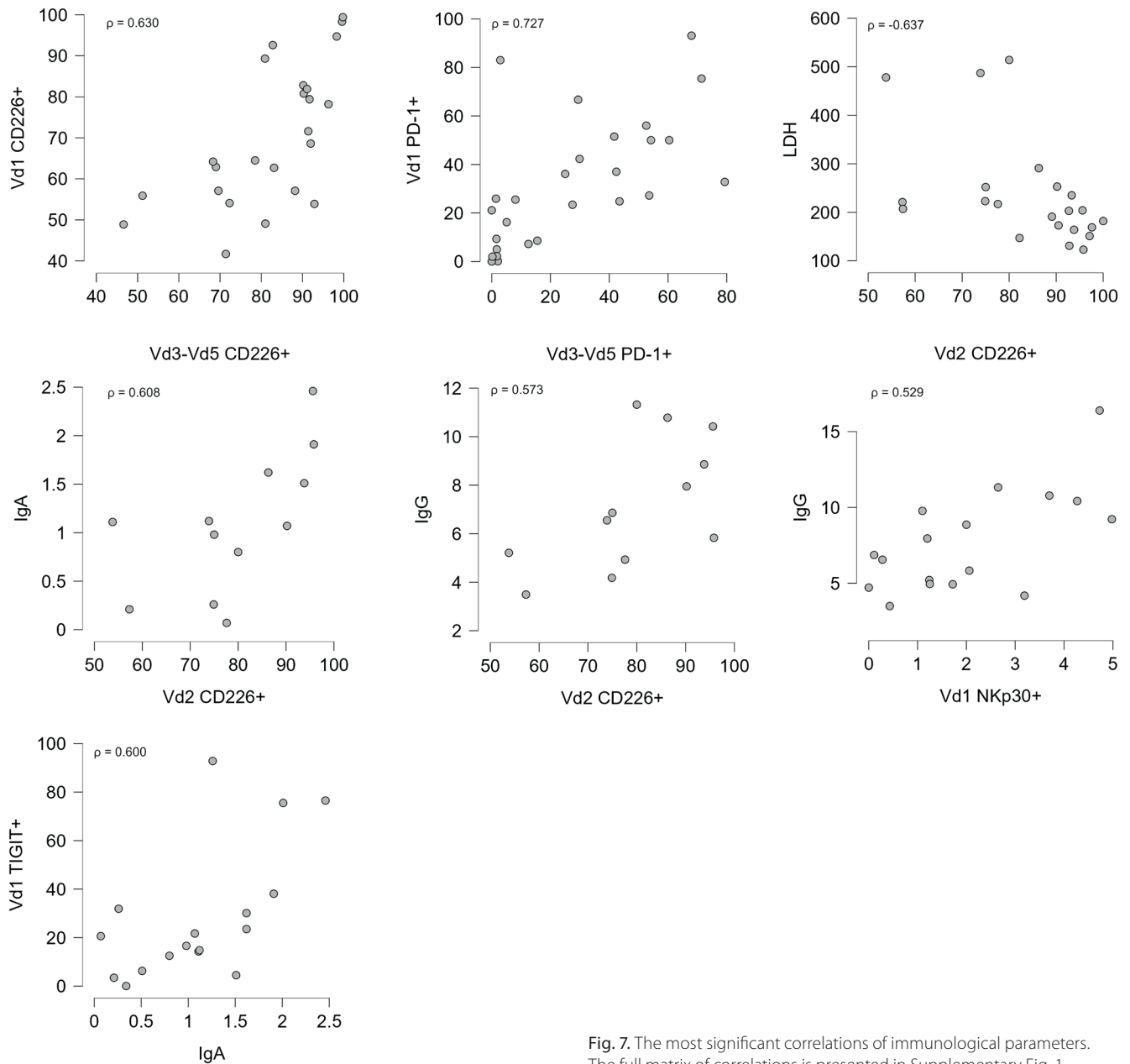
Fig. 7. The most significant correlations of immunological parameters. The full matrix of correlations is presented in Supplementary Fig. 1

Supplementary data

The Supplementary materials are available at https://zenodo.org/doi/10.5281/zenodo.10848380. The package includes the following files:

Supplementary Fig. 1. Gating strategy.

Supplementary Fig. 2. The full matrix of correlations.

Supplementary Fig. 3. Scatter plots for each correlation pair.

Supplementary Table 1. Exact p-values for intergroup comparisons.

Data availability

The datasets generated and/or analyzed during the current study are available from the corresponding author on reasonable request.

Consent for publication

Not applicable.

ORCID iDs

Michał K. Zarobkiewicz https://orcid.org/0000-0003-0788-6353
Natalia Lehman https://orcid.org/0000-0003-2324-5679
Wioleta Kowalska https://orcid.org/0000-0003-2324-5679
Izabela Dąbrowska https://orcid.org/0000-0003-0930-5874
Agnieszka Bojarska-Junak https://orcid.org/0000-0003-2340-9442

References

1. Seifert M, Sellmann L, Bloehdorn J, et al. Cellular origin and pathophysiology of chronic lymphocytic leukemia. *J Exp Med*. 2012;209(12):2183–2198. doi:10.1084/jem.20120833
2. Tietsche De Moraes Hungria V, Chiattone C, Pavlovsky M, et al. Epidemiology of hematologic malignancies in real-world settings: Findings from the Hemato-Oncology Latin America Observational Registry Study. *J Glob Oncol*. 2019;2019:1–19. doi:10.1200/JGO.19.00025
3. Watson L, Wyld P, Catovsky D. Disease burden of chronic lymphocytic leukaemia within the European Union. *Eur J Haematol*. 2008;81(4):253–258. doi:10.1111/j.1600-0609.2008.01114.x
4. Hallek M, Cheson BD, Catovsky D, et al. iwCLL guidelines for diagnosis, indications for treatment, response assessment, and supportive management of CLL. *Blood*. 2018;131(25):2745–2760. doi:10.1182/blood-2017-09-806398
5. Wodarz D, Garg N, Komarova NL, et al. Kinetics of CLL cells in tissues and blood during therapy with the BTK inhibitor ibrutinib. *Blood*. 2014;123(26):4132–4135. doi:10.1182/blood-2014-02-554220
6. Riches JC, Davies JK, McClanahan F, et al. T cells from CLL patients exhibit features of T-cell exhaustion but retain capacity for cytokine production. *Blood*. 2013;121(9):1612–1621. doi:10.1182/blood-2012-09-457531
7. Forconi F, Moss P. Perturbation of the normal immune system in patients with CLL. *Blood*. 2015;126(5):573–581. doi:10.1182/blood-2015-03-567388
8. Vlachonikola E, Stamatopoulos K, Chatzidimitriou A. T cells in chronic lymphocytic leukemia: A two-edged sword. *Front Immunol*. 2021;11:612244. doi:10.3389/fimmu.2020.612244
9. Simões C, Silva I, Carvalho A, et al. Quantification and phenotypic characterization of peripheral blood Vδ1⁺ T cells in chronic lymphocytic leukemia and monoclonal B cell lymphocytosis. *Cytometry B Clin Cytom*. 2019;96(2):164–168. doi:10.1002/cyto.b.21645
10. Shiromizu CM, Jancic CC. γδ T lymphocytes: An effector cell in autoimmunity and infection. *Front Immunol*. 2018;9:2389. doi:10.3389/fimmu.2018.02389
11. Pang DJ, Neves JF, Sumaria N, Pennington DJ. Understanding the complexity of γδ T-cell subsets in mouse and human. *Immunology*. 2012;136(3):283–290. doi:10.1111/j.1365-2567.2012.03582.x
12. Kondo M, Izumi T, Fujieda N, et al. Expansion of human peripheral blood gamma and delta T cells using zoledronate. *J Vis Exp*. 2011;55:3182. doi:10.3791/3182
13. Zarobkiewicz MK, Bojarska-Junak AA. The mysterious actor: γδ T lymphocytes in chronic lymphocytic leukaemia (CLL). *Cells*. 2022;11(4):661. doi:10.3390/cells11040661
14. Almeida AR, Correia DV, Fernandes-Platzgummer A, et al. Delta one T cells for immunotherapy of chronic lymphocytic leukemia: Clinical-grade expansion/differentiation and preclinical proof of concept. *Clin Cancer Res*. 2016;22(23):5795–5804. doi:10.1158/1078-0432.CCR-16-0597
15. Poggi A, Venturino C, Catellani S, et al. Vδ1 T lymphocytes from B-CLL patients recognize ULBP3 expressed on leukemic B cells and upregulated by *trans*-retinoic acid. *Cancer Res*. 2004;64(24):9172–9179. doi:10.1158/0008-5472.CAN-04-2417
16. Rai KR, Sawitsky A, Cronkite EP, Chanana AD, Levy RN, Pasternack BS. Clinical staging of chronic lymphocytic leukemia. *Blood*. 1975;46(2):219–234. PMID:1139039.
17. Gao J, Aksoy BA, Dogrusoz U, et al. Integrative analysis of complex cancer genomics and clinical profiles using the cBio portal. *Sci Signal*. 2013;6(269):pl1. doi:10.1126/scisignal.2004088
18. Cerami E, Gao J, Dogrusoz U, et al. The cBio cancer genomics portal: An open platform for exploring multidimensional cancer genomics data. *Cancer Discov*. 2012;2(5):401–404. doi:10.1158/2159-8290.CD-12-0095
19. Landau DA, Tausch E, Taylor-Weiner AN, et al. Mutations driving CLL and their evolution in progression and relapse. *Nature*. 2015;526(7574):525–530. doi:10.1038/nature15395
20. Mohr A, Cumin M, Bagacean C, et al. The regulatory capacity of B cells directs the aggressiveness of CLL. *Oncoimmunology*. 2019;8(3):1554968. doi:10.1080/2162402X.2018.1554968
21. Zarobkiewicz M, Kowalska W, Chocholska S, et al. High M-MDSC percentage as a negative prognostic factor in chronic lymphocytic leukaemia. *Cancers (Basel)*. 2020;12(9):2614. doi:10.3390/cancers12092614
22. Annese T, Tamma R, Ribatti D. Update in TIGIT immune-checkpoint role in cancer. *Front Oncol*. 2022;12:871085. doi:10.3389/fonc.2022.871085
23. De Weerdt I, Hofland T, Lameris R, et al. Improving CLL Vγ9Vδ2-T-cell fitness for cellular therapy by ex vivo activation and ibrutinib. *Blood*. 2018;132(21):2260–2272. doi:10.1182/blood-2017-12-822569
24. Coscia M, Vitale C, Peola S, et al. Dysfunctional Vγ9Vδ2 T cells are negative prognosticators and markers of dysregulated mevalonate pathway activity in chronic lymphocytic leukemia cells. *Blood*. 2012;120(16):3271–3279. doi:10.1182/blood-2012-03-417519
25. Tokuyama H, Hagi T, Mattarollo SR, et al. Vγ9Vδ2 T cell cytotoxicity against tumor cells is enhanced by monoclonal antibody drugs: Rituximab and trastuzumab. *Int J Cancer*. 2008;122(11):2526–2534. doi:10.1002/ijc.23365
26. Pende D, Bottino C, Castriconi R, et al. PVR (CD155) and Nectin-2 (CD112) as ligands of the human DNAM-1 (CD226) activating receptor: Involvement in tumor cell lysis. *Mol Immunol*. 2005;42(4):463–469. doi:10.1016/j.molimm.2004.07.028
27. Yeo J, Ko M, Lee DH, Park Y, Jin HS. TIGIT/CD226 axis regulates antitumor immunity. *Pharmaceuticals (Basel)*. 2021;14(3):200. doi:10.3390/ph14030200
28. Wang X, Mou W, Han W, et al. Diminished cytolytic activity of γδ T cells with reduced DNAM-1 expression in neuroblastoma patients. *Clin Immunol*. 2019;203:63–71. doi:10.1016/j.clim.2019.04.006
29. Veuillen C, Rey J, Castellano R, et al. Defective triggering of NK cells results in primary CLL cells resistance to cytotoxicity. *Blood*. 2011;118(21):3876. doi:10.1182/blood.V118.21.3876.3876
30. Yu X, Harden K, C Gonzalez L, et al. The surface protein TIGIT suppresses T cell activation by promoting the generation of mature immunoregulatory dendritic cells. *Nat Immunol*. 2009;10(1):48–57. doi:10.1038/ni.1674
31. Harjunpää H, Guillerey C. TIGIT as an emerging immune checkpoint. *Clin Exp Immunol*. 2020;200(2):108–119. doi:10.1111/cei.13407
32. Jin Z, Lan T, Zhao Y, et al. Higher TIGIT⁺CD226⁻γδ T cells in patients with acute myeloid leukemia. *Immunol Invest*. 2022;51(1):40–50. doi:10.1080/08820139.2020.1806868

33. Bartkowiak J, Błoński JZ, Niewiadomska H, Kulczycka D, Robak T. Characterization of γδ T cells in peripheral blood from patients with B-cell chronic lymphocytic leukaemia. *Biomed Lett*. 1998;58(228):19–30.

34. Lawand M, Déchanet-Merville J, Dieu-Nosjean MC. Key features of gamma-delta T-cell subsets in human diseases and their immunotherapeutic implications. *Front Immunol*. 2017;8:761. doi:10.3389/fimmu.2017.00761

35. Hus I, Podhorecka M, Bojarska-Junak A, et al. The clinical significance of ZAP-70 and CD38 expression in B-cell chronic lymphocytic leukaemia. *Ann Oncol*. 2006;17(4):683–690. doi:10.1093/annonc/mdj120

36. Autore F, Strati P, Innocenti I, et al. LDH levels predict progression-free survival in treatment-naïve patients with trisomy 12 chronic lymphocytic leukemia. *Blood*. 2016;128(22):3211. doi:10.1182/blood.V128.22.3211.3211

37. Hallek M. Chronic lymphocytic leukemia: 2020 update on diagnosis, risk stratification and treatment. *Am J Hematol*. 2019;94(11):1266–1287. doi:10.1002/ajh.25595

38. Spaner DE, Venema R, Huang J, et al. Association of blood IgG with tumor necrosis factor-alpha and clinical course of chronic lymphocytic leukemia. *EBioMedicine*. 2018;35:222–232. doi:10.1016/j.ebiom.2018.08.045

39. Ishdorj G, Streu E, Lambert P, et al. IgA levels at diagnosis predict for infections, time to treatment, and survival in chronic lymphocytic leukemia. *Blood Adv*. 2019;3(14):2188–2198. doi:10.1182/bloodadvances.2018026591

Differential expression of miRNA-769-5p and Smad2 in patients with or without oral cGVHD

*Xiang-Zhi Yong[1,2,B–E], *Yu-Xi Zhou[1,B,C], Tian-Tian Wu[1,3,C], Qiao-Zhi Jiang[1,2,B], Zhen-Min Liu[1,4,C], Zhong-Ming Zhang[5,B], Rong-Quan He[6,C], Zhi-Guang Huang[7,C], Gang Chen[7,C,E], Renchuan Tao[1,2,A,E,F]

[1] College of Stomatology, Guangxi Medical University, Nanning, China

[2] Guangxi Health Commission Key Laboratory of Prevention and Treatment for Oral Infectious Diseases, Nanning, China

[3] Guangxi Key Laboratory of AIDS Prevention and Treatment, Guangxi Medical University, Nanning, China

[4] Guangxi Key Laboratory of Oral and Maxillofacial Rehabilitation and Reconstruction, Nanning, China

[5] Department of Hematology, The First Affiliated Hospital of Guangxi Medical University, Nanning, China

[6] Department of Oncology, The First Affiliated Hospital of Guangxi Medical University, Nanning, China

[7] Department of Pathology, The First Affiliated Hospital of Guangxi Medical University, Nanning, China

A – research concept and design; B – collection and/or assembly of data; C – data analysis and interpretation;
D – writing the article; E – critical revision of the article; F – final approval of the article

Address for correspondence
Renchuan Tao
E-mail: taorenchuan@gxmu.edu.cn

Abstract

Background. Oral chronic graft-versus-host disease (cGVHD) impacts quality of life of patients after allogeneic hematopoietic stem cell transplantation (allo-HSCT). However, its precise pathogenesis remains unknown, with potential associations with differential microRNA (miRNA) expression and the TGF-β/Smad signaling pathway.

Objectives. This study aims to explore miRNA expression profiles in the peripheral blood of oral cGVHD patients, focusing on miRNA-769-5p and its relationship with Smad2.

Materials and methods. Peripheral venous blood samples were collected for RNA extraction from 8 patients with oral cGVHD, 8 patients without cGVHD and 8 participants from the healthy control group. The miRNA library was constructed using the Illumina Hiseq 2500 platform. We focused on identifying miRNAs associated with the TGF-β/Smad signaling pathway and subsequently conducted validation experiments. The oral cGVHD and without cGVHD groups were each expanded to include 15 individuals. Peripheral blood samples were subjected to polymerase chain reaction (PCR) analysis to assess miRNA levels and to evaluate Smad2 mRNA levels in peripheral blood mononuclear cells (PBMC). Additionally, enzyme-linked immunosorbent assay (ELISA) was conducted to determine the Smad2 protein levels in peripheral blood.

Results. The most significantly differentially expressed miRNAs among the 3 groups were miRNA-505-5p and miRNA-769-5p. Kyoto Encyclopedia of Genes and Genomes (KEGG) pathway analysis indicated an enrichment of the target genes of miRNA-769-5p in the TGF-β signaling pathway. It was observed that miRNA-769-5p expression was higher in patients without oral cGVHD in comparison to those with oral cGVHD. Receiver operating characteristic (ROC) analysis demonstrated that miRNA-769-5p holds diagnostic value for oral cGVHD. As a target of miRNA-769-5p, Smad2 mRNA exhibited a negative correlation with it. Moreover, both Smad2 mRNA and protein levels were higher in patients with oral cGVHD as opposed to those without cGVHD.

Conclusions. Differential expression of miRNAs, particularly the downregulation of miRNA-769-5p, may influence the development of oral cGVHD by diminishing its inhibitory effect on the TGF-β/Smad signaling pathway through its interaction with Smad2.

Key words: oral mucosa, allogeneic hematopoietic stem cell transplantation, miRNAs, chronic graft-versus-host-disease

Background

Chronic graft-versus-host disease (cGVHD) is the leading cause of death following allogeneic hematopoietic stem cell transplantation (allo-HSCT).[1] As an alloimmune and autoimmune disease, it is characterized by lichenoid changes and fibrosis affecting various tissues, thereby compromising organ function.[2] Its clinical signs manifest first in the mucosal tissues.[3] The oral cavity is the primary organ affected by cGVHD, with oral manifestations occurring in 45−83% of cGVHD patients.[4] Encompassing lichen planus-like changes, erythema, ulceration, mucoceles, etc., the clinical presentation of oral cGVHD is diverse and can affect any sites within the oral cavity, including the oral mucosa, salivary glands and periodontium.[5,6] Lichen planus-like changes, marked by hyperkeratotic white lines and lacy-appearing lesions on the oral mucosa, serve as the diagnostic feature of oral cGVHD among its oral manifestations.[7] Our previous study showed that these lichen planus-like changes persist even when the systemic symptoms of cGVHD in patients are well controlled.[8] The repercussions of oral cGVHD significantly impact patient's quality of life, particularly in terms of eating and nutrient absorption.[9] Furthermore, oral cGVHD poses a risk for the development of oral squamous cell carcinomas (OSCCs).[10,11] Given the adverse effects of oral cGVHD on both oral and systemic health, raising awareness is crucial for understanding its occurrence and progression.

The pathogenesis of cGVHD, especially in the oral context, is intricate and remains controversial. Recent studies have shed light on the role of microRNAs (miRNAs) in cGVHD pathogenesis.[12] Reikvam et al. were the first to report miRNA serum profiles in cGVHD,[13] and miRNA profiles from plasma extracellular vesicles (EVs) have been considered markers of cGVHD onset.[14] However, owing to the distinct microenvironments of various organs and tissues, the miRNAs associated with the disease also exhibit variations.[15,16] Consequently, it prompts the question of whether miRNA profiles also change in oral cGVHD patients and how these changes impact the disease.

In our previous research, we uncovered an imbalance of cytokines associated with the TGF-β/Smad pathway in oral cGVHD patients.[17] TGF-β/Smad represents a major subfamily within the TGF-β signaling pathway. Phosphorylation of drosophila mothers against decapentaplegic protein 2 (Smad2) serves to activate this pathway, subsequently exerting its effects.[18] Research supports the involvement of the TGF-β/Smad signaling pathway in the initiation and progression of cGVHD,[19] and it has been shown that therapeutic intervention targeting this pathway can effectively manage cGVHD.[20] Furthermore, it is worth noting that Smads can be subject to regulation by miRNAs.[21,22] This leads us to question whether patients with oral cGVHD may exhibit aberrant miRNA expression profiles that influence the TGF-β/Smad pathway and contribute to the development of oral cGVHD.

Objectives

This study aimed to investigate miRNA expression profiles in the peripheral blood of patients affected by oral cGVHD, with a specific focus on miRNA-769-5p and its relationship with Smad2. We aim to provide an initial exploration of the correlation between miRNA-769-5p and Smad2 and their potential influences on oral cGVHD.

Materials and methods

Study groups and approval

The oral cGVHD group comprised patients whose clinical manifestations of cGVHD exclusively affected the oral cavity. The group without cGVHD comprised patients who underwent transplantation more than a year prior and did not develop cGVHD. The healthy control group comprised healthy volunteers.

All study participants were recruited from Guangxi Medical University (Nanning, China). Informed consent, consistent with the principles of the Declaration of Helsinki, was obtained from all study participants. The research protocol received approval from the Research Ethics Committee of Guangxi Medical University (approval No. IRB: 20170301-4). All procedures adhered to the relevant guidelines and regulations.

Study design

Eight individuals were recruited for sampling in each group for RNA sequencing analysis. To further validate the RNA sequencing results in both the oral cGVHD and without cGVHD groups, an additional 7 individuals were included in each group, resulting in a total of 15 individuals in each group for polymerase chain reaction (PCR)-based testing and analysis.

Clinical examination

The oral cGVHD diagnosis and grading were determined based on established diagnostic and scoring criteria.[7] Oral discomfort was assessed using a Visual Analogue Scale (VAS). Demographic information was collected through a structured questionnaire, and clinical evaluations and examinations were recorded.

RNA sequencing

Peripheral venous blood was collected from 8 participants in each of the 3 groups. Total RNA was isolated from the whole blood using TRIZOL (Invitrogen, Waltham, USA) to create the miRNA library. Sequencing and the subsequent analysis of miRNA differential expression were performed on the Illumina Hiseq 2500 platform by LC-Bio (Hangzhou, China).

qPCR

Peripheral venous blood samples were collected, and total RNA was extracted using TRIzol (Invitrogen) to measure miRNA levels. Concurrently, peripheral blood mononuclear cells (PBMCs) were isolated and subjected to RNA extraction to determine the Smad2 mRNA levels. The RNA was subsequently reverse-transcribed into cDNA utilizing TruScript™ First Strand cDNA Synthesis Kit. Quantitative real-time polymerase chain reaction (qPCR) was conducted using qTOWER 2.2 system (Analytik Jena AG, Jena, Germany). Cel-miR-39-5p served as the control for miRNA detection, while GAPDH acted as the control for Smads mRNA. Primer sequences are provided in Table 1. Data analysis was performed using the following formula: $R = 2^{-(\Delta Ct\ sample\ -\ \Delta Ct\ control)}$.

ELISA

Plasma samples from participants in the oral cGVHD and without cGVHD groups were collected and subjected to analysis using a human Smad2 immunoblot assay enzyme-linked immunosorbent assay (ELISA) kit (Cusabio, Wuhan, China). Spectrophotometric measurements were taken at 450 nm using the Wellscan Mk3 instrument (Thermo Fisher Scientific, Waltham, USA).

Luciferase reporter assay

The 3'-UTR of Smad2, containing either wild-type (WT) or mutated (MUT) binding sites for miRNA-769_5p, was amplified and inserted into the pGL3 vector to generate the plasmids pGL3-WT-Smad2-3'-UTR or pGL3-MUT-Smad2-3'-UTR, respectively. In the luciferase reporter assay, HEK-293 cells were co-transfected with the luciferase reporter vectors and miRNA-769-5p mimics, or their respective negative controls, using Lipofectamine LTX (Invitrogen). The pRL-TK plasmid (Promega, Madison, USA) served as a normalization control. After 24 h of incubation, luciferase activity was measured using a Luciferase Reporter Assay kit (Promega) following the manufacturer's instructions.

Statistical analyses

RNA sequencing results were expressed as the normalized fragments per kilo base per million mapped reads (FPKM) (log base per million reads) and subjected to analysis of variance (ANOVA) testing. The miRNAs with differential expression were defined based on a Benjamini–Hochberg adjusted p-value <5% and |log2 (fold-change FC) | ≥1. Significant differential miRNAs were then analyzed for target gene prediction using TargetScan (https://www.targetscan.org/vert_80/)[23] and miRWalk (http://mirwalk.umm.uni-heidelberg.de).[24] The resulting overlapping datasets were subsequently utilized for the Kyoto Encyclopedia of Genes and Genomes (KEGG) pathway enrichment analysis with the aid of OmicStudio (LC-Bio). In the following experiments, we employed the Shapiro–Wilk normality test to evaluate the distribution of the data (Supplementary Table 1). The miRNA expression displayed skewness and underwent transformation using the Box–Cox method to conform to a normal distribution. Differences in miRNA and Smad2 expression between groups were assessed using t-test. Diagnostic analysis was conducted through receiver operating characteristic (ROC) curve analysis. Furthermore, after assigning ranks to miRNA-769 based on its expression values, Spearman's correlation method was utilized to assess its association with Smad2. A p-value of less than 0.05 was considered statistically significant. The statistical software IBM SPSS v. 22.0 (IBM Corp., Armonk, USA) was utilized for data analysis.

Results

miRNAs differential expression among allo-HSCT patients and healthy controls

The demographic and clinical characteristics of the study participants are presented in Table 2. Among all 3 groups, a total of 518 miRNAs were expressed. After conducting an ANOVA analysis (details not presented), it was found that 191 of these miRNAs exhibited differential expression (Fig. 1). The most significantly differentially expressed miRNAs were identified as miRNA-505-5p and miRNA-769-5p (Table 3), sorted in descending order of significance based on p-values. Enrichment analysis of these 2 miRNAs was conducted using KEGG pathway functional annotation (Fig. 2,3).

Table 1. Primer information

Name	Sequence (5'to3')
has-miR-769-5p	F: TCGCGTGAGACCTCTGGG R: GTCGTATCCAGTGCAGGGTCCGAGGTATTCGCACTGGATACGACAGCTCA
cel-miR-39-5p	F: TGGGAGCTGATTTCGTCTTG R: GTCGTATCCAGTGCAGGGTCCGAGGTATTCGCACTGGATACGACTATTAC
Smad2	F: TGTTAACCGAAATGCCACGGTA R: GGCTCTGCACAAAGATTGCACTA
GAPDH	F: GCACCGTCAAGGCTGAGAAC R: TGGTGAAGACGCCAGTGGA

Table 2. Demographic and clinical characteristics of study participants

Demographic and clinical information	Oral cGVHD (n = 8)	Without cGVHD (n = 8)	Healthy control (n = 8)
Demographic information			
Age (years, M ±SD)	35.12 ±14.38	34.37 ±15.31	32.12 ±4.79
Gender (male/female)	6/2	6/2	6/2
Donor			
Donor relationship (unrelated/related)	1/6	3/5	/
HLA match (non-identical/identical)	5/3	4/4	/
Blood type (non-identical/identical)	5/3	4/4	/
Cell source			
BMT/PBSCT/BMT+PBSCT/BMT+CBT	0/5/3/0	0/4/3/1	/
Clinical sign			
Severity score of oral manifestation	4.25 ±2.19	0	0
Oral pain VAS scores	4.5 ±2.39	0	0

M ±SD – mean ± standard deviation; cGVHD – chronic graft-versus-host disease; HLA – human leukocyte antigen; BMT – bone marrow transplantation; PBSCT – peripheral blood stem cell transplantation; CBT – cord blood transplantation.

Table 3. The information of top 2 different expression miRNAs

Statistical information	Normalized FPKM of miR-505-5p (miR sequence: GGGAGCCAGGAAGTATTGATGT)			Normalized FPKM of miR-769-5p (miR sequence: TGAGACCTCTGGGTTCTGAGCT)		
	oral cGVHD (n = 8)	without cGVHD (n = 8)	healthy control (n = 8)	oral cGVHD (n = 8)	without cGVHD (n = 8)	healthy control (n = 8)
M ±SD	202.625 ±48.928	301.000 ±48.196	169.500 ±36.493	1145.250 ±196.738	1178.125 ±223.850	752.250 ±161.667
Levene's test for variance homogeneity H_0: Equal variances H_1: Unequal variance	0.337			0.482		
p-value for Levene's test	0.718			0.624		
ANOVA for difference among groups H_0: equal means among groups H_1: unequal means among groups	18.561			11.723		
p-value for ANOVA	<0.001 (2.26E-05)			<0.001 (3.83E-04)		
df	23			23		

M ±SD – mean ± standard deviation; ANOVA – analysis of variance; cGVHD – chronic graft-versus-host disease; H_0 – null hypothesis; H_1 – alternative hypothesis; df – degrees of freedom.

The KEGG results indicated that target genes of miRNA-769-5p were enriched in the TGF-β signaling pathway (Fig. 3). While high-throughput sequencing indicated a modest reduction in miRNA-769-5p abundance in the oral cGVHD group compared to the without cGVHD group, the observed difference was not statistically significant.

Lower expressions of miRNA-769-5p in patients with oral cGVHD

To further validate the differential expression of miRNA-769-5p, we expanded the sample size to include 15 patients in both the oral cGVHD and without cGVHD groups (Table 4), and conducted verification through PCR analysis. It was observed that the expression of miRNA-769-5p

was higher in patients without oral cGVHD compared to those with oral cGVHD (Table 5, Fig. 4). Among 30 patients after allo-HSCT (both the oral cGVHD and without cGVHD groups), ROC analysis indicated that miRNA-769-5p holds a certain diagnostic value for oral cGVHD, with an area under the curve (AUC) of 0.809, signifying a moderate diagnostic efficacy (95% confidence interval (95% CI): 0.657, 0.961; p = 0.004, Fig. 5).

Higher expressions of Smad2 in patients with oral cGVHD

Following predictions made by TargetScan and miR-Walk, Smad2 was validated as a potential target gene of miRNA-769-5p through a dual-luciferase test (Fig. 6).

Table 4. Demographic and clinical characteristics of study participants

Demographic and clinical information	Oral cGVHD (n = 15)	Without cGVHD (n = 15)
Demographic information		
Age (years, M ±SD)	33.33 ±16.70	33.40 ±12.61
Gender (male/female)	12/3	11/4
Donor		
Donor relationship (unrelated/related)	4/11	5/10
HLA match (non-identical/identical)	8/7	7/8
Blood type (non-identical/identical)	7/8	8/7
Cell source		
BMT/PBSCT/BMT+PBSCT/BMT+CBT	0/5/10/0	0/8/7/0
Clinical sign		
Severity score of oral manifestation	4.27 ±2.22	0
Oral pain VAS scores	3.40 ±2.72	0

M ±SD – mean ± standard deviation; VAS – Visual Analogue Scale; cGVHD – chronic graft-versus-host disease; HLA – human leukocyte antigen; BMT – bone marrow transplantation; PBSCT – peripheral blood stem cell transplantation; CBT – cord blood transplantation.
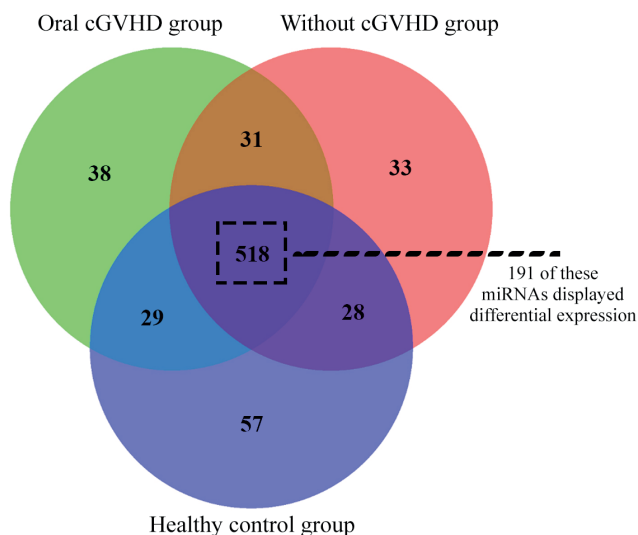
Fig. 1. Venn diagrams of miRNA profiles of the 3 groups. Among the 3 groups (oral chronic graft-versus-host disease (cGVHD) group, without cGVHD group and the healthy control group), a total of 518 miRNAs were expressed. After conducting an analysis of variance (ANOVA) analysis (details not presented), it was found that 191 of these miRNAs exhibited differential expression
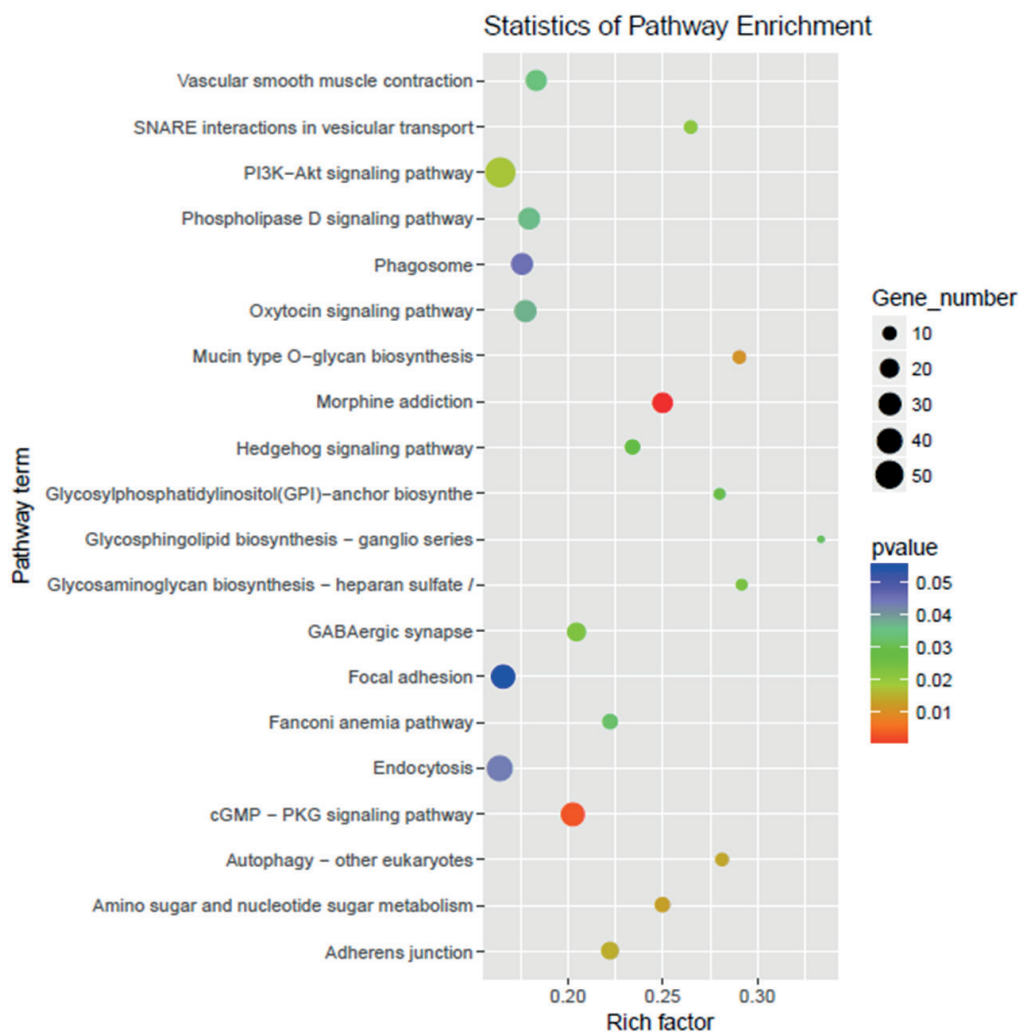
Fig. 2. Kyoto Encyclopedia of Genes and Genomes (KEGG) pathway enrichment of the target genes for miRNA-505-5p. Y-axis: pathway names, x-axis: rich factor. Bubble colors represent significance, with deeper red indicating smaller p-values and more prominent statistical significance. The size of the bubbles reflects the number of genes associated with the pathway

Fig. 3. Kyoto Encyclopedia of Genes and Genomes (KEGG) pathway enrichment of the target genes for miRNA-769-5p. Y-axis: pathway names, x-axis: rich factor. Bubble colors represent significance, with deeper red indicating smaller p-values and more prominent statistical significance. The size of the bubbles reflects the number of genes associated with the pathway. The blue frames denote the TGF-β/Smad signaling pathways

Table 5. Differences in miRNA and Smad2 expression between groups

Statistical information	miR-769-5p*		Smad2 mRNA		Smad	
	oral cGVHD (n = 15)	without cGVHD (n = 15)	oral cGVHD (n = 15)	without cGVHD (n-15)	oral cGVHD (n = 15)	without cGVHD (n = 15)
M ±SD	−4.342 ±2.726	−0.447 ±2.004	1.455 ±0.432	1.019 ±0.361	77.238 ±13.318	62.799 ±15.238
Levene's test for variance homogeneity H_0: equal variances H_1: unequal variance	2.326		<0.001		0.002	
p-value for Levene's test	0.138		0.993		0.963	
t-test for difference between groups H_0: equal means for 2 groups H_1: unequal means for 2 groups	−4.459		3.000		2.763	
p-value for t-test	<0.001		0.006		0.010	
df	28		28		28	
95% CI	upper	−2.106		0.733		25.142	
	lower	−5.686		0.138		3.734	

cGVHD – chronic graft-versus-host disease; H_0 – null hypothesis; H_1 – alternative hypothesis; df – degrees of freedom; 95% CI – 95% confidence interval. M ±SD – mean ± standard deviation.

Among 30 patients after allo-HSCT, a negative correlation was observed between miRNA-769-5p and Smad2 mRNA (r = −0.635, 95% CI: −0.8136, −0.3460; p < 0.001, Fig. 7).

Additionally, both Smad2 mRNA and protein levels were higher in the patients with oral cGVHD compared to those without cGVHD (Table 5, Fig. 8).
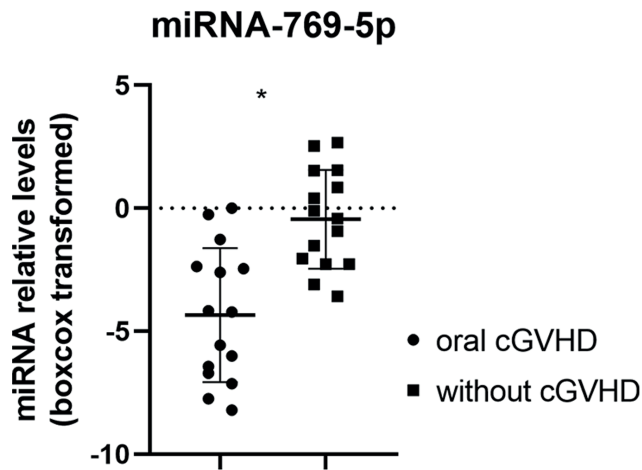
Fig. 4. Different expression of miRNA-769-5p between the oral chronic graft-versus-host disease (cGVHD) and without cGVHD groups. The expression data of miRNA-769-5p were transformed using the Box–Cox method. The differences were measured with t-test. The bars represent the mean and standard deviation (M ±SD). The expression of miRNA-769-5p was higher in patients without oral cGVHD compared to those with oral cGVHD

*oral cGVHD compared to without cGVHD, t = −4.459, degrees of freedom (df) = 28, 95% confidence interval (95% CI): −5.686, −2.106; p < 0.001, tested using t-test.
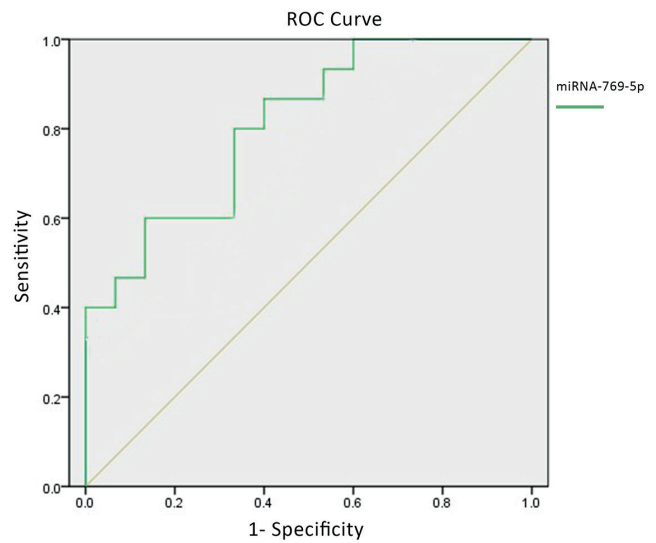
Fig. 5. Receiver operating characteristic (ROC) curve of circulating miRNA-769-5p in the peripheral blood. Among the 30 patients after allogeneic hematopoietic stem cell transplantation (allo-HSCT) (both the oral chronic graft-versus-host disease (cGVHD) and without cGVHD groups), ROC analysis indicated that miRNA-769-5p holds a certain diagnostic value for oral cGVHD, with an area under the curve (AUC) of 0.809, signifying a moderate diagnostic efficacy (95% confidence interval (95% CI): 0.657, 0.961; p = 0.004)

Fig. 6. Dual-luciferase detection of the interaction between hsa-miR-769-5p and *Smad2*. *Smad2* was validated as a potential target gene of miRNA-769-5p. The difference was measured with t-test. The bars represented mean and standard deviation (M ±SD)

*Smad2 wild-type (WT)+mimics negative control (NC) vs Smad2 WT+miR-769-5p mimics, t = 7.021, degrees of freedom (df) = 4, 95% confidence interval (95% CI): −0.507, −0.220, p = 0.002; NS Smad2 mutant-type (MUT)+mimics, NC+Smad2 MUT+miR-769-5p mimics, t = 1.114, df = 4, 95% CI: −0.204, 0.477; p = 0.328.
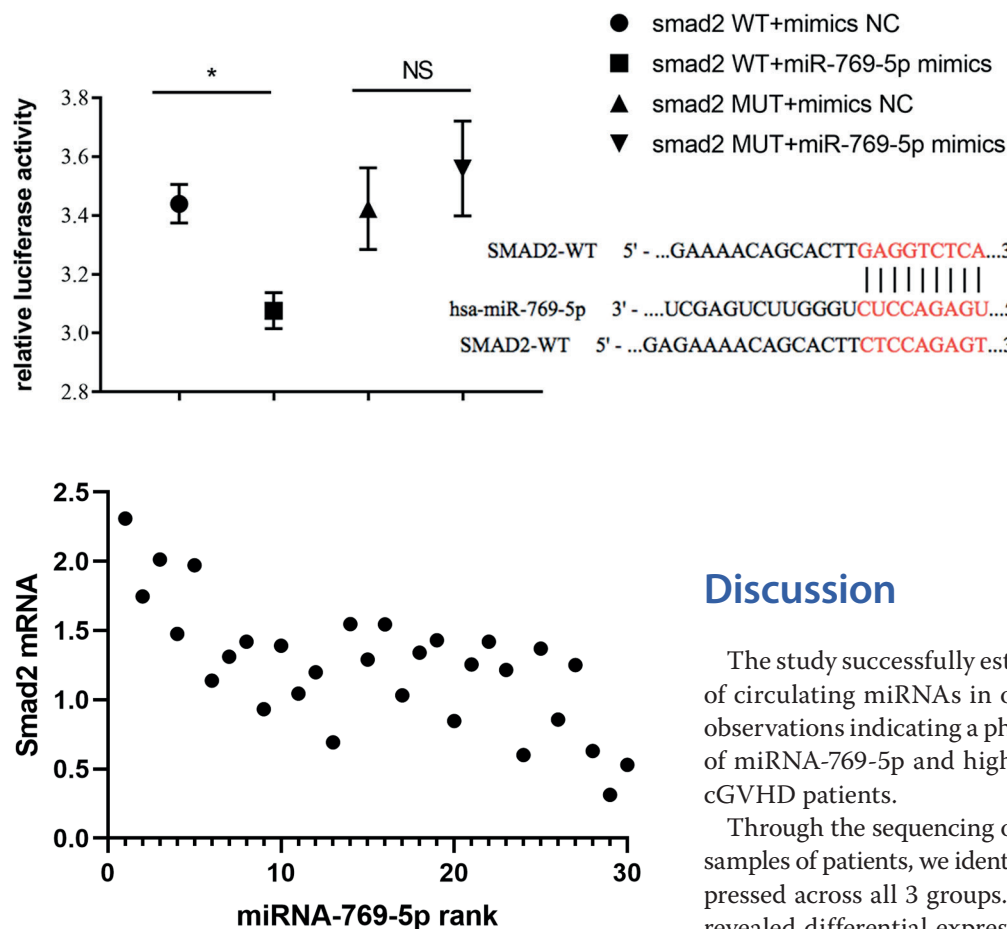
Fig. 7. The relationship between miRNA-769-5p and Smad2 mRNA in peripheral blood mononuclear cells (PBMCs). Among 30 patients after allogeneic hematopoietic stem cell transplantation (allo-HSCT), a negative correlation was observed between miRNA-769-5p and Smad2 mRNA (r = −0.635, 95% confidence interval (95% CI): −0.814, −0.346; p < 0.001)

Discussion

The study successfully established an expression profile of circulating miRNAs in oral cGVHD and made initial observations indicating a phenomenon of a low expression of miRNA-769-5p and high expression of Smad2 in oral cGVHD patients.

Through the sequencing of miRNAs in peripheral blood samples of patients, we identified a total of 518 miRNAs expressed across all 3 groups. Subsequent ANOVA analysis revealed differential expression in 191 of these miRNAs. Guided by the ranking of p-values, we selected the top 2 miRNAs for KEGG pathway analysis, which unveiled an enrichment of target genes for miRNA-769-5p within the TGF-β signaling pathway. Based on the sequencing
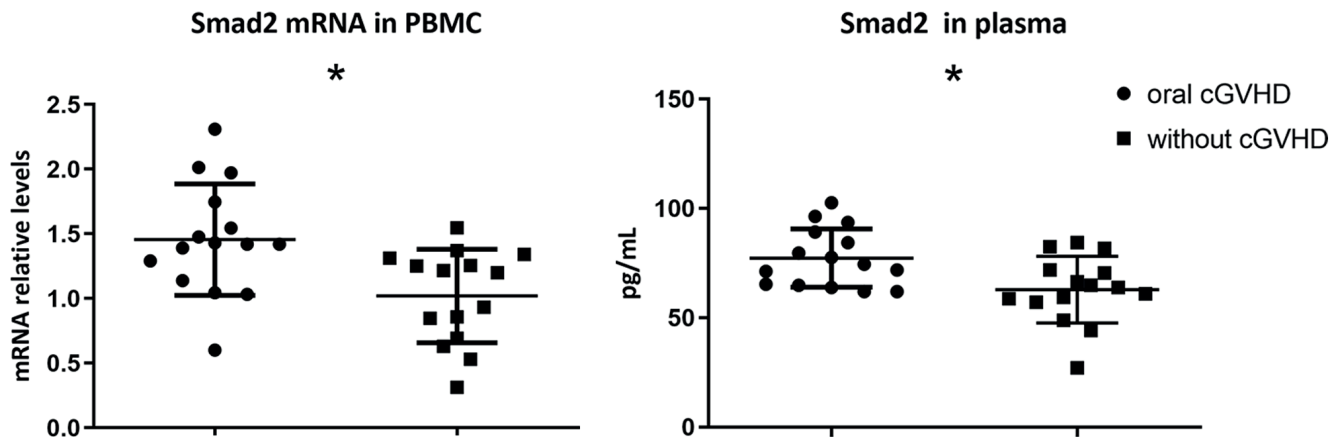
Fig. 8. Different expressions in Smad2 between the oral chronic graft-versus-host disease (cGVHD) and without cGVHD groups. The differences were measured with t-test. The bars represented mean and standard deviation (M ±SD). Both Smad2 mRNA and protein levels were higher in patients with oral cGVHD compared to those without cGVHD

*oral cGVHD compared to without cGVHD, $t_{smad2\ mRNA}$ = 3.000, degrees of freedom (df) = 28, 95% confidence interval (95% CI): 0.138, 0.733; p = 0.006; t_{smad2} = 2.763, df = 28, 95% CI: 3.734, 25.142; p = 0.010, tested with t-test.

results, we expanded the sample size and conducted PCR validation, which revealed the lower expression of miRNA-769-5p in oral cGVHD. Importantly, it was ascertained that miRNA-769-5p holds diagnostic significance in the context of oral cGVHD.

Research on miRNA-769-5p has primarily centered on its involvement in cancer. Studies have revealed its function as an oncogene in gastric cancer,[25] hepatocellular carcinoma[26] and prostate cancer.[27] Conversely, in oral squamous cell carcinoma (OSCC), elevated miRNA-769-5p expression has been found to inhibit tumor cell proliferation, migration and invasion while promoting apoptosis.[28] Studies have shown that patients after allo-HSCT are 2–3 times more likely to develop solid tumors than healthy individuals.[29] About 1/3 of solid tumors are secondary tumors in the skin and mucosa of recipients of transplants, with OSCC accounting for 50% of these patients.[30,31] Consequently, the question arises as to whether the low expression of miRNA-769-5p in oral cGVHD patients is one of the factors predisposing them to the development of oral cancer, a matter that warrants further consideration.

Furthermore, the study unveiled that the overexpression of miR-769-5p has the potential to alleviate tissue fibrosis by modulating the TGF-β/Smad signaling pathway.[32] It is well-established that the TGF-β/Smad signaling pathway can stimulate tissue fibrosis.[33] Both mRNA and protein levels were higher in the oral cGVHD group than those in patients without cGVHD. The high expression of Smad2 hinted at the activation of TGF-β/Smads, which leads to oral cGVHD. In this study, after being predicted using TargetScan and miRWalk, we verified that Smad2 was the target gene of miRNA-769-5p using the dual-luciferase test. A negative relationship between miRNA-769-5p and Smad2 mRNA was also observed. Fibrosis is a feature of oral cGVHD, and the effective

treatment of cGVHD often involves inhibiting the TGF-β/Smad signaling pathway.[34] Consequently, the high expression of miRNA-769-5p in patients without oral cGVHD may also act to suppress the expression of SMADs, subsequently inhibiting the activation of the TGF-β/Smad signaling pathway, ultimately leading to a reduction in fibrosis and symptom relief.

Additionally, it is noteworthy that the TGF-β/Smad signaling pathway is involved in Th17/Treg immuno-reactions.[35] In patients suffering from skin cGVHD, the study identified a dysregulation in cytokine secretion, such as TGF-β, alongside an imbalance in Th17/Treg cell ratios.[36] In our earlier research, we also observed imbalances in cytokines related to Th17 and Treg cells in oral cGVHD.[17] Previous studies have demonstrated that downregulating Smad2 can mitigate the severity of cGVHD[20] by not only reducing fibrosis[37] but also by inhibiting the generation of Th17.[38] The investigations further emphasized that by inhibiting the TGF-β/Smad pathway, Th17-mediated immune responses could be effectively controlled, thus ameliorating murine cardiac transplant rejection.[39] Therefore, the high expression of miRNA-769-5p in patients without oral cGVHD may serve to modulate the immune response by suppressing the TGF-β/Smad pathway, ultimately reducing the manifestation of oral cGVHD symptoms.

Limitations

In this study, we have examined the distinctive expression patterns of miRNAs in patients affected by oral cGVHD. We have also undertaken an initial exploration of the potential relationship between miRNA-769-5p and Smad2 differential expression and oral cGVHD. Nevertheless, the precise mechanistic interactions of miRNAs influencing the development of diseases require further

in-depth exploration and validation through in vitro experiments. Additionally, during the sequencing phase, we observed lower expression levels of miRNA-769-5p in the peripheral blood of healthy volunteers compared to individuals with oral cGVHD and those without it. However, this study did not proceed to validate these findings using PCR. Subsequent research could involve further validation and exploration of the implications of elevated miRNA-769-5p expression in post-transplant patients.

Conclusions

Differential expression of miRNAs, particularly the downregulation of miRNA-769-5p, may influence the development of oral cGVHD by diminishing its inhibitory effect on the TGF-β/Smad signaling pathway through its interaction with Smad2. This interaction potentially plays a significant role in the pathogenesis of oral cGVHD and offers a promising avenue for further research and therapeutic exploration.

Supplementary data

The Supplementary materials are available at https://doi.org/10.5281/zenodo.10551750. The package includes the following file:

Supplementary Table 1. Normality test for the data distribution.

Data availability

The datasets generated and/or analyzed during the current study are available from the corresponding author upon reasonable request.

Consent for publication

Not applicable.

ORCID iDs

Xiang-Zhi Yong ⓘ https://orcid.org/0000-0002-0208-9171
Yu-Xi Zhou ⓘ https://orcid.org/0000-0001-9496-975X
Tian-Tian Wu ⓘ https://orcid.org/0000-0002-0843-5186
Qiao-Zhi Jiang ⓘ https://orcid.org/0000-0001-7908-8583
Zhen-Min Liu ⓘ https://orcid.org/0000-0002-4299-1231
Zhong-Ming Zhang ⓘ https://orcid.org/0000-0003-1537-9685
Rong-Quan He ⓘ https://orcid.org/0000-0002-7752-2080
Zhi-Guang Huang ⓘ https://orcid.org/0000-0003-4457-9491
Gang Chen ⓘ https://orcid.org/0000-0003-2402-2987
Renchuan Tao ⓘ https://orcid.org/0000-0002-9647-0757

References

1. Kröger N, Solano C, Wolschke C, et al. Antilymphocyte globulin for prevention of chronic graft-versus-host disease. *N Engl J Med*. 2016; 374(1):43–53. doi:10.1056/NEJMoa1506002
2. Tollemar V, Garming Legert K, Sugars RV. Perspectives on oral chronic graft-versus-host disease from immunobiology to morbid diagnoses. *Front Immunol*. 2023;14:1151493. doi:10.3389/fimmu.2023.1151493
3. MacDonald KPA, Hill GR, Blazar BR. Chronic graft-versus-host disease: Biological insights from preclinical and clinical studies. *Blood*. 2017;129(1):13–21. doi:10.1182/blood-2016-06-686618
4. Fall-Dickson JM, Pavletic SZ, Mays JW, Schubert MM. Oral complications of chronic graft-versus-host disease. *J Natl Cancer Inst Monogr*. 2019;2019(53):lgz007. doi:10.1093/jncimonographs/lgz007
5. Bassim CW, Fassil H, Mays JW, et al. Oral disease profiles in chronic graft versus host disease. *J Dent Res*. 2015;94(4):547–554. doi:10.1177/0022034515570942
6. Haverman TM, Raber-Durlacher JE, Raghoebar II, et al. Oral chronic graft-versus-host disease. *J Am Dent Assoc*. 2020;151(11):846–856. doi:10.1016/j.adaj.2020.08.001
7. Jagasia MH, Greinix HT, Arora M, et al. National Institutes of Health Consensus Development Project on Criteria for Clinical Trials in Chronic Graft-versus-Host Disease: I. The 2014 Diagnosis and Staging Working Group Report. *Biol Blood Marrow Transplant*. 2015;21(3):389–401.e1. doi:10.1016/j.bbmt.2014.12.001
8. Xiao LT, Peng YT, Tao RC, et al. Oral mucosa health status among patients after allogeneic hematopoietic stem cell transplantation in Guangxi district [in Chinese]. *J Oral Sci Res*. 2011;27(10):881–885. https://www.cnki.net/KCMS/detail/detail.aspx?dbcode=CJFD&dbname=CJFD2011&filename=KQYZ201110015&uniplatform=OVERSEA&v=dTrPAV-h1ZE9xeOJrTgb-L7gcsaevGIb4eqTX0SyjoTQB43bRJHQ3csVBT0_2-jQ. Accessed July 12, 2023.
9. Bassim CW, Fassil H, Dobbin M, et al. Malnutrition in patients with chronic GVHD. *Bone Marrow Transplant*. 2014;49(10):1300–1306. doi:10.1038/bmt.2014.145
10. Wu T, Liu Z, Yong X, et al. P16-positive secondary tongue squamous cell carcinoma following allogeneic hematopoietic stem cell transplantation: A case report and literature review. *Oral Oncol*. 2021;121: 105399. doi:10.1016/j.oraloncology.2021.105399
11. Liu Z, Peng Y, Yong X, et al. A case report of secondary oral squamous cell carcinoma after allogeneic hematopoietic stem cell transplantation. *Oral Oncol*. 2020;109:104629. doi:10.1016/j.oraloncology.2020.104629
12. Salvi V, Gianello V, Tiberio L, Sozzani S, Bosisio D. Cytokine targeting by miRNAs in autoimmune diseases. *Front Immunol*. 2019;10:15. doi:10.3389/fimmu.2019.00015
13. Reikvam H, Vo AK, Johansen S, et al. MicroRNA serum profiles and chronic graft-versus-host disease. *Blood Adv*. 2022;6(18):5295–5306. doi:10.1182/bloodadvances.2021005930
14. Łacina P, Crossland RE, Wielińska J, et al. Differential expression of miRNAs from extracellular vesicles in chronic graft-versus-host disease: A preliminary study. *Adv Clin Exp Med*. 2022;32(5):539–544. doi:10.17219/acem/155373
15. Vajari MK, Moradinasab S, Yousefi A, Bashash D. Noncoding RNAs in diagnosis and prognosis of graft-versus-host disease (GVHD). *J Cell Physiol*. 2022;237(9):3480–3495. doi:10.1002/jcp.30830
16. Lv Q, Tian Z, Dong E, Cao X. Tissue/organ-specialized immunologic features and disease mechanisms [in Chinese]. *Chin Sci Bull*. 2012;36: 3450–3458. doi:10.1360/972012-1602
17. Yong X, Peng Y, Liu Z, et al. Analysis of serum and salivary cytokines among patients with oral cGVHD after Allo-HSCT. *Oral Dis*. 2021;27(5): 1320–1324. doi:10.1111/odi.13658
18. Wang H, Li M, Fei L, et al. Bone marrow-derived mesenchymal stem cells transplantation attenuates renal fibrosis following acute kidney injury in rats by diminishing pericyte-myofibroblast transition and extracellular matrix augment. *Transplant Proc*. 2023;55(1):225–234. doi:10.1016/j.transproceed.2022.12.002
19. Zhang H, Liu J, Sun Y, et al. Nestin⁺ mesenchymal stromal cells fibrotic transition mediated by CD169⁺ macrophages in bone marrow chronic graft-versus-host disease. *J Immunol*. 2023;211(7):1154–1166. doi:10.4049/jimmunol.2200558
20. Marinelli Busilacchi E, Costantini A, Mancini G, et al. Nilotinib treatment of patients affected by chronic graft-versus-host disease reduces collagen production and skin fibrosis by downmodulating the TGF-β and p-SMAD pathway. *Biol Blood Marrow Transplant*. 2020;26(5):823–834. doi:10.1016/j.bbmt.2020.01.014
21. Li S, Fan Q, He S, Tang T, Liao Y, Xie J. MicroRNA-21 negatively regulates Treg cells through a TGF-β1/Smad-independent pathway in patients with coronary heart disease. *Cell Physiol Biochem*. 2015;37(3):866–878. doi:10.1159/000430214

22. Liang J, Zhu W, Zhang Z, et al. MicroRNA-199a-3p enhances expressions of fibrosis-associated genes through targeting Smad1 in mouse cardiac fibroblasts [in Chinese]. *J Southern Med Univ.* 2018;38(10): 1203–1208. https://kns.cnki.net/kcms/detail/44.1627.R.20181026. 2108.040.html. Accessed July 12, 2023.

23. Agarwal V, Bell GW, Nam JW, Bartel DP. Predicting effective microRNA target sites in mammalian mRNAs. *eLife.* 2015;4:e05005. doi:10.7554/ eLife.05005

24. Sticht C, De La Torre C, Parveen A, Gretz N. miRWalk: An online resource for prediction of microRNA binding sites. *PLoS One.* 2018;13(10): e0206239. doi:10.1371/journal.pone.0206239

25. Luan PB, Jia XZ, Yao J. MiR-769-5p functions as an oncogene by downregulating RYBP expression in gastric cancer. *Eur Rev Med Pharmacol Sci.* 2020;24(12):6699–6706. doi:10.26355/eurrev_202006_21657

26. Xian Y, Wang L, Yao B, et al. MicroRNA-769-5p contributes to the proliferation, migration and invasion of hepatocellular carcinoma cells by attenuating RYBP. *Biomed Pharmacother.* 2019;118:109343. doi:10. 1016/j.biopha.2019.109343

27. Lee D. miR-769-5p is associated with prostate cancer recurrence and modulates proliferation and apoptosis of cancer cells. *Exp Ther Med.* 2021;21(4):335. doi:10.3892/etm.2021.9766

28. Zhou Y, Xu XM, Feng Y. MiR-769-5p inhibits cancer progression in oral squamous cell carcinoma by directly targeting JAK1/STAT3 pathway. *Neoplasma.* 2020;67(3):528–536. doi:10.4149/neo_2020_190703N582

29. Shimada K, Yokozawa T, Atsuta Y, et al. Solid tumors after hematopoietic stem cell transplantation in Japan: Incidence, risk factors and prognosis. *Bone Marrow Transplant.* 2005;36(2):115–121. doi:10.1038/ sj.bmt.1705020

30. Mawardi H, Elad S, Correa ME, et al. Oral epithelial dysplasia and squamous cell carcinoma following allogeneic hematopoietic stem cell transplantation: Clinical presentation and treatment outcomes. *Bone Marrow Transplant.* 2011;46(6):884–891. doi:10.1038/bmt.2011.77

31. Santarone S, Natale A, Angelini S, et al. Secondary oral cancer following hematopoietic cell transplantation. *Bone Marrow Transplant.* 2021;56(5):1038–1046. doi:10.1038/s41409-020-01147-z

32. Bontempi G, Terri M, Garbo S, et al. Restoration of WT1/miR-769-5p axis by HDAC1 inhibition promotes MMT reversal in mesenchymal-like mesothelial cells. *Cell Death Dis.* 2022;13(11):965. doi:10.1038/ s41419-022-05398-0

33. Chen C, Chen J, Wang Y, et al. Ganoderma lucidum polysaccharide inhibits HSC activation and liver fibrosis via targeting inflammation, apoptosis, cell cycle, and ECM-receptor interaction mediated by TGF-β/Smad signaling. *Phytomedicine.* 2023;110:154626. doi:10.1016 /j.phymed.2022.154626

34. Mays J, Fassil H, Edwards D, Pavletic S, Bassim C. Oral chronic graft-versus-host disease: Current pathogenesis, therapy, and research. *Oral Dis.* 2013;19(4):327–346. doi:10.1111/odi.12028

35. Wang F, Yang Y, Li Z, et al. Mannan-binding lectin regulates the Th17/ Treg axis through JAK/STAT and TGF-β/SMAD signaling against *Candida albicans* infection . *J Inflamm Res.* 2022;15:1797–1810. doi:10.2147/ JIR.S344489

36. Yang H. Clinical observation and pathogenetic study on the sclerodermatous chronic graft-versus-host disease after hematopoietic stem cell transplantation [in Chinese] [doctoral thesis]. Guangzhou, China: Southern Medical University; 2016. https://www.cnki.net/ KCMS/detail/detail.aspx?dbcode=CMFD&dbname=CMFD201701&fi lename=1016269721.nh&uniplatform=OVERSEA&v=89vORq70QkQ PcXUbbRKeCe9ngGsu99_fKuM-4NUeQ3--TCIaBX21cNuVLWHQEszv. Accessed July 12, 2023.

37. Chen H, Moreno-Moral A, Pesce F, et al. WWP2 regulates pathological cardiac fibrosis by modulating SMAD2 signaling. *Nat Commun.* 2019;10(1):3616. doi:10.1038/s41467-019-11551-9

38. Martinez GJ, Zhang Z, Reynolds JM, et al. Smad2 positively regulates the generation of Th17 Cells. *J Biol Chem.* 2010;285(38):29039–29043. doi:10.1074/jbc.C110.155820

39. Wang YY. Deletion of Smad3 improves cardiac allograft rejection in mice [in Chinese] [doctoral thesis]. Hangzhou, China: Zhejiang University; 2016. https://www.cnki.net/KCMS/detail/detail.aspx?dbcode =CDFD&dbname=CDFDLAST2017&filename=1016282995.nh&uni platform=OVERSEA&v=hth6zz6Eq-DdKsHO0-j8PxdBDGnbyCr531H ZQMkrQMHkAFR6V1yEve9t5b_S_sHQ. Accessed July 12, 2023.

Association between skin lymphangiogenesis parameters and arterial hypertension status in patients: An observational study

Angelika Chachaj[1,A–F], Ivana Stanimirova[2,C,D,F], Mariusz Chabowski[3,4,B,F], Agnieszka Gomułkiewicz[5,B,F], Paweł Hodurek[6,B,F], Natalia Glatzel-Plucińska[5,B,F], Mateusz Olbromski[5,B,F], Aleksandra Piotrowska[5,B,F], Aleksandra Kuzan[6,B,F], Jędrzej Grzegrzółka[5,B,F], Katarzyna Ratajczak-Wielgomas[5,B,F], Aleksandra Nowak[5,B,F], Ewa Szahidewicz-Krupska[7,B,F], Jerzy Wiśniewski[8,B,F], Mariusz A. Bromke[5,B,F], Marzenna Podhorska-Okołów[9,B,F], Andrzej Gamian[10,B,F], Dariusz Janczak[11,B,F], Piotr Dzięgiel[5,12,B,E,F], Andrzej Szuba[1,A,C,E,F]

[1] Department of Angiology and Internal Medicine, Wroclaw Medical University, Poland

[2] Institute of Chemistry, University of Silesia, Katowice, Poland

[3] Department of Surgery, 4th Military Hospital in Wroclaw, Poland

[4] Division of Anesthesiological and Surgical Nursing, Department of Nursing and Obstetrics, Wroclaw Medical University, Poland

[5] Division of Histology and Embryology, Department of Human Embryology and Morphology, Wroclaw Medical University, Poland

[6] Department of Medical Biochemistry, Wroclaw Medical University, Poland

[7] Department and Clinic of Internal and Occupational Diseases and Hypertension, Wroclaw Medical University, Poland

[8] Faculty of Chemistry, Wroclaw University of Science and Technology, Poland

[9] Division of Ultrastructure Research, Wroclaw Medical University, Poland

[10] Institute of Immunology and Experimental Therapy, Polish Academy of Sciences, Wrocław, Poland

[11] Department of Vascular, General and Transplantation Surgery, Wroclaw Medical University, Poland

[12] Department of Physiotherapy, University School of Physical Education, Wrocław, Poland

A – research concept and design; B – collection and/or assembly of data; C – data analysis and interpretation;
D – writing the article; E – critical revision of the article; F – final approval of the article

Address for correspondence
Angelika Chachaj
E-mail: angelika__chachaj@wp.pl

Conflict of interest
None declared

Abstract

Background. Recent studies have indicated that the skin lymphatic system and interstitium may play a role in the pathophysiology of arterial hypertension (AH).

Objectives. We aimed to determine whether the set of pathway parameters described previously in rodents would allow for the distinction between hypertensive and normotensive patients.

Materials and methods. Molecular and histopathological parameters from the skin and blood of patients with AH (AH group, n = 53), resistant AH (RAH group, n = 32) and control (C group, n = 45) were used, and a statistical multivariate bootstrap methodology combining partial least squares-discriminant analysis (PLS-DA) and selectivity ratio (SR) were applied.

Results. The C vs RAH model presented the best prediction performance (AUC test = 0.90) and had a sensitivity and specificity of 73.68% and 83.33%, respectively. However, the parameters selected for the C vs AH group model were the most important for the pathway described in the rodent model, i.e., greater density of the skin lymphatic vessels (D2-40 expression) and greater number of macrophages (CD68 expression), higher expression of the messenger ribonucleic acid (mRNA) of nuclear factor of activated T cells 5 (NFAT5), vascular endothelial growth factor C (VEGF- C) and podoplanin (PDPN) in the skin, greater concentration of hyaluronic acid (HA) in the skin, and lower serum concentration of VEGF-C.

Conclusions. Our study suggests that the NFAT5/VEGF-C/lymphangiogenesis pathway, previously described in rodent studies, may also be present in human HA. Further experiments are needed to confirm our findings.

Key words: lymphangiogenesis, chemometrics, salt-sensitivity, nuclear factor of activated T cells 5 (NFAT5), vascular endothelial growth factor C (VEGF-C)

64

A. Chachaj et al. Lymphatic system in arterial hypertension

Background

The lymphatic system is complementary to the circulatory system, and its principal function is to maintain fluid homeostasis and prevent tissue edema.[1] There is growing evidence that the lymphatic system of the skin interstitium may also play an essential role in the pathophysiology of arterial hypertension (AH).[2–5]

Previous rodent studies revealed that sodium ions (Na+) accumulate in the skin in an osmotically inactive form, binding to glycosaminoglycans (GAGs).[6–9] The [23]Na magnetic resonance imaging ([23]Na-MRI) studies confirmed that Na+ is also stored in human skin and (in smaller quantities) in muscles.[10,11] The increased skin Na+ content in rodents resulted in more intensive GAGs skin synthesis,[2] polymerization and degree of sulfation.[9,12,13] A higher concentration of Na+ in the skin of rodents resulted in hypertonic stress and subsequent stimulation of a pathway that started with infiltration of the skin by macrophages[14] and activation of nuclear factor of activated T cells 5 (NFAT5).[15] The next step was macrophage secretion of vascular endothelial growth factor C (VEGF-C)[14] and activation of lymphangiogenesis in the skin.[2] Blocking the macrophages – VEGF-C – lymphangiogenesis axis in the skin of rodents fed a high-sodium diet by genetic or pharmacological interventions resulted in salt-sensitive AH.[3,4]

The regulatory pathway proposed in the experimental rodent model may be protective in AH. Vascular endothelial growth factor C, as the main stimulator of lymphangiogenesis, is also a regulator of the lymphatic vessels' pump activity[16] and a known inducer of the endothelial nitric oxide synthase (eNOS) expression, associating with the vasodilation of blood vessels and, potentially, with lowering blood pressure via NO elevation.[2,13,17] Moreover, newly formed lymphatic vessels might enable the removal of Na+ and water from the skin interstitium.[2–5,18,19]

Our previous studies demonstrated that the lymphatic system and the skin interstitium may also play a role in the pathophysiology of AH in humans. In our 1st study, we demonstrated that the hypertensive and control groups did not differ in the skin concentration of Na+, that a higher skin concentration of Na+ was associated with increased water content, and that the patients with resistant hypertension had a higher number of macrophages in the skin and lower concentration of serum VEGF-C than the control group.[20] Our 2nd study showed that the patients with hypertension and a higher concentration of Na+ in the skin had a significantly greater density of skin lymphatic vessels, and that skin water content correlated with factors associated with lymphangiogenesis in the skin, i.e., messenger ribonucleic acid (mRNA) expression of NFAT5, VEGF-C, and podoplanin (PDPN), and number of macrophages (expression of CD68).[21] We managed to separate a group of patients with AH that most closely matched the experimental rodent model of salt-sensitive hypertension in the histological and molecular assessment (it was the group of patients with AH and a high Na+ concentration in the skin), and there were some significant relationships among the parameters important in the pathway described in rodents. However, the direct differences in the individual parameters important for this pathway between hypertensive and normotensive groups were mainly insignificant.[21]

In the present study, we addressed whether it is possible to determine the sets of parameters important for the NFAT5-VEGF-C-lymphangiogenesis pathway to distinguish hypertensive from normotensive patients. Mathematically, this can be done using a multivariate discriminant analysis.[22,23] Therefore, we applied a multivariate bootstrap method that combined partial least squares-discriminant analysis (PLS-DA) and the selectivity ratio (SR).

Objectives

To determine whether the pathway parameters previously described in rodents would allow for distinguishing hypertensive and normotensive patients.

Materials and methods

Study design

Molecular and histopathological parameters from the skin and blood of patients with AH and without AH (control group) were used, and a statistical multivariate bootstrap methodology combing PLS-DA and SR was applied.

Participants

Patients hospitalized in the Department of Surgery in the 4th Military Hospital in Wrocław (Poland), with and without AH, who had undergone elective surgery with an abdominal skin incision, were enrolled in the study. The participants represent a continuous population of those with planned surgical intervention of abdominal skin incisions. Among the most common indications for abdominal surgery were abdominal aortic aneurysm, Leriche's syndrome, gallstones, and abdominal hernia.

The exclusion criteria were secondary hypertension, diabetes mellitus, kidney failure, and a body mass index (BMI) >40 kg/m^2.

To ensure that the groups did not differ in age, we removed patients under or equal to 50 years from the control group. We also removed 1 patient with a BMI of 42.9 kg/m^2 because this patient was enrolled in our study incorrectly (BMI > 40 kg/m^2 was an exclusion criterion). Additionally, we removed 1 patient with a BMI of 38.1 kg/m^2 from the AH group because this BMI value was significantly higher than the BMI values in all other patients. The study groups did not differ in sex. The measurements of 1 control patient (patient No. 46 from the control group) were
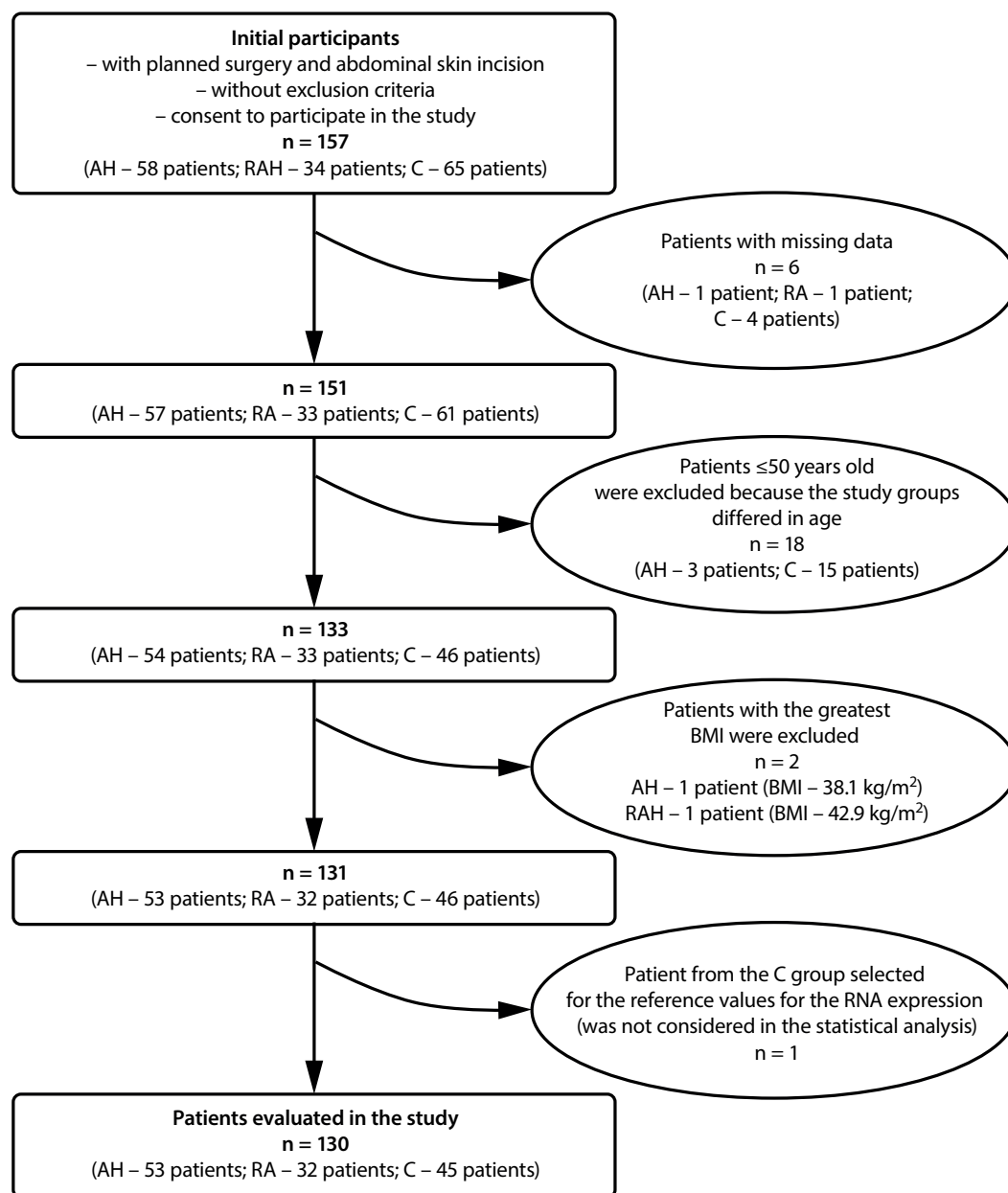
Fig. 1. Patient selection flowchart

AH – group with arterial hypertension; RAH – group with resistant arterial hypertension; C – control group; BMI – body mass index.

selected as the reference values for estimating the RNA expression parameters. This patient was not considered in the statistical analysis in this study. A flowchart of patient selection is presented in Fig. 1.

The Bioethical Commission of Wroclaw Medical University approved the study protocol (approval No. KB-578/2012). All of the participants were informed about the purpose of the study, and written informed consent was signed by every patient before their inclusion. The study was conducted following the principles outlined in the Declaration of Helsinki.

Study groups

We evaluated the following study groups: 1) with AH (patients with AH who required no more than 3 antihypertensive drugs to control their blood pressure, n = 53; among them, there were 9 patients with AH recognized as de novo); 2) with resitant AH (RAH) (RAH patients with AH who required more than 3 different antihypertensive drugs to control their blood pressure, n = 32); 3) control (C) group (patients without AH, n = 45).

Diagnosis of AH was defined as systolic blood pressure (SBP) ≥140 mm Hg and/or diastolic blood pressure (DBP) ≥90 mm Hg.[24] Blood pressure measurements were repeated using the Riva–Rocci method in a seated rest period during daily hospitalization, also in the control group. The final AH diagnosis, or lack of such diagnosis, was based on carefully analyzing each patient's medical history and clinical evaluation, including repeated blood pressure measurements. Most patients qualified to the AH group had the AH diagnosis stated in the past and had been taking antihypertensive medications before admission to the hospital. Blood pressure measurements were

66

A. Chachaj et al. Lymphatic system in arterial hypertension

the basis for qualifying the patients with AH to the group with resistant AH (the RAH group) or controlled AH with less than 3 drugs (the AH group). Moreover, among patients without diagnosis of AH at admission to the hospital (initially the control patients), those with repeated blood pressure values above 140/90 mm Hg were diagnosed with AH recognized as de novo, and they started to take the antihypertensive treatment. They were finally qualified for the group with AH (the AH group).

Variables

Skin samples were taken from abdominal skin at the beginning of surgery at the site of the planned surgical incision. They were then cut into smaller parts and placed in appropriate test tubes (for histological examination, Na^+ concentration, water content, hyaluronic acid (HA), real-time polymerase chain reaction (PCR), and protein assessment with western blot), as previously described.[21]

We took the following parameters into account in the statistical analysis: skin Na^+, water content in the skin, HA in the skin (HA, as a significant component of GAGs in the skin,[25] which can leave the skin interstitium through the lymphatic vessels and is present in the bloodstream[26]), skin mRNA expression of NFAT5, VEGF-C, and PDPN, number of macrophages (as CD68 expression) in the skin, and the density of lymphatic vessels in the skin (as the PDPN/D2-40 expression). In addition, we also considered the expression of CD31 in the skin (regarded as a blood endothelium marker; however, in light of recent findings, CD31 is a pan-endothelial marker and may also be detected on several immune cells and lymphatic endothelium cells),[27–30] VEGF-D mRNA (another known stimulator of the process of lymphangiogenesis), skin tumor necrosis factor alpha (TNF-α) mRNA (as a marker of inflammation in the skin),[31] plasma concentrations of HA, Na^+, K^+, and creatinine, and the parameters which have been suggested to be the markers of salt-sensitivity, i.e., plasma renin activity (PRA),[32,33] plasma concentration of N-terminal pro atrial natriuretic peptide (NT-proANP)[34,35] and serum concentration of circulating VEGF-C.[36]

Detailed descriptions of the study samples and laboratory procedures were published elsewhere,[21] except the method used to evaluate the expression of CD31 in the skin, which was described below.

Immunohistochemistry of CD31 expression in the skin

Immunohistochemical (IHC) reactions were performed on 4-μm thick paraffin sections, as previously described. As primary antibodies (20 min incubation), mouse monoclonal against CD31 (clone JC70A, ready-to-use, IR610; Dako, Glostrup, Denmark) was used. Expression of CD31 was assessed according to the Weidner method.[37] The IHC reactions were evaluated with a BX-41 light microscope (Olympus Corp., Tokyo, Japan). First, the slides were examined under low magnification (×100) to identify areas with the highest vascular density (hotspots). Then, under ×400 magnification, stained vessels were counted in 3 hotspots. The final score for each slide was presented as a mean number of vessels per mm^2. Any stained cells were counted as a single microvessel, even in the absence of a vessel lumen.[37]

Statistical univariate and multivariate chemometric analysis

Univariate and multiple analyses used a classic and nonparametric analysis of variance (ANOVA) for the initial data categorization. The Kolmogorov–Smirnov test was also used to assess whether each sample was drawn from a normally distributed population. As a nonparametric variant of classic ANOVA, the Kruskal–Wallis test was used, followed by a post hoc Dunn's test with the Sidak adjustment formula.[38] Any values missing completely at random (ca. 7.6%) were not considered in the comparisons. A $χ^2$ test assessed whether the hypertension diagnosis and family history of hypertension were independent and if AH diagnosis and gender were independent.

The strategy for a multivariate discriminant analysis combined a PLS-DA with the SR method for selecting the most important parameters for distinguishing 2 respective groups. A bootstrapped method, with a replacement, was used to estimate the quality of the models with the selected parameters, and the prediction was evaluated for the test set. The sensitivity, specificity and efficiency were presented as figures of merit to evaluate any model's prediction ability. To obtain a representative model set that contained samples that described all of the variability that was characteristic for each group (e.g., C, AH or RAH) and was balanced to avoid the recalculation of the cutoff value in the PLS discriminant model,[39] the Kennard and Stone algorithm[40] was used. Thus, 26 samples were considered in the model set for each of the 3 pair–group comparisons, while the remaining samples (n_C = 19, n_{AH} = 27 and n_{RAH} = 6) were placed in the respective test set. The complexity of every PLS-DA model for each bootstrapped sample (out of 1,000) was selected automatically after a leave-one-sample-out cross-validation procedure. Since the data contained missing values, the Kennard and Stone algorithm was modified to estimate the distances using the partial distance strategy,[41] with which the squared Euclidean distance was only calculated for the observed elements, and the result was proportionally rescaled to account for missing values. An expectation–maximization approach in PLS-DA[42,43] was adopted to manage the incomplete model sets and to perform the prediction for the incomplete test sets. The strategy may be described using, e.g., the C vs RAH model. First, a bootstrap sample (26 C and 26 RAH samples) for the model set was created by randomly withdrawing samples from each group with

a replacement. Then, a PLS-DA model of a given complexity was constructed for the autoscaled parameters, and the respective SR values for all of the parameters (1 SR value for each parameter), or the area under the receiver operating curve (AUC) value for the entire model, were estimated. This calculation was repeated for 1,000 different bootstrap samples, and the respective 1,000 SR values for each variable were used to obtain the estimates of the mean and standard deviation (M ±SD) or a histogram of the AUC values. A cutoff value for the average SR values was then selected, considering the relationship between the average discriminative power of any parameter and the selectivity ratio, which was 0.1 in this case. A bootstrap procedure was used to evaluate the average AUC values and the uncertainty of the model with a reduced number of parameters and, finally, to obtain the prediction for the test set. The scheme of the entire procedure was presented elsewhere.[44]

All calculations employed Statistical Toolbox 8.0 with MATLAB 7.0 (R14) (https://www.mathworks.com), and in-house tested and validated algorithms were performed on a personal computer (Intel(R) Pentium(R) M, 1.60GHz with 2GB RAM) using the Microsoft Windows XP (service pack 2) operating system (Microsoft Corp., Redmond, USA).

Results

Univariate analysis

The study groups did not differ in the mean age or sex values. The hypertensive groups had significantly higher BMI than the control group (p = 0.003, Kruskal–Wallis test). The basic demographic and medical data of all studied groups are listed in Table 1.

A comparison of the primary groups using ANOVA and Kruskal–Wallis tests showed that the concentrations of Na^+ in the skin were similar in the hypertensive and control groups. Only the mean and median values of creatinine and renin concentration in plasma in the RAH group and NFAT5, VEGF-C and PDPN mRNA expressions in the skin in the AH group were found to be significantly higher than in the C group.

Multivariate models using a partial least squares-discriminant analysis

The next hypothesis was whether the changes in the combination of the studied parameters were responsible for distinguishing any 2 defined groups. To describe the relationship among all of the parameters and determine which of them might be responsible for distinguishing the normotensive individuals from the non-resistant hypertensive patients (C vs AH), the normotensive individuals from patients with resistant hypertension (C vs RAH) and the non-resistant and resistant hypertensive patients (AH vs RAH), multivariate discriminant models used a PLS-DA was constructed under the assumption that a linear combination of parameters (not a single parameter) might be responsible for describing the differences between any 2 groups. This is a straightforward assumption to account for any covariance/correlations among all of the parameters and the impact of these relationships in the discriminant analysis, which is impossible to conduct using univariate analysis.

First, the quality of the 3 pairwise multivariate discriminant PLS-DA models (C vs AH, C vs RAH and AH vs RAH) was evaluated and described by the average and

Table 1. Selected demographic and medical parameters of the studied groups

Parameter		C group (n = 45)	AH group (n = 53)	RAH group (n = 32)	p-value
Age, mean ±SD (min–max)		65 ±7 (56–81)	68 ±8 (51–89)	67 ±8 (56–81)	0.092*
BMI [kg/m²], mean ±SD		25.4 ±3.6	27.0 ±3.2	28.6 ±4.0#	0.003*
Male gender [%]		68.9	73.6	68.8	0.842**
SBP [mm Hg], mean ±SD		124.23 ±8.76	140.16 ±15.42#	148.14 ±19.66#	<0.001*
DBP [mm Hg], mean ±SD		77.63 ±5.28	83.47 ±8.13#	84.90 ±13.31#	0.003*
Number of antihypertensive medications used by the patients [%]	1 medication	–	30.6	–	–
	2 medications	–	44.9	–	
	3 medications	–	24.5	59.4	
	4 medications	–	–	28.1	
	5 medications	–	–	12.5	
Mean time from diagnosis of hypertension [years]		–	9.6	12.5	–
Family history of hypertension [%]		14.3	44.0	51.7	0.008**

* Kruskal–Wallis test (Kolmogorov–Smirnov normality test for all parameters p < 0.001); ** χ^2 test. # statistically significant differences vs C group in the multiple comparison Dunn–Sidak post hoc testing; C – control group; AH – group with arterial hypertension; RAH – group with resistant arterial hypertension; SD – standard deviation; BMI – body mass index; SBP – systolic blood pressure; DBP – diastolic blood pressure.

A

B

C
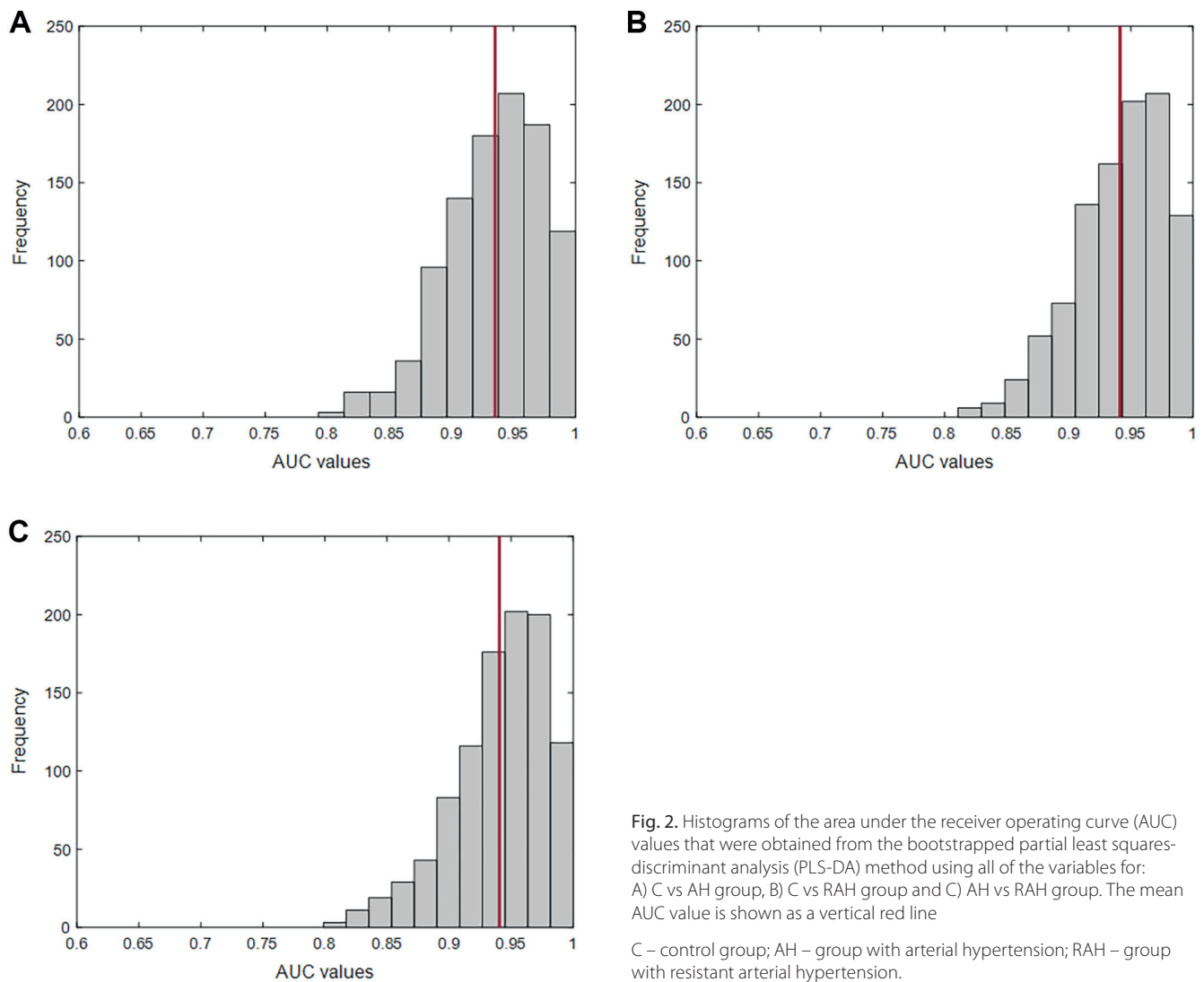
Fig. 2. Histograms of the area under the receiver operating curve (AUC) values that were obtained from the bootstrapped partial least squares-discriminant analysis (PLS-DA) method using all of the variables for: A) C vs AH group, B) C vs RAH group and C) AH vs RAH group. The mean AUC value is shown as a vertical red line

C – control group; AH – group with arterial hypertension; RAH – group with resistant arterial hypertension.

Table 2. The average area under the receiver operating curve (AUC) values (uncertainty in the AUC evaluation) for the model and the AUC values for the test set that were obtained from partial least squares-discriminant analysis (PLS-DA). Sensitivity, specificity and efficiency for the test sets with all of the variables

Model	Average AUC values for model set	AUC for test set	PLS-DA (complexity)	Sensitivity [%]	Specificity [%]	Efficiency [%]
C vs AH	0.94 ±0.04	0.70	3	94.74	44.44	65.22
C vs RAH	0.94 ±0.04	0.95	3	84.21	100.00	88.00
AH vs RAH	0.94 ±0.04	0.70	3	37.04	100.00	48.48

C – control group; AH – group with arterial hypertension; RAH – group with resistant arterial hypertension.

standard error values of the AUC, which was estimated for 1,000 bootstrapped samples, with a replacement. The AUC values measure the model's ability to distinguish between the groups, with a higher AUC indicating a better model. The statistical analysis section describes the selection of a balanced model and test sets. The histograms of the AUC values (the mean AUC value is presented by a vertical red line) are presented in Fig. 2. The sensitivity, specificity and efficiency of the prediction are listed in Table 2.

From the results presented in Table 2, the best prediction was obtained from the model built to distinguish the resistant hypertensive group from the control group (AUC_{test} = 0.95). The best prediction expression means that the sensitivity, specificity and efficiency estimated for the independent tests set were as close as possible to 100%. The test samples were not used to build the model. Three normotensive individuals were incorrectly recognized as resistant hypertensive patients, and this resulted in a sensitivity of 84.21%. The model had the highest specificity

Table 3. Univariate, multivariate and descriptive statistics for the parameters that were found to be the most important using the selectivity ratio – partial least squares-discriminant analysis (SR-PLS-DA). Bootstrapping was used to estimate the mean selectivity ratio (SR) for each parameter. A cutoff value of 0.10 for average SR was used to select the important parameters (*)

Parameters	Mean values of parameters ±SD			Kruskal–Wallis test p-value	Parameters selected (*) by SR-PLS-DA in all models (average SR > 0.10)		
	C group (n = 45)	AH group (n = 53)	RAH group (n = 32)		C vs AH	C vs RAH	AH vs RAH
Plasma Na$^+$ [mmol/L^{-1}]	140.67 ±3.23	140.85 ±3.11	141.21 ±2.70	0.632	*	–	*
Plasma K$^+$ [mmol/L^{-1}]	4.20 ±0.40	4.28 ±0.48	4.47 ±0.54	0.117	*	*	*
Plasma creatinine [mg/dL^{-1}]	0.82 ±0.18	0.91 ±0.26	1.06 ±0.40#	0.022	*	*	*
eGFR [mL/min^{-1}]	92.16 ±27.34	86.93 ±28.63	90.44 ±32.48	0.624	*	*	*
Plasma NT-proANP [nmol/L^{-1}]	2.69 ±1.64	3.15 ±2.17	3.69 ±2.89	0.500	*	*	*
Plasma renin activity [uIU/mL^{-1}]	75.69 ±52.15	186.76 ±332.96	291.05 ±428.40#	0.018	*	*	–
Skin lymphatic vessels, D2-40 [um^2]	7,889.59 ±4,684.28	9,392.61 ±5,090.00	8,193.45 ±4,525.78	0.301	*	–	*
Skin CD68 [number of macrophages/mm^{-2}]	4.33 ±3.69	7.05 ±11.58	4.06 ±5.85	0.179	*	–	*
Skin log (NFAT5 mRNA)	0.66 ±0.50	0.97 ±0.40#	0.90 ±0.41	0.003	*	*	–
Skin log (VEGF-C mRNA)	0.47 ±0.33	0.65 ±0.30#	0.60 ±0.34	0.029	*	*	–
Skin log (VEGF-D mRNA)	0.52 ±0.51	0.60 ±0.45	0.48 ±0.53	0.299	–	–	*
Skin log (PDPN mRNA)	0.50 ±0.60	0.82 ±0.51#	0.74 ±0.54	0.008	*	*	–
Serum VEGF-C [pg/mL^{-1}]	4,784.11 ±1,800.16	4,483.74 ±1,668.33	4,084.76 ±1,667.89	0.122	*	*	–
Serum VEGF-D [pg/mL^{-1}]	343.78 ±150.98	338.60 ±139.29	317.00 ±156.66	0.466	–	–	*
Skin water [% of dry weight]	53.13 ±39.92	52.7 ±40.81	35.36 ±18.47	0.063	–	*	*
Skin hyaluronic acid [mg/g^{-1}]	0.56 ±0.25	0.74 ±0.81	0.54 ±0.24	0.714	*	*	*
Skin blood vessels, CD31 [v/mm^{-2}]	12.45 ±5.79	13.32 ±7.44	12.67 ±8.23	0.443	–	–	–
Skin log (TNF-α mRNA)	–0.10 ±0.29	–0.13 ±0.33	–0.12 ±0.29	0.880	–	–	–
Serum hyaluronic acid [ng/mL^{-1}]	40.51 ±40.04	45.15 ±38.07	42.38 ±36.55	0.316	–	–	–
Skin Na$^+$ [mg/kg^{-1}]	624.97 ±485.04	567.79 ±409.64	583.45 ±353.69	0.939	–	–	–

Normality test (Kolmogorov–Smirnov): failed for all parameters (p < 0.001); #statistically significant differences vs C group in the multi-comparison Dunn–Sidak post hoc testing; SD – standard deviation; C – control group; AH – group with arterial hypertension; RAH – group with resistant arterial hypertension; Na$^+$– sodium, K$^+$ – potassium; eGFR – estimated glomerular filtration rate; NT-proANP – N-terminal proatrial natriuretic peptide; NFAT5 – nuclear factor of activated T cells 5; VEGF-C – vascular endothelial growth factor C; VEGF-D – vascular endothelial growth factor D; PDPN – podoplanin; TNF-α – tumor necrosis factor alpha.

(100%), indicating that all resistant hypertensive patients were correctly recognized. A specificity of 100% was also obtained for the model built to distinguish between non-resistant and resistant hypertensive patients (AH vs RAH in Table 2). However, this model had very poor sensitivity (37.04%), and the probability of correctly identifying a non-resistant hypertensive patient (AH patient) was very low. In contrast, the probability of an incorrect identification of an AH patient as an RAH patient was relatively high. Indeed, the model that described the differences between the normotensive individuals and the non-resistant hypertensive patients (C vs AH) showed a relatively high sensitivity of 94.74%, but a low specificity (44.44%). This suggests that the probability of incorrectly recognizing a normotensive patient as non-resistant hypertensive was very low. In contrast, the probability of incorrectly identifying a non-resistant hypertensive patient as normotensive was relatively high. Thus, all of the parameters that were usually considered to describe the mechanism of Na$^+$ regulation in the skin are best explained by the differences between normotensive and resistant hypertensive individuals.

An important question was whether reducing the number of parameters would also provide a good description of the models regarding the sensitivity, specificity and prediction efficiency. The parameters were selected using the SR approach in PLS-DA, and the method is abbreviated as SR-PLS-DA.[45–47] The SR is a figure of merit that describes the importance (in terms of the explained variance) of each parameter in the model construction. The larger the SR value for a parameter, the more important it is in explaining the differences between the groups in the PLS-DA model. The SR values for each parameter were estimated during the bootstrapping procedure (1,000 bootstrapped samples), and parameters with average SR values (e.g., the average value of 1,000 SR values obtained for each parameter) larger than 0.10 were selected as important. The descriptive statistics for the parameters found to be the most important in each model are shown in Table 3.

Table 4. The average area under the receiver operating curve (AUC) values (uncertainty in the AUC estimation) for the model and test sets with the selected variables from the selectivity ratio – partial least squares-discriminant analysis (SR-PLS-DA). Sensitivity, specificity and efficiency for the test sets with selected variables are marked by an asterisk (*). in Table 3. The cutoff value for selectivity ratio (SR) in all of the models was 0.10

Model	Average AUC values for model set	AUC for test set	PLS-DA (complexity)	Sensitivity [%]	Specificity [%]	Efficiency [%]
C vs AH	0.90 ±0.04	0.68	2	89.47	33.33	56.52
C vs RAH	0.89 ±0.04	0.90	2	73.68	83.33	76.00
AH vs RAH	0.87 ±0.05	0.73	2	22.22	100.00	36.36

C – control group; AH – group with arterial hypertension; RAH – group with resistant arterial hypertension.

The C vs AH and AH vs RAH models used 11 of the 20 parameters, but only 6 selected parameters (54%) were common. The parameters important for differentiating C and RAH were unimportant for distinguishing the AH and RAH patients, and it was renin, log (NFAT5 mRNA), log (VEGF-C mRNA), log (PDPN mRNA), and serum VEGF-C. Conversely, the parameters important for distinguishing AH and RAH groups that were unimportant for distinguishing the C and RAH groups were plasma Na$^+$, D2-40, CD68, log (VEGF-D mRNA), and serum VEGF-D. The C vs AH model required a larger number of parameters (13 of the 20) and had a larger number of parameters that were common with the other 2 models (ten common parameters concerning the C vs RAH model and 8 common parameters compared to those that had been used with the AH vs RAH model). Specifically, skin water, log (VEGF-D mRNA) and serum VEGF-D were unimportant for distinguishing the normotensive and non-resistant hypertensive patients. Still, they were found to be important in the other 2 models.

The performance of the models with the selected parameters was re-evaluated using the bootstrapping procedure; the results are presented in Table 4. Once again, the best performance for the test set (AUC_{test} = 0.90) was obtained when differentiating the normotensive individuals from the resistant hypertensive patients. Compared to the model with all parameters, this model had a lower sensitivity, specificity and efficiency for the test set. However, the C vs AH model also had a very poor specificity (33.33%), while the AH vs RAH model had a very low sensitivity (22.22%).

Discussion

The group in our study that most corresponded to the sequence of events documented in the rodents' skin was the AH group. The parameters that distinguished AH group from C group were also important for the mechanism presented in the studies of Machnik et al.,[2,3] Wiig et al.[4] and Nikpey et al.,[5] i.e., a greater density of lymphatic vessels (expressed as D2-40), a greater number of macrophages in the skin (expressed as CD68), a higher expression of NFAT5, VEGF-C and PDPN mRNA, a higher concentration of HA in the skin, and a lower concentration of serum VEGF-C. As in the studies of Machnik et al.,[2,3] the expression of TNF-α mRNA was not important for differentiating the studied groups.

Although more than a dozen years have passed since the NFAT5-VEGF-C lymphangiogenesis pathway was described in experimental AH rodent studies,[2–5] our studies (this and recently published) are the first human studies that directly translate the rodent model of the involvement of the lymphatic system in the pathogenesis of AH to the patients. Studying this mechanism in humans is challenging since the pathogenesis of human AH is heterogeneous, and salt sensitivity is only one of the causes. That may be the reason why the groups in our study did not differ significantly in the majority of parameters important for studying the pathway using univariate analysis (except for the higher NFAT5, VEGF-C and PDPN mRNA expression in the skin in the AH compared to the C group). By utilizing a multivariate discriminant analysis method, such as PLS-DA, we could provide additional evidence that the mechanisms observed in the skin of rodents may also be applicable to humans.

The dominant pathophysiological mechanisms that led to resistant hypertension were probably various in the RAH group, which we primarily hypothesized would be the most salt-sensitive.[48] The lack of a tendency to lower PRA values in the RAH group might suggest mechanisms other than salt sensitivity,[32,33] which led to resistant hypertension in this group. Another explanation is that there was an insufficient activation of the NFAT5-VEGF-C pathway and, therefore, no effect on the increase in the number of macrophages and the density of lymphatic vessels in the skin in the RAH group.

Interestingly, the lower concentration of skin water in the RAH group was one of the parameters that differentiated the RAH group from the C or AH group. This observation might have resulted from increased vascular contraction and arterial remodeling, characteristic of long-lasting resistant AH.[49] The greater vascular resistance might be associated with a decreased filtration from the capillaries at the microcirculation level and, therefore, there was a lower skin water content. It might be an important observation concerning the pathophysiology of the NFAT5–VEGF-C–lymphangiogenesis pathway because we showed in our previous study that the skin water content was strongly associated with lymphangiogenesis

in the skin, i.e., it was associated with greater mRNA expression of NFAT5, VEGF-C and PDPN, and a number of macrophages.[21]

Assuming that the skin water content triggers skin lymphangiogenesis, a smaller amount of water passing through the skin microcirculatory system through vessels hardened by long-lasting hypertension might result in inadequately activated NFAT5-VEGF-C-lymphangiogenesis in patients with RAH. However, this suspicion requires further elucidation.

In this study, the concentration of Na^+ in the skin did not differ in hypertensive and the control groups, as we had previously reported.[20] Moreover, the amount of skin Na^+ was not responsible for the differentiation between pairs of studied groups in the multivariate analysis. However, we would expect a difference in the skin Na^+ concentrations if the healthy individuals in an experiment consumed excessive amounts of salt in their diets and the results of measuring Na^+ in their skin were compared with those of healthy subjects. In our study, we did not control the intake of dietary salt. Therefore, some normotensive individuals could have had higher levels of skin Na^+ than usual. In comparison, the hypertensive patients could have had lower levels of skin Na^+ than the control due to the administration of antihypertensive medications or because of following a low-sodium diet, which is usually prescribed for patients with AH.

In our study, the patients in the RAH group had a higher BMI than the C group. However, we do not consider the difference in BMI as a limiting factor. The relationship between the higher body weight (BMI approx. 30 kg/m^2) and AH has been well documented,[50,51] as patients with primary hypertension in the same age group generally present a higher BMI.

Limitations

The main limitations of the study were previously described in detail.[20,21] Additionally, there is the marginal possibility of patients' incorrect classification to hypertensive groups based on medical history and non-standardized BP measurement without ambulatory blood pressure monitoring (ABPM), especially since the patients were pre-surgical. The patients from the control group did not have AH because neither the medical history nor measurements during hospitalization indicated it. The group with hypertension treated with <3 antihypertensive drugs mainly consisted of patients with a previously diagnosed and treated AH (before hospitalization), and only 9 patients from this group had AH diagnosed de novo, based on blood pressure measurements during hospitalization. Even if we assume that some of the patients with AH recognized de novo were included in the AH group (the AH group) instead of the control group (elevated blood pressure might be only a result of perioperative stress or "white coat" AH in some of these patients), the differences
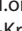
between the control group and the group with HA (the AH group) would be less significant. The group with resistant hypertension (the RAH group) might also include some patients with non-resistant AH. Still, such a possible incorrect classification of some patients would only reduce the differences between the AH and the RAH groups, not increase them. Therefore, the small risk associated with incorrect patient classification to both AH groups (AH and RAH) in our study only reduced differences among the study groups and did not increase them. The equalization of the study groups in age achieved by eliminating patients under or equal to 50 years old instead of the process of matching the patients might also be considered as a limiting factor.

The lack of sodium sensitivity testing in our patients is another important study's limitation. However, our priority was examining the skin, which was only possible in patients who had undergone surgery with an abdominal incision. It would have been ethically debatable to perform a sodium sensitivity test on patients awaiting surgery. The precise protocol requires one week of low and then one week of high salt intake. A shorter procedure consisting of administering intravenous saline and then furosemide is not accurate.[52] Moreover, a possible dietary interview with our patients about their salt intake would not have enabled us to identify a salt-sensitive group – it might have been more confusing than helpful. Most of our participants took several antihypertensive medications, including diuretics, usually for a long time. Determining the impact of such drugs on the concentration of Na^+ in the skin and on the investigated mechanism was also not possible.[11] Moreover, every disease, taking any medications currently and in the past, the patient's hormonal state, and indication for surgery might impact the studied mechanism. The number of such influencing parameters is countless and completely unknown. Therefore, when we planned our study, we decided on a simple qualification of patients based on the division with and without hypertension after confirming the absence of exclusion criteria used in our research.

Conclusions

The results of our study, specifically the differentiation between the AH group and the respective C group, suggest that the NFAT5–VEGF-C–lymphangiogenesis pathway, previously described in experimental AH in rodent studies, might also be present in humans. However, it was only an observational study. Further experiments are needed to prove our findings. Regulation of this pathway also requires further research. Such investigations are worth the effort because establishing the exact role of the lymphatic system in the pathophysiology of AH would provide a basis for searching for new therapeutic agents for this disease.

ORCID iDs

Angelika Chachaj ⬤ https://orcid.org/0000-0001-8087-8005
Ivana Stanimirova ⬤ https://orcid.org/0000-0003-4966-3246
Mariusz Chabowski ⬤ https://orcid.org/0000-0002-9232-4525
Agnieszka Gomułkiewicz ⬤ https://orcid.org/0000-0003-2256-1055
Paweł Hodurek ⬤ https://orcid.org/0000-0002-6364-0879
Natalia Glatzel-Plucińska ⬤ https://orcid.org/0000-0001-6901-1240
Mateusz Olbromski ⬤ https://orcid.org/0000-0002-1972-1524
Aleksandra Piotrowska ⬤ https://orcid.org/0000-0003-4093-7386
Aleksandra Kuzan ⬤ https://orcid.org/0000-0003-4264-8174
Jędrzej Grzegrzółka ⬤ https://orcid.org/0000-0002-1548-279X
Katarzyna Ratajczak-Wielgomas
　　⬤ https://orcid.org/0000-0001-6175-2204
Ewa Szahidewicz-Krupska ⬤ https://orcid.org/0000-0002-4446-6991
Jerzy Wiśniewski ⬤ https://orcid.org/0000-0003-2831-7643
Mariusz A. Bromke ⬤ https://orcid.org/0000-0002-0806-6608
Marzenna Podhorska-Okołów
　　⬤ https://orcid.org/0000-0003-2215-5997
Andrzej Gamian ⬤ https://orcid.org/0000-0002-2206-6591
Dariusz Janczak ⬤ https://orcid.org/0000-0003-4671-9128
Piotr Dzięgiel ⬤ https://orcid.org/0000-0002-8292-1385
Andrzej Szuba ⬤ https://orcid.org/0000-0002-7555-6201

References

1. Wiig H, Swartz MA. Interstitial fluid and lymph formation and transport: Physiological regulation and roles in inflammation and cancer. *Physiol Rev*. 2012;92(3):1005–1060. doi:10.1152/physrev.00037.2011

2. Machnik A, Neuhofer W, Jantsch J, et al. Macrophages regulate salt-dependent volume and blood pressure by a vascular endothelial growth factor-C-dependent buffering mechanism. *Nat Med*. 2009; 15(5):545–552. doi:10.1038/nm.1960

3. Machnik A, Dahlmann A, Kopp C, et al. Mononuclear phagocyte system depletion blocks interstitial tonicity-responsive enhancer binding protein/vascular endothelial growth factor C expression and induces salt-sensitive hypertension in rats. *Hypertension*. 2010;55(3): 755–761. doi:10.1161/HYPERTENSIONAHA.109.143339

4. Wiig H, Schröder A, Neuhofer W, et al. Immune cells control skin lymphatic electrolyte homeostasis and blood pressure. *J Clin Invest*. 2013;123(7):2803–2815. doi:10.1172/JCI60113

5. Nikpey E, Karlsen TV, Rakova N, Titze JM, Tenstad O, Wiig H. High-salt diet causes osmotic gradients and hyperosmolality in skin without affecting interstitial fluid and lymph. *Hypertension*. 2017;69(4): 660–668. doi:10.1161/HYPERTENSIONAHA.116.08539

6. Ivanova L, Archibasova V, Shterental' I. Sodium-depositing function of the skin in white rats [in Russian]. *Fiziol Zh SSSR Im I M Sechenova*. 1978;64(3):358–363. PMID:648666.

7. Arkhibasova V, Ivanova L, Podsekaeva G, Natochin I. Possibilities of deposition of electrolytes in the skin in different states of water-salt metabolism [in Russian]. *Fiziol Zh SSSR Im I M Sechenova*. 1983; 69(10):1352–1356. PMID:6641985.

8. Schafflhuber M, Volpi N, Dahlmann A, et al. Mobilization of osmotically inactive Na$^+$ by growth and by dietary salt restriction in rats. *Am J Physiol Renal Physiol*. 2007;292(5):F1490–F1500. doi:10.1152/ajprenal.00300.2006

9. Heer M, Frings-Meuthen P, Titze J, et al. Increasing sodium intake from a previous low or high intake affects water, electrolyte and acid–base balance differently. *Br J Nutr*. 2009;101(9):1286. doi:10.1017/S0007114508088041

10. Kopp C, Linz P, Dahlmann A, et al. ^{23}Na magnetic resonance imaging-determined tissue sodium in healthy subjects and hypertensive patients. *Hypertension*. 2013;61(3):635–640. doi:10.1161/HYPERTENSIONAHA.111.00566

11. Dahlmann A, Dörfelt K, Eicher F, et al. Magnetic resonance-determined sodium removal from tissue stores in hemodialysis patients. *Kidney Int*. 2015;87(2):434–441. doi:10.1038/ki.2014.269

12. Titze J, Lang R, Ilies C, et al. Osmotically inactive skin Na$^+$ storage in rats. *Am J Physiol Renal Physiol*. 2003;285(6):F1108–F1117. doi:10.1152/ajprenal.00200.2003

13. Titze J, Machnik A. Sodium sensing in the interstitium and relationship to hypertension. *Curr Opin Nephrol Hypertens*. 2010;19(4):385–392. doi:10.1097/MNH.0b013e32833aeb3b

14. Müller S, Quast T, Schröder A, et al. Salt-dependent chemotaxis of macrophages. *PLoS One*. 2013;8(9):e73439. doi:10.1371/journal.pone.0073439

15. Miyakawa H, Woo SK, Dahl SC, Handler JS, Kwon HM. Tonicity-responsive enhancer binding protein, a Rel-like protein that stimulates transcription in response to hypertonicity. *Proc Natl Acad Sci U S A*. 1999; 96(5):2538–2542. doi:10.1073/pnas.96.5.2538

16. Breslin JW, Gaudreault N, Watson KD, Reynoso R, Yuan SY, Wu MH. Vascular endothelial growth factor-C stimulates the lymphatic pump by a VEGF receptor-3-dependent mechanism. *Am J Physiol Heart Circ Physiol*. 2007;293(1):H709–H718. doi:10.1152/ajpheart.00102.2007

17. Lahdenranta J, Hagendoorn J, Padera TP, et al. Endothelial nitric oxide synthase mediates lymphangiogenesis and lymphatic metastasis. *Cancer Res*. 2009;69(7):2801–2808. doi:10.1158/0008-5472.CAN-08-4051

18. Karlsen TV, Nikpey E, Han J, et al. High-salt diet causes expansion of the lymphatic network and increased lymph flow in skin and muscle of rats. *Arterioscler Thromb Vasc Biol*. 2018;38(9):2054–2064. doi:10.1161/ATVBAHA.118.311149

19. Kwon S, Agollah GD, Sevick-Muraca EM, Chan W. Altered lymphatic function and architecture in salt-induced hypertension assessed by near-infrared fluorescence imaging. *J Biomed Opt*. 2012;17(8): 080504-1. doi:10.1117/1.JBO.17.8.080504

20. Chachaj A, Puła B, Chabowski M, et al. Role of the lymphatic system in the pathogenesis of hypertension in humans. *Lymph Res Biol*. 2018;16(2):140–146. doi:10.1089/lrb.2017.0051

21. Chachaj A, Stanimirova I, Chabowski M, et al. Sodium accumulation in the skin is associated with higher density of skin lymphatic vessels in patients with arterial hypertension. *Adv Med Sci*. 2023;68(2): 276–289. doi:10.1016/j.advms.2023.08.001

22. Wold H. Nonlinear iterative partial least squares (NIPALS) modelling: Some current developments. In: Krishnaiah PR, ed. *Multivariate Analysis–III. Proceedings of the Third International Symposium on Multivariate Analysis Held at Wright State University, Dayton, Ohio, June 19–24, 1972*. Cambridge, USA: Academic Press; 1973:383–407. doi:10.1016/B978-0-12-426653-7.50032-6

23. De Jong S. SIMPLS: An alternative approach to partial least squares regression. *Chemom Intell Lab Syst*. 1993;18(3):251–263. doi:10.1016/0169-7439(93)85002-X

24. Williams B, Mancia G, Spiering W, et al. 2018 ESC/ESH Guidelines for the management of arterial hypertension: The Task Force for the management of arterial hypertension of the European Society of Cardiology and the European Society of Hypertension. *J Hypertens*. 2018;36(10):1953–2041. doi:10.1097/HJH.0000000000001940

25. Liang J, Jiang D, Noble PW. Hyaluronan as a therapeutic target in human diseases. *Adv Drug Deliv Rev*. 2016;97:186–203. doi:10.1016/j.addr.2015.10.017

26. Kyosseva SV, Harris EN, Weigel PH. The hyaluronan receptor for endocytosis mediates hyaluronan-dependent signal transduction via extracellular signal-regulated kinases. *J Biol Chem*. 2008;283(22): 15047–15055. doi:10.1074/jbc.M709921200

27. Podgrabinska S, Braun P, Velasco P, et al. Molecular characterization of lymphatic endothelial cells. *Proc Natl Acad Sci U S A*. 2002;99(25): 16069–16074. doi:10.1073/pnas.242401399

28. Hattori H. Caution should be taken in using CD31 for distinguishing the vasculature of lymph nodes. *J Clin Pathol*. 2003;56(8):638–639. PMID:12890824. PMCID:PMC1770018.

29. McKenney JK, Weiss SW, Folpe AL. CD31 expression in Intratumoral macrophages: A potential diagnostic pitfall. *Am J Surg Pathol*. 2001; 25(9):1167–1173. doi:10.1097/00000478-200109000-00007

30. Rütsche D, Michalak-Micka K, Zielinska D, et al. The role of CD200–CD200 receptor in human blood and lymphatic endothelial cells in the regulation of skin tissue inflammation. *Cells*. 2022;11(6):1055. doi:10.3390/cells11061055

31. Rodriguez-Iturbe B, Pons H, Quiroz Y, Johnson RJ. The immunological basis of hypertension. *Am J Hypertens*. 2014;27(11):1327–1337. doi:10.1093/ajh/hpu142

32. Ferri C, Di Francesco L, Baldoncini R, et al. Sodium-modulating hormones and the pressor response to sodium chloride in essential arterial hypertension [in Italian]. *Ann Ital Med Int*. 1993;8(2):89–94. PMID:8353025.

33. Overlack A, Ruppert M, Kolloch R, et al. Divergent hemodynamic and hormonal responses to varying salt intake in normotensive subjects. *Hypertension*. 1993;22(3):331–338. doi:10.1161/01.HYP.22.3.331

34. Melander O, Frandsen E, Groop L, Hulthén UL. Plasma ProANP$_{1-30}$ reflects salt sensitivity in subjects with heredity for hypertension. *Hypertension*. 2002;39(5):996–999. doi:10.1161/01.HYP.0000017552.91014.2A

35. Melander O, Wowern FV, Frandsen E, et al. Moderate salt restriction effectively lowers blood pressure and degree of salt sensitivity is related to baseline concentration of renin and N-terminal atrial natriuretic peptide in plasma. *J Hypertens*. 2007;25(3):619–627. doi:10.1097/HJH.0b013e328013cd50

36. Liu F, Mu J, Yuan Z, et al. Aberrant lymphatic system during salt loading in normotensive salt-sensitive Asians. *Med Sci Monit*. 2011;17(10):CR542–CR546. doi:10.12659/MSM.881978

37. Weidner N, Semple JP, Welch WR, Folkman J. Tumor angiogenesis and metastasis: Correlation in invasive breast carcinoma. *N Engl J Med*. 1991;324(1):1–8. doi:10.1056/NEJM199101033240101

38. Johnson RA, Wichern DW. *Applied Multivariate Statistical Analysis*. 6th ed. Upper Saddle River, USA: Pearson/Prentice Hall; 2007. https://www.webpages.uidaho.edu/~stevel/519/Applied%20Multivariate%20Statistical%20Analysis%20by%20Johnson%20and%20Wichern.pdf.

39. Brereton RG, Lloyd GR. Partial least squares discriminant analysis: Taking the magic away. *J Chemom*. 2014;28(4):213–225. doi:10.1002/cem.2609

40. Kennard RW, Stone LA. Computer-aided design of experiments. *Technometrics*. 1969;11(1):137–148. doi:10.1080/00401706.1969.10490666

41. Eirola E, Doquire G, Verleysen M, Lendasse A. Distance estimation in numerical data sets with missing values. *Inform Sci*. 2013;240:115–128. doi:10.1016/j.ins.2013.03.043

42. Walczak B, Massart DL. Dealing with missing data. *Chemom Intell Lab Syst*. 2001;58(1):15–27. doi:10.1016/S0169-7439(01)00131-9

43. Stanimirova I, Serneels S, Van Espen PJ, Walczak B. How to construct a multiple regression model for data with missing elements and outlying objects. *Anal Chim Acta*. 2007;581(2):324–332. doi:10.1016/j.aca.2006.08.014

44. Ząbek A, Stanimirova I, Deja S, et al. Fusion of the 1H NMR data of serum, urine and exhaled breath condensate in order to discriminate chronic obstructive pulmonary disease and obstructive sleep apnea syndrome. *Metabolomics*. 2015;11(6):1563–1574. doi:10.1007/s11306-015-0808-5

45. Kvalheim OM. Interpretation of partial least squares regression models by means of target projection and selectivity ratio plots. *J Chemom*. 2010;24(7–8):496–504. doi:10.1002/cem.1289

46. Kvalheim OM, Arneberg R, Bleie O, Rajalahti T, Smilde AK, Westerhuis JA. Variable importance in latent variable regression models. *J Chemom*. 2014;28(8):615–622. doi:10.1002/cem.2626

47. Kvalheim OM, Karstang TV. Interpretation of latent-variable regression models. *Chemom Intell Lab Syst*. 1989;7(1–2):39–51. doi:10.1016/0169-7439(89)80110-8

48. Pimenta E, Gaddam KK, Oparil S, et al. Effects of dietary sodium reduction on blood pressure in subjects with resistant hypertension: Results from a randomized trial. *Hypertension*. 2009;54(3):475–481. doi:10.1161/HYPERTENSIONAHA.109.131235

49. Touyz RM, Alves-Lopes R, Rios FJ, et al. Vascular smooth muscle contraction in hypertension. *Cardiovasc Res*. 2018;114(4):529–539. doi:10.1093/cvr/cvy023

50. Landi F, Calvani R, Picca A, et al. Body mass index is strongly associated with hypertension: Results from the Longevity Check-up 7+ Study. *Nutrients*. 2018;10(12):1976. doi:10.3390/nu10121976

51. Linderman GC, Lu J, Lu Y, et al. Association of body mass index with blood pressure among 1.7 million Chinese adults. *JAMA Netw Open*. 2018;1(4):e181271. doi:10.1001/jamanetworkopen.2018.1271

52. De La Sierra A, Giner V, Bragulat E, Coca A. Lack of correlation between two methods for the assessment of salt sensitivity in essential hypertension. *J Hum Hypertens*. 2002;16(4):255–260. doi:10.1038/sj.jhh.1001375

Optimizing screening cutoffs for drugs of abuse in hair using immunoassay for forensic applications

Arianna Giorgetti[1,C,D], Jennifer P. Pascali[1,E], Guido Pelletti[1,A,F],
Marco Garagnani[1,A], Raffaella Roffi[1,C], Marialuisa Grech[2,E], Paolo Fais[1,E]

[1] Department of Medical and Surgical Sciences, Unit of Legal Medicine, University of Bologna, Italy

[2] Azienda Unità Sanitaria Locale di Bologna, Italy

A – research concept and design; B – collection and/or assembly of data; C – data analysis and interpretation;
D – writing the article; E – critical revision of the article; F – final approval of the article

Abstract

Background. In forensic toxicology, positive immunoassay (IA) test results do not hold forensic validity and need to be confirmed with mass spectrometry (MS). On the other hand, a negative result is a strong indication that the drug and/or the drug metabolites are not present in the sample and that confirmatory analyses are not necessary. Consequently, a negative IA result must have forensic validity since it can be admitted in court during a trial.

Objectives. Screening cutoffs for the analysis of hair samples using immunoassays (IAs) were retrospectively optimized based on the Society of Hair Testing (SoHT) confirmation cutoffs and the utility of the test for forensic applications was discussed.

Materials and methods. Hair samples taken from 150 patients with a history of drug addiction were analyzed with ILab 650, Werfen (Milan, Italy) using DRI® reagents. Confirmatory analyses were subsequently performed using the ACQUITY UPLC® System, Waters Corporation (Milford, USA). Screening cutoffs were retrospectively optimized using receiver operating characteristic (ROC) analysis.

Results. A total of 162 single positive results were obtained for confirmatory analysis (10 for amphetamines/methamphetamines, 11 for MDMA, 37 for cocaine, 40 for THC, 33 for methadone, and 31 for opiates). The optimized screening cutoffs were 0.27 IA ng/mg for amphetamines, 0.51 IA ng/mg for MDMA, 0.59 IA ng/mg for cocaine, 0.14 IA ng/mg for cannabinoids, 0.63 IA ng/mg for methadone, and 0.26 IA ng/mg for opiates. An area under the curve (AUC) greater than 0.95 was obtained with very high sensitivity and specificity for all drugs.

Conclusions. The presented screening method proved to be a useful technique on hair samples for the classes of drugs most commonly found in Italy and Europe and can be applied to forensic analysis.

Key words: forensic sciences, forensic toxicology, immunoassay

76

A. Giorgetti et al. Screening optimization of drugs in hair

Background

The analysis of hair matrix is an elaborate and time-consuming multi-step process. The first step involves a wash to eliminate external contamination, followed by hair segmentation or pulverization and extraction (liquid/liquid, solid phase, solid phase micro-extraction). In most laboratories, the instrumental analysis is performed with immunoassay (IA) screening followed by chromatography (gas, liquid) coupled with mass spectrometry (MS).[1]

Immunoassays were the first technique used to detect drug use in hair and, since then, IA techniques have been widely used in forensic toxicology as screening tests.[2,3] However, positive results from an IA test do not hold forensic validity due to its risk of improper interpretation of test results and should be confirmed using a MS-based technique.[4,5] On the other hand, a negative result strongly suggests that neither the drug nor its metabolites are detected in the sample, making further confirmation analysis unnecessary.[6] Therefore, a negative result, since it is not followed by confirmation analysis, is often presented in court during a trial and can hold forensic validity.[5] To achieve this result, the cutoff used to distinguish negative and positive screening samples needs to be optimized to avoid false negative (FN) values (i.e., sensitivity close to 100%).[7]

Most IA implementations are tailored for clinical contexts involving urine specimens, where concentrations and thresholds tend to be higher compared to levels in hair and blood samples. Consequently, the screening analysis of hair samples might lead to the omission of substances of forensic significance, and screening cutoffs must be tested and optimized concerning the cutoffs used for confirmation, which can vary according to the purpose of the analysis.[8,9] In forensics, reference cutoffs are those reported by the Society of Hair Testing (SoHT),[10] which enables the identification of drug use against external contamination or passive exposure.[11]

Prior research has indicated that IA technology was highly effective in assessing urine, serum,[12] and, more recently, whole blood taken from living subjects[13] or post-mortem.[6]

Objectives

In the present paper, screening results using hair samples taken from patients in therapy for drug addiction obtained through DRI® IA (amphetamines, cannabinoids, cocaine, methadone, and opiates) were compared to the quantitative results of the toxicological analysis performed using ultra-performance liquid chromatography coupled to tandem MS (UPLC-MS/MS). Screening cutoffs were then retrospectively optimized based on SoHT[14] confirmation cutoffs.

Materials and methods

Samples

Head hair samples from 150 patients with a history of drug addiction and undergoing treatment at the substance abuse service were collected from January 2022 to March 2023 in the metropolitan area of Bologna, Italy. After performing the analysis for clinical purposes, an aliquot was taken and stored according to the 2022 SoHT Consensus on general recommendations for hair testing. For the purpose of this study, the samples were treated completely anonymously.[10] The samples consisted of head hair, ranging from 3 to 6 cm in length, and were collected by cutting as close to the skin as possible. The hair strands were maintained in alignment until analysis. Toxicological analyses were performed within 72 h of sampling. Two analyses were performed on each sample, an IA analysis using ILab 650 (Werfen, Milan, Italy) and a UPLC-MS/MS analysis using an ACQUITY UPLC® System (Waters Corporation, Milford, USA). The 1st IA test was utilized as the screening test to be optimized, and the 2nd test (UPLC-MS/MS) as the confirmatory test.

Immunoassay analysis

Six drugs/classes were assessed: amphetamines/methamphetamines, MDMA, cocaine, cannabinoids, methadone, and opiates.

Reagents

The following reagents were used: DRI® Amphetamines Assay, DRI® Ecstasy Assay, DRI® DRI® Cocaine Metabolite Assay, DRI® Cannabinoid Assay, DRI® Methadone Assay, and the DRI® Opiate Assay.[15] The hair assay cutoffs for the original IA application were opiates 0.2 ng/mg (REF W150135, anti-morphine antibodies), methadone 0.2 ng/mg (REF W150596; anti-methadone antibodies), cocaine metabolite 0.2 ng/mg (REF W150055; anti-benzoylecgonine antibodies), amphetamines 0.2 ng/mg (REF W150017; anti-amphetamine and anti-methamphetamine antibodies), MDMA (ecstasy) 0.2 ng/mg (REF W15100075; anti-MDMA antibodies), and cannabinoids 0.1 ng/mg (REF W150185; anti-THCCOOH antibodies).

Sample preparation

Sample preparation followed the manufacturer's suggestions, as follows: an aliquot of 33 mg of hair matrix finely chopped in 2–3-mm-long fragments were placed in a glass tube with a screw cap. To exclude the possibility of positivity due to external contamination, 1 mL of SLV-VMA-T washing solution (Comedical, Trento, Italy; REF SSSLVT000050) was added to the tube with the sample, gently mixed for about 30 s, and then the solution was

removed. After washing, 400 μL of VMA-T (Comedical; REF SSVMAT001007) extraction reagent was added to the test tube and incubated for 1 h at 100°C. After cooling at room temperature, the sample was centrifuged for 5 min at 3,000 g. Immunoassay analysis was performed using an ILab-650 Clinical Chemistry System (Werfen).

Calibrators and control samples

Calibration was performed using a 5-point calibration curve (0 included) with "CAL VMA-T calibrators Drugs of abuse and medicaments in hair" (Comedical; REF SSCALT000008)[16] as follows: amphetamines (0–0.50–1.00–2.00–4.00 ng/mg), ecstasy (0–0.45–0.90–1.80–3.60 ng/mg), cocaine (0–0.45–0.90–1.80–3.60 ng/mg), cannabinoids (0–0.12–0.24–0.48–0.96 ng/mg), opiates (0–0.40–0.80–1.60–3.20 ng/mg), and methadone (0–0.80–1.60–3.20–6.40 ng/mg). Quality control (QC) samples for each drug were performed using TricoCheck® (Comedical; REF SSVMAT001007), as follows: amphetamines 0.85 ng/mg, ecstasy 1.25 ng/mg, cocaine 1.05 ng/mg, cannabinoids 0.45 ng/mg, methadone 1.68 ng/mg, and opiates 1.10 ng/mg.

Cross-reactions among classes of drugs

Concerning possible cross-reactions, positive and negative lists for each test are provided by the manufacturer in their performance guides.[15] Cross-reactivity for each class of drugs was also assessed internally by adding QC concentrations (2 for each drug) to blank blood samples. Given that we did not detect any cross-reactions among the various drug classes included in the study, samples testing positive for more than one drug were individually considered for data analysis for each specific drug. When expressing the IA values for drugs of abuse, it is not advisable to use "ng/mg" since IA tests provide semi-quantitative results. Therefore, when referencing IA tests, "ng/mg" should be interpreted as "ng/mg IA units".

UPLC-MS/MS analysis

A minimum quantity of 25 mg was needed to perform the analysis. For extraction, 0.3 mL of a mixture of methanol/water (1:1, v/v) with 0.1% formic acid was added to the hair sample and incubated at 45°C overnight. For analysis, after centrifugation, 2 μL were injected into the UPLC-MS/MS system. We utilized an ACQUITY UPLC® System (Waters Corporation) equipped with a C18 column (2.1×150 mm, 1.8 μm; Waters Corporation). Mobile phase A consisted of a 5 mM ammonium formate aqueous solution, while mobile phase B was composed of acetonitrile, with both phases containing 0.1% formic acid.

Analytes were eluted at a flow rate of 0.4 mL/min. The elution gradient started at 13% B, isocratic for 0.5 a min; from 0.5 to 10.0 min, it was increased to 50% B, from 10.0 to 12.5 min, it was increased to 95% B, and from 12.5 to 15 min it was decreased to 13% B.

The column temperature was maintained at 50°C. The method was internally validated for a range of analytes, including morphine, codeine, dihydrocodeine, 6-monoacetylmorphine, heroin, tramadol, methadone, MDMA, MDEA (3,4-methylenedioxy-N-ethylamphetamine), MDA (3,4-methylenedioxyamphetamine), methamphetamine, amphetamine, cocaine, benzoylecgonine, cocaethylene, and THC, with a linearity range of 0.1–1 ng/mg, in line with the cutoff for identifying drug users proposed by SoHT.[14] The method was fully validated according to European Medicines Agency (EMA) guidelines,[17] by assessing selectivity, linearity, accuracy, precision, limit of quantification (LOQ), limit of detection (LOD), matrix effect, and recovery. The first point on the calibration curve was considered the lower limit of quantification (LLOQ). R^2 values exceeded 0.99 for all tested molecules. All parameters tested were within acceptable limits.

Study design and statistical analyses

For identifying positive cases, the cutoffs proposed by the SoHT were used.[14] Table 1 reports the class of drugs of the IAs and the corresponding confirmation parameters. All 150 samples were analyzed using IAs as the screening test, and with UPLC-MS/MS as the confirmatory test.

To optimize the screening cutoffs, the result of the IA test was semi-quantitatively expressed in terms of "ng/mg IA units"; the results of the confirmatory analysis were considered positive when the SoHT criteria were respected, considering the main analyte and, when necessary, metabolites. As an example, for a positive cocaine result, the SoHT document assumed that "The presence of benzoylecgonine, norcocaine, cocaethylene, hydroxyl-cocaines, or hydroxy-benzoylecgonine must be considered

Table 1. Confirmation cutoffs for each class of drugs

Immunoassay test (IA)	Confirmation (LC-MS/MS)	Confirmation cutoff [ng/mg]
Amphetamine	amphetamine methamphetamine	0.20
MDMA	MDMA	0.20
Cocaine	cocaine[1]	0.50
Cannabinoids	THC	0.05
Methadone	methadone	0.20
Opiates	morphine codeine dihydrocodeine 6-monoacetylmorphine heroin tramadol	0.20

[1] with the presence of metabolites (benzoylecgonine, norcocaine, cocaethylene, hydroxyl-cocaines or hydroxy-benzoylecgonine);
IA – immunoassay; LC-MS/MS – ultra-performance liquid chromatography coupled to tandem mass spectrometry; MDMA – 3,4-methyl-enedioxy-methamphetamine; THC –tetrahydrocannabinol.

78

A. Giorgetti et al. Screening optimization of drugs in hair

to confirm use". Then, the result is considered "positive" at confirmation analysis only when cocaine was found above the cutoff, with the presence of a metabolite.

Receiver operating characteristic (ROC) curves were built using GraphPad Prism 9.5.1 software (GraphPad Software, San Diego, USA), which computes them from raw data. To this scope, screening results testing negative by UPLC/MSMS were inserted as "negative", while screening results corresponding to a positive result by UPLC/MSMS were inserted as "positive". Due to the cross-reactivity of the IA amphetamines test to methamphetamine, for the optimization of the amphetamines IA test, the sample was considered positive on confirmation analysis when the presence of amphetamine or methamphetamine above the confirmation cutoff was assessed. A sample was considered positive for cocaine when the presence of cocaine above the confirmation cutoff and metabolites were assessed, as requested by SoHT guidelines. A sample was considered positive for opiates when a result was positive for morphine, codeine, dihydrocodeine, 6-monoacetylmorphine, heroin, or tramadol above the confirmation cutoffs. A sample was considered positive for MDMA, cannabinoids and methadone when the presence of MDMA, THC and methadone, respectively, were encountered.

The ability of a test to discriminate between positive and negative samples is provided as the area under the ROC curve (area under the curve (AUC)) calculated with a standard error (SE) and 95% confidence interval (95% CI), as well as a p-value. The software automatically tabulates and plots the sensitivity and specificity of the test using each value in the data table as a possible cutoff value. A likelihood ratio is additionally calculated. Screening cutoff values were retrospectively optimized using contingency tables and assessed through ROC analysis. The SE of the area is calculated using the equation from Hanley and McNeil.[18]

We determined the optimal cutoff by summing the sensitivity and specificity. Sensitivity, calculated as TP/(TP+FN), and specificity, calculated as TN/(TN+FP), were determined using the numbers of true positives (TP), true negatives (TN), false positives (FP), and false negatives (FN). In cases where the sensitivity at the optimized cutoffs was less than 1, we retrospectively calculated the cutoff with a sensitivity equal to 1, referred to as the "highest sensitivity cutoff" (HS cutoff). Since the samples were processed anonymously for the purposes of this study, which did not involve the collection of any personal data, obtaining ethical approval was deemed unnecessary.

Results

Overall, 150 hair samples were analyzed. Since there was no cross-reactivity detected among various drug classes, multiple drugs found in the same sample were individually considered for statistical analysis. A total of 162 single

positive results were obtained during confirmatory analysis (10 for amphetamine/methamphetamine, 11 for MDMA, 37 for cocaine, 40 for THC, 33 for methadone, and 31 for opiates). Optimized screening cutoffs for IA test using ROC analysis were as follows:

- 0.27 IA ng/mg for amphetamines;
- 0.51 IA ng/mg for MDMA;
- 0.59 IA ng/mg for cocaine;
- 0.14 IA ng/mg for cannabinoids;
- 0.63 IA ng/mg for methadone;
- 0.26 IA ng/mg for opiates.

For the compounds that did not reach 100% sensitivity at the optimized cutoff, HS-cutoffs were calculated, as follows: 0.21 IA ng/mg for amphetamines (specificity: 86.4%), 0.24 IA ng/mg for cocaine (specificity: 82.0%) and 0.03 IA ng/mg for cannabinoids (specificity: 66.4%). The ROC curves and a graphical representation of plots of positive and negative results at the optimized cutoffs are presented in Fig. 1 and Fig. 2.

An AUC greater than 0.95 was obtained for all drugs. Table 2 shows the sensitivity and specificity for all optimized cutoffs.

Discussion

In this study, the cutoffs obtained through IA-based screening were optimized with respect to forensic interpretative cutoffs.[14] In the routine of hair analysis, the optimized screening cutoff and the confirmation cutoff should not be confused.[11] For IA screening, the use of cutoffs is an attempt to limit the number of FP cases, thus limiting the number of confirmation analyses performed, which are expensive and time-consuming, whilst not missing TP results. Immunoassays, although simple to perform, are prone to interferences that can cause FN or FP. On the other hand, the use of confirmation cutoffs comes from the consensus document of the SoHT, which produced cutoff values for a range of analytes to differentiate between deliberate drug consumption and the possibility of incidental exposure or endogenous production.[14] These are not analytical cutoffs, and analyte concentrations below these values may indicate deliberate administration.[11] The proposed approach ensures that the screening test is optimized not only with the analytical result of the laboratory, often identified with the LLOQ, but with the interpretative cutoff.

Moreover, the screening results should be interpreted in semi-quantitative terms (expressed as IA ng/mg units), as the numerical result cannot be directly compared to the confirmation cutoff. For instance, concerning cocaine, the test has a higher affinity for benzoylecgonine, while the interpretative SoHT cutoff requires the presence of cocaine above a certain value, coupled with the presence of metabolites. Consequently, we may encounter higher concentrations in the screening results that cannot be equated to those of the confirmation cutoff.
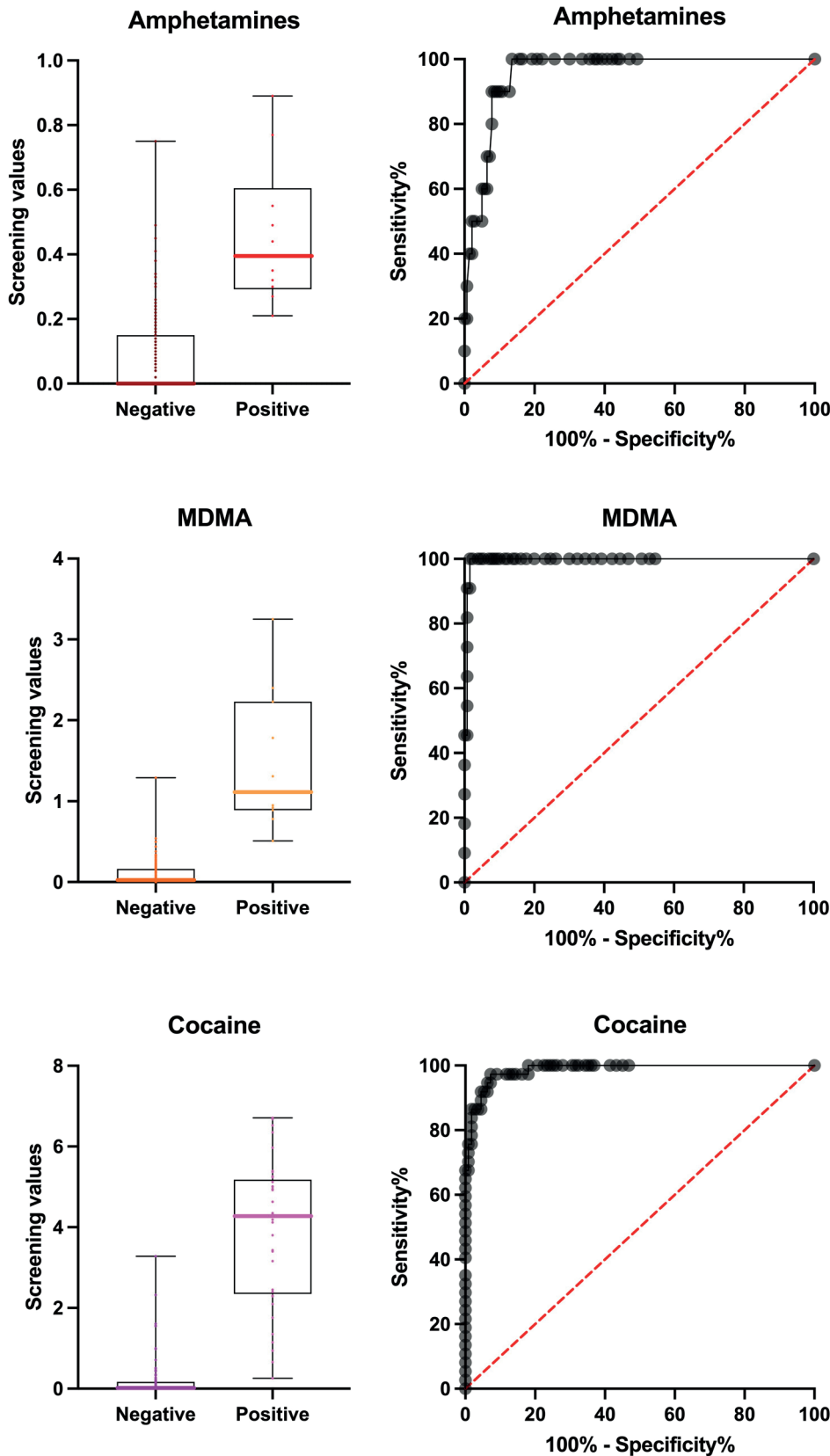
Fig. 1. Plots (left) and receiver operating characteristic (ROC) curves (right) for amphetamines, MDMA and cocaine. The plots depict 1st quartile (Q1) and 3rd quartile (Q3) (represented by black thin lines) and the median (represented as the height of the columns)

All semi-quantitative optimized cutoffs showed satisfying results in terms of sensitivity and specificity, with a value of sensitivity greater than 90% and a very good AUC for all compounds. The AUC is a reliable parameter that considers both sensitivity and specificity and, hence, directly measures the diagnostic power of the test. These AUC results indicate the reliability of the optimized cutoffs for all the molecules tested.[9] Some laboratories that perform hair testing during their daily routines report positive identifications to analytical limits routinely (i.e.,

Cannabinoids
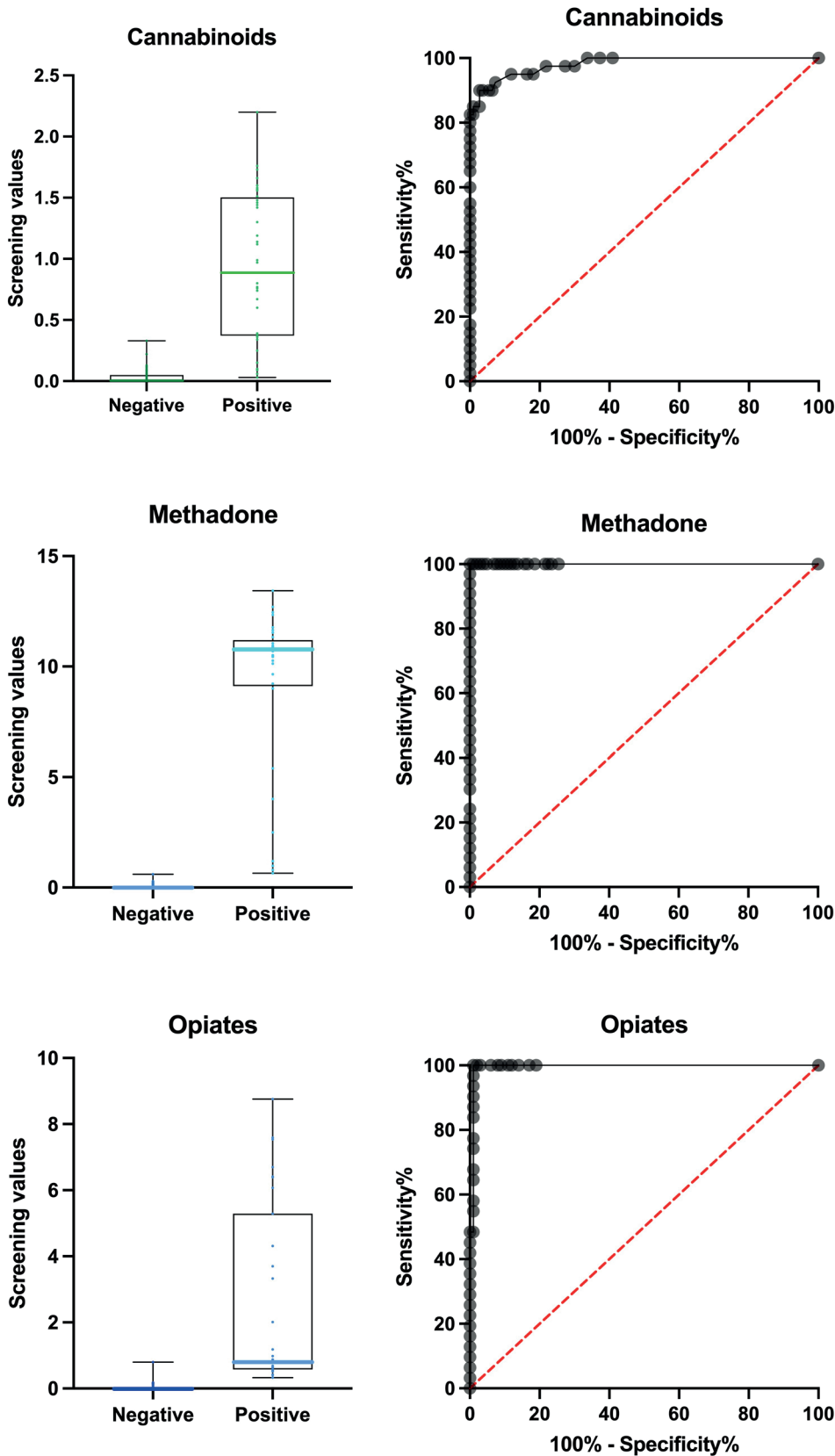
Methadone

Opiates

Fig. 2. Plots and receiver operating characteristic (ROC) curves for cannabinoids, methadone and opiates. The plots depict 1st quartile (Q1) and 3rd quartile (Q3) (represented by black thin lines) and the median (represented as the height of the columns)

LOQ or LOD), risking giving a false impression of past drug use. Other laboratories use either the SoHT or "in-house" cutoff values and may report the same analytical result as "negative" or "not detected", thus risking not

supplying valuable information in the context of a particular case.[11]

The results of this study showed that the proposed screening technique at the optimized cutoffs exhibits

Table 2. Results obtained for each class of drugs. For each class of drugs, optimized cutoffs along with main statistical results are reported

Optimized cutoff	Amphetamines	MDMA	Cocaine	Cannabinoids	Methadone	Opiates
AUC	0.956	0.995	0.986	0.981	1.000	0.994
SE	0.018	0.005	0.007	0.010	<0.001	0.005
95% CI	0.920–0.991	0.986–1.000	0.973–1.000	9.961–1.000	(0.999–1.000>*	0.985–1.000
p[H]	<0.001	<0.001	<0.001	<0.001	<0.001	<0.001
O cutoff	0.270	0.510	0.590	0.140	0.630	0.260
Sensitivity (%)	90.000	100.000	97.300	90.000	100.000	100.000
95% CI	59.600–99.500	74.100–100.000	86.200–99.900	77.000–96.000	89.600–100.000	89.000–100.000
Specificity (%)	92.100	98.500	92.800	97.300	100.000	99.000
95% CI	86.500–95.600	94.600–99.700	86.400–96.300	92.300–99.300	96.400–100.000	94.600–100.000
HS cutoff	0.210	–	0.240	0.030	–	–
Sensitivity (%)	100.000	–	100.000	100.000	–	–
95% CI	72.300–100.000	–	90.600–100.000	91.200–100.000	–	–
Specificity (%)	86.400	–	82.000	66.400	–	–
95% CI	79.800–91.100	–	73.800–88.000	57.100–74.500	–	–

AUC – area under the curve; O cutoff – optimized cutoff; HS cutoffs – cutoffs with highest sensitivity, which correspond to optimized cutoff for MDMA, methadone and opiates. *Due to the property of AUC (≤1.000), symmetrical interval (0.999–1.001) was truncated on the right to (0.999–1.000); p[H] – level of statistical significance of the Hanley–McNeil method; 95% CI – 95% confidence interval; SE – standard error; HS – high sensitivity.

a very high sensitivity for all drugs, avoiding the FN rate with an acceptable level of specificity even using HS-cutoffs namely cutoffs with a sensitivity of 100%. Depending on the analysis's purpose, each laboratory may opt to use either the optimized cutoffs or the HS-cutoffs. For example, in fields such as analyses for driving license regranting or other forensic areas where FN is not accepted, the HS-cutoff may see a broader application. Conversely, in other fields with a high volume of analyses and patient assessments guided by clinical and anamnestic parameters, laboratories might choose the optimized cutoff for cost-effectiveness reasons, involving closer short-term monitoring of select patients.

Contrary to what was previously observed in the blood,[6,13] hair tests are reliable for the screening of amphetamines, as the biogenic amines, mainly responsible for FP results in blood, are not present in the hair matrix. The use of the term "cutoff" instead of "LLOQ" was deliberate, specifically to denote a threshold where the laboratory can make a decision based on its cost-effectiveness requirements regarding whether to confirm the sample. It extends beyond being solely an analytical result, as it would be in the case of LLOQ.

In recent years, numerous forensic toxicology laboratories have shifted from immunoenzymatic techniques to multi-targeted methods utilizing MS-based approaches, allowing for the simultaneous detection of a wider range of molecules.[19,20] However, the importance of retaining an immunoenzymatic technique resides in having a distinct method for confirmation. This proves particularly advantageous for laboratories that may lack either 2 MS-based techniques or 2 divergent methods for conducting both screening and confirmation analyses. Such laboratories could find benefit in employing immunoenzymatic techniques, especially for analyses with high sample volumes.

Forensic toxicology plays a primary role in the research within the field of biomedical-legal sciences,[21,22] and in recent years, it has mainly focused on MS-based techniques, which have high sensitivity and specificity. We believe that the robustness of the preliminary experiment could pave the way for further validation studies on IA tests, encompassing a larger number of samples and other drugs of forensic interest.

Limitations

The study sample consisted of hair samples taken from a specific population, namely patients with a drug use disorder, primarily undergoing maintenance therapy with methadone. Consequently, the results related to methadone may be overestimated due to elevated methadone levels in the samples, which are much higher than the confirmatory cutoff. This could stem from methadone maintenance therapy in positive study participants and the absence of patients with irregular methadone intake in our study population. To address this limitation, screening cutoffs should be refined using a larger sample size and diverse populations of forensic relevance. This method was optimized for the drugs of abuse most commonly found in drivers in our country,[22] but other substances that can influence the ability to drive, such as prescription drugs,[23] were not included. Therefore, in the future, the screening panel should be extended to common prescription drugs (benzodiazepines and medical opioids). Regarding the sample size, a power

82

A. Giorgetti et al. Screening optimization of drugs in hair

analysis was not applied, but the samples received during a specific time period were analyzed according to the casework requirements. This has been specified in the limitations of the study.

Conclusions

Compared to routine urine or blood drug testing, IAs for hair analysis are not commonly employed due to the low concentrations required for this purpose. The study's strengths lie in the optimization of IA cutoffs with interpretative values, a substantial sample size, and the achievement of a high level of sensitivity and specificity at the optimized cutoff points, along with a very high AUC during ROC analysis. In conclusion, this screening method has demonstrated its utility when applied to hair samples for the most commonly detected drug classes in Italy and Europe. It can find application in both forensic and clinical analyses.

Data availability

The datasets generated and/or analyzed during the current study are available from the corresponding author on reasonable request.

Consent for publication

Not applicable.

ORCID iDs

Arianna Giorgetti https://orcid.org/0000-0002-0441-9787
Jennifer P. Pascali https://orcid.org/0000-0002-1363-3400
Guido Pelletti https://orcid.org/0000-0003-3263-1758
Marco Garagnani https://orcid.org/0000-0002-4320-2556
Paolo Fais https://orcid.org/0000-0002-2270-9956

References

1. Kintz P. Hair analysis in forensic toxicology: An updated review with a special focus on pitfalls. *Curr Pharm Des*. 2018;23(36):5480–5486. doi:10.2174/1381612823666170929155628

2. Swanson DM, Pearson JM, Evans-Nguyen T. Comparing ELISA and LC–MS-MS: A simple, targeted postmortem blood screen. *J Anal Toxicol*. 2022;46(7):797–802. doi:10.1093/jat/bkab104

3. Kahl KW, Seither JZ, Reidy LJ. LC-MS-MS vs ELISA: Validation of a comprehensive urine toxicology screen by LC-MS-MS and a comparison of 100 forensic specimens. *J Anal Toxicol*. 2019;43(9):734–745. doi:10.1093/jat/bkz066

4. Italian Forensic Toxicologists Association (GTFI). Linee Guida per la Determinazione di Sostanze Stupefacenti e Psicotrope su Campioni Biologici con Finalità Tossicologico-Forensi e Medico-Legali. Rome, Italy: Italian Forensic Toxicologists Association (GTFI); 2022. https://www.gtfi.it/wp-content/uploads/2023/02/LineeGuidaGTFI-MaterialeBiologico-rev06-08giu2022.pdf. Accessed October 16, 2023.

5. Busardò FP, Pacifici R, Pichini S. Mass spectrometry vs. immunoassay in clinical and forensic toxicology: Qui modus in rebus est? *Clin Chem Lab Med*. 2017;55(10):e236–e237. doi:10.1515/cclm-2017-0418

6. Pelletti G, Rossi F, Garagnani M, et al. Optimization of cloned enzyme donor immunoassay cut-offs for drugs of abuse in post-mortem whole blood. *Forensic Sci Int*. 2020;312:110291. doi:10.1016/j.forsciint.2020.110291

7. Musshoff F, Kirschbaum KM, Graumann K, Herzfeld C, Sachs H, Madea B. Evaluation of two immunoassay procedures for drug testing in hair samples. *Forensic Sci Int*. 2012;215(1–3):60–63. doi:10.1016/j.forsciint.2011.03.030

8. Svaizer F, Lotti A, Gottardi M, Miozzo MP. Buprenorphine detection in hair samples by immunometric screening test: Preliminary experience. *Forensic Sci Int*. 2010;196(1–3):118–120. doi:10.1016/j.forsciint.2009.12.047

9. Agius R, Nadulski T. Utility of ELISA screening for the monitoring of abstinence from illegal and legal drugs in hair and urine. *Drug Test Anal*. 2014;6(Suppl1):101–109. doi:10.1002/dta.1644

10. Society of Hair Testing (SoHT). Consensus on general recommendations for hair testing consensus revision: Presented in Verona, June 10, 2022 following the expert meeting in Malaga, March 4–5, 2022. 2022. https://www.soht.org/images/pdf/General_Consensus_Hair_Testing_2022.pdf. Accessed October 16, 2023.

11. Cuypers E, Flanagan RJ. The interpretation of hair analysis for drugs and drug metabolites. *Clin Toxicol*. 2018;56(2):90–100. doi:10.1080/15563650.2017.1379603

12. Musshoff F, Wolters T, Lott S, Ippisch J, Gradl S, Madea B. Optimization and validation of CEDIA drugs of abuse immunoassay tests in serum and urine on an Olympus AU 400. *Drug Test Anal*. 2013;5(5):366–371. doi:10.1002/dta.1454

13. Pelletti G, Garagnani M, Rossi F, Roffi R, Barone R, Pelotti S. Optimization of cloned enzyme donor immunoassay cut-offs for drugs of abuse in whole blood of drivers involved in road accidents. *Forensic Sci Int*. 2019;294:27–33. doi:10.1016/j.forsciint.2018.10.023

14. Society of Hair Testing (SoHT). Consensus on drugs of abuse (DOA) testing in hair. Society of Hair Testing (SoHT); 2021. https://www.soht.org/images/pdf/Consensus_DoA_2021.pdf. Accessed October 16, 2023.

15. Werfen. QuantilLab reagents. Milan, Italy: Werfen; 2023. https://www.werfen.com/it/it/reagenti-quantilab. Accessed October 18, 2023.

16. Baumgartner MR, Guglielmello R, Fanger M, Kraemer T. Analysis of drugs of abuse in hair: Evaluation of the immunochemical method VMA-T vs. LC–MS/MS or GC–MS. *Forensic Sci Int*. 2012;215(1–3):56–59. doi:10.1016/j.forsciint.2011.08.025

17. European Medicines Agency (EMA). Guideline on Bioanalytical Mehod Validation, 21 Jul 2011. Amsterdam, the Netherlands: European Medicines Agency (EMA); 2011. https://www.ema.europa.eu/en/documents/scientific-guideline/guideline-bioanalytical-method-validation_en.pdf. Accessed October 16, 2023.

18. Hanley JA, McNeil BJ. The meaning and use of the area under a receiver operating characteristic (ROC) curve. *Radiology*. 1982;143(1):29–36. doi:10.1148/radiology.143.1.7063747

19. D'Ovidio C, Locatelli M, Perrucci M, et al. LC-MS/MS application in pharmacotoxicological field: Current state and new applications. *Molecules*. 2023;28(5):2127. doi:10.3390/molecules28052127

20. Rubicondo J, Scuffi L, Pietrosemoli L, et al. A new multi-analyte LC–MS-MS screening method for the detection of 120 NPSs and 49 drugs in hair. *J Anal Toxicol*. 2023;46(9):e262–e273. doi:10.1093/jat/bkac093

21. Boscolo-Berto R, Viel G, Cecchi R, et al. Journals publishing biomedicolegal research in Europe. *Int J Legal Med*. 2012;126(1):129–137. doi:10.1007/s00414-011-0620-3

22. Viel G, Boscolo-Berto R, Cecchi R, Bajanowski T, Vieira ND, Ferrara SD. Bio-medicolegal scientific research in Europe: A country-based analysis. *Int J Legal Med*. 2011;125(5):717–725. doi:10.1007/s00414-011-0576-3

23. Pelletti G, Verstraete AG, Reyns T, et al. Prevalence of therapeutic drugs in blood of drivers involved in traffic crashes in the area of Bologna, Italy. *Forensic Sci Int*. 2019;302:109914. doi:10.1016/j.forsciint.2019.109914

Polish cross-cultural adaptation of a disease-specific quality-of-life instrument: The Penn Acoustic Neuroma Quality-of-Life Scale

Katarzyna Bieńkowska[1,A–D,F], Barbara Kostecka[1,A–D,F], Mirosław Ząbek[2,3,4,A–C,E,F], Andrzej Kokoszka[1,A–D,F],
Sebastian Dzierzęcki[4,A–C,E,F], Ewelina Cichoń[5,6,A–C,E,F], Grzegorz Turek[3,A–C,E,F]

[1] Second Department of Psychiatry, Medical University of Warsaw, Poland

[2] Department of Neurosurgery, Postgraduate Medical Centre, Warsaw, Poland

[3] Department of Neurosurgery, Bródno Masovian Hospital, Warsaw, Poland

[4] Gamma Knife Centre, Warsaw, Poland

[5] Department of Psychology, Faculty of Applied Studies, Psychology Research Unit for Public Health, University of Lower Silesia DSW, Wrocław, Poland

[6] Faculty of Health Sciences, Wroclaw Medical University, Poland

A – research concept and design; B – collection and/or assembly of data; C – data analysis and interpretation;
D – writing the article; E – critical revision of the article; F – final approval of the article

Abstract

Background. The medical community has shown a growing interest in developing methods for measuring and comparing objective patient outcomes coupled with subjective patient assessments. Questionnaires enable healthcare professionals to obtain the patient's perspective about their experienced vestibular schwannomas (VS) symptoms quickly. To date, in Poland, a cross-cultural adapted version of a disease-specific questionnaire for the measurement of quality of life (QoL) in patients with VS has not been produced.

Objectives. This study aimed to adapt the questionnaire evaluating disease-specific QoL in patients with VS (Penn Acoustic Neuroma Quality-of-Life Scale; PANQOL) to Polish and evaluate its psychometric properties.

Materials and methods. One-hundred twenty-four patients aged between 24 and 85 years (mean (M) = 60.17 ±standard deviation (SD) = 13.27) diagnosed with VS and treated with Gamma Knife were included in the study. We used a questionnaire translated from English into Polish by a bilingual professional, verified through a back-translation. The final version consisted of 26 items. The internal consistency of the Polish version of the PANQOL scale domains was measured using the Cronbach's alpha (α). To verify the validity of PANQOL subscales, a correlation analysis was conducted between the domains of PANQOL and other questionnaires, including the Assessment of Quality of Life (AQoL-8D), the Glasgow Benefit Inventory (GBI), the 5 Well-Being Index (WHO-5), the Skarzynski Tinnitus Scale (STS) for the presence of dizziness, and the Gardner–Robertson classes.

Results. The majority of PANQOL domains showed excellent or good internal consistency (for a PANQOL total of 0.934; for subscales in the range of 0.916–0.424). Our analysis showed strong correlations between the total PANQOL score and AQoL-8D utility score, as well as between the subscales. We observed weak to moderately significant relationships between GBI and PANQOL domains (r = 0.18–0.43), the WHO-5 (r = 0.18–0.56) and the STS scale (r = −0.40− −0.19).

Conclusions. The results demonstrated that the POL-PANQOL is a reliable and valid questionnaire for measuring QoL.

Key words: quality of life, adaptation, psychometrics, vestibular schwannomas, Penn Acoustic Neuroma Quality-of-Life scale

84

K. Bieńkowska et al. Adaptation of the PANQOL questionnaire

Background

Over the last decade, the medical community has shown a growing interest in developing methods for measuring and comparing objective patient outcomes coupled with subjective patient assessments.[1] The World Health Organization (WHO) indicates that currently the measure of success for medicine is not only treatment but also the improvement in health-related quality of life (QoL) in psychological and social areas. Using health-related QoL questionnaires, it is possible to assess the impact of disease and treatment on the patient's daily life not only in terms of physical health but also in psychological and social areas.[2] Two types of standardized questionnaires can be used for QoL assessments – generic or disease-specific. A generic questionnaire may be less sensitive in the assessment of changes related to a disease or treatment. Therefore, disease-specific questionnaires are dedicated to patients diagnosed with a particular entity, and the tools are designed to consider symptoms or various health aspects that may be affected by the disease.

Vestibular schwannomas (VS) are slow-growing benign intracranial tumors arising from the Schwann cells of the vestibular part of cranial nerve VIII.[3,4] The most common symptoms include unilateral or asymmetric hearing loss (94%), tinnitus (83%), dizziness or vertigo, and facial paralysis. The availability of high-resolution magnetic resonance imaging (MRI) has contributed to an increase in the detection rate of VS (completely asymptomatic or with only minor clinical symptoms). If the patient presents with only minor symptoms, the assessment of QoL is an important factor in medical decision-making and helps understand the patient's perspective.[5]

To date, most studies that assessed QoL in patients with VS were performed using generic questionnaires, which may be inadequately sensitive to changes in clinical status and insufficient to provide meaningful data for a specific patient population. Only a few retrospective studies in patients with VS evaluated QoL using disease-specific questionnaires,[1,6,7] especially the Penn Acoustic Neuroma Quality-of-Life scale (PANQOL). What is more, another methodology for QoL measurement in patients with VS after treatment, proposed by the European Association of Neuro-Oncology, does not indicate which treatment options have the greatest impact on QoL improvements.[8] Thus, there is a need for the adaptation and validation of a disease-specific questionnaire. So far, in Poland, a cross-cultural adapted version of a disease-specific questionnaire for the measurement of QoL in patients with VS has not been produced.

Objectives

This study aimed to adapt the PANQOL, designed and validated by Shaffer et al.,[5] to Polish context and evaluate its psychometric properties.

Materials and methods

Study design

From June 2021 to August 2022, patients diagnosed with VS were recruited. They received a package with 2 copies of the informed consent form, 5 questionnaires including the PANQOL-POL, Glasgow Benefit Inventory (GBI), Assessment of Quality of Life 8-Dimension (AQoL-8D), Skarzynski Tinnitus Scale (STS), and WHO–5 Well-being Index, and a demographic survey.

Ethics approval and consent to participate

The study was conducted in accordance with the ethical principles of the Declaration of Helsinki, and the study protocol was approved by the institutional review board at the Centre of Postgraduate Medical Education, Warsaw, Poland (approval No. 37/2021 issued on May 12, 2021). Every patient enrolled in the study signed an informed consent form after receiving the necessary information from an investigator prior to their participation in the study.

Cross-cultural adaptation of the PANQOL

The PANQOL is a questionnaire established by Shaffer et al.[5] to evaluate disease-specific QoL in patients with VS. The authors based it on the system that classifies outcomes in terms of body dysfunction, activity restriction and effects on participation in society. They created the first questionnaire for patients with VS that not only involves reporting symptoms but reflects QoL impairment at all 3 levels mentioned above and includes issues specifically identified by patients.[5]

The questionnaire consists of 26 items grouped into 7 domains: Hearing (4), Balance (6), Facial Function (3), Pain (1), Anxiety (4), Energy (6), and General Health (2). The responses are provided with a rating scale from 1 (strongly disagree) to 5 (strongly agree). The total score was obtained by calculating the average number of points from the 7 domain scores. Higher scores are interpreted as a better health-related QoL. The values of test–retest reliability and internal consistency were high.[1,5] Domain scores were obtained by calculating the average number of points from responses to items assigned to a particular domain. So far, the PANQOL has been adapted and translated into Dutch,[9] Spanish,[10] French,[11] Japanese,[12] and Hindi.[13]

The PANQOL-POL adaptation was based on guidelines by Beaton et al.[14] The first step of the adaptation process was to obtain permission from the authors. The translation process was conducted in accordance with Guidelines for the Cross-Cultural Adaptation Process by Beaton et al.[14]

Translation method

Stage 1: Translation of the PANQOL into Polish was conducted by a clinical psychologist (Polish-English native

speaker, not directly engaged in the study) and by a translation agency (bilingual translator, English native-speaker from Cracow, Poland). The translation agency was not informed about the aim of the study, and the translators had different backgrounds.

Stage 2: Synthesis of the translation was performed by a translator and 2 observers from the study team. The result of this stage was to produce 1 translated version.

Stage 3: The 3rd stage was to conduct a back-translation. Two bilingual professionals (from the translation agency) translated the questionnaire back into the original language, and we received 2 back translations.

Stage 4: The Expert Committee of 5 specialists in the fields of neurosurgery, psychiatry and clinical psychology assessed the translation. Polish and English versions were compared with each other, and after some corrections, the best version was finally chosen.

Questionnaires

The AQoL-8D developed by Hawthorne[15] consists of 35 items covering 8 dimensions: Independent Living, Pain, Senses, Mental Health, Happiness, Coping, Relationships, and Self-Worth, as well as Super dimensions: Physical and Psycho-Social. The Polish version of this questionnaire, adapted by Obrycka et al.,[16] has good psychometric properties and is a valid and reliable measure of QoL. The total score of the AQoL-8D and subscales were used to check the validity of the Polish version of the PANQOL.

The GBI was designed by Robinson et al.[17] and intended for single-use post-intervention as a measure of change related to a specific medical procedure, especially for otolaryngological interventions. The tool consists of 18 items. The questions are related to aspects of general, social and physical health. The scores range from –100 to +100 (max benefit). The Physical Health subscale was used to check the validity of the Polish version of the PANQOL for the General Health subscale.

The STS was established by Skarzynski et al.[18] to evaluate tinnitus complaints, either with normal or impaired hearing. The scale consists of 15 items grouped into 3 subscales: psychological distress, functioning and coping. Scores are expressed on a scale from 0 to 100, where 0 means no difficulties. The total score of STS was used to check the validity of the Polish version of the PANQOL for the Hearing subscale.

The WHO-5 was established by Hajos et al.[19] and adapted by Cichoń et al.[20] This is an unidimensional 5-item tool used to measure general emotional wellbeing. The scores are summed with higher scores indicating better emotional wellbeing. The total score of the WHO-5 was used to check the validity of the PANQOL-POL for the subscales of Energy and Anxiety.

A demographic survey included questions about sex, age, residence, education, employment, economic status, marital status, and comorbidities.

Statistical and psychometric analyses

Data analysis was performed using IBM SPSS v. 28.0 for Windows (IBM Corp., Armonk, USA). The level of significance was calculated with a 95% confidence interval (95% CI) ($p < 0.05$).

The basic descriptive statistical data for age with sociodemographic and categorical variables were reported as frequencies and percentages (Supplementary Table 1). A descriptive statistical analysis was performed for all questionnaire measurements (GBI, WHO-5, STS, PANQOL, and AQoL-8D). The means (M), medians (Me), quartiles (Q1; Q3), standard deviations (SD), as well as minimum and maximum values are presented in Supplementary Table 2. We verified data distribution for skewness and kurtosis considering standard errors and the results of the Kolmogorov–Smirnov test.

In the next step, the internal consistency of the Polish version of the PANQOL scale domains was measured using Cronbach's alpha (α). The value of alpha describes the extent to which the items on a scale measure the same concept or construct.[21] The commonly accepted interpretation of Cronbach's alpha was as follows: ≥0.91 (if alpha is too high (about > 0.95), it may suggest that some items are redundant, as they are testing the same question but in a different manner[22]) – excellent; <0.80−0.90 > – good; <0.70−0.80 – acceptable; <0.60−0.70 – questionable; 0.50−0.60 – poor; and ≤0.50 – unacceptable.

To verify the validity of the PANQOL subscales, a correlation analysis was conducted, where the Pearson's correlation coefficients (for quantitative variables) using the bootstrap method were estimated between the domains of PANQOL and GBI, WHO-5, STS, and AQoL-8D subscales. The assumption of Pearson's correlation analysis about the linearity was checked using scatter plots. The validation was based on correlations with questionnaires measuring the same or similar construct, correlating with the relevance of the QoL variable. The bias-corrected and accelerated (BCa) bootstrap method using 1000 resamples was used as the recommended technique for calculating confidence intervals in the cases where statistics did not address data normality.[23–25]

We also compared the results of the PANQOL dimensions between patients with and without dizziness after Gamma Knife surgery (GKS).

Results

Sociodemographic data

The study sample included 124 patients diagnosed with VS and treated with GKS. The mean age of patients was 60.17 years (SD = 13.27). Most patients were women (n = 77; 62.10%). In total, 106 (86.18%) patients had secondary or higher education, and the majority assessed their economic status as medium (73.98%). A total of 51

(41.46%) and 64 (52.03%) patients were employed or retired, respectively. Gardner–Robertson (GR) classes I and II after surgery were seen in 25.64% and 24.36% of patients, respectively. Most patients (30.77%) after surgery were assigned to class III according to the GR classification (details presented in Supplementary Table 1), while 10.26% of participants were classified as level V in GR scale which is interpreted as „Deaf". Descriptive statistical data based on the results obtained from questionnaires are presented in Supplementary Table 2. Most participants had grade 1 according to the House–Brackmann (HB) scoring system, interpreted as a normal function, and facial paralysis was not reported.

PANQOL-POL domain internal consistency

The internal consistency of the PANQOL-POL scale domains is presented in Table 1. Our analysis showed that most PANQOL domains showed excellent or good internal consistencies. The Facial Function and Hearing subscales reached acceptable internal consistencies (α > 0.7). The General Health domain showed an unacceptable internal consistency (α < 0.5). The low value of alpha may be due to the number of questions in that set (only 2 items).

Table 1. Internal consistencies (Cronbach's alpha) of the Polish version of the PANQOL

PANQOL dimension	M	SD	Cronbach's alpha	Number of items
Anxiety	63.60	24.67	0.897	4
Facial	74.65	21.85	0.730	3
General Health	47.61	18.25	0.424	2
Balance	62.19	25.07	0.916	6
Hearing	54.23	21.30	0.748	4
Energy	57.81	24.05	0.879	6
Pain	58.87	30.61	–[a]	1
Total	59.76	16.75	0.934	26

PANQOL – Penn Acoustic Neuroma Quality-of-Life Scale; M – mean; SD – standard deviation; [a] the Pain subscale consists of only 1 item and thus Cronbach's alpha is not applicable.

Measurement with questionnaires: Correlations with PANQOL-POL scores

Pearson's product–moment correlation coefficients (r) were calculated to examine the interdimensional correlations between the PANQOL domains and the AQoL-8D dimensions. These are presented in Table 2.

The PANQOL Facial Function subscale was weakly but significantly correlated with all AQoL-8D domains (r = 0.2–0.4). The PANQOL Facial Function subscale had the strongest correlation with the Relationships (r = 0.39; Boot95% BCa CI: 0.229–0.530) and Independent Living (r = 0.38; Boot95% BCa CI: 0.223–0.527) values.

The PANQOL Anxiety domain was also significantly correlated with all AQoL-8D domains (from a r = 0.25 for the Senses value (Boot95% BCa CI: 0.047–0.444) to a r = 0.61 for the Utility score (Boot95% BCa CI: 0.430–0.741).

The PANQOL General Health domain showed moderately significant correlations with the Independent Living, Happiness, Coping, Relationships, Self-Worth, Pain, Senses, and Mental Health dimensions. The strongest correlations were observed between the PANQOL General Health domain and the Utility score (r = 0.65; Boot95% BCa CI: 0.537–0.738) as well as the Physical super dimension (r = 0.65; Boot95% BCa CI: 0.512–0.751).

The PANQOL Balance and Hearing subscales were weakly or moderately correlated with all AQoL-8D domains (r = 0.28–0.55). The strongest correlations were observed between the PANQOL Balance domain and the Psycho-social super dimension value (r = 0.53; Boot95% BCa CI: 0.394 – 0.647), while the PANQOL Hearing subscale had the strongest relationship with the Senses value (r = 0.55; Boot95% BCa CI: 0.431–0.664).

The PANQOL Energy dimension was moderately or strongly correlated with all AQoL-8D domains (r = 0.40–0.66). The strongest correlation was observed between the PANQOL Energy subscale and Utility score (r = 0.66; Boot95% BCa CI: 0.528–0.760).

Similarly, the PANQOL total score was moderately or strongly correlated with all AQoL-8D domains (r = 0.52–0.71). The strongest correlation was observed between the PANQOL total score and Utility score (r = 0.71; Boot95% BCa CI: 0.598–0.807).

The PANQOL Balance and Hearing subscales were weakly or moderately correlated with all AQoL-8D domains (r = 0.28–0.55). The strongest correlations were observed between the PANQOL Balance domain and Psycho-social super dimension (r = 0.53; Boot95% BCa CI: 0.394 – 0.647), while the PANQOL Hearing subscale had the strongest relationships with the Senses value (r = 0.55; Boot95% BCa CI: 0.431–0.664).

The weakest relationships were observed between the PANQOL Pain dimension and all AQoL-8D domains (r = 0.18–0.51). There was no significant correlation between this PANQOL subscale and Mental Health, whereas the strongest correlations were observed for the PANQOL Pain subscale and Pain value (r = 0.51; Boot95% BCa CI: 0.360–0.629). The strongest significant interdimensional correlations are presented in Supplementary Table 3.

Next, Pearson's product–moment correlation coefficients (r) with the 95% BCa confidence intervals from 1000 bootstrap replications were estimated to test the correlations between the PANQOL domains and WHO-5 scores (Supplementary Table 4). All PANQOL domains were significantly weakly or moderately correlated with WHO-5 scores (r = 0.18–0.56). The strongest correlation was observed between the PANQOL General Health domain and WHO-5 results (r = 0.56; Boot95% BCa CI: 0.429–0.671).

Table 2. The results of Pearson's correlations (r) for PANQOL and AQoL-8D subscales; the bootstrap[a] method was used

Statistics		AQoL-8D										
		Utility score	Inde-pen-dent living value	Hap-piness value	Mental health value	Coping value	Rela-tion-ships value	Self-worth value	Pain value	Senses value	Psycho-social super dimen-sion	Physical super dimen-sion
PANQOL Facial												
r		**0.372**	**0.384**	**0.275**	**0.256**	**0.232**	**0.388**	**0.321**	**0.230**	**0.333**	**0.346**	**0.311**
p-value		<0.001	<0.001	0.002	0.004	0.010	<0.001	<0.001	0.010	<0.001	<0.001	<0.001
Bootstrap 95% BCa	LL	0.203	0.223	0.118	0.083	0.039	0.229	0.124	0.052	0.139	0.190	0.138
	UL	0.518	0.527	0.419	0.393	0.389	0.530	0.483	0.397	0.498	0.495	0.454
PANQOL Anxiety												
r		**0.607**	**0.338**	**0.539**	**0.570**	**0.580**	**0.489**	**0.546**	**0.415**	**0.252**	**0.416**	**0.570**
p-value		<0.001	<0.001	<0.001	<0.001	<0.001	<0.001	<0.001	<0.001	0.005	<0.001	<0.001
Bootstrap 95% BCa	LL	0.430	0.136	0.409	0.412	0.416	0.322	0.379	0.258	0.047	0.244	0.413
	UL	0.741	0.540	0.650	0.694	0.705	0.631	0.676	0.562	0.444	0.579	0.701
PANQOL General												
r		**0.648**	**0.480**	**0.522**	**0.609**	**0.513**	**0.554**	**0.457**	**0.512**	**0.398**	**0.578**	**0.648**
p-value		<0.001	<0.001	<0.001	<0.001	<0.001	<0.001	<0.001	<0.001	<0.001	<0.001	<0.001
Bootstrap 95% BCa	LL	0.537	0.340	0.365	0.494	0.358	0.398	0.312	0.380	0.278	0.472	0512
	UL	0.738	0.607	0.656	0.704	0.656	0.682	0.573	0.625	0.519	0.671	0.751
PANQOL Balance												
r		**0.467**	**0.491**	**0.286**	**0.354**	**0.335**	**0.398**	**0.314**	**0.430**	**0.384**	**0.527**	**0.366**
p-value		<0.001	<0.001	0.001	<0.001	<0.001	<0.001	<0.001	<0.001	<0.001	<0.001	<0.001
Bootstrap 95% BCa	LL	0.321	0.358	0.123	0.205	0.177	0.250	0.144	0.274	0.263	0.394	0.207
	UL	0.602	0.617	0.442	0.488	0.490	0.540	0.470	0.579	0.506	0.647	0.523
PANQOL Hearing												
r		**0.482**	**0.325**	**0.297**	**0.320**	**0.363**	**0.449**	**0.417**	**0.312**	**0.554**	**0.449**	**0.371**
p-value		<0.001	<0.001	<0.001	<0.001	<0.001	<0.001	<0.001	<0.001	<0.001	<0.001	<0.001
Bootstrap 95% BCa	LL	0.315	0.170	0.111	0.134	0.180	0.270	0.245	0.132	0.431	0.293	0.176
	UL	0.628	0.482	0.454	0.489	0.516	0.599	0.563	0.478	0.664	0.592	0.555
PANQOL Energy												
r		**0.662**	**0.459**	**0.514**	**0.584**	**0.561**	**0.617**	**0.554**	**0.402**	**0.451**	**0.517**	**0.655**
p-value		<0.001	<0.001	<0.001	<0.001	<0.001	<0.001	<0.001	<0.001	<0.001	<0.001	<0.001
Bootstrap 95% BCa	LL	0.528	0.308	0.382	0.465	0.405	0.492	0.410	0.246	0.279	0.379	0.539
	UL	0.760	0.600	0.632	0.683	0.687	0.724	0.665	0.530	0.584	0.636	0.754
PANQOL Pain												
r		0.344	0.311	0.189	00.118	0.268	0.265	0.276	0.508	0.233	0.452	0.183
p-value		<0.001	<0.001	0.037	0.195	0.003	0.003	0.002	<0.001	0.009	<0.001	0.042
Bootstrap 95% BCa	LL	0.152	0.127	−0.014	−0.105	0.064	0.080	0.090	0.360	0.056	0.298	−0.045
	UL	0.502	0.454	0.358	0.317	0.432	0.421	0.434	0.629	0.394	0.575	0.376
PANQOL Total												
r		0.712	0.558	0.517	0.547	0.570	0.624	0.577	0.574	0.515	0.661	0.608
p		<0.001	<0.001	<0.001	<0.001	<0.001	<0.001	<0.001	<0.001	<0.001	<0.001	<0.001
Bootstrap 95% BCa	LL	0.598	0.419	0.378	0.372	0.439	0.498	0.420	0.442	0.358	0.554	0.468
	UL	0.807	0.676	0.629	0.689	0.689	0.727	0.708	0.694	0.642	0.757	0.741

PANQOL – Penn Acoustic Neuroma Quality-of-Life Scale; AQoL-8D – Assessment of Quality of Life 8-Dimension; Bootstrap 95% BCa – the bias-corrected and accelerated (BCa) 95% bootstrap confidence interval; LL and UL – lower and upper limit of 95% confidence interval. Values in bold are significant at 95% confidence limit; [a] bootstrap 1000 samples.

In the next step, Pearson's product–moment correlation coefficients (r) with the 95% BCa confidence intervals from 1000 bootstrap replications were also estimated to test the correlations between PANQOL domains and GBI dimensions (Supplementary Table 5).

Only the GBI Support subscale was not significantly correlated with PANQOL domains. The observed significant relationships between the GBI and PANQOL domains were weak (r = 0.18–0.43). The strongest correlation was observed between the PANQOL General Health domain and GBI total results (r = 0.43; Boot95% BCa CI: 0.268–0.567) as well as between the PANQOL General Health domain and GBI General subscale (r = 0.42; Boot95% BCa CI: 0.255–0.567).

We also estimated Pearson's product–moment correlation coefficients (r) with the 95% BCa CIs from 1000 bootstrap replications to test the correlations between the PANQOL domains and the STS scale (Supplementary Table 6).

The STS scale was negatively and weakly correlated with 4 PANQOL domains: General Health (r = -0.19; Boot95% BCa CI: −0.347– −0.022), Hearing (r = −0.40; Boot95% BCa CI: −0.544– −0.249), Energy (r = −0.22; Boot95% BCa CI: −0.391– −0.050), and total PANQOL scores (r = −0.26; Boot95% BCa CI: −0.428– −0.093). Thus, the more tinnitus complaints (STS score), the lower the scores in the General Health, Hearing and Energy domains and the aggregate results of PANQOL.

Dizziness after surgery and PANQOL results

Further, we compared the PANQOL Balance subscale results between patients with and without dizziness after surgery (Supplementary Table 7). Patients without dizziness obtained higher PANQOL scores (M = 78.43; SD = 20.25) than those with dizziness after surgery (M = 48.14; SD = 19.74); t(121) = 8.39; 95% BCa CI: 23.28 – 37.34. The effect size was large (Cohen's d = 1.52).

Discussion

The purpose of this study was to conduct the first adaptation of the disease-specific questionnaire for patients with VS to Polish conditions and to evaluate its psychometric properties based on data obtained from 124 patients, the largest group in which adaptations have been performed so far. The results of the study demonstrate that the PANQOL-POL is a valid and reliable instrument to measure disease-specific QoL in patients with VS. Our analysis showed that most PANQOL domains had excellent or good internal consistency measured with Cronbach's alpha; similar values were reported in the original version of this tool presented by Shaffer et al.[5] Only the General Health domain showed unacceptable internal consistency (α < 0.5), as in the Japanese adaptation.[9,12] The low value

of alpha may be due to the small number of questions in that set (only 2 items). Nishiyama et al.[12] emphasized that clinicians need to be careful in interpreting the General Health domain score. As in previous adaptations conducted by van Leeuwen et al.[9] (PANQOL-Dutch), Nishiyama et al.[12] (PANQOL-Japanese) and Pattankar et al.[13] (PANQOL-Hindi), we did not determine the internal consistency for the Pain domain because it included only a single item.

To verify the validity of the PANQOL subscales, a correlation analysis was conducted between the domains of PANQOL and the following questionnaires: AQoL-8D, GBI, WHO-5 and STS, as well as the presence of dizziness and GR classes. In the previous non-Polish adaptations (such as Japanese, Dutch and Hindi), the PANQOL total score was correlated with the 36-Item Short Form Health Survey (SF-36). In the Polish adaptation, we decided to use the AQoL-8D questionnaire as we focused on patients with hearing loss and this tool is frequently used in this group of patients. Our analysis showed a strong correlation between the PANQOL total score and the AQoL-8D Utility score. Strong correlations were found between subscales AQoL-8D Pain and PANQOL Pain, AQOL-8D Physical super dimension and PANQOL General Health, AQOL-8D Utility and PANQOL Energy, and AQOL-8D Senses and PANQOL Hearing. Furthermore, the PANQOL Hearing subscale was correlated with GR classes, and the results showed that the higher the GR class (greater degree of hearing impairment), the lower the scores on the PANQOL, which is interpreted as a worse QoL. Moreover, the analysis showed a relationship between lower anxiety according to the PANQOL and better coping in daily life. All PANQOL domains were significantly weakly or moderately correlated with WHO-5 scores. The strongest correlation was observed between the PANQOL General Health domain and WHO-5 results, which could be interpreted that patients who assessed their general health as better also reported better mental health functioning. We observed a correlation between the PANQOL General Health domain and GBI total results. Patients who reported better general health also reported higher benefits after GKS treatment.

The PANQOL Facial Function domain had the strongest correlation with the Relationships value. It needs to be highlighted that most participants had grade 1 according to the HB scoring system, which is interpreted as a normal function, and facial paralysis was not reported. Patients achieved high scores (M = 74.65; S = 21.85) in the PANQOL Facial Function domain, which is consistent with our medical data (patients did not have facial nerve dysfunction). In the Hindi adaptation of the PANQOL conducted by Pattankar et al.,[13] the PANQOL Facial Function domain had poor correlation with SF-36 dimensions. We also compared the results of the PANQOL Balance subscale between patients with and without dizziness after surgery. The results showed that patients who did not report dizziness obtained better scores in the PANQOL Balance. Moreover, the more tinnitus complaints (STS

score), the lower scores in General Health, Hearing and Energy domains and the total results of the PANQOL.

The PANQOL is a disease-specific questionnaire including questions about symptoms. The results of our study indicate a strong correlation between the general and specific questionnaires. Therefore, we propose that the PANQOL be used to assess quality of life in patients with VS.

Limitations

The General Health domain showed unacceptable internal consistency ($\alpha < 0.5$) for the Polish version of the scale. The low value of alpha may be due to the number of questions in that set (only 2 items). Clinicians need to be careful in interpreting the General Health domain scores, and to assess it, additional questionnaires should be applied. Quality of life is a subjective construct and multiple factors may have an impact on the health-related QoL of patients. According to the Central Brain Tumor Registry in the USA, the incidence increases between the 65–74-year-old age group without a sex difference.[26] In our study, the study group could be more representative in terms of gender distribution. Vestibular schwannoma occurs with the same frequency in both sexes.

Conclusions

The present report is the first adaptation of a disease-specific questionnaire for patients with VS to Polish conditions. The results demonstrated that the Polish version of PANQOL is a reliable and valid questionnaire.

Supplementary data

The Supplementary materials are available at https://doi.org/10.5281/zenodo.10933235. The package includes the following files:

Supplementary Table 1. Demographic and medical characteristics of the patients (n = 124)

Supplementary Table 2. Descriptive statistics of questionnaires used in the study.

Supplementary Table 3. The strongest correlations between AQoL-8D and PANQOL subscales (n = 123).

Supplementary Table 4. Pearson's correlations (r) for PANQOL subscales and WHO-5_ the bootstrap method was used.

Supplementary Table 5. Pearson's correlations (r) for PANQOL subscales and GBI_ the bootstrap method was used.

Supplementary Table 6. Pearson's correlations (r) for PANQOL subscales and STS_ the bootstrap method was used.

Supplementary Table 7. Comparison of patients with and without dizziness after Gamma Knife surgery based on the PANQOL Balance subscale scores.

Data availability

The datasets generated and/or analyzed during the current study are available from the corresponding author on reasonable request.

Consent for publication

Every patient was informed and gave their consent to the statistical processing and anonymous publication of their answers before participating in this study.

ORCID iDs

Katarzyna Bienkowska   https://orcid.org/0000-0002-3390-3244
Barbara Kostecka   https://orcid.org/0000-0002-0531-3642
Grzegorz Turek   https://orcid.org/0000-0002-0609-5819
Miroslaw Zabek   https://orcid.org/0000-0001-6847-2424
Andrzej Kokoszka   https://orcid.org/0000-0003-4518-5494
Sebastian Dzierzęcki   https://orcid.org/0000-0002-8262-1999
Ewelina Cichoń   https://orcid.org/0000-0001-5728-3003

References

1. Carlson ML, Tveiten OV, Driscoll CL, et al. Long-term quality of life in patients with vestibular schwannoma: An international multicenter cross-sectional study comparing microsurgery, stereotactic radiosurgery, observation, and nontumor controls. *J Neurosurg*. 2015; 122(4):833–842. doi:10.3171/2014.11.JNS14594
2. World Health Organization (WHO). The World Health Organization quality of life assessment (WHOQOL): Position paper from the World Health Organization. *Soc Sci Med*. 1995;41(10):1403–1409. doi:10.1016/0277-9536(95)00112-K
3. Fabbris C, Gazzini L, Paltrinieri D, Marchioni D. Exclusive surgical treatment for vestibular schwannoma regrowth or recurrence: A meta-analysis of the literature. *Clin Neurol Neurosurg*. 2020;193:105769. doi:10.1016/j.clineuro.2020.105769
4. Balossier A, Régis J, Reyns N, et al. Repeat stereotactic radiosurgery for progressive vestibular schwannomas after previous radiosurgery: A systematic review and meta-analysis. *Neurosurg Rev*. 2021; 44(6):3177–3188. doi:10.1007/s10143-021-01528-y
5. Shaffer BT, Cohen MS, Bigelow DC, Ruckenstein MJ. Validation of a disease-specific quality-of-life instrument for acoustic neuroma: The Penn Acoustic Neuroma Quality-of-Life Scale. *Laryngoscope*. 2010;120(8): 1646–1654. doi:10.1002/lary.20988
6. McLaughlin EJ, Bigelow DC, Lee JYK, Ruckenstein MJ. Quality of life in acoustic neuroma patients. *Otol Neurotol*. 2015;36(4):653–656. doi:10.1097/MAO.0000000000000674
7. Miller LE, Brant JA, Chen J, Kaufman AC, Ruckenstein MJ. Hearing and quality of life over time in vestibular schwannoma patients: Observation compared to stereotactic radiosurgery. *Otol Neurotol*. 2019; 40(8):1094–1100. doi:10.1097/MAO.0000000000002334
8. Goldbrunner R, Weller M, Regis J, et al. EANO guideline on the diagnosis and treatment of vestibular schwannoma. *Neurooncology*. 2020; 22(1):31–45. doi:10.1093/neuonc/noz153
9. Van Leeuwen BM, Herruer JM, Putter H, Jansen JC, Van Der Mey AGL, Kaptein AA. Validating the Penn Acoustic Neuroma Quality of Life Scale in a sample of Dutch patients recently diagnosed with vestibular schwannoma. *Otol Neurotol*. 2013;34(5):952–957. doi:10.1097/MAO.0b013e31828bb2bb
10. Medina MDM, Carrillo A, Polo R, et al. Validation of the Penn Acoustic Neuroma Quality-of-Life Scale (PANQOL) for Spanish-speaking patients. *Otolaryngol Head Neck Surg*. 2017;156(4):728–734. doi:10.1177/0194599816688640
11. Oddon PA, Montava M, Salburgo F, Collin M, Vercasson C, Lavieille JP. Conservative treatment of vestibular schwannoma: Growth and Penn Acoustic Neuroma Quality of Life scale in French language. *Acta Otorhinolaryngol Ital*. 2017;37(4):320–327. doi:10.14639/0392-100X-1094

12. Nishiyama T, Oishi N, Kojima T, et al. Validation and multidimensional analysis of the Japanese Penn Acoustic Neuroma Quality-of-life Scale. *Laryngoscope*. 2020;130(12):2885–2890. doi:10.1002/lary.28488

13. Pattankar S, Churi O, Misra B. Validation of the Penn Acoustic Neuroma Quality of Life (PANQOL) Scale for Hindi-speaking patients recently diagnosed with vestibular schwannoma. *Neurol India*. 2022; 70(3):978. doi:10.4103/0028-3886.349775

14. Beaton DE, Bombardier C, Guillemin F, Ferraz MB. Guidelines for the process of cross-cultural adaptation of self-report measures. *Spine (Phila Pa 1976)*. 2000;25(24):3186–3191. doi:10.1097/00007632-200012150-00014

15. Hawthorne G. Assessing utility where short measures are required: Development of the Short Assessment of Quality of Life-8 (AQoL-8) instrument. *Value Health*. 2009;12(6):948–957. doi:10.1111/j.1524-4733.2009.00526.x

16. Obrycka A, Padilla JL, Lorens A, Skarzynski PH, Skarzynski H. Validation of AQoL-8D: A health-related quality of life questionnaire for adult patients referred for otolaryngology. *Eur Arch Otorhinolaryngol*. 2022;279(2):653–662. doi:10.1007/s00405-021-06689-6

17. Robinson K, Gatehouse S, Browning GG. Measuring patient benefit from otorhinolaryngological surgery and therapy. *Ann Otol Rhinol Laryngol*. 1996;105(6):415–422. doi:10.1177/000348949610500601

18. Skarżyński H, Gos E, Raj-Koziak D, Skarżyński PH. Skarzynski Tinnitus Scale: Validation of a brief and robust tool for assessing tinnitus in a clinical population. *Eur J Med Res*. 2018;23(1):54. doi:10.1186/s40001-018-0347-4

19. Hajos TRS, Pouwer F, Skovlund SE, et al. Psychometric and screening properties of the WHO-5 well-being index in adult outpatients with type 1 or type 2 diabetes mellitus. *Diabet Med*. 2013;30(2):e63–e69. doi:10.1111/dme.12040

20. Cichoń E, Kiejna A, Kokoszka A, et al. Validation of the Polish version of WHO-5 as a screening instrument for depression in adults with diabetes. *Diabetes Res Clin Pract*. 2020;159:107970. doi:10.1016/j.diabres.2019.107970

21. Nunnally JC, Bernstein IH. *Psychometric Theory*. 3rd ed. New York, USA: McGraw-Hill; 1994. ISBN:978-0-07-107088-1.

22. Streiner DL. Starting at the beginning: An introduction to coefficient alpha and internal consistency. *J Pers Assessment*. 2003;80(1):99–103. doi:10.1207/S15327752JPA8001_18

23. Efron B. The bootstrap and modern statistics. *J Am Stat Assoc*. 2000; 95(452):1293–1296. doi:10.1080/01621459.2000.10474333

24. Bishara AJ, Hittner JB. Reducing bias and error in the correlation coefficient due to nonnormality. *Educ Psychol Meas*. 2015;75(5):785–804. doi:10.1177/0013164414557639

25. Haukoos JS, Lewis RJ. Advanced statistics: Bootstrapping confidence intervals for statistics with "difficult" distributions. *Acad Emerg Med*. 2005;12(4):360–365. doi:10.1197/j.aem.2004.11.018

26. Kshettry VR, Hsieh JK, Ostrom QT, Kruchko C, Barnholtz-Sloan JS. Incidence of vestibular schwannomas in the United States. *J Neurooncol*. 2015;124(2):223–228. doi:10.1007/s11060-015-1827-9

Protective effect of clotrimazole on lung injury in an experimental model of ruptured abdominal aortic aneurysm

Zerrin Pulathan[1,A,C–F], Şaban Murat Ergene[2,B], Gökalp Altun[1,C,D], Esin Yuluğ[3,B,D], Ahmet Menteşe[4,B,D]

[1] Department of Cardiovascular Surgery, Faculty of Medicine, Karadeniz Technical University, Trabzon, Turkey

[2] Department of Cardiovascular Surgery, Faculty of Medicine, Recep Tayyip Erdoğan University, Rize, Turkey

[3] Department of Histology and Embryology, Faculty of Medicine, Karadeniz Technical University, Trabzon, Turkey

[4] Department of Medical Biochemistry, Faculty of Medicine, Karadeniz Technical University, Trabzon, Turkey

A – research concept and design; B – collection and/or assembly of data; C – data analysis and interpretation;
D – writing the article; E – critical revision of the article; F – final approval of the article

Address for correspondence
Zerrin Pulathan
E-mail: zerrin.pulathan@gmail.com

Abstract

Background. Lungs are the target organs most affected by ischemia/reperfusion (I/R) injury, which is exacerbated when hemorrhagic shock occurs. Suppressing various proinflammatory cytokines, inflammation and oxidation that initiate and aggravate lung damage with various drugs or methods provides significant benefits in preventing lung damage.

Objectives. This study aims to evaluate the protective effect of clotrimazole (CLT), an antimycotic drug, on lung injury and systemic inflammatory response in rats by creating an experimental model of a ruptured abdominal aortic aneurysm (RAAA).

Materials and methods. Thirty-six male Sprague Dawley rats were randomly divided into 5 groups: sham, sham+CLT, sham+polyethylene glycol (PEG), shock+ischemia/reperfusion (SIR), and SIR+CLT. Saline, CLT and PEG were administered in the sham groups without shock and I/R. The hemorrhagic shock was developed in SIR groups by drawing blood for 1 h to keep the mean arterial pressure at 50 mm Hg. After 60 min, the SIR+CLT group was given 20 mg/kg CLT; then, the aortic clamps were opened, and rats were left for 120 min of reperfusion. The blood taken to create hemorrhagic shock was returned in a controlled manner during this time. At the end of the reperfusion procedure, samples were taken for cytokine levels in serum and lung tissue and for other biochemical analyses. Blood gas, histopathological examination and wet/dry weight measurements were performed to assess lung injury.

Results. An increase was observed in all parameters in the SIR group compared to the sham group. In the SIR+CLT group, the serum myeloperoxidase (MPO), tumor necrosis factor alpha (TNF-α), lung MPO values, histologically lung injury scores, and lung tissue wet/dry ratio were decreased significantly when compared to the SIR group (p < 0.05).

Conclusions. These results indicate that CLT may reduce the systemic inflammatory response and lung injury due to shock and I/R in an experimental model of RAAA.

Key words: IL-6, TNF-α, hemorrhagic shock, clotrimazole, aortic ischemia/reperfusion

92

Z. Pulathan et al. Clotrimazole protects against lung injury

Background

A ruptured abdominal aortic aneurysm (RAAA) is an emergency of cardiovascular surgery today, with high mortality and morbidity rates. Although endovascular repair has reduced the mean mortality to 26.8% in the treatment of RAAA, the mortality of open surgical repair is still around 40%.[1] One of the important reasons that increase mortality after ruptured aortic aneurysm treatment is pulmonary complications such as respiratory failure, pneumonia and acute respiratory distress syndrome (ARDS).[2] Pulmonary complications, seen at a 36–41% rate, are related to blood and fluid transfusions, cross-clamping duration and systemic inflammatory response.[3] Mortality ranges from 27% to 45% in cases with ARDS, depending on the severity of the clinical picture. Unlike other ischemia/reperfusion (I/R) injuries, 2 critical clinical events occur in RAAA. One of these is hypovolemic shock, which causes systemic hypoxia in all tissues due to bleeding. The other is lower body ischemia due to cross-clamping during treatment and reperfusion injury seen afterward. After RAAA surgery, high levels of cytokines, such as tumor necrosis factor alpha (TNF-α) and interleukin 6 (IL-6), which increase inflammation, are high.[4] This has been associated with ARDS and increased mortality.[5,6] Activated neutrophils accumulate in the subendothelial space, releasing reactive oxygen species (ROS) and oxidative damage.[7] Ischemia causes an increase in calcium permeability by promoting its entry into cells. The intracellular accumulation of calcium ions (Ca^{++}) because of changes in the permeability of the plasma membrane and the decrease in its active ATP-depended transport results in the activation of phospholipases and proteases.[8]

Clotrimazole (CLT), an azole antifungal drug (1-2 chlorophenyl-diphenyl methyl-1H- imidazole), is frequently used for prophylaxis and treatment of candidiosis following transplantation.[9] In addition, it is used in treating diseases such as malaria, sickle cell anemia, tuberculosis, and rheumatoid arthritis, and is effective as an antiapoptotic and immunosuppressive agent.[10] Also, it has been reported that CLT acts by inhibiting both cytochrome P450 (CYP2, CYP3A) and Ca^{2+}-linked K^{+} channels.[11] These include the depleting intracellular calcium-dependent potassium channels and inhibiting voltage-dependent calcium channels in the sarcoplasmic reticulum Ca^{+2}-ATPase.[12] In this way, CLT has been shown to prevent the formation of free oxygen radicals in the organism for various reasons.[13] Some cytochrome P450 epoxygenases catalyze the formation of anti-inflammatory epoxyeicosatrienoic acids (EETs) from arachidonic acid. Epoxyeicosatrienoic acids inhibit inflammation by reducing nuclear factor-kappa B (NF-κB) activation. Thus, EETs play essential roles in various biological activities such as blood pressure regulation and cardioprotection.[14] Epoxyeicosatrienoic acids also show an anti-inflammatory effect on vascular remodeling by regulating TNF-α-induced VCAM-1 expression, therefore providing

endothelial protection.[15] In addition, its anti-inflammatory and antioxidant efficacy has been shown by numerous studies. Clotrimazole also exerts anti-inflammatory effects by inhibiting NF-kB-dependent cytokines such as TNF-α and IL-8 in vivo and in vitro.[16] Clotrimazole also suppresses NOS-mediated ROS production while increasing adenosine triphosphate (ATP) production in mitochondria in I/R injury by inhibiting the entry of Ca^{2+} via transient receptor potential (TRPM2) channels.[17]

Objectives

The aim of this study was to investigate the potential anti-inflammatory and antioxidant effects of CLT in the systemic circulation and lung tissue in an experimental model of ruptured abdominal aortic aneurysm simulating hypovolemic shock and I/R.

Materials and methods

Chemicals

Clotrimazole (1-[2-Chlorophenyl] diphenyl methyl-1H-imidazole, Cas No. 23593-75-1) and PEG, the solvent of CLT (Polyethylene glycol 400, Cas No: 25322-68-3) were purchased from Sigma-Aldrich (St. Louis, USA). Ketamine hydrochloride (Ketalar, 500 mg/10 mL) was obtained from Pfizer (New York, USA), and xylazine hydrochloride (Rompun 2%) was obtained from Bayer (Leverkusen, Germany).

Animals

Thirty-six Sprague Dawley rats were used, weighing 420 ±56 g and aged 4–5 months. Before the experiment, the rats were kept in wire cages in a 12-hour light/dark cycle at 24–26°C and a relative humidity of 50 ±10%. Rats were acclimated to the environment and treated under ethical animal use and care principles. Twelve hours before the experiment, nutrition, but not water, was stopped. First, rats were randomly divided into 2 main groups: sham (Sh) and shock+ischemia/reperfusion (SIR). Sham groups were redivided into 3 groups as sh (n = 6), Sh+clotrimazole (Sh+CLT; n = 6) and Sh+polyethylene glycol (Sh+PEG; n = 6). Shock+ischemia/reperfusion groups were also divided into SIR (n = 9) and SIR+CLT (n = 9). The number of animals was determined using the power analysis method. A minimum sample size of 6 animals per group would provide the appropriate power (1 − β = 0.8) to identify significant (α = 0.05) differences in malondialdehyde (MDA), considering large effect size d = 2.0, with a variance test. Sample size calculation was performed using inG*Power 3.1.9.2 (Kiel University, Kiel, Germany) for 2 individual comparisons between 2 groups (Sh-Sh+CLT-Sh+PEG and Sh-SIR-SIR+CLT). For SIR and

Table 1. Experimental groups and applied procedures

Groups	n	Shock 60 min	Drug 1 mL	Ischemia 60 min	Reperfusion 120 min
Sh	6	–	saline	–	–
Sh+CLT	6	–	CLT	–	–
Sh+PEG	6	–	PEG	–	–
SIR	9	+	saline	+	+
SIR+CLT	9	+	CLT	+	+

Sh – sham; CLT – clotrimazole; PEG – polyethylene glycol; SIR – shock+ischemia/reperfusion.

SIR+CLT groups, to minimize the effect of mortality, 9 rats have been included in the study. Eventually, the experiment was continued with a total of 5 groups (Table 1).

Ethical standards

This experimental study was approved by Karadeniz Technical University Animal Experiments Local Ethics Committee (approval No. 2019/33). All experiments were blinded and randomized according to the ARRIVE (Animal Research: Reporting of In Vivo Experiments) guidelines by a separate researcher who created the experimental protocol and performed the experiments at Karadeniz Technical University Surgical Practice and Research Center.[18]

Surgical procedures

In this study, we used the ruptured abdominal aortic aneurysm model in rats developed for the first time in 1995 by Lindsay et al.[19] Sham groups underwent no surgical procedure except for aortic exploration. Shock+ischemia/reperfusion groups experienced hypovolemic shock for 60 min, ischemia for 60 min and reperfusion for 120 min (Table 1). Rats were anesthetized without disrupting spontaneous breathing. For this purpose, xylazine hydrochloride was administered intramuscularly (im.) at 10 mg/kg, and ketamine hydrochloride was administered im. at a dose of 50 mg/kg and repeated when necessary. A catheter was inserted through the right carotid artery for arterial pressure monitoring. The left internal jugular vein was catheterized for blood and fluid replacement (Novacath; Medipro, Los Angeles, USA). During the experiment, the rats' blood pressure, heart rate, rectal temperature, and respiratory rate were monitored (Nikon Kohden BSM-4113; Nikon Corp., Tokyo, Japan). The rectal temperature was kept around 36.5°C using a heat lamp. For insensible fluid losses, saline (0.9% NaCl) was infused at 3 mL/kg/h (Perfusor Compact S; Brown, Melsungen, Germany). Blood was drawn from the carotid artery cannula using a heparinized plastic syringe until mean arterial pressure (MAP) decreased to 50 mm Hg to induce hypovolemic shock in the SIR groups. The amount of blood drawn was less than 30% of the total blood volume. At the 45 min of hemorrhagic shock and its equivalent duration, 1 mL of saline was given to the rats in the Sh and SIR groups, 1 mL of PEG to the Sh+PEG group, and 30 mg/kg of CLT to the Sh+CLT and SIR+CLT groups intraperitoneally (ip.), and laparotomy and aortic exploration was performed at the 60 min. After 60 min of hypovolemic shock, systemic heparinization was performed. The abdominal aorta was then clamped in 2 places, above the supramesenteric and iliac bifurcation, resulting in lower torso ischemia. Half of the blood drawn from the rats was reinfused into the jugular vein. Thus, surgical treatment and resuscitation were simulated. Once the aortic clamps were opened, the abdomen was closed using a 5/0 prolene suture, and rats were allowed 120 min of reperfusion. The remaining blood was reinfused, Ringer's lactate solution was given when needed, and MAP was maintained at 100 mm Hg.

Sample preparation

At the end of the reperfusion, all rats were euthanized by exsanguination. Arterial blood samples were taken for blood gas and biochemical analysis. Lung tissues were removed, part of the left lung was frozen at −80°C for biochemical analysis, and the remainder was fixed in formaldehyde for histopathological examinations. The right lung was reserved for wet/dry weight measurements.

Biochemical analysis

The amount of MDA in rat blood samples was measured using the thiobarbituric acid reactive substance (TBARS) method developed by Yagi in 1984.[20] As a result of the measurement, plasma MDA amounts were calculated as nanomoles per milliliter (nmol/mL). Serum MPO levels were determined using the enzyme-linked immunosorbent assay (ELISA) kit (cat. No. BMS622; Bender MedSystems, Vienna, Austria). Results are shown in nanograms per milliliter (ng/mL). Serum TNF-α levels were determined using the same ELISA kit. Results are given in picogram per milliliter (pg/mL). Serum IL-6 levels were also determined using the same ELISA kit. Results are given in picogram per milliliter (pg/mL). Ischemia-modified albumin (IMA) measurement was evaluated with the rapid and colorimetric determination method developed by Bar et al.[21] Results are reported in absorbance units (ABSU). At the end of the experiment, blood was taken from the heparinized syringe

94

Z. Pulathan et al. Clotrimazole protects against lung injury

via the carotid artery and transferred to the cartridge, and blood gases were measured (IRMA TruPoint Blood Analysis System, Guangzhou, China). A piece of lung tissue was homogenized, and MDA levels in tissues were studied with the thiobarbituric acid method developed by Mihara and Uchiyama in 1978.[22] Uchiyama Tissue MDA levels were expressed as nmol MDA/g wet tissue. Tissue MPO levels were determined using the ELISA kit (cat. No. HK105; Hycult Biotech, Uden, the Netherlands). The results are given in ng/mL per gram of wet tissue.

For lung wet/dry weight measurements, the right lung was separated from other tissues and weighed on a microbalance. After 48 h at 70°C, it was weighed again. The wet/dry ratio was calculated, and the increase was interpreted in favor of pulmonary edema.

Histopathology

For histopathological examination, the tissues were processed employing a standard paraffin-embedded technique. Then, the sections prepared this way were stained with hematoxylin and eosin (H&E). An experienced histologist, unaware of the study groups, performed a histopathological evaluation. In the damage scoring of lung tissues, 5 different areas at high magnification (×400) (Olympus Bx51; Olympus Corp., Tokyo, Japan) in the lung preparation of each group were evaluated semi-quantitatively according to the criteria described below. Microscopic damage scoring was performed on a 4-grade scale: Grade 0. Normal lung morphology: Grade 1. Mild intra-alveolar edema and mild inflammatory cell infiltration: Grade 2. Moderate alveolar edema and moderate inflammatory cell infiltration: Grade 3. Severe alveolar edema, severe inflammatory cell infiltration, and focal hemorrhage: Grade 4. Diffuse inflammatory cell infiltration and alveolar damage.

Statistical analyses

Statistical analysis was performed using the IBM SPSS v. 23.0 software (IBM Corp., Armonk, USA). The levels of serum biomarkers, arterial blood and lung tissue findings have been presented as median and interquartile ranges (IQRs). The statistical significance of the levels of serum biomarkers, arterial blood, and lung tissue findings has been tested within Sham – sham+CLT – sham+PEG and sham – SIR – SIR+CLT with the Kruskal–Wallis test. Post hoc analysis within subgroups was tested with the Dunn's test and Bonferroni adjustment. Due to the small number of samples, nonparametric methods were chosen. Test statistics, degrees of freedom (df) values, p-values and adjusted p-values have been given in the results section. The levels of parameters among groups have also been shown via boxplot graphics with data points. A p-value under 0.05 indicates statistical significance.

Results

Biochemical results in blood serum are shown in Table 2 and Fig. 1. One of the reactions caused by free oxygen radicals is lipid peroxidation, and one of the end products of lipid peroxidation is MDA.

There was no statistically significant differences between levels of serum MDA across groups of Sh-Sh+PEG and Sh+CLT (v = 0.495, df = 2, p = 0.781), and Sh, SIR and SIR+CLT (Kruskal-Wallis test H-statistic = 4.43, df = 2, p = 0.109).

Measuring serum MPO values gives information about neutrophil activation. There was a significant difference across groups of Sh, Sh+PEG and Sh+CLT (Kruskal–Wallis test H-statistic = 9.579, df = 2, p < 0.01), and Sh, SIR and SIR+CLT (Kruskal–Wallis test H-statistic = 20.250, df = 2, p < 0.001). Serum MPO levels were significantly higher in the Sh+CLT group than in the Sh+PEG group (Dunn's test statistic = 9.500, adj. p = 0.006). Serum MPO levels were also significantly higher in the SIR group compared to Sh (Dunn's test statistic = −16.500, adj. p < 0.001) and SIR+CLT groups (Dunn's test statistic = 9.500, p < 0.03).

There were no statistically significant differences between the levels of serum TNF-α across Sh, Sh+PEG and Sh+CLT groups (Kruskal–Wallis test H-statistic = 4.643, df = 2; p = 0.098), but there was a significant difference between Sh, SIR and SIR+CLT groups (Kruskal–Wallis test H-statistic = 13.302, df = 2; p = 0.001). The TNF-α

Table 2. Serum biochemical parameters in all groups

Parameters median (IQR)	Sh (n = 6)	Sh+CLT (n = 6)	Sh+PEG (n = 6)	SIR (n = 9)	SIR+CLT (n = 9)
MDA [nmol/mL]	1.54 (0.26)	1.41 (0.60)	1.57 (0.51)	2.11 (2.97)	1.76 (0.87)
MPO [ng/mL]	83.72 (6.52)	87.30 (6.91)[a]	75.13 (11.66)[a]	397.63 (40.81)[b]	179.65 (50.74)[b]
TNF-α [pg/mL]	154.28 (13.08)	155.16 (24.29)	167.85 (18.45)	260.83 (77.07)[b]	221.21 (61.59)[b]
IL-6 [pg/mL]	163.25 (40.56)	143.17 (49.62)	158.86 (55.20)	189.67 (102.85)	179.61 (41.37)
IMA [ABSU]	0.61 (0.34)	0.84 (0.42)	0.69 (0.48)	0.98 (0.74)[c]	0.90 (0.09)

MDA – malondialdehyde; MPO – myeloperoxidase; TNF-α – tumor necrosis factor alpha; IL-6 – interleukin 6; IMA – ischemia-modified albumin; Sh – sham; CLT – clotrimazole; PEG – polyethylene glycol; SIR – shock+ischemia/reperfusion. Values are given as median (interquartile range (IQR)). The Kruskal–Wallis test was used for the analysis. Post hoc analysis within subgroups was tested with the Dunn's test and Bonferroni adjustment; [a] p < 0.05 compared the results between between Sh+CLT and Sh+PEG; [b] p < 0.05 compared the results between Sh – SIR and SIR – SIR+CLT; [c] p < 0.05 compared the results between Sh and SIR.
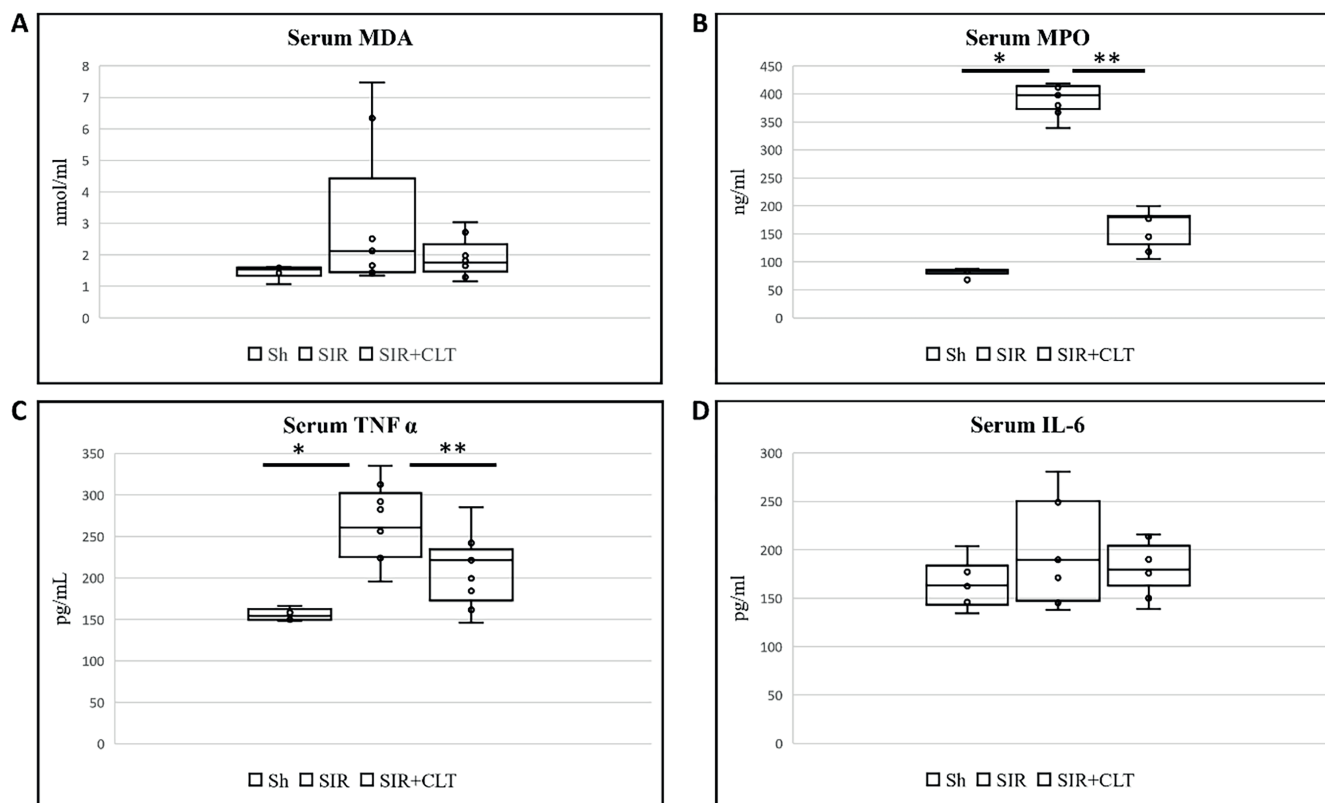
Fig. 1. A. MDA – serum malondialdehyde; B. MPO – serum myeloperoxidase; C. TNF-α –serum tumor necrosis factor alpha; D. IL-6 – serum interleukin 6; Sh – sham; SIR –shock+ischemia/reperfusion; SIR+CLT – SIR+clotrimazole. Boxes show median and interquartile range (IQR) (25–75 percentiles), and the end of whiskers show min–max values; data are presented using the Kruskal–Wallis test. Post hoc analysis within subgroups was assessed with the Dunn's test and Bonferroni adjustment

* p < 0.001 for serum MPO and p = 0.001 for serum TNF-α when comparing Sh and SIR groups; ** p = 0.021 for serum MPO and p = 0.003 for serum TNF-α when comparing SIR and SIR+CLT groups.

values were significantly higher in the SIR group compared to the Sh (Dunn's test statistic = −13.556; adj. p < 0.001) and SIR+CLT groups (Dunn's test statistic = 12.400; p < 0.003).

There were no statistically significant differences between the levels of serum IL-6 across Sh, Sh+PEG and Sh+CLT groups (Kruskal–Wallis test H-statistic = 0.246, df = 2; p = 0.884), and Sh, SIR and SIR+CLT groups (Kruskal–Wallis test H-statistic = 1.960, df = 2; p = 0.375).

Ischemia-modified albumin is a marker that shows tissue hypoxia. It is sensitive to ischemia but not specific to any particular tissue. There were no statistically significant differences between the levels of serum IMA across Sh, Sh+PEG and Sh+CLT groups (Kruskal–Wallis test H-statistic = 0.667, df = 2; p = 0.717), but there was a significant difference between Sh, SIR and SIR+CLT groups (Kruskal–Wallis test H-statistic = 6.529, df = 2; p < 0.04). Serum IMA was higher among the SIR group than the Sh group (Dunn's test statistic = −9.333; adj. p < 0.04).

Upon examination of arterial blood gases, it was observed that both metabolic and respiratory acidosis developed in the SIR and SIR+CLT groups, in comparison to the sham groups (Table 3).

There were no statistically significant differences between the levels of PH across Sh, Sh+PEG and Sh+CLT groups (Kruskal–Wallis test statistics = 2.783, df = 2; p = 0.249). Still, there was a significant difference between Sh, SIR and SIR+CLT (Kruskal–Wallis test H-statistic = 14.537, df = 2; p < 0.001). The PH in SIR group was significantly lower than in the Sh (Dunn's test statistic = 13.722; adj. p < 0.001) and SIR+CLT groups (Dunn's test statistic = −8.333; adj. p < 0.04).

There were no statistically significant differences between the levels of PaO_2 across Sh, Sh+PEG and Sh+CLT groups (Kruskal–Wallis test H-statistic = 2.321, df = 2; p = 0.994), and Sh and SIR groups. There were no statistically significant differences in the level of $PaCO_2$ across Sh, Sh+PEG and Sh+CLT groups (Kruskal–Wallis test H-statistic = 0.012, df = 2; p = 0.313), and across Sh, SIR and SIR+CLT groups (Kruskal–Wallis test H-statistic = 1.913, df = 2; p = 0.384).

There were no statistically significant differences regarding the level of HCO_3 across Sh, Sh+PEG and Sh+CLT groups (Kruskal–Wallis test H-statistic = 0.672, df = 2; p = 0.714), but there was a significant difference between Sh, SIR and SIR+CLT groups (Kruskal–Wallis test H-statistic = 12.742, df = 2; p = 0.002). The HCO_3 in the SIR group was significantly lower than in the Sh group (Dunn's test statistic = 13.278; adj. p = 0.001).

96

Z. Pulathan et al. Clotrimazole protects against lung injury

Table 3. Arterial blood gas values in all groups

Parameters median (IQR)	Sh (n = 6)	Sh+CLT (n = 6)	Sh+PEG (n = 6)	SIR (n = 9)	SIR+CLT (n = 9)
pH	7.37 (0.05)	7.40 (0.17)	7.43 (0.07)	7.26 (0.18)[a]	7.34 (0.06)
PaO_2	99.60 (25.00)	90.95 (38.70)	103.90 (13.80)	104.00 (20.10)	115.40 (37.40)
$PaCO_2$	41.75 (9.30)	44.05 (21.00)	42.20 (13.70)	37.00 (10.70)	38.00 (15.20)
HCO_3 [mEq/L]	25.75 (2.40)	27.00 (11.50)	25.30 (7.60)	13.60 (8.00)[b]	19.40 (50.30)
BE [mmol/L]	0.90 (2.30)	2.30 (3.30)	1.15 (3.00)	−13.30 (9.80)[b]	−6.00 (6.60)

PaO_2 – arterial partial oxygen pressure; $PaCO_2$ – arterial partial pressure of carbon dioxide; HCO_3 – bicarbonate; BE – base excess; Sh – sham; CLT – clotrimazole; PEG – polyethylene glycol; SIR – shock+ischemia/reperfusion. Values are given as median (interquartile range (IQR)). Data are presented using the Kruskal–Wallis test. Post hoc analysis within subgroups was tested with the Dunn's test and Bonferroni adjustment; [a] p < 0.05 compared the results between SIR – Sh and SIR – SIR+CLT, [b] p < 0.05 compared the results between Sh and SIR.

Table 4. Lung tissue findings in all groups

Parameters median (IQR)	Sh (n = 6)	Sh+CLT (n = 6)	Sh+PEG (n = 6)	SIR (n = 9)	SIR+CLT (n = 9)
MDA [nmol/mL]	465.59 (70.56)[a]	455.37 (82.04)	479.95 (137.54)	631.81 (95.15)	582.47 (83.10)
MPO [ng/mL]	5361.32 (703.77)	5780.96 (538.36)	5273.26 (264.63)	6626.55 (812.59)[b]	5659.79 (857.31)
Wet/dry weight ratio	2.48 (0.37)	2.26 (0.32)	2.30 (0.64)	5.47 (1.08)[b]	3.76 (0.87)[b]
Lung injury score	0.50 (1.00)	1.00 (1.00)[c]	1.00 (0.00)	3.00 (1.00)[d]	2.00 (2.00)

MDA – malondialdehyde; MPO – myeloperoxidase; Sh – sham; CLT – clotrimazole; PEG – polyethylene glycol; SIR – shock+ischemia/reperfusion. Values are given as median (interquartile range (IQR)). Data are presented using the Kruskal–Wallis test. Post hoc analysis within subgroups was tested with the Dunn's test and Bonferroni adjustment. [a] p < 0.05 compared the results between Sh – SIR and Sh – SIR+CLT; [b] p < 0.05 compared the results between SIR-Sh and SIR-SIR+CLT; [c] p < 0.05 compared the results between Sh and Sh+CLT; [d] p < 0.05 compared the results between Sh and SIR.

There were no statistically significant differences concerning base excess (BE) levels across Sh, Sh+PEG and Sh+CLT groups (Kruskal–Wallis test H-statistic = 1.770, df = 2; p = 0.413). Still, there was a significant difference between Sh, SIR and SIR+CLT groups (Kruskal–Wallis test H-statistic = 15.676, df = 2; p < 0.001). The BE in the SIR group was significantly lower than in the Sh group (Dunn's test statistic = 14.677; adj. p < 0.001).

Lung tissue

Biochemical results, lung injury score and wet/dry ratio in lung tissue are shown in Table 4 and Fig. 2.

There were no statistically significant differences between the levels of lung tissue MDA across Sh, Sh+PEG and Sh+CLT groups (Kruskal–Wallis test H-statistic = 0.152, df = 2; p = 0.927), but there was a significant difference between Sh, SIR and SIR+CLT groups (Kruskal–Wallis test H-statistic = 13.548, df = 2; p < 0.001). The lung tissue MDA in the Sh group was significantly lower than in the SIR group (Dunn's test statistic = −13.278; adj. p < 0.001) and in the SIR+CLT group (Dunn's test statistic = −10.722; adj. p < 0.02). There were no statistically significant differences between the levels of lung tissue MPO across Sh, Sh+PEG and Sh+CLT groups (Kruskal–Wallis test H-statistic = 2.889, df = 2; p = 0.236) but there was a significant difference between Sh, SIR and SIR+CLT groups (Kruskal–Wallis test H-statistic = 11.382, df = 2; p = 0.003). The lung tissue MPO in the SIR group was significantly higher than in the Sh group (Dunn's test

statistic = −11.333; adj. p = 0.007) and in the SIR+CLT group (Dunn's test statistic = 8.889; adj. p < 0.03).

Histopathological findings of lung injury in the experimental groups are presented in Fig. 3. Diffuse alveolar edema, intra-alveolar and inter-alveolar hemorrhage, and neutrophil infiltration were observed in the SIR group. There were significant differences between the levels of lung injury scores across Sh, Sh+PEG and Sh+CLT groups (Kruskal–Wallis test H-statistic = 6.611, df = 2; p = 0.037), and Sh, SIR and SIR+CLT groups (Kruskal–Wallis test H-statistic = 13.158, df = 2; p < 0.001). The lung injury scores in the Sh+CLT group (Dunn's test statistic = −6.250; adj. p = 0.045) and in the SIR group (Dunn's test statistic = −13.056; adj. p < 0.001) were significantly higher than in the Sh and SIR+CLT groups (p = 0.011). There were no statistically significant differences between the levels of weight/dry weight ratio across Sh, Sh+PEG and Sh+CLT groups (Kruskal–Wallis test H-statistic = 2.279, df = 2; p = 0.320), but there was a significant difference between Sh, SIR and SIR+CLT groups (Kruskal–Wallis test H-statistic = 19.604, df = 2; p < 0.001). The weight/dry weight ratio in the SIR group was significantly higher than in the Sh group (Dunn's test statistic = −16.222; adj. p < 0.001) and in the SIR+CLT group (Dunn's test statistic = 8.889; adj. p < 0.03).

Discussion

The surgical treatment of RAAA involves 2 essential processes. The 1st is the "hypovolemic shock" phase caused
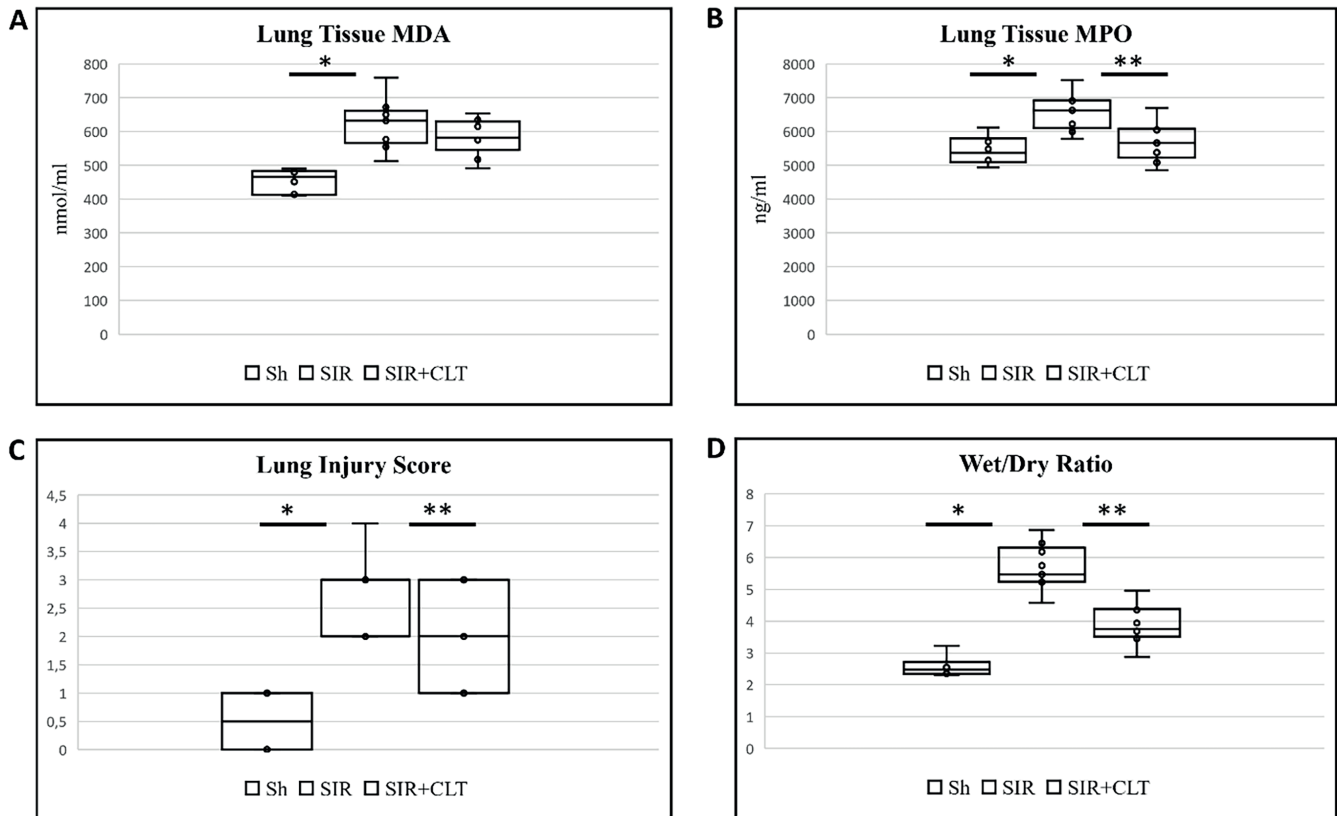
Fig. 2. A. MDA – lung tissue malondialdehyde; B. MPO – lung tissue myeloperoxidase; C. lung injury score; D. Wet/dry ratio in sham (Sh), shock+ischemia/reperfusion (SIR) and SIR+clotrimazole (SIR+CLT) groups. Boxes show median and interquartile range (IQR) (25–75 percentiles), and the end of whiskers show min–max values; data are presented using the Kruskal–Wallis test. Post hoc analysis within subgroups was evaluated with the Dunn's test and Bonferroni adjustment

*p = 0.001 for lung tissue MDA; *p = 0.007 for lung tissue MPO; *p = 0.001 for lung injury score, and *p < 0.001 for wet/dry ratio when comparing Sh and SIR groups; **p = 0.023 for lung tissue MPO; **p = 0.011 for lung injury score; **p = 0.021 for wet/dry ratio when comparing SIR and SIR+CLT groups.
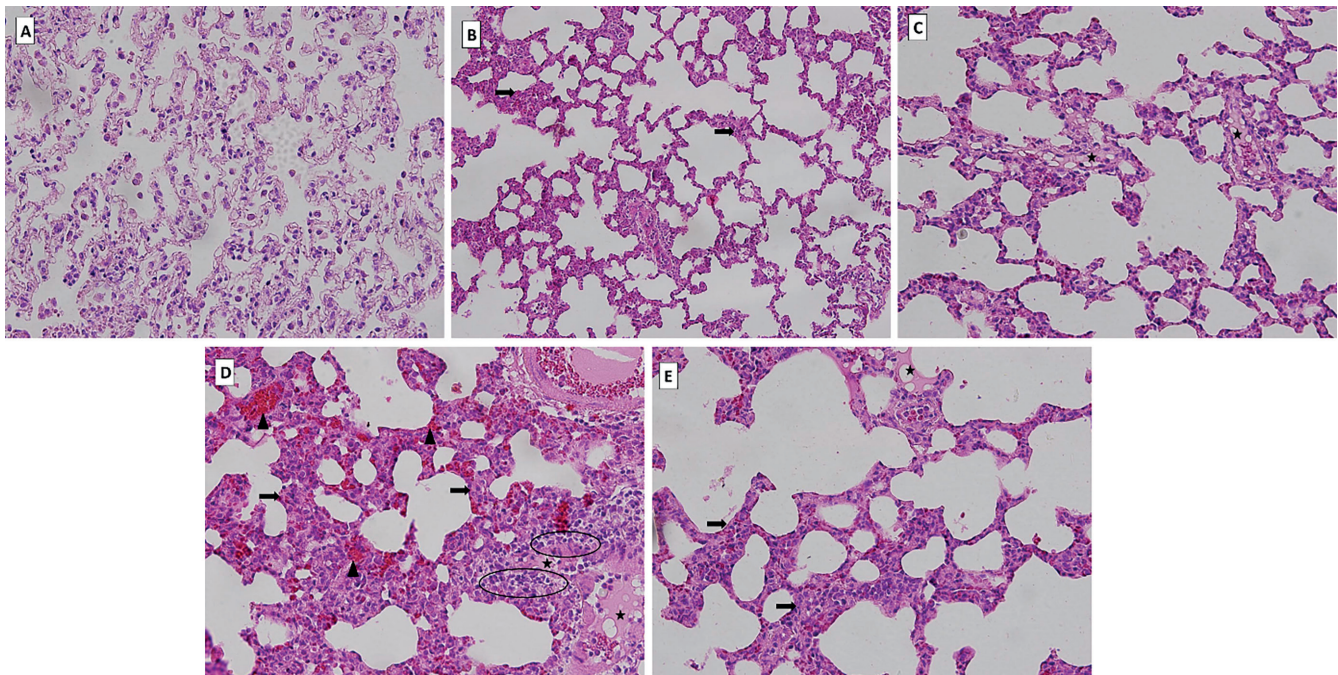
Fig. 3. Histopathological changes of lung tissues in groups. A. Sham (Sh) group; B. Sham+ clotrimazole (Sh+CLT) group; C. Sham+polyethylene glycol (Sh+PEG) group; D. Shock+ischemia/reperfusion (SIR) group; E. SIR+CLT group. Normal histopathological finding in the Sh group. Localized thickening of the alveolar epithelium (arrow) in the Sh+CLT group. There is a small amount of interalveolar edema (star) in the Sh+PEG group. Diffuse alveolar edema (star), intra-alveolar and inter-alveolar hemorrhage (arrowhead), neutrophil infiltration (ellipse), and epithelial thickening (arrow) in the SIR group. Moderate intraalveolar edema (star) and alveolar epithelial thickening (arrow) in the SIR+CLT group (hematoxylin & eosin (H&E) ×200).

by aortic rupture, resulting in total body hypoperfusion. The 2nd is the "clamp" phase, which is the most critical part of the surgical treatment and leads to lower body ischemia.[19] Temporary clamping of the aorta or its major visceral branches at the infradiaphragmatic segment can cause damage to organs that are directly exposed to ischemia, including the bowel and kidney, and to the distant target organs, particularly the lungs.[7] Total body hypoperfusion due to hemorrhagic shock or lower body ischemia due to aortic clamping alone does not cause sufficient organ damage and increased mortality.[6,23–25] Due to these 2 crucial ischemic conditions and subsequent reperfusion in RAAA operations, mortality remains high, and multiple organ failures occur.[5,7] Although many physiopathological factors that cause shock and I/R injury are considered, the main factor is free oxygen radicals that appear in the reperfusion phase. The main source of free radicals that are held responsible for reperfusion injury are neutrophils that are activated both in shock and in ischemia and reperfusion phases.[6,8,26] The systemic inflammatory effects of neutrophils cause varying degrees of damage to many organs and tissues.[7] The lungs have a very capacious endothelial surface due to the pulmonary capillary bed. After reperfusion of ischemic tissues, the pulmonary capillary bed acts as a filter. Platelet microaggregates formed during vascular stasis are retained in the lungs after reperfusion. Following the adhesion of neutrophils to the lung endothelium, proteolytic enzymes and free oxygen radicals are released, and lung damage develops accordingly.[27,28] The severity of lung failure varies depending on the duration, severity of the hemorrhagic shock and the patient's lung reserves.

In our study, we examined lung injury and the effect of CLT on this injury in the RAAA model, where shock and ischemia/reperfusion can be simulated together. We determined serum MDA, MPO, TNF-α, IMA levels, and lung tissue MDA and MPO levels. In addition to biochemical analyses, we evaluated the lung damage by examining the lung tissue histopathologically; we also examined the rats for pulmonary edema using wet/dry weight ratios calculation.

Serum and lung tissue MDA values are an important test showing lipid peroxidation and, therefore, the presence of free oxygen radicals. Although lung damage and lipid peroxidation occurred in the SIR group, the MDA value change was insignificant. Usul et al. found a significant decrease in MDA values in the medulla spinalis tissue after aortic I/R in rats given CLT.[29] We used CLT in similar doses, but both our experimental model and the tissues we examined were different. In our model, more oxygen radicals have been formed, and the drug might have failed to suppress this, or the transition of CLT to the medulla spinalis tissue might have been different. This suggests additional experimental work is needed in this regard.

Clotrimazole suppresses neutrophil activation in the systemic circulation and lung tissue, the most crucial distant organ. Thapa et al. stated that in the experimental colitis

model, tissue MPO activity decreased in the CLT group and approached the control group at a dose of 50 mg/kg compared to 10 mg/kg.[16] Cekic et al. showed that the concentration of MPO in the lung and pancreas tissue of rats with necrotizing pancreatitis decreased significantly in the CLT group.[30] Wilson et al. showed that CLT reduces neutrophil cell infiltration in candida-infected vaginal cell cultures, thus inhibiting the production of proinflammatory cytokines, especially IL-8.[31] There is no evidence that CLT suppresses neutrophil activation in both the systemic circulation and the distant organ. Our study is the first in this regard.

Tumor necrosis factor alpha is a proinflammatory cytokine and a potent chemoattractant. Liu et al. showed that transmembrane peripheral blood leukocytes inhibit TNF-α in lung damage caused by lipopolysaccharide and function as a protective agent through its anti-inflammatory effect.[32] In our study, TNF-α values decreased significantly in the SIR+CLT group compared to the SIR group. This showed that CLT significantly suppresses the systemic inflammatory response. Our findings are compatible with other studies. Thapa et al. showed that CLT inhibited the NF-κB-dependent cytokines TNF-α and IL-8 in vivo and in vitro, ameliorating inflammation and abnormal angiogenesis in an experimental colitis model.[16] They also demonstrated that CLT dose-dependently inhibited the expression of TNF-α-induced adhesion molecules and angiogenesis in vivo in the chorioallantoic membrane (CAM) model, inhibiting ROS production and NF-kB translocation, thereby reducing inflammation in CAM tissue.[33] In an in vitro study with cardiac myocytes, Roberge et al. showed that CLT inhibits TNF-α and prevents the death of cardiomyocyte cells by inhibiting the TRPM2 channel.[34] TRPM2 is a Ca^{2+}-permeable cationic channel of the transient receptor potential (TRP) superfamily linked to apoptotic signaling.[35]

Studies have shown that IMA increases due to hypoxia or I/R, sepsis, acute infection, and advanced cancer.[36,37] However, in our research, the IMA value did not decrease significantly in the group receiving CLT. This is the same characteristic as serum MDA values. With these findings, we can conclude that CLT does not show a prominent antioxidant property.

Interleukin 6 is a soluble mediator with pleiotropic effects on inflammation, immune response and hematopoiesis.[38] It initiates and stimulates oxidation in neutrophils and increases ICAM-1 release from endothelial cells and endothelial permeability. Shields and Waldow et al. used IL-6 as a marker in their experimental studies and showed the changes in IL-6 levels with the methods they applied.[39,40] Harkin et al. demonstrated the severity of lung injury with IL-6 levels in a similar experimental study.[23] Swartbol et al. demonstrated that IL-6 reaches peak values between 6 h and 7 days after surgery in different case series during surgical and endovascular treatment of non-RAAAs and RAAAs.[41] Makar et al. found that IL-6 levels were significantly higher in patients with RAAA who

underwent open surgery than those who received endovascular therapy. They showed that they decreased after the 5th day in both groups.[42] The fact that IL-6 levels did not decrease significantly in the SIR+CLT group in our study can be explained by the higher release of IL-6 in the reperfusion phase. The 2-hour reperfusion time in our study may have needed to be increased to show this change.

In the blood gas analysis, significant metabolic and respiratory acidosis developed in the SIR groups. Confirming significant lung damage, this unfortunately did not improve significantly in CLT-treated rats. This situation can also be explained by the spontaneous breathing of the rats and the lack of use of buffering drugs. Also, the reperfusion time of 120 min might have been adequate. Clotrimazole is known to be a CYP2 and TRPM2 channel inhibitor. Shimizu et al. demonstrated the protective effect of CLT as a specific TRMP2 channel inhibitor in experimental focal cerebral ischemia.[43] Studies showing the efficacy of CLT in shock or I/R are needed.

According to our results, when the groups were compared regarding parameters such as histopathological samples, lung injury score and wet/dry weight ratio, the damage that can lead to ARDS in the postoperative period in patients with RAAA, such as alveolar edema, epithelial thickening, alveolar hemorrhage, and leukocyte infiltration seen in the SIR group, was significantly reduced by CLT. Unfortunately, we could not find any other in vivo experimental shock or I/R study that investigated the inhibitory effect of CLT to compare with our findings. The effect of CLT on EETs catalyzed by cytochrome P450 epoxygenases has not been investigated. Examining this pathway may be a good step to see the effects of CLT on blood pressure, pulmonary vascular bed and endothelial functions.[15]

Limitations

In this study, we tried to investigate the protective effect of CLT on lung injury of shock and I/R through inflammation, oxidation and NF-kB-dependent cytokine pathways. It will be more enlightening to show whether CYP2 and TRPM2 channel inhibition are effective in the activity of CLT.

Conclusions

In our study, significant tissue damage occurred in the RAAA model in which hemorrhagic shock, aortic ischemia and reperfusion were simulated together, resulting in substantial pulmonary edema. This damage was significantly reduced when treated with CLT. The administration of CLT provided effective suppression of both systemic and local inflammatory responses, as well as neutrophil infiltration, thereby mitigating lung damage in a rat model of experimental RAAA.

Data availability

The datasets generated and/or analyzed during the current study are available from the corresponding author on reasonable request.

Consent for publication

Not applicable.

ORCID iDs

Zerrin Pulathan https://orcid.org/0000-0002-3317-9970
Şaban Murat Ergene https://orcid.org/0000-0003-1806-3168
Gökalp Altun https://orcid.org/0000-0003-1116-6594
Esin Yuluğ https://orcid.org/0000-0002-8857-9234
Ahmet Menteşe https://orcid.org/0000-0003-2036-5317

References

1. Wanhainen A, Verzini F, Van Herzeele I, et al. Editor's Choice: European Society for Vascular Surgery (ESVS) 2019 Clinical Practice Guidelines on the Management of Abdominal Aorto-iliac Artery Aneurysms. *Eur J Vasc Endovasc Surg*. 2019;57(1):8–93. doi:10.1016/j.ejvs.2018.09.020
2. Bown MJ, Nicholson ML, Bell PRF, Sayers RD. The systemic inflammatory response syndrome, organ failure, and mortality after abdominal aortic aneurysm repair. *J Vasc Surg*. 2003;37(3):600–606. doi:10.1067/mva.2003.39
3. Edwards ST, Schermerhorn ML, O'Malley AJ, et al. Comparative effectiveness of endovascular versus open repair of ruptured abdominal aortic aneurysm in the Medicare population. *J Vasc Surg*. 2014;59(3):575–582.e6. doi:10.1016/j.jvs.2013.08.093
4. Stilo F, Catanese V, Nenna A, et al. Biomarkers in EndoVascular Aneurysm Repair (EVAR) and abdominal aortic aneurysm: Pathophysiology and clinical implications. *Diagnostics*. 2022;12(1):183. doi:10.3390/diagnostics12010183
5. Wu MY, Yiang GT, Liao WT, et al. Current mechanistic concepts in ischemia and reperfusion injury. *Cell Physiol Biochem*. 2018;46(4):1650–1667. doi:10.1159/000489241
6. Adam DJ, Lee AJ, Ruckley CV, Bradbury AW, Ross JA. Elevated levels of soluble tumor necrosis factor receptors are associated with increased mortality rates in patients who undergo operation for ruptured abdominal aortic aneurysm. *J Vasc Surg*. 2000;31(3):514–519. PMID:10709065.
7. Zhaosheng J, Ka C, Daqing M. Perioperative "remote" acute lung injury: Recent update. *J Biomed Res*. 2017;31(3):197. doi:10.7555/JBR.31.20160053
8. Ferrari RS, Andrade CF. Oxidative stress and lung ischemia–reperfusion injury. *Oxid Med Cell Longev*. 2015;2015:590987. http://www.hindawi.com/journals/omcl/2015/590987 Accessed June 15, 2023.
9. Uno T, Wada K, Matsuda S, et al. Effects of clotrimazole on tacrolimus pharmacokinetics in patients with heart transplants with different *CYP3A5* genotypes. *Eur J Clin Pharmacol*. 2019;75(1):67–75. doi:10.1007/s00228-018-2558-6
10. Iannelli A, De Sousa G, Zucchini N, Saint-Paul MC, Gugenheim J, Rahmani R. Anti-apoptotic pro-survival effect of clotrimazole in a normothermic ischemia reperfusion injury animal model. *J Surg Res*. 2011;171(1):101–107. doi:10.1016/j.jss.2010.03.035
11. Bartolommei G, Tadini-Buoninsegni F, Hua S, Moncelli MR, Inesi G, Guidelli R. Clotrimazole inhibits the Ca^{2+}-ATPase (SERCA) by interfering with Ca^{2+} binding and favoring the E2 conformation. *J Biol Chem*. 2006;281(14):9547–9551. doi:10.1074/jbc.M510550200
12. Crowley PD, Gallagher HC. Clotrimazole as a pharmaceutical: Past, present and future. *J Appl Microbiol*. 2014;117(3):611–617. doi:10.1111/jam.12554
13. Lee DU, Ji MJ, Kang JY, Kyung SY, Hong JH. Dust particles-induced intracellular Ca^{2+} signaling and reactive oxygen species in lung fibroblast cell line MRC5. *Korean J Physiol Pharmacol*. 2017;21(3):327. doi:10.4196/kjpp.2017.21.3.327

14. Liu JY, Yang J, Inceoglu B, et al. Inhibition of soluble epoxide hydrolase enhances the anti-inflammatory effects of aspirin and 5-lipoxygenase activation protein inhibitor in a murine model. *Biochem Pharmacol*. 2010;79(6):880–887. doi:10.1016/j.bcp.2009.10.025

15. Shi Z, He Z, Wang DW. CYP450 epoxygenase metabolites, epoxyeicosatrienoic acids, as novel anti-inflammatory mediators. *Molecules*. 2022;27(12):3873. doi:10.3390/molecules27123873

16. Thapa D, Lee JS, Park SY, et al. Clotrimazole ameliorates intestinal inflammation and abnormal angiogenesis by inhibiting interleukin-8 expression through a nuclear factor-κB-dependent manner. *J Pharmacol Exp Ther*. 2008;327(2):353–364. doi:10.1124/jpet.108.141887

17. Miller BA, Wang J, Song J, et al. Trpm2 enhances physiological bioenergetics and protects against pathological oxidative cardiac injury: Role of Pyk2 phosphorylation. *J Cell Physiol*. 2019;234(9):15048–15060. doi:10.1002/jcp.28146

18. Kilkenny C, Browne WJ, Cuthill IC, Emerson M, Altman DG. Improving bioscience research reporting: The ARRIVE Guidelines for Reporting Animal Research. *PLoS Biol*. 2010;8(6):e1000412. doi:10.1371/journal.pbio.1000412

19. Lindsay TF, Walker PM, Romaschin A. Acute pulmonary injury in a model of ruptured abdominal aortic aneurysm. *J Vasc Surg*. 1995;22(1):1–8. doi:10.1016/S0741-5214(95)70081-1

20. Yagi K. Assay for blood plasma or serum. *Methods Enzymol*. 1984;105:328–331. doi:10.1016/S0076-6879(84)05042-4

21. Bar-Or D, Curtis G, Rao N, Bampos N, Lau E. Characterization of the Co^{2+} and Ni^{2+} binding amino-acid residues of the N-terminus of human albumin: An insight into the mechanism of a new assay for myocardial ischemia. *Eur J Biochem*. 2001;268(1):42–48. doi:10.1046/j.1432-1327.2001.01846.x

22. Uchiyama M, Mihara M. Determination of malonaldehyde precursor in tissues by thiobarbituric acid test. *Anal Biochem*. 1978;86(1):271–278. doi:10.1016/0003-2697(78)90342-1

23. Harkin DW, Marron CD, Rother RP, Romaschin A, Rubin BB, Lindsay TF. C5 complement inhibition attenuates shock and acute lung injury in an experimental model of ruptured abdominal aortic aneurysm. *Br J Surg*. 2005;92(10):1227–1234. doi:10.1002/bjs.4938

24. Ozan Karakişi S, Hemşinli D, Tümkaya L, Ergene Ş, Mercantepe T, Yılmaz A. Resveratrol against lung injury in an ischemia/reperfusion model of abdominal aortic rupture. *Turk Gogus Kalp Damar Cerrahisi Derg*. 2021;29(3):330–338. doi:10.5606/tgkdc.dergisi.2021.21737

25. Faria I, Thivalapill N, Makin J, Puyana JC, Raykar N. Bleeding, hemorrhagic shock, and the global blood supply. *Crit Care Clin*. 2022;38(4):775–793. doi:10.1016/j.ccc.2022.06.013

26. Den Hengst WA, Gielis JF, Lin JY, Van Schil PE, De Windt LJ, Moens AL. Lung ischemia-reperfusion injury: A molecular and clinical view on a complex pathophysiological process. *Am J Physiol Heart Circ Physiol*. 2010;299(5):H1283–H1299. doi:10.1152/ajpheart.00251.2010

27. Matthay MA, Zemans RL, Zimmerman GA, et al. Acute respiratory distress syndrome. *Nat Rev Dis Primers*. 2019;5(1):18. doi:10.1038/s41572-019-0069-0

28. Laubach VE, Sharma AK. Mechanisms of lung ischemia–reperfusion injury. *Curr Opin Organ Transplant*. 2016;21(3):246–252. doi:10.1097/MOT.0000000000000304

29. Usul H, Arslan E, Cansever T, Cobanoglu U, Baykal S. Effects of clotrimazole on experimental spinal cord ischemia/reperfusion injury in rats. *Spine (Phila Pa 1976)*. 2008;33(26):2863–2867. doi:10.1097/BRS.0b013e3181906e6d

30. Cekic AB, Alhan E, Usta A, Türkyılmaz S, Kural BV, Erçin C. Effects of clotrimazol on the acute necrotizing pancreatitis in rats. *Inflammation*. 2013;36(6):1576–1583. doi:10.1007/s10753-013-9702-3

31. Wilson D, Hebecker B, Moyes DL, et al. Clotrimazole dampens vaginal inflammation and neutrophil infiltration in response to *Candida albicans* infection. *Antimicrob Agents Chemother*. 2013;57(10):5178–5180. doi:10.1128/AAC.01244-13

32. Liu X, Jiang Y, Chen B, Qiu X, He S. Effects of membrane-type PBLs on the expression of TNF-α and IL-2 in pulmonary tissue of SD rats after LPS-induced acute lung injury. *Adv Clin Exp Med*. 2022;32(1):71–79. doi:10.17219/acem/152739

33. Thapa D, Lee JS, Park MA, et al. Inhibitory effects of clotrimazole on TNF-α-induced adhesion molecule expression and angiogenesis. *Arch Pharm Res*. 2009;32(4):593–603. doi:10.1007/s12272-009-1416-6

34. Roberge S, Roussel J, Andersson DC, et al. TNF-mediated caspase-8 activation induces ROS production and TRPM2 activation in adult ventricular myocytes. *Cardiovasc Res*. 2014;103(1):90–99. doi:10.1093/cvr/cvu112

35. Sumoza-Toledo A, Penner R. TRPM2: A multifunctional ion channel for calcium signalling. *J Physiol*. 2011;589(7):1515–1525. doi:10.1113/jphysiol.2010.201855

36. Güney T, Kocman AE, Ozatik O, Akyüz F. The effect of fucoidin on kidney and lung injury in a rat infrarenal aortic ischemia–reperfusion model. *Perfusion*. 2022;37(2):198–207. doi:10.1177/0267659120982839

37. Eroğlu O, Türkmen S, Menteşe A, et al. The diagnostic value of ischemia-modified albumin in the diagnosis of aortic pathology. *Turk J Med Sci*. 2014;44:62–67. doi:10.3906/sag-1206-94

38. Tanaka T, Narazaki M, Kishimoto T. IL-6 in inflammation, immunity and disease. *Cold Spring Harb Perspect Biol*. 2014;6(10):a016295. doi:10.1101/cshperspect.a016295

39. Shields CJ. Hypertonic saline infusion for pulmonary injury due to ischemia–reperfusion. *Arch Surg*. 2003;138(1):9–14. doi:10.1001/archsurg.138.1.9

40. Waldow T, Alexiou K, Witt W, et al. Protection against acute porcine lung ischemia/reperfusion injury by systemic preconditioning via hind limb ischemia. *Transplant Int*. 2005;18(2):198–205. doi:10.1111/j.1432-2277.2004.00005.x

41. Swartbol P, Truedsson L, Norgren L. The inflammatory response and its consequence for the clinical outcome following aortic aneurysm repair. *Eur J Vasc Endovasc Surg*. 2001;21(5):393–400. doi:10.1053/ejvs.2001.1352

42. Makar RR, Badger SA, O'Donnell ME, et al. The inflammatory response to ruptured abdominal aortic aneurysm is altered by endovascular repair. *Int J Vasc Med*. 2013;2013:482728. doi:10.1155/2013/482728

43. Shimizu T, Dietz RM, Cruz-Torres I, et al. Extended therapeutic window of a novel peptide inhibitor of TRPM2 channels following focal cerebral ischemia. *Exp Neurol*. 2016;283:151–156. doi:10.1016/j.expneurol.2016.06.015

Penehyclidine hydrochloride alleviates LPS-induced inflammatory responses and oxidative stress via ROS/Nrf2/HO-1 activation in RAW264.7 cells

Qiongmei Guo[1,A–F], Chunyan Zhang[2,3,B–D,F], Jingui Gao[4,A,C,F], Wenjing Shi[4,A–C,F], Xiaozhi Liu[3,5,B–D,F]

[1] Department of Anesthesiology, The First Hospital of Hebei Medical University, Shjiazhuang, China

[2] Medical Research Center, The 5th Center Hospital of Tianjin, China

[3] Tianjin Key Laboratory of Epigenetic for Organ Development of Preterm Infants, The 5th Center Hospital of Tianjin, China

[4] Department of Anesthesiology, The Second Hospital of Hebei Medical University, Shjiazhuang, China

[5] Pediatric Center, The 5th Center Hospital of Tianjin, China

A – research concept and design; B – collection and/or assembly of data; C – data analysis and interpretation;
D – writing the article; E – critical revision of the article; F – final approval of the article

Address for correspondence
Jingui Gao
E-mail: gjingui@126.com

Abstract

Background. Inflammation is a biological response of the immune system to harmful stimuli. Penehyclidine hydrochloride (PCH) can alleviate inflammation and oxidative stress by activating reactive oxygen species (ROS), nuclear factor erythroid 2-related factor (Nrf2) and heme oxygenase 1 (HO-1) in animal models, but there is a lack of cellular evidence.

Objectives. This study investigated the effects of PHC on lipopolysaccharide (LPS)-induced inflammation response and oxidative stress in RAW264.7 cells.

Materials and methods. RAW264.7 cells were treated with 1 µg/mL or 5 µg/mL of PHC, with interleukin 6 (IL-6), tumor necrosis factor alpha (TNF-α), IL-1β, and prostaglandin E2 (PGE2) levels measured with enzyme-linked immunosorbent assay (ELISA) and nitric oxide (NO) measured using the Griess test. Reactive oxygen species were examined with flow cytometry and immunofluorescence, and b-related factor 2 (BRF-2) and NAD(P)H-quinone oxidoreductase 1 (NQO1) using western blot.

Results. Penehyclidine hydrochloride partly, but substantially, reversed LPS-related NO and PGE2 production by RAW264.7 cells in a dose-dependent manner and suppressed LPS-induced expression of IL-6, TNF-α and IL-1β messenger ribonucleic acid (mRNA), secretion of IL-6, TNF-α and IL-1β, and ROS production. Lipopolysaccharide stimulation did not affect Nrf2, heme oxygenase 1 (HO-1) or NQO1 protein expression in RWA264.7 cells not treated with PHC. However, PHC treatment significantly elevated Nrf2, HO-1 and NQO1 protein in LPS-treated RWA264.7 cells, an effect that was dose-dependent. The ROS scavenging using N-acetyl-L-cysteine abolished the PHC-induced upregulation of Nrf2 and HO-1.

Conclusions. Penehyclidine hydrochloride may alleviate LPS-induced inflammation and oxidative stress by activating Nrf2 signaling in RAW264.7 macrophages. These findings suggest that PHC could alleviate inflammation by targeting activated macrophages.

Key words: macrophages, inflammation, lipopolysaccharide, oxidative stress, penehyclidine hydrochloride

Background

Inflammation represents a critical biological response of the immune system to harmful stimuli such as pathogenic organisms, injured cells and tissues, toxic molecules, and irradiation.[1] Although inflammation is necessary to the normal healing process by promoting the disposal of injured cells and pathogenic organisms,[2,3] uncontrolled or excessive inflammation can trigger acute and/or chronic damage in multiple organs, leading to disease.[1,4] Inflammation can even promote the growth of tumor cells and cancers.[5] The cytokine storm resulting from acute excessive immune and inflammatory reactions is also involved in the morbidity and mortality of several conditions like sepsis and coronavirus disease-19 (COVID-19).[6,7] Low-grade chronic inflammation is involved in conditions such as type 2 diabetes, obesity and hypertension, and contributes to the development of complications and associated diseases.[8,9]

Uncontrolled inflammation is characterized by the overproduction of pro-inflammatory modulators, including nitric oxide (NO), prostaglandin E2 (PGE2) and cytokines,[10] playing a key role in the pathogenetic mechanisms of various chronic disorders, e.g., cardiovascular diseases, type 2 diabetes, rheumatoid arthritis, and cancers.[11] Therefore, targeting inflammation is a promising avenue for chronic disease prevention and treatment.[11–13]

Inflammation is also involved in neurological and psychiatric disease development and progression.[14–18] There is a functional interplay between the central and autonomic nervous systems, and prefrontal cortex disruption may contribute to irregular behavioral responses, leading to many cognitive dysfunctions common in neurological diseases.[19] In this regard, some anti-inflammatory drugs (e.g., celecoxib and aspirin) or drugs with pleiotropic anti-inflammatory effects (e.g., pioglitazone, statins and minocycline) function in bipolar disorder, major depressive disorder and schizophrenia, given that baseline inflammation is present.[20]

Inflammation is a complex process involving several cell types and mechanisms,[1,21] with macrophages critical in its initiation, maintenance and resolution. Indeed, they can be activated and deactivated by different cytokines produced during inflammatory processes. Activating cytokines and signals include interferon gamma (IFNγ) granulocyte-monocyte colony-stimulating factor, tumor necrosis factor alpha (TNF-α), bacterial lipopolysaccharide (LPS), extracellular matrix proteins, and chemical mediators. On the other hand, deactivating cytokines and signals include interleukin (IL)-10, transforming growth factor beta (TGF-β), and the removal or deactivation of mediators.[22,23]

Oxidative stress contributes significantly to inflammatory reactions observed in chronic disorders,[24] involves cellular damage that can trigger immune cells and processes,[25,26] and occurs when the reactive oxygen species (ROS) exceed antioxidant capacity.[26] Reactive oxygen species are normal by-products of adenosine triphosphate (ATP) production by the mitochondria, but can increase under pathogenic conditions.[27] In addition, some immune cells can produce ROS to destroy pathogens and abnormal cells.[28] Besides consuming antioxidant compounds, several innate antioxidant mechanisms exist in mammals.[29,30]

Nuclear factor erythroid 2-related factor (Nrf2) is a pleiotropic transcription factor that induces defense mechanisms counteracting oxidative stress and inflammation. During oxidative stress, Nrf2 upregulates multiple genes responsible for antioxidant activity, including heme oxygenase 1 (HO-1), which reduces oxidative stress by clearing heme, and NAD(P)H-quinone oxidoreductase 1 (NQO1), that prevents hydroquinone conversion to ROS.[31] Besides its role in oxidative stress, the Nrf2 activation mediates the anti-inflammatory features of some commonly used nonsteroidal anti-inflammatory drugs,[32] suggesting a contribution of Nrf2 in the crosstalk between inflammation and oxidative stress. It can also decrease the transcription of pro-inflammatory cytokines in activated macrophages.[33]

Penehyclidine hydrochloride ($C_{20}H_{29}NO_2$·HCl; PHC) is an anticholinergic drug designed by the Chinese Academy of Military Sciences that exhibits substantial peripheral and central anticholinergic activities by simultaneously binding to the M and N cholinergic receptors.[34] It is widely used in China as a reversal drug for treating organophosphorus poisoning and a pre-anesthetic medication to reduce respiratory secretion and vagus nerve reflex.[35] Penehyclidine hydrochloride also possesses anti-inflammatory and antioxidant properties, demonstrating protective effects on inflammation and oxidative stress-related disorders such as heart ischemia/reperfusion, acute kidney injury and septic shock.[36–38] Furthermore, PHC can attenuate the Toll-like receptors in inflammatory chronic lung diseases[39] and acute lung injury,[40] and has been shown to decrease the postoperative expression of pro-inflammatory cytokines[41] and reduce cerebral injury in models of cardiopulmonary bypass by decreasing inflammation and neuronal apoptosis.[42] Toxicity and adverse events associated with PHC are dry mouth, flushing and dry skin. High doses can cause dizziness, urinary retention, delirium, and elevated body temperature.[35]

Studies have shown that PHC induces Nrf2/HO-1 signaling in acute lung/kidney damage triggered by ischemia/reperfusion or rhabdomyolysis in animal models, along with suppressing ROS and pro-inflammatory cytokine production, e.g., TNF-α, IL-6 and IL-1β.[36,43,44] However, there is still a lack of cellular evidence of Nrf2/HO-1 pathway involvement in the anti-inflammatory and antioxidant activities of PHC.

Activated macrophages are a major source of pro-inflammatory mediators in the development of inflammation,[45] and LPS-stimulated murine RAW264.7 macrophages are widely used in inflammation research.[46]

In this study, we performed dose–response experiments on the anti-inflammatory and antioxidant activities of PHC and the PHC-induced alterations in Nrf2 signaling

in LPS-treated RAW264.7 cells. The study provides cellular evidence of Nrf2 pathway involvement in the anti-inflammatory and antioxidant activities of PHC, serving as a potential therapeutic target for managing inflammatory diseases.

Objectives

This study aimed to investigate the effects of PHC on LPS-induced inflammatory responses and oxidative stress in RAW264.7 cells.

Methods

Cell culture

RAW264.7 cells, provided by The Central Laboratory of Peking University Binhai Hospital (Beijing, China), underwent culture in Dulbecco's modified Eagle's medium (DMEM; Thermo Fisher Scientific, Waltham, USA) containing high glucose, 10% fetal bovine serum (Thermo Fisher Scientific), 100 IU/mL penicillin and 100 IU/mL streptomycin (Solarbio Life Science, Beijing, China), at 37°C with 5% CO_2.

Cell Counting Kit-8 (CCK-8) assay

Cell viability was assessed using Cell Counting Kit-8 (CCK-8; Solarbio Life Science, Beijing, China) as directed by the manufacturer.[47] RAW264.7 cells were cultured in 96-well microplates (Corning Company, Corning, USA) at a density of 5×10^3/well. Cells were serum starved overnight and administered various PHC doses (0, 1, 5, 10, 20, and 40 µg/mL; Jinzhou Aohong Pharmaceutical Industry Co., Ltd., Jinzhou, China) for 24 h. Doses as high as 40 µg/mL have not been reported in the literature previously, and such a wide range of increasing doses was chosen for this study to verify the toxicity of PHC on RAW264.7 cells and provide a basis for dose selection for future studies. The results of cell viability showed that PHC concentrations ranging from 1 µg/mL to 10 µg/mL had no significant effect on RAW264.7 cell viability. Thus, we treated RAW264.7 cells with 1 µg/mL or 5 µg/mL PHC in the subsequent experiments. Cell Counting Kit-8 solution (10 µL) was added to each well, and absorbance (A) was measured at 450 nm after incubation for 1 h at 37°C using an Epoch microplate spectrophotometer (BioTek, Winooski, USA). Cell viability was calculated as (A−A0)/A0 × 100%.

Enzyme-linked immunosorbent assay

RAW264.7 cells underwent culture in 6-well plates at 2.5×10^6/well. After overnight serum starvation, cells were administered 1 µg/mL LPS (O111:B4; #L4391; Sigma-Aldrich, St. Louis, USA) with or without 1 µg/mL or 5 µg/mL PHC

in serum-deprived DMEM for 24 h.[47] Serum-free medium was used as a negative control. The culture medium was collected for measuring IL-6, TNF-α, IL-1β, and PGE2 using specific enzyme-linked immunosorbent assay (ELISA) kits (R&D Systems, Shanghai, China) as directed by the manufacturer.

Nitric oxide measurement using the Griess reagent

RAW264.7 cells underwent the treatments outlined above. Secreted NO concentration was measured using an NO assay kit containing Griess reagent (Beyotime Biotechnology, Shanghai, China) as directed by the manufacturer.[48]

Flow cytometry

Intracellular ROS was assessed using flow cytometry.[49] Cells washed with phosphate-buffered saline (PBS) underwent a 20-min incubation with dichlorofluorescein diacetate (DCFH-DA; 10 µM) at 37°C. Fluorescence intensity was obtained with a DxFLEX flow cytometer (Beckman Coulter, Brea, USA), with FlowJo 10.8.1 (FlowJo LLC, Ashland, USA) used for analysis.

Immunofluorescence staining

Intracellular ROS was detected using DCFH-DA staining.[49] Briefly, RAW264.7 cells underwent a 20-min incubation with DCFH-DA (10 µM) (Reactive Oxygen Species Assay Kit, S0033S; Beyotime Biotechnology) at 37°C, fluorescence was visualized, and images were acquired under a Zeiss LSM 800 confocal laser scanning microscope (Carl Zeiss AG, Jena, Germany).

Quantitative reverse transcription polymerase chain reaction

Total ribonucleic acid (RNA) was isolated with an Eastep® Super RNA extraction kit (Shanghai Promega Biological Products, Shanghai, China) as instructed by the manufacturer.[50] After complementary DNA (cDNA) synthesis, quantitative reverse transcription polymerase chain reaction (qRT-PCR) was carried out with SYBR green and the following primers (Genewitz, South Plainfield, USA):
β-actin,
5'-GTGACGTTGACATCCGTAAAGA-3' (sense) and
5'-GCCGGACTCATCGTACTCC-3' (antisense);
IL-6,
5'-TGATGGATGCTACCAAACTGGA-3' (sense) and
5'-TGTGACTCCAGCTTATCTCTTGG-3' (antisense);
inducible NO synthase (iNOS),
5'-GCGCTCTAGTGAAGCAAAGC-3' (sense) and
5'-GGGATTCTGGAACATTCTGTGC-3' (antisense);
IL-1β,
5'-TGCCACCTTTTGACAGTGATG-3' (sense) and
5'-ATGTGCTGCTGCGAGATTTG-3' (antisense);

104

Q. Guo et al. PHC alleviates inflammation via ROS/Nrf2/HO-1

TNF-α,
5'-CCCTCACACTCACAAACCAC-3' (sense) and
5'-ACAAGGTACAACCCATCGGC-3' (antisense).

The $2^{-\Delta\Delta CT}$ method was utilized for data analysis.

Western blot

RAW264.7 cell lysis used radioimmunoprecipitation assay (RIPA) buffer, with supernatants collected after a 10-min centrifugation at 4°C (12,000 r/min). A bicinchoninic acid assay (BCA) (P0010S; Beyotime Biotechnology) was performed for protein quantitation. Identical quantities of total protein (40 μg) were resolved using 12% sodium dodecyl-sulfate polyacrylamide gel electrophoresis (SDS-PAGE) and transferred onto polyvinylidene fluoride (PVDF) membranes. The specimens were blocked with 5% nonfat milk for 1 h at ambient, followed by overnight incubation with primary antibodies against Nrf2 (1:1,000; #12721S; Cell Signaling Technology (CST), Danvers, USA), HO-1 (1:1,000; #43966S; CST), NQO1 (1:1000; #ab28947; Abcam, Cambridge, UK), GAPDH (1:1,000; #5174S; CST), or β-tubulin (1:1000; #ab18207; Abcam) at 4°C. Next, washing with tris-buffered saline containing 0.1% Tween 20 (TBST) was performed, with subsequent incubation with secondary antibodies for 1 h at ambient temperature. Protein bands were visualized with the enhanced chemiluminescence kit (Advansta, Menlo Park, USA) and analyzed using ImageJ (National Institutes of Health (NIH), Bethesda, USA).

Statistical analyses

The analysis employed GraphPad Prism 9 (GraphPad Software, San Diego, USA), with Fig. 1,2 using 6 data points and Fig. 3,4 using 3 data points. Differences in characteristics between groups were analyzed using the Kruskal–Wallis test with Dunn's post hoc tests, with p < 0.05 indicating statistical significance.

Results

PHC suppressed LPS-associated NO and PGE2 production in RAW264.7 cells

In order to select the appropriate PHC treatment doses, we examined RAW264.7 cell viability after administering diverse PHC concentrations and found that PHC ranging from 1 μg/mL to 10 μg/mL had no marked effects (Fig. 1A and Supplementary Tables 1,2). Thus, the subsequent assays used 1 μg/mL or 5 μg/mL PHC to remain below the toxicity threshold. For evaluating PHC's effect on LPS-related inflammation, RAW264.7 cells were treated with various PHC concentrations in the presence of LPS. Lipopolysaccharide dramatically enhanced NO and PGE2 production by RAW264.7 cells (Fig. 1B,C and Supplementary Tables 3–6). Penehyclidine hydrochloride partly but

substantially reversed LPS-related NO and PGE2 production in a dose-dependent manner, with the same trend observed for iNOS mRNA expression (Fig. 1D and Supplementary Tables 7,8). In addition, compared to untreated round-shaped RAW264.7 cells, LPS-stimulated cells became rod-shaped, bearing pseudopodia. Of note, the morphological alterations were alleviated by PHC treatment dose-dependently (Fig. 1E). The above findings indicated that PHC inhibited LPS-related inflammation in macrophages.

PHC suppressed LPS-induced expression and secretion of pro-inflammatory cytokines in RAW264.7 cells

To assess PHC's effect on LPS-associated inflammation, we determined the expression and secretion of pro-inflammatory cytokines in RAW264.7 cells administered LPS and PHC. As depicted in Fig. 2A–F and Supplementary Tables 9–20, LPS dramatically elevated IL-6, TNF-α and IL-1β mRNA amounts and secretion, and these effects were partially but significantly attenuated by PHC dose-dependently. The above data suggested that PHC suppressed LPS-related inflammation in macrophages.

PHC abrogated LPS-induced ROS production in RAW264.7 cells

In order to examine PHC's effect on LPS-induced oxidative stress, we determined ROS production in RAW264.7 cells administered with LPS and PHC. DCFH-DA-based flow cytometry analysis (Fig. 3A,B and Supplementary Tables 21–23) and immunofluorescence (Fig. 3C,D and Supplementary Tables 24–26) consistently showed that PHC dose-dependently and remarkably abrogated LPS-stimulated ROS production. These data suggested that PHC alleviated LPS-induced oxidative stress in macrophages.

PHC activated Nrf2 signaling in RAW264.7 cells

In order to investigate Nrf2 pathway involvement in PHC's effect in RWA264.7 cells, we determined the protein amounts of Nrf2 and its target genes HO-1 and NQO1 in RWA264.7 cells. As depicted in Fig. 4A,B and Supplementary Tables 27–34, LPS stimulation did not affect the protein expression of Nrf2, HO-1 and NQO1 in cells without PHC. However, PHC treatment significantly elevated Nrf2, HO-1 and NQO1 protein in LPS-treated cells dose-dependently.

We also focused on the effects of the ROS scavenger n-acetyl-l-cysteine (NAC) on PHC-induced Nrf2 and HO-1. Penehyclidine hydrochloride at a concentration of 5 μg/mL significantly upregulated Nrf2 expression, but this was significantly inhibited by NAC. Moreover, PHC at a concentration of 5 μg/mL showed a similar trend in nuclear HO-1 expression, although the difference was not statistically significant, possibly due to limitations
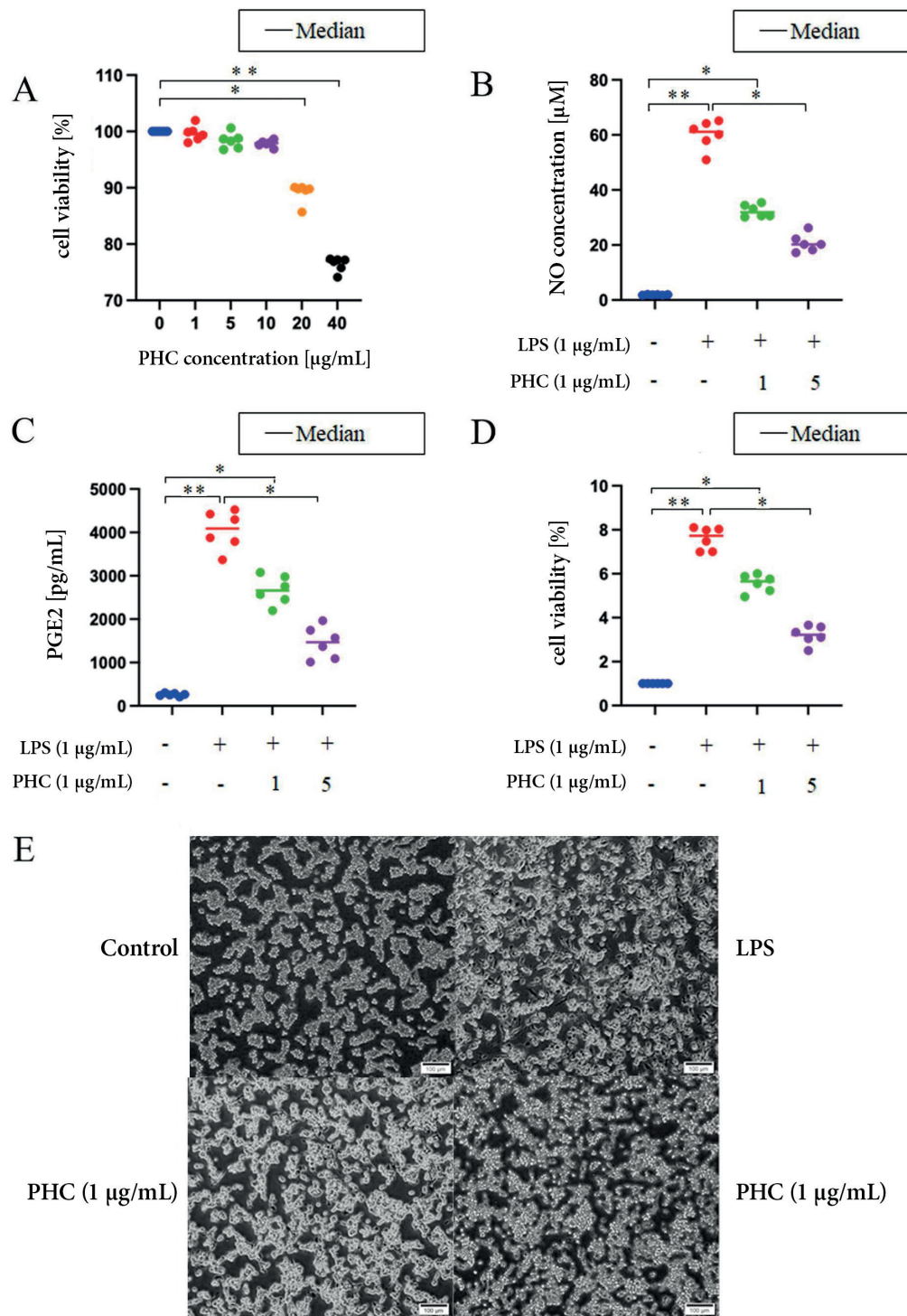
Fig. 1. Penehyclidine hydrochloride (PHC) inhibited lipopolysaccharide (LPS)-induced nitric oxide (NO) and prostaglandin E2 (PEG2) production in RAW264.7 cells. A. RAW264.7 cells were serum starved overnight and administered PHC at various concentrations (0, 1, 5, 10, 20, and 40 μg/mL) for 24 h. Untreated cells were used as a negative control. The Cell Counting Kit-8 (CCK-8) assay was used to determine cell viability. B–E. RAW264.7 cells were administered 1 μg/mL LPS alone or in combination with 1 μg/mL or 5 μg/mL PHC for 24 h. Nitric oxide (B) and PGE2 (C) were measured in the cell culture medium. Quantitative reverse transcription polymerase chain reaction (qRT-PCR) was conducted to determine the messenger ribonucleic acid (mRNA) expression of inducible nitric oxide synthase (iNOS) (D) in RAW264.7 cells. Cell morphology (E) was observed under a bright-field microscope at ×10 magnification. Data are mean ± standard deviation (mean ± SD)

$*p < 0.05$; $**p < 0.01$ ($n = 6$). Differences in characteristics between groups were analyzed using the Kruskal–Wallis test with Dunn's post hoc test.

in sample size. These findings suggest that the activation of Nrf2/HO-1 in macrophages by PHC is associated with ROS (Fig. 4C and Supplementary Tables 35–40).

Discussion

This study showed that PHC could reverse LPS-related NO and PGE2 production in RAW264.7 cells. PHC also suppressed LPS-induced IL-6, TNF-α and IL-1β mRNA expression, IL-6, TNF-α and IL-1β secretion, and ROS production. LPS stimulation did not affect Nrf2, HO-1 and NQO1 protein expression in RWA264.7 cells without PHC, but PHC treatment elevated Nrf2, HO-1 and NQO1 protein after LPS treatment. Reactive oxygen species scavenging using NAC abolished the PHC-induced upregulation of Nrf2 and HO-1, highlighting the role of ROS in the process. Therefore, PHC partially abrogated LPS-related overproduction of pro-inflammatory mediators and ROS in RAW264.7 cells, and, in the presence of LPS,
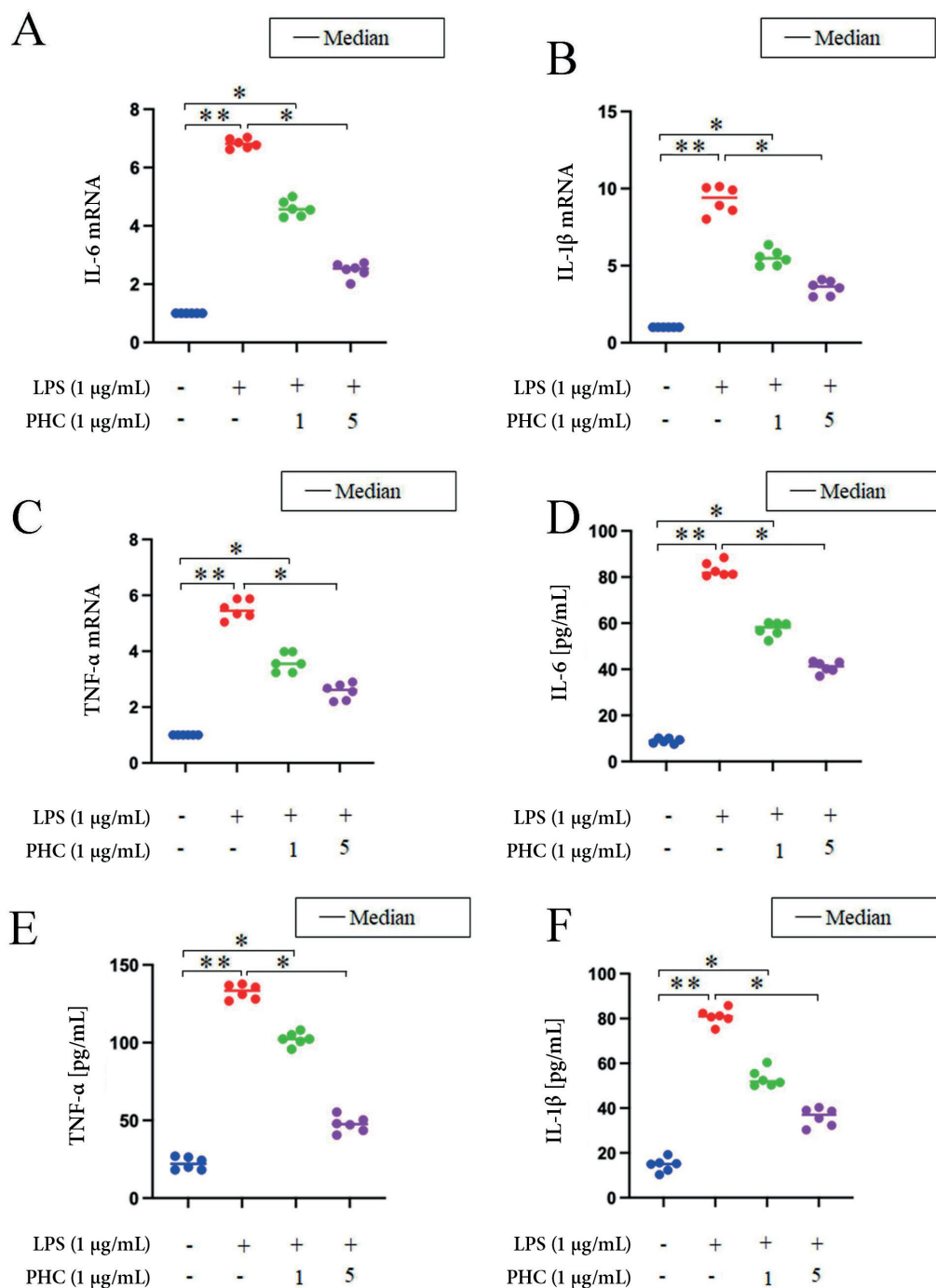
Fig. 2. Penehyclidine hydrochloride (PHC) suppressed lipopolysaccharide (LPS)-induced expression and secretion of pro-inflammatory cytokines of RAW264.7 cells. RAW264.7 cells were administered 1 μg/mL LPS alone or in combination with 1 μg/mL or 5 μg/mL PHC for 24 h. A–C. Quantitative reverse transcription polymerase chain reaction (qRT-PCR) was performed to determine messenger ribonucleic acid (mRNA) levels of interleukin (IL)-6, IL-1β and tumor necrosis factor alpha (TNF-α) in cells; D,E. Enzyme-linked immunosorbent assay (ELISA) was conducted to measure IL-6, IL-1β and TNF-α in the cell culture medium

*p < 0.05; **p < 0.01 (n = 6). Differences in characteristics between groups were analyzed using the Kruskal–Wallis test with Dunn's post hoc test.

PHC enhanced Nrf2, HO-1 and NQO1 protein expression. These findings suggest that PHC may enhance Nrf2 signaling in activated macrophages, and could serve as an anti-inflammatory and antioxidant compound for managing inflammatory disorders.

Penehyclidine hydrochloride toxicity on RAW264.7 cells was examined. Weng et al. demonstrated that PHC ranging from 1 μg/mL to 5 μg/mL did not change the activity of cultured alveolar macrophages but dose-dependently reduced LPS-mediated apoptosis.[51] Penehyclidine hydrochloride can also decrease neuronal apoptosis in the context of inflammation caused by cardiopulmonary bypass.[42] Our results showed

that PHC concentrations ranging from 1 μg/mL to 10 μg/mL had no significant effect on RAW264.7 cell viability. Thus, we treated RAW264.7 cells with 1 μg/mL or 5 μg/mL PHC in the subsequent experiments. Selecting the lowest doses could ensure the avoidance of possible PHC toxicity.

Lipopolysaccharide promoted the release of pro-inflammatory factors such as NO, PGE2, IL-6, IL-1β, and TNF-α, consistent with the known effects of LPS.[10,52,53] Meanwhile, LPS-induced ROS production by RAW264.7 cells was similar to previous reports.[54,55] These data suggest that an in vitro inflammation and oxidative stress model was successfully established.
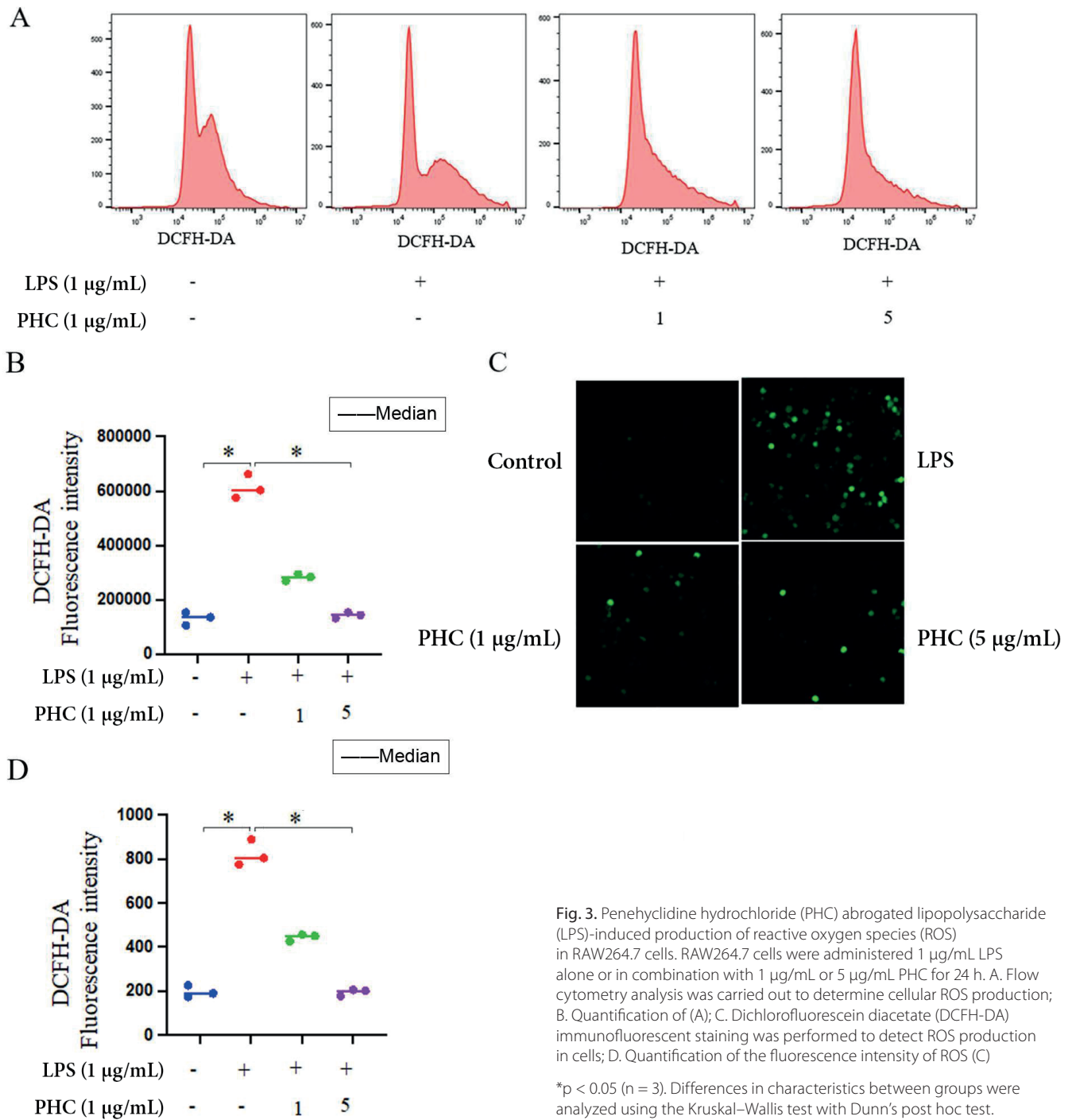
Fig. 3. Penehyclidine hydrochloride (PHC) abrogated lipopolysaccharide (LPS)-induced production of reactive oxygen species (ROS) in RAW264.7 cells. RAW264.7 cells were administered 1 μg/mL LPS alone or in combination with 1 μg/mL or 5 μg/mL PHC for 24 h. A. Flow cytometry analysis was carried out to determine cellular ROS production; B. Quantification of (A); C. Dichlorofluorescein diacetate (DCFH-DA) immunofluorescent staining was performed to detect ROS production in cells; D. Quantification of the fluorescence intensity of ROS (C)

*p < 0.05 (n = 3). Differences in characteristics between groups were analyzed using the Kruskal–Wallis test with Dunn's post hoc test.

Macrophages are among the first immune cells to encounter pathogenic organisms and other stimuli, and activated macrophages are important sources of pro-inflammatory cytokines.[22,23] Polarized macrophages are important in the pathogenetic mechanisms of inflammatory diseases by inducing the production of pro-inflammatory mediators.[56] As shown above, PHC effectively reversed LPS-associated excessive synthesis of pro-inflammatory factors and ROS, suggesting that PHC may alleviate the inflammatory response of macrophages.

Oxidative stress is critical in the etiology and perpetuation of inflammation.[57] Recently, Liu et al. reported that

PHC administration enhanced Nrf2 expression while suppressing mouse lung inflammation resulting from renal ischemia/reperfusion.[43] Similarly, Yang et al. found that PHC upregulated Nrf2 and HO-1 while suppressing the production of pro-inflammatory cytokines and ROS in renal ischemia/reperfusion-induced injured lungs. Furthermore, PHC-induced protection is lost in Nrf2^{−/−} mice, suggesting that Nrf2 is essential for the protective role of PHC against inflammation and oxidative stress.[44] However, whether PHC affects Nrf2 signaling in macrophages remains unknown.

A protective role for PHC in LPS-associated inflammation and oxidative stress has been extensively demonstrated

Fig. 4. Penehyclidine hydrochloride (PHC) induced nuclear factor erythroid 2-related factor (Nrf2) signaling in RAW264.7 cells. RAW264.7 cells were administered 1 μg/mL lipopolysaccharide (LPS) alone or in combination with 1 μg/mL or 5 μg/mL PHC for 24 h. Immunoblot was conducted to determine the protein expression of Nrf2 (A, 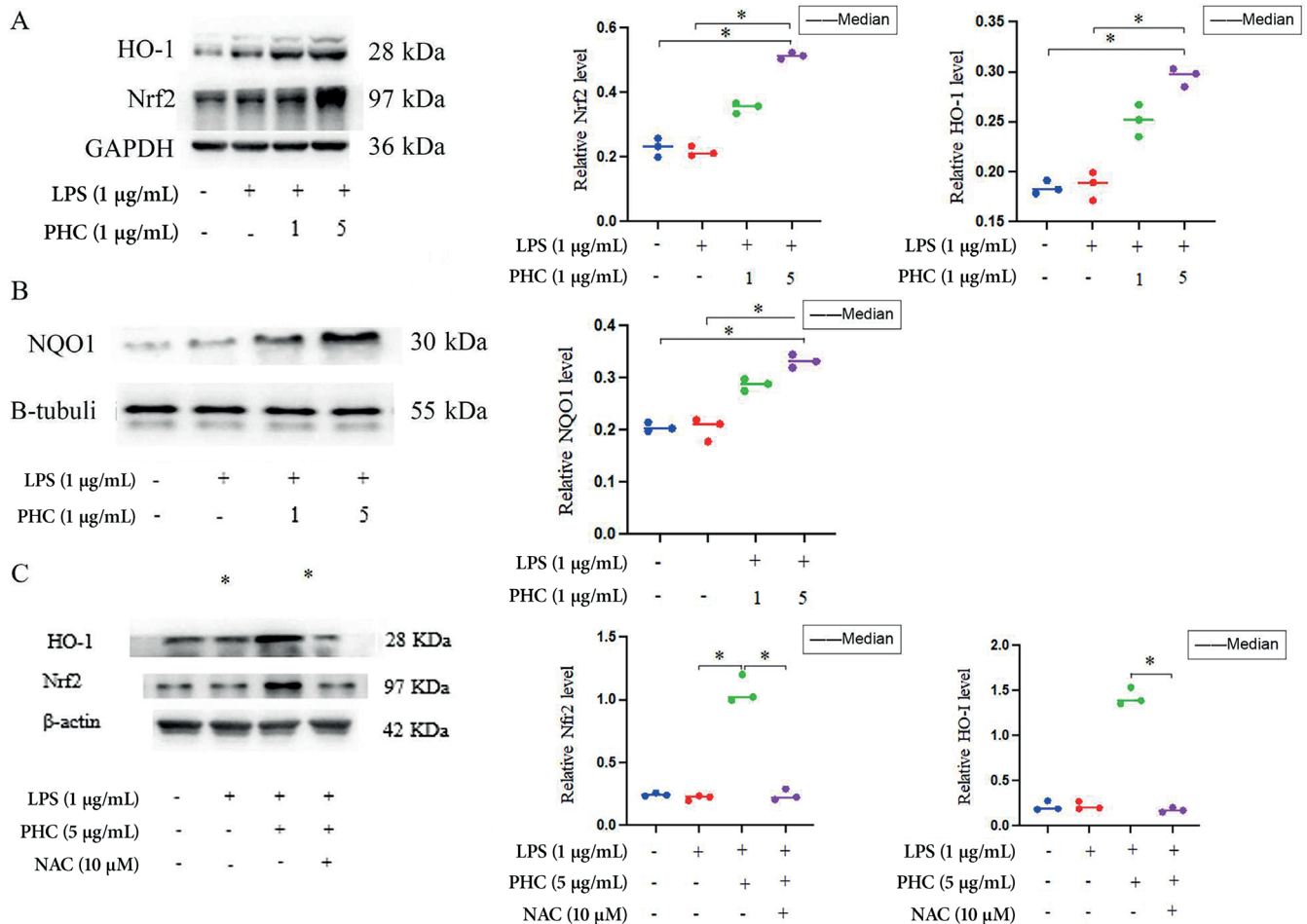left panel), heme oxygenase (HO)-1 (A, right panel) and NAD(P)H-quinone oxidoreductase 1 (NQO1) (B); C. RAW264.7 cells were administered LPS (1 μg/mL), LPS (1 μg/mL) + PHC (5 μg/mL) or LPS (1 μg/mL) + PHC (5 μg/mL) + N-acetyl-L-cysteine (NAC; 10 μM). The left panel shows Nrf2, and the right panel shows HO-1. Immunoblot was carried out to determine the protein expression of HO-1 and Nrf2, with glyceraldehyde 3-phosphate dehydrogenase (GAPDH) or β-actin as an internal reference

*$p < 0.05$ (n = 3). Differences in characteristics between groups were analyzed using the Kruskal–Wallis test with Dunn's post hoc test.

in animal models. Indeed, Guo et al. found that PHC alleviated LPS-associated acute lung injury and lung inflammation in a rat model, accompanied by considerable reductions in TNF-α, IL-8 and IL-6 in bronchoalveolar lavage fluid and downregulation of iNOS expression in the lung tissue.[58] Ye et al. revealed that PHC inhibits LPS-associated lung myeloperoxidase expression and ROS production in rats.[59] Furthermore, PHC can attenuate the impact of Toll-like receptors in models of inflammatory chronic lung diseases[39] and acute lung injury.[40] Similarly, PHC decreases serum TNF-α and IL-1β while improving renal function indicators in rats with LPS-induced acute kidney injury.[60] In humans, PHC decreased the expression of pro-inflammatory cytokines after surgery.[41] At the cellular level, PHC inhibited NO, PGE2, IL-1β, and TNF-α release in LPS-activated microglia,[61] and reduced the inflammatory response in cultured human pulmonary microvascular endothelial cells after LPS stimulation, reflected by lower secretion of lactate dehydrogenase, TNF-α and IL-6, and attenuated

expression of vascular cell adhesion molecule 1 (VCAM-1) and intercellular cell adhesion molecule-1 (ICAM-1).[62]

N-acetyl-l-cysteine has been shown to downregulate Nrf2/HO-1 signaling in the presence of hydrogen peroxide (H_2O_2) in MC3T3-E1 preosteoblasts[63] and attenuate kaempferol-induced Nrf2 interaction with the HO-1 promoter and subsequent HO-1 expression.[64] Our findings suggest that Nrf2/HO-1 signaling induction by PHC in macrophages is ROS-dependent. The findings are consistent with Zhu et al., who demonstrated that Nrf2 decreased the transcription of pro-inflammatory cytokines in activated macrophages.[33] Therefore, it is our opinion that PHC could have a role in managing disorders involving inflammation and oxidative stress. Of course, such management is outside the approved indications, and studies are necessary to examine the possibility, efficacy and safety of using PHC for acute or chronic inflammatory diseases. Acute and chronic inflammatory diseases carry high morbidity and mortality worldwide, and the available

treatments have limited efficacy. As such, exploring novel strategies warrants attention.

Several points require further elucidation. For example, in Fig. 3C, only a select number of cells showed increased ROS levels instead of a universal increase across all treated cells. Unfortunately, the present study cannot provide the answer. In order to understand what is happening in those cells, microdissection and single-cell omics will be necessary but were not performed in the present study. Compared with the control group, the cells in the LPS group showed a general increase in ROS levels, and this difference was dose-dependent. In addition, the western blots appeared to show secondary bands, and since there are different post-translational modifications and different forms of proteins, multiple bands can be recognized by the same antibody. Still, the target bands were analyzed according to the molecular weight of the corresponding marker, and the trend of the bands was consistent. Nonetheless, the nature of the protein modifications and isoforms could be investigated. Furthermore, LPS stimulation did not affect Nrf2, HO-1 and NQO1 protein expression in RWA264.7 cells without PHC. It could be hypothesized that the effect of PHC is specific to Nrf2, HO-1 and NQO1 elevation instead of a reversal of the effects of LPS, but the present study was not designed to examine such mechanisms, and additional studies are necessary.

Limitations

This study failed to verify that PHC can relieve LPS-stimulated macrophage inflammation and oxidative stress through the Nrf2 signaling pathway by silencing the expression of Nrf2. Inflammation is a complex process involving several effectors, pathways and cells. Future studies should use agonists, antagonists, and knockout/silenced cell and animal models to examine the involvement of these effectors, pathways and cells in the mechanisms involved in PHC modulation of inflammation and oxidative stress.

Only 1 µg and 5 µg doses were explored and were selected because they were far below the toxic dose, avoiding any risk of interference from PHC toxicity. In addition, starting with a small dose that works is consistent with clinical dosing principles, where anticholinergics have been found to increase the incidence of postoperative cognitive impairment in the elderly.[41] Still, future studies should include doses up to 20 µg to determine the exact dose-dependency of the effects of PHC. Therefore, the results of this study need further verification.

Conclusions

In conclusion, PHC may alleviate LPS-induced inflammation and oxidative stress while activating Nrf2 signaling in RAW264.7 macrophages. These findings suggest that PHC could be used for inflammation therapy by targeting activated macrophages.

Supplementary data

The Supplementary materials are available at https://doi.org/10.5281/zenodo.10622908. The package contains the following files:

Supplementary Table 1. Descriptive statistics for CCK-8 for Fig. 1A.

Supplementary Table 2. Kruskal–Wallis test results ($H = 29.44$, $p < 0.0001$) for CCK-8 for Fig. 1A.

Supplementary Table 3. Descriptive statistics for NO concentrations for Fig. 1B.

Supplementary Table 4. Kruskal–Wallis test results for NO concentrations for Fig. 1B ($H = 21.62$, $p < 0.0001$).

Supplementary Table 5. Descriptive statistics for PGE2 for Fig. 1C.

Supplementary Table 6. Kruskal–Wallis test results ($H = 21.60$, $p < 0.0001$) for PGE2 for Fig. 1C.

Supplementary Table 7. Descriptive statistics for iNOS mRNA for Fig. 1D.

Supplementary Table 8. Kruskal–Wallis test results ($H = 21.93$, $p < 0.0001$) for iNOS mRNA for Fig. 1D.

Supplementary Table 9. Descriptive statistics for IL-6 mRNA for Fig. 2A.

Supplementary Table 10. Kruskal–Wallis test results ($H = 21.93$, $p < 0.0001$) for IL-6 mRNA for Fig. 2A.

Supplementary Table 11. Descriptive statistics for IL-1 mRNA for Fig. 2B.

Supplementary Table 12. Kruskal–Wallis test results ($H = 21.93$, $p < 0.0001$) for IL-1mRNA for Fig. 2B.

Supplementary Table 13. Descriptive statistics for TNF-α mRNA for Fig. 2C.

Supplementary Table 14. Kruskal–Wallis test results ($H = 21.93$, $p < 0.0001$) for TNF-α mRNA for Fig. 2C

Supplementary Table 15. Descriptive statistics for IL-6 for Fig. 2D.

Supplementary Table 16. Kruskal–Wallis test results ($H = 21.60$, $p < 0.0001$) for IL-6 for Fig. 2D.

Supplementary Table 17. Descriptive statistics for TNF-α for Fig. 2E.

Supplementary Table 18. Kruskal–Wallis test results ($H = 21.62$, $p < 0.0001$) for TNF-α for Fig. 2E.

Supplementary Table 19. Descriptive statistics for IL-1α for Fig. 2F.

Supplementary Table 20. Kruskal–Wallis test results ($H = 21.60$, $p < 0.0001$) for IL-1 for Fig. 2F.

Supplementary Table 21. Raw data for ROS for Fig. 3B.

Supplementary Table 22. ROS descriptive statistics for Fig. 3B.

Supplementary Table 23. Kruskal–Wallis test results ($H = 9.359$, $p = 0.0020$) for ROS for Fig. 3B.

Supplementary Table 24. Raw data for ROS for Fig. 3D.

Supplementary Table 25. Descriptive statistics for ROS for Fig. 3D.

Supplementary Table 26. Kruskal–Wallis test results ($H = 9.359$, $p = 0.0020$) for ROS for Fig. 3D.

Supplementary Table 27. Raw data for Nrf2 for Fig. 4A.

Supplementary Table 28. Descriptive statistics for Nrf2 for Fig. 4A.

Supplementary Table 29 Kruskal–Wallis test results (H = 9.359, p = 0.0020) for Nrf2 for Fig. 4A.

Supplementary Table 30. Raw data for HO-1 for Fig. 4A.

Supplementary Table 31. Descriptive statistics for HO-1 for Fig. 4A.

Supplementary Table 32. Kruskal–Wallis test results (H = 9.359, p = 0.0020) for HO-1 for Fig. 4A.

Supplementary Table 33. Descriptive statistics for NQO1 for Fig. 4B.

Supplementary Table 34. Kruskal–Wallis test results (H = 9.359, p = 0.0020) for NQO1 for Fig. 4B.

Supplementary Table 35. Raw data for Nrf2 for Fig. 4C.

Supplementary Table 36. Descriptive statistics for Nrf2 for Fig. 4C.

Supplementary Table 37. Kruskal–Wallis test results (h = 7.308, p = 0.0328) for Nrf2 for Fig. 4C.

Supplementary Table 38. Raw data for HO-1 for Fig. 4C.

Supplementary Table 39. Descriptive statistics for HO-1 for Fig. 4C.

Supplementary Table 40. Kruskal–Wallis test results (H = 7.205, p = 0.0328) for HO-1 for Fig. 4C.

Note: In Supplementary Tables 3–40: A – control group, B – LPS group, C – LPS+PHC (1 μG/mL) group, D – LPS+PHC (5 μg/mL) group.

Data availability

The datasets generated and/or analyzed during the current study are available from the corresponding author on reasonable request.

Consent for publication

Not applicable.

ORCID iDs

Qiongmei Guo ⬤ https://orcid.org/0009-0003-8952-2795
Chunyan Zhang ⬤ https://orcid.org/0000-0002-4329-1739
Jingui Gao ⬤ https://orcid.org/0000-0002-3944-443X
Wenjing Shi ⬤ https://orcid.org/0009-0009-7643-4415
Xiaozhi Liu ⬤ https://orcid.org/0000-0002-5640-4472

References

1. Chen L, Deng H, Cui H, et al. Inflammatory responses and inflammation-associated diseases in organs. *Oncotarget*. 2018;9(6):7204–7218. doi:10.18632/oncotarget.23208
2. Karin M, Clevers H. Reparative inflammation takes charge of tissue regeneration. *Nature*. 2016;529(7586):307–315. doi:10.1038/nature17039
3. Wang Z, Qi F, Luo H, Xu G, Wang D. Inflammatory microenvironment of skin wounds. *Front Immunol*. 2022;13:789274. doi:10.3389/fimmu.2022.789274
4. Bennett JM, Reeves G, Billman GE, Sturmberg JP. Inflammation: Nature's way to efficiently respond to all types of challenges. Implications for understanding and managing "the epidemic" of chronic diseases. *Front Med (Lausanne)*. 2018;5:316. doi:10.3389/fmed.2018.00316
5. Zhao H, Wu L, Yan G, et al. Inflammation and tumor progression: Signaling pathways and targeted intervention. *Sig Transduct Target Ther*. 2021;6(1):263. doi:10.1038/s41392-021-00658-5
6. Fajgenbaum DC, June CH. Cytokine storm. *N Engl J Med*. 2020;383(23):2255–2273. doi:10.1056/NEJMra2026131
7. Chousterman BG, Swirski FK, Weber GF. Cytokine storm and sepsis disease pathogenesis. *Semin Immunopathol*. 2017;39(5):517–528. doi:10.1007/s00281-017-0639-8
8. Tsalamandris S, Antonopoulos AS, Oikonomou E, et al. The role of inflammation in diabetes: Current concepts and future perspectives. *Eur Cardiol*. 2019;14(1):50–59. doi:10.15420/ecr.2018.33.1
9. Ellulu MS, Patimah I, Khaza'ai H, Rahmat A, Abed Y. Obesity and inflammation: The linking mechanism and the complications. *Arch Med Sci*. 2017;4:851–863. doi:10.5114/aoms.2016.58928
10. Lin CY, Wang WH, Chen SH, et al. Lipopolysaccharide-induced nitric oxide, prostaglandin E2, and cytokine production of mouse and human macrophages are suppressed by pheophytin-b. *Int J Mol Sci*. 2017;18(12):2637. doi:10.3390/ijms18122637
11. Sugimoto MA, Sousa LP, Pinho V, Perretti M, Teixeira MM. Resolution of inflammation: What controls its onset? *Front Immunol*. 2016;7:160. doi:10.3389/fimmu.2016.00160
12. Todoric J, Antonucci L, Karin M. Targeting inflammation in cancer prevention and therapy. *Cancer Prev Res*. 2016;9(12):895–905. doi:10.1158/1940-6207.CAPR-16-0209
13. Goldfine AB, Shoelson SE. Therapeutic approaches targeting inflammation for diabetes and associated cardiovascular risk. *J Clin Invest*. 2017;127(1):83–93. doi:10.1172/JCI88884
14. Tanaka M, Toldi J, Vécsei L. Exploring the etiological links behind neurodegenerative diseases: Inflammatory cytokines and bioactive kynurenines. *Int J Mol Sci*. 2020;21(7):2431. doi:10.3390/ijms21072431
15. Tanaka M, Tóth F, Polyák H, Szabó Á, Mándi Y, Vécsei L. Immune influencers in action: Metabolites and enzymes of the tryptophan–kynurenine metabolic pathway. *Biomedicines*. 2021;9(7):734. doi:10.3390/biomedicines9070734
16. Tanaka M, Vécsei L. Monitoring the redox status in multiple sclerosis. *Biomedicines*. 2020;8(10):406. doi:10.3390/biomedicines8100406
17. Tanaka M, Szabó Á, Spekker E, Polyák H, Tóth F, Vécsei L. Mitochondrial impairment: A common motif in neuropsychiatric presentation? The link to the tryptophan–kynurenine metabolic system. *Cells*. 2022;11(16):2607. doi:10.3390/cells11162607
18. Tanaka M, Vécsei L. Editorial of Special Issue 'Dissecting Neurological and Neuropsychiatric Diseases: Neurodegeneration and Neuroprotection.' *Int J Mol Sci*. 2022;23(13):6991. doi:10.3390/ijms23136991
19. Battaglia S, Cardellicchio P, Di Fazio C, Nazzi C, Fracasso A, Borgomaneri S. Stopping in (e)motion: Reactive action inhibition when facing valence-independent emotional stimuli. *Front Behav Neurosci*. 2022;16:998714. doi:10.3389/fnbeh.2022.998714
20. Fitton R, Sweetman J, Heseltine-Carp W, Van Der Feltz-Cornelis C. Anti-inflammatory medications for the treatment of mental disorders: A scoping review. *Brain Behav Immun Health*. 2022;26:100518. doi:10.1016/j.bbih.2022.100518
21. Furman D, Campisi J, Verdin E, et al. Chronic inflammation in the etiology of disease across the life span. *Nat Med*. 2019;25(12):1822–1832. doi:10.1038/s41591-019-0675-0
22. Mosser DM, Edwards JP. Exploring the full spectrum of macrophage activation. *Nat Rev Immunol*. 2008;8(12):958–969. doi:10.1038/nri2448
23. Orecchioni M, Ghosheh Y, Pramod AB, Ley K. Macrophage polarization: Different gene signatures in M1(LPS+) vs. classically and M2(LPS–) vs. alternatively activated macrophages. *Front Immunol*. 2019;10:1084. doi:10.3389/fimmu.2019.01084
24. Pizzino G, Irrera N, Cucinotta M, et al. Oxidative stress: Harms and benefits for human health. *Oxid Med Cell Longev*. 2017;2017:8416763. doi:10.1155/2017/8416763
25. Khansari N, Shakiba Y, Mahmoudi M. Chronic inflammation and oxidative stress as a major cause of age-related diseases and cancer. *Recent Pat Inflamm Allergy Drug Discov*. 2009;3(1):73–80. doi:10.2174/187221309787158371
26. Sharifi-Rad M, Anil Kumar NV, Zucca P, et al. Lifestyle, oxidative stress, and antioxidants: Back and forth in the pathophysiology of chronic diseases. *Front Physiol*. 2020;11:694. doi:10.3389/fphys.2020.00694
27. Zorov DB, Juhaszova M, Sollott SJ. Mitochondrial reactive oxygen species (ROS) and ROS-induced ROS release. *Physiol Rev*. 2014;94(3):909–950. doi:10.1152/physrev.00026.2013

28. Bassoy EY, Walch M, Martinvalet D. Reactive oxygen species: Do they play a role in adaptive immunity? *Front Immunol*. 2021;12:755856. doi:10.3389/fimmu.2021.755856

29. Surai PF, Earle-Payne K. Antioxidant defences and redox homeostasis in animals. *Antioxidants (Basel)*. 2022;11(5):1012. doi:10.3390/antiox11051012

30. Pamplona R, Constantini D. Molecular and structural antioxidant defenses against oxidative stress in animals. *Am J Physiol Regul Integr Comp Physiol*. 2011;301(4):R843–R863. doi:10.1152/ajpregu.00034.2011

31. Jiang T, He Y. Recent advances in the role of nuclear factor erythroid-2-related factor 2 in spinal cord injury: Regulatory mechanisms and therapeutic options. *Front Aging Neurosci*. 2022;14:851257. doi:10.3389/fnagi.2022.851257

32. Eisenstein A, Hilliard BK, Pope SD, et al. Activation of the transcription factor NRF2 mediates the anti-inflammatory properties of a subset of over-the-counter and prescription NSAIDs. *Immunity*. 2022;55(6):1082–1095.e5. doi:10.1016/j.immuni.2022.04.015

33. Zhu H, Jia Z, Li Y. Nrf2 signaling in macrophages. *React Oxyg Species (Apex)*. 2016;2(6):417–420. doi:10.20455/ros.2016.875

34. Han XY, Liu H, Liu CH, et al. Synthesis of the optical isomers of a new anticholinergic drug, penehyclidine hydrochloride (8018). *Bioorg Med Chem Lett*. 2005;15(8):1979–1982. doi:10.1016/j.bmcl.2005.02.071

35. Wang Y, Gao Y, Ma J. Pleiotropic effects and pharmacological properties of penehyclidine hydrochloride. *Drug Des Devel Ther*. 2018;12:3289–3299. doi:10.2147/DDDT.S177435

36. Zhao W, Huang X, Zhang L, et al. Penehyclidine hydrochloride pretreatment ameliorates rhabdomyolysis-induced AKI by activating the Nrf2/HO-1 pathway and alleviating endoplasmic reticulum stress in rats. *PLoS One*. 2016;11(3):e0151158. doi:10.1371/journal.pone.0151158

37. Zhan J, Liu Y, Zhang Z, Chen C, Chen K, Wang Y. Effect of penehyclidine hydrochloride on expressions of MAPK in mice with CLP-induced acute lung injury. *Mol Biol Rep*. 2011;38(3):1909–1914. doi:10.1007/s11033-010-0310-0

38. Tan H, Lin D, Wang Z, Yang Y, Ma J. Cardioprotective time-window of penehyclidine hydrochloride postconditioning: A rat study. *Eur J Pharmacol*. 2017;812:48–56. doi:10.1016/j.ejphar.2017.07.003

39. Xiao HT, Liao Z, Tong RS. Penehyclidine hydrochloride: A potential drug for treating COPD by attenuating Toll-like receptors. *Drug Des Devel Ther*. 2012;6:317–322. doi:10.2147/DDDT.S36555

40. Wu X, Liu H, Song X, et al. Penehyclidine hydrochloride inhibits TLR4 signaling and inflammation, and attenuates blunt chest trauma and hemorrhagic shock-induced acute lung injury in rats. *Mol Med Rep*. 2018;17(5):6327–6336. doi:10.3892/mmr.2018.8644

41. Hongyu X, Qingting W, Xiaoling S, Liwu Z, Ailing Y, Xin L. Penehyclidine hydrochloride on postoperatively cognitive function. *Med Hypotheses*. 2019;129:109246. doi:10.1016/j.mehy.2019.109246

42. Cao HJ, Sun YJ, Zhang TZ, Zhou J, Diao YG. Penehyclidine hydrochloride attenuates the cerebral injury in a rat model of cardiopulmonary bypass. *Can J Physiol Pharmacol*. 2013;91(7):521–527. doi:10.1139/cjpp-2012-0329

43. Liu Z, Li Y, Yu L, Chang Y, Yu J. Penehyclidine hydrochloride inhibits renal ischemia/reperfusion-induced acute lung injury by activating the Nrf2 pathway. *Aging*. 2020;12(13):13400–13421. doi:10.18632/aging.103444

44. Yang Q, Li L, Liu Z, Li C, Yu L, Chang Y. Penehyclidine hydrochloride ameliorates renal ischemia reperfusion-stimulated lung injury in mice by activating Nrf2 signaling. *Bioimpacts*. 2021;12(3):211–218. doi:10.34172/bi.2021.23401

45. Kany S, Vollrath JT, Relja B. Cytokines in inflammatory disease. *Int J Mol Sci*. 2019;20(23):6008. doi:10.3390/ijms20236008

46. Facchin BM, Dos Reis GO, Vieira GN, et al. Inflammatory biomarkers on an LPS-induced RAW 264.7 cell model: A systematic review and meta-analysis. *Inflamm Res*. 2022;71(7–8):741–758. doi:10.1007/s00011-022-01584-0

47. Yang Q, Liu X, Yao Z, Mao S, Wei Q, Chang Y. Penehyclidine hydrochloride inhibits the release of high-mobility group box 1 in lipopolysaccharide-activated RAW264.7 cells and cecal ligation and puncture–induced septic mice. *J Surg Res*. 2014;186(1):310–317. doi:10.1016/j.jss.2013.08.015

48. Han B, Dai Y, Wu H, et al. Cimifugin inhibits inflammatory responses of RAW264.7 cells induced by lipopolysaccharide. *Med Sci Monit*. 2019;25:409–417. doi:10.12659/MSM.912042

49. Han S, Gao H, Chen S, et al. Procyanidin A1 alleviates inflammatory response induced by LPS through NF-κB, MAPK, and Nrf2/HO-1 pathways in RAW264.7 cells. *Sci Rep*. 2019;9(1):15087. doi:10.1038/s41598-019-51614-x

50. Li T, Chen X, Qian Y, et al. A synthetic BRET-based optogenetic device for pulsatile transgene expression enabling glucose homeostasis in mice. *Nat Commun*. 2021;12(1):615. doi:10.1038/s41467-021-20913-1

51. Weng J, Chen M, Lin Q, Chen J, Wang S, Fang D. Penehyclidine hydrochloride defends against LPS-induced ALI in rats by mitigating endoplasmic reticulum stress and promoting the Hes1/Notch1 pathway. *Gene*. 2019;721:144095. doi:10.1016/j.gene.2019.144095

52. Baek SH, Park T, Kang MG, Park D. Anti-inflammatory activity and ROS regulation effect of sinapaldehyde in LPS-stimulated RAW 264.7 macrophages. *Molecules*. 2020;25(18):4089. doi:10.3390/molecules25184089

53. Muniandy K, Gothai S, Badran KMH, Suresh Kumar S, Esa NM, Arulselvan P. Suppression of proinflammatory cytokines and mediators in LPS-induced RAW 264.7 macrophages by stem extract of *Alternanthera sessilis* via the inhibition of the NF-κ B pathway. *J Immunol Res*. 2018;2018:3430684. doi:10.1155/2018/3430684

54. Bist G, Pun NT, Magar TBT, et al. Inhibition of LPS-stimulated ROS production by fluorinated and hydroxylated chalcones in RAW 264.7 macrophages with structure-activity relationship study. *Bioorg Med Chem Lett*. 2017;27(5):1205–1209. doi:10.1016/j.bmcl.2017.01.061

55. Ma Y, Tang T, Sheng L, et al. Aloin suppresses lipopolysaccharide-induced inflammation by inhibiting JAK1-STAT1/3 activation and ROS production in RAW264.7 cells. *Int J Mol Med*. 2018;42(4):1925–1934. doi:10.3892/ijmm.2018.3796

56. Atri C, Guerfali F, Laouini D. Role of human macrophage polarization in inflammation during infectious diseases. *Int J Mol Sci*. 2018;19(6):1801. doi:10.3390/ijms19061801

57. De Almeida AJPO, De Almeida Rezende MS, Dantas SH, et al. Unveiling the role of inflammation and oxidative stress on age-related cardiovascular diseases. *Oxid Med Cell Longev*. 2020;2020:1954398. doi:10.1155/2020/1954398

58. Guo Y, Wei M, Yan Z, Wang G. Penehyclidine hydrochloride attenuates LPS-induced acute lung injury in rats [in Chinese]. *Xi Bao Yu Fen Zi Mian Yi Xue Za Zhi*. 2017;33(11):1486–1490. PMID:29268851.

59. Ye S, Yang X, Wang Q, Chen Q, Ma Y. Penehyclidine hydrochloride alleviates lipopolysaccharide-induced acute lung injury by ameliorating apoptosis and endoplasmic reticulum stress. *J Surg Res*. 2020;245:344–353. doi:10.1016/j.jss.2019.07.080

60. Cao HJ, Yu DM, Zhang TZ, et al. Protective effect of penehyclidine hydrochloride on lipopolysaccharide-induced acute kidney injury in rat. *Genet Mol Res*. 2015;14(3):9334–9342. doi:10.4238/2015.August.10.14

61. Huang C, He J, Chen Y, Zhang Y, Chen C. Penehyclidine hydrochloride inhibits the LPS-induced inflammatory response in microglia. *J Surg Res*. 2014;188(1):260–267. doi:10.1016/j.jss.2013.12.011

62. Zheng F, Xiao F, Yuan QH, et al. Penehyclidine hydrochloride decreases pulmonary microvascular endothelial inflammatory injury through a beta-arrestin-1-dependent mechanism. *Inflammation*. 2018;41(5):1610–1620. doi:10.1007/s10753-018-0804-9

63. Lee D, Kook SH, Ji H, et al. N-acetyl cysteine inhibits H_2O_2-mediated reduction in the mineralization of MC3T3-E1 cells by down-regulating Nrf2/HO-1 pathway. *BMB Rep*. 2015;48(11):636–641. doi:10.5483/BMBRep.2015.48.11.112

64. Yang CC, Hsiao LD, Wang CY, et al. HO-1 upregulation by kaempferol via ROS-dependent Nrf2-ARE cascade attenuates lipopolysaccharide-mediated intercellular cell adhesion molecule-1 expression in human pulmonary alveolar epithelial cells. *Antioxidants (Basel)*. 2022;11(4):782. doi:10.3390/antiox11040782

Bergapten attenuates human papillary thyroid cancer cell proliferation by triggering apoptosis and the GSK-3β, P13K and AKT pathways

Jingjing Li[1,A,D], Shaik A. Hussain[2,A,C], Jayasimha R. Daddam[3,A,B,D], Mengjie Sun[4,A,F]

[1] Department of Otolaryngology, The Second Affiliated Hospital of Xi'an Jiaotong University, China

[2] Department of Zoology, College of Science, King Saud University, Riyad, Saudi Arabia

[3] Department of Animal Sciences, Michigan State University, East Lansing, USA

[4] Department of Oncology, Xi'an Gaoxin Hospital, China

A – research concept and design; B – collection and/or assembly of data; C – data analysis and interpretation;
D – writing the article; E – critical revision of the article; F – final approval of the article

Address for correspondence
Mengjie Sun
E-mail: smj6177@sina.com

Abstract

Background. Over the past few decades, thyroid cancer (TC) incidence has steadily increased globally. The most common TC is human papillary thyroid carcinoma (PTC), which is poorly responsive to the current treatments. Hence, finding a successful therapeutic is urgently required.

Objectives. Bergapten (BG) is a furanocoumarin, a natural psoralen derivative isolated from numerous species of citrus and bergamot oil that has demonstrated anti-tumor activity. However, there are no reports available on the efficacy of BG on PTC cells.

Materials and methods. The current research investigated the anti-cancer activity of BG on human BCPAP cells, with cytotoxicity and apoptosis evaluated using MTT assay, AO/EB, DAPI, PI, ELISA, mRNA, and western blot.

Results. Bergapten (control group, 10 µM/mL and 15 µM/mL) inhibited PTC cell proliferation and stimulated apoptosis by enhancing Bax and caspase and reducing Bcl-2, cyclin-D1, c-myc, and survivin in a dose-dependent manner. Furthermore, BG expressively attenuated PI3K/AKT/GSK-3β signaling, creating an uneven Bax/Bcl-2 ratio that triggered Cyt-c, caspase cascade and apoptosis in human PTC cells.

Conclusions. Our findings emphasize that BG has the potential to be used as a protective natural remedy for human PTC cells.

Key words: apoptosis, thyroid cancer, papillary thyroid cancer, bergapten, PI3K/AKT/GSK-3β

Background

Thyroid cancer (TC) is the most common endocrine cancer, responsible for 96% of all new and 66.8% of deaths due to endocrine cancers.[1,2] Papillary thyroid cancer (PTC) is the primary cause behind the rise in TC cases in the USA,[3] with PTC subtypes accounting for 74–80% of all TC cases.[4] The overall death rate from PTC is greater than that of other endocrine cancers, despite recent data on the 5-year survival of TC in China showing notable advancement. Well-differentiated TC is treated employing various methods, including radioactive iodine,[5] thyroid hormone suppression therapy and surgical excision. However, as TC disparity decreases, standard surgical techniques, including Iodine-131 (I131) excision, no longer produce favorable partially segregated thyroid results.[6] Hence, novel treatments or potential biological mechanisms for cell cycle regulation, proliferation and apoptosis need to be identified to reduce the prevalence of tumors and improve prognosis in PTC patients.

Natural products were once believed to be crucial for developing novel and effective anti-cancer treatments. The naturally occurring psoralen analog bergapten (BG), a furanocoumarin, is found in the roots and fruits of many different plants, including *Angelica archangelica* L., and it has been demonstrated that BG (5-methoxypsoralen) has anti-proliferative effects against many carcinomas.[7,8] According to previous research, psoralen can combat the growth of skin and breast cancer cells, and BG prevents the growth of MCF-7-TR1 and MCF-7 cells that are resistant to tamoxifen.[9] Other research revealed that BG has anti-inflammatory, anti-cancer and hepatoprotective properties,[10] while multiple investigations have shown BG to suppress topoisomerase-1 and COX-2.[11,12] These results demonstrate that BG stimulates different signaling pathways and possesses promising anti-cancer properties. However, an in-depth understanding of the molecular effects of BG on PTC cells requires more research.

The cell cycle is a highly controlled biological process that includes the G1, S, G2, and M phases in sequence, with its regular progression controlled by several cyclin-dependent kinases (CDKs) and related cyclins. The most critical area of study is cell proliferation, caused by uncontrolled cell proliferation that is central to tumor formation.[13] Controlled cell death, or apoptosis, is a common target for many management strategies and plays a crucial role in cancer treatment. The morphological changes occurring in dying cells include cell disappearance, membrane blebbing, DNA fragmentation, chromatin reduction, and loss of organelle integrity.[14] Both extrinsic and intrinsic mechanisms may be potential causes of apoptosis,[15] with apoptotic pathways that promote orderly, non-inflammatory cell death connected to caspase cysteine proteases family activation.[16]

The PI3K/AKT apoptotic signaling pathway is widely observed in many malignant cells, with numerous downstream substrates of PI3K/AKT signaling, including GSK-3β and Bax, contributing to the therapeutic conflict in tumor cells and cell death prevention.[17] According to recent research, human lung carcinoma cells undergoing apoptosis and G1 phase cell cycle arrest were more susceptible to BG than normal lung cancer cells.[18,19] Therefore, the present study examined BG's ability to inhibit tumor growth in PTC cells and the related signaling cascades.

Objectives

The study aimed to further understand BG functions using BCPAP human PTC cells to assess cytotoxicity and potential molecular effects such as promoting cell viability, cell cycle regulation and apoptosis. Such an approach should provide a preliminary description of BG's ability to inhibit cell proliferation and induce apoptosis in PTC cells.

Materials and methods

Chemicals

Bergapten, RPMI-1640, fetal bovine serum (FBS), antibiotics, phosphate-buffered saline (PBS), dimethyl sufloxide (DMSO), 3-(4,5-dimethylthiazol-2-yl)-2,5-diphenyltetrazolium bromide (MTT), acridine orange/ethidium bromide (AO/EB), 4′,6-diamidino-2-phenylindole (DAPI), propidium iodide (PI), and sodium dodecyl-sulfate (SDS) were obtained from Gibco (Thermo Fisher Scientific, Waltham, USA). Enzyme-linked immunosorbent assay (ELISA) kits were purchased from Cayman Chemicals (Ann Arbor, USA), and the antibodies for western blot analysis were acquired from Beyotime Biotechnology (Shanghai, China).

Cell culture

The BCPAP human PTC cells were purchased from Shanghai Aiyan Biotechnology Co., Ltd (Shanghai, China) and cultured in RPMI 1640 medium containing FBS (10%), penicillin (100 U/mL) and streptomycin (100 U/mL), maintained at 37°C in a humid environment with 5% CO_2.

Cell cytotoxicity assay

The MTT was used to measure cell growth.[20] The BCPAP cells were cultured at 37°C in a moist incubator with 5% CO_2 after being seeded into 96-well plates (1×10^5 cells per well). The cells were separated after overnight incubation, cleaned with PBS, and treated with different concentrations of BG (control group, 2.5, 5, 10, 15, 20, and 25 μM/mL) for 1 day. To allow the mitochondrial dehydrogenase to transform MTT into insoluble formazan crystals, MTT (100 μL) solution was added to the control and treated PTC cells, and the cells were incubated for an additional 4 h. The formazan

crystals dissolved when DMSO (150 μL) was added, and optical density (OD) was determined at 490 nm (Bio-Tek Instruments, Winooski, USA). Using Sigma Plot™ software, 4 parameter logistic function dose-response curves were used to calculate the IC50. Further research was then conducted using the selected concentrations.

Acridine orange/ethidium bromide labelling to assess apoptosis

Acridine orange/ethidium bromide (AO/EB) staining identified apoptotic PTC cell morphology after exposure to BG at concentrations of 10 μM and 15 μM.[21] The BC-PAP cells were cultured for a day after adding 10 μM and 15 μM BG. The AO/EB dye mixture (100 g/mL of each dye) was added to all groups (control, 10 μM and 15 μM BG treated with BCPAP), the unbound dye was removed using a PBS wash, and the cells were left at room temperature for 20 min in the dark before being observed under a fluorescence microscope (IXdrop Standard Microscope; Olympus Corp., Tokyo, Japan).

Examining apoptosis using DAPI staining

Human PTC cells were treated with BG (control, 10 μM and 15 μM) in 96-well plates and then fixed with paraformaldehyde (4%) for 10 min at 37°C. The treated BCPAP cells were stained with DAPI for 10 min to analyze the cellular changes associated with apoptosis according to a previously described method.[22] The dyed samples were mounted on glass slides and examined using fluorescence microscopy (Nikon Eclipse TS100; Nikon Corp., Tokyo, Japan).

Examining apoptosis using propidium iodide staining

Propidium iodide (PI) staining was employed to examine the apoptotic nuclei of BCPAP cells. The PTC cells were incubated with doses of BG (control, 10 μM/mL and 15 μM/mL) for 2 days. Following the incubation, the treated cells were collected and stained with PI.[23] A fluorescence microscope (Nikon Eclipse TS100; Nikon Corp.) was used to observe the red fluorescence emitting from the nuclei.

Measurement of caspase-9 and caspase-8

Apoptosis was determined by measuring caspase-9 and caspase-8 in 3 independent replicates using an ELISA kit following the manufacturer's protocol.

Determination of mRNA expression

Whole RNA was isolated from BCPAP cells according to the company's guidelines using TRIzol® reagent (Abcam, Cambridge, USA). Using a high-capacity complementary DNA (cDNA) reverse transcription kit (Abcam), the extracted

RNA was reverse transcribed into cDNA following the manufacturer's procedures, and the cDNAs were examined using the Fast Start SYBR Green Master mix (Abcam). The band intensity was examined by employing 1.5% agarose gels exposed to electrophoresis and measured using ImageJ v. 1.48 software (National Institutes of Health (NIH), Bethesda, USA):

cyclin D1
F: 5′-CTGTTTGGCGTTTCCCAGAGTCATC-3′
R: 5′-AGCCTCCTCCTCACAACCTCTC-3′
Bcl-2
F: 5′-ATGTGTGTGTGTGGAGAGGCTCAA-3′
R: 5′-GAGAGACAGCCAGGAAATCAA-3′
Bax
F: 5′-ATGTTTTCTGACGGCAACTTC-3′
R: 5′-AGTCCAATGTCCAGCCCAT-3′
caspase-3
F: 5′-TGTTTGTGTGCTTCTGAGCC-3′
R: 5′-CACGCCATGTCATCATCAAC-3′
c-Myc
F: 5′-ACCCTTGCCGCATCCACGAAAC-3′
R: 5′-CGTAGTCGAGGTCATAGTTGGTTGGTTGG-3′
survivin
F: 5′-GGACCACCGCATCTACAT-3′
R: 5′-CAAGTCTGGCTCGTTCAGT-3′

Western blot study

Human BCPAP cells were exposed to BG (control, 10 μM/mL and 15 μM/mL) and cultured for 1 day. Using an ice-cold lysis solution containing protease inhibitors, cell lysates were formed for western blotting, and the protein content was measured using a Protein BCA Assay Kit (Pierce Chemical Co., Rockford, USA). The proteins were electrophoretically scattered for a brief period and transferred to a polyvinyl fluoride (PVDF) film, which was blocked and then probed overnight at 4°C using 1:1,000 dilutions of P13K, AKT, GSK-3β, and β-actin primary antibodies. Secondary antibodies (1:5,000) were then added, and the LI-COR Odessey imaging system (Lincoln, USA) was used to stain and visualize the bands to detect the presence of proteins. Densitometry was used to evaluate and quantify the protein band using ImageJ.

Statistical analyses

The statistical analysis employed GraphPad Prism v. 8.0.2 (GraphPad Software, San Diego, USA) and IBM SPSS software v. 25 (IBM Corp., Armonk, USA), with data presented as the median (min and max). Since the sample size was too small to assess data distribution, the differences between groups were analyzed using the non-parametric Kruskal–Wallis test with Dunn's post hoc test. Statistics for the Kruskal–Wallis tests are presented in Table 1 and the Supplementary material. A statistically significant difference was considered when $p < 0.05$. All tests in this study were bilateral.

Table 1. The results of the Kruskal–Wallis test with a correction for controlling I-type error (Dunn's test)

Explained variable	C vs 10 µM	C vs 15 µM	10 µM vs 15 µM
Caspase-9	0.092	0.01522	0.390
Caspase-8	0.136	0.01522	0.198
Cyclin-D1	0.153	0.01522	0.153
Bcl-2	0.152	0.01522	0.152
Bax	0.154	0.01522	0.154
Caspase-3	0.154	0.01522	0.154
C-Myc	0.154	0.01522	0.154
Survivin	0.153	0.01522	0.153
PI3K	0.152	0.01522	0.152
AKT	0.153	0.01522	0.153
GSK-3β	0.153	0.01522	0.153

C – control group; 10 µM – 10 µM bergapten group;
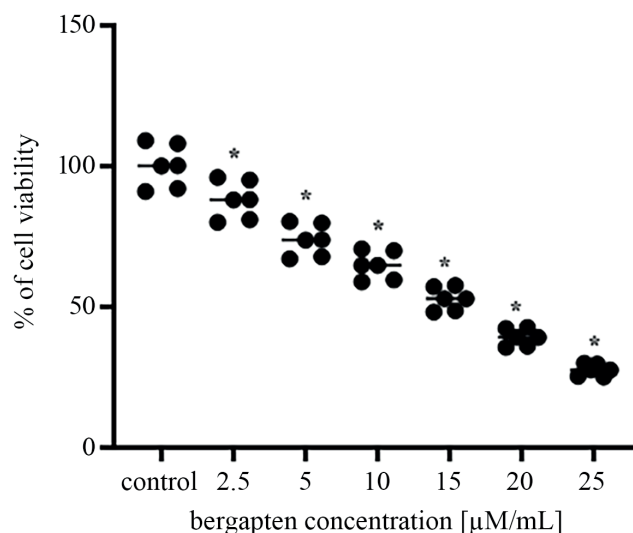15 µM – 15 µM bergapten group.

Fig. 1. Bergapten (BG) inhibits human papillary thyroid carcinoma (PTC) cell viability. Human PTC BCPAP cells were treated with various doses of BG (5–20 µM/mL) for 1 day. A 3-(4,5-dimethylthiazol-2-yl)-2,5-diphenyltetrazolium bromide (MTT) assay was used to calculate cell proliferation. This figure presents data (black dots) and the medians (horizontal lines)

*$p < 0.001$ compared to the control group (Table 2)

Results

Effect of BG on human PTC cells that are cytotoxicity

The MTT assay was used to assess BCPAP human PTC cell cytotoxicity using different doses of BG (control group, 2.5, 5, 10, 15, 20, and 25 µM/mL). Bergapten improved the cytotoxic and anti-proliferative properties of BCPAP cancer cells in a dose-dependent manner, with a BG dose of less than 10 µM unable to inhibit PTC cell proliferation. However, when treated with 10 µM/mL and 15 µM of BG, 2 PTC cells (BCPAP) showed lower proliferation, and increasing BG to 20 µM destroyed both PTC cells. The BG IC50 value for both PTC cells was 15 µM, according to the MTT assay. As a result, the inhibitory concentration levels of 10 µM/mL and 15 µM BG were chosen for further testing (Table 2, Fig. 1).

Human PTC cell apoptosis was caused by BG as determined by AO/EB staining

Apoptotic changes were seen in human PTC cells using AO/EB dual-labeling. Untreated BCPAP appeared as uniformly pigmented viable green cells, while PTC cells treated with BG (10 µM/mL and 15 µM) exhibited greater apoptotic alterations than the control in a concentration-dependent manner. Human PTC cells treated with 10 µM BG showed early apoptotic bodies, compacted chromatin

and vivid greenish-yellow areas caused by membrane blebbing. After 15 µM BG treatment, BCPAP cells exhibited late apoptotic changes such as chromatin condensation, fragmented nuclei and membrane blebbing. BCPAP cells were orange-red and had lost membrane integrity (Fig. 2).

DAPI staining of human PTC cells

To identify healthy and viable cells, human PTC cells were labeled with DAPI. In contrast to untreated PTC cells, BG-treated BCPAP cancer cells displayed improved nuclear morphology and nuclear body disintegration, leading to apoptosis. When BCPAP cells were exposed to BG (10 µM/mL and 15 µM/mL), they experienced chromatin condensation, membrane blebbing, nuclear envelop disintegration, and cellular collapse. These findings showed that BG induced apoptosis in a dose-dependent manner (Fig. 3).

BG triggered apoptosis in human PTC cells, as evidenced by PI staining

PTC cells died in a dose-dependent manner after being treated with BG. Compared to untreated control BCPAP cells, BG (10 µM/mL and 15 µM/mL) supplementation

Table 2. Comparison of the studied groups

Variables	Control	2.5 µM	5 µM	10 µM	15 µM	20 µM	25 µM	p-value*
MTT	100.01 (91.00–109.00)	88.02 (80.09–95.93)	73.76 (67.09–80.37)	64.74 (58.90–70.56)	52.91 (48.15–57.67)	39.20 (35.67–42.73)	27.60 (25.12–30.08)	<0.001

10 µM – 10 µM bergapten group; 15 µM – 15 µM bergapten group. Data were presented as median (min and max); *p-value was generated from Kruskal–Wallis test. There was a significant difference among all groups in the Dunn's test.
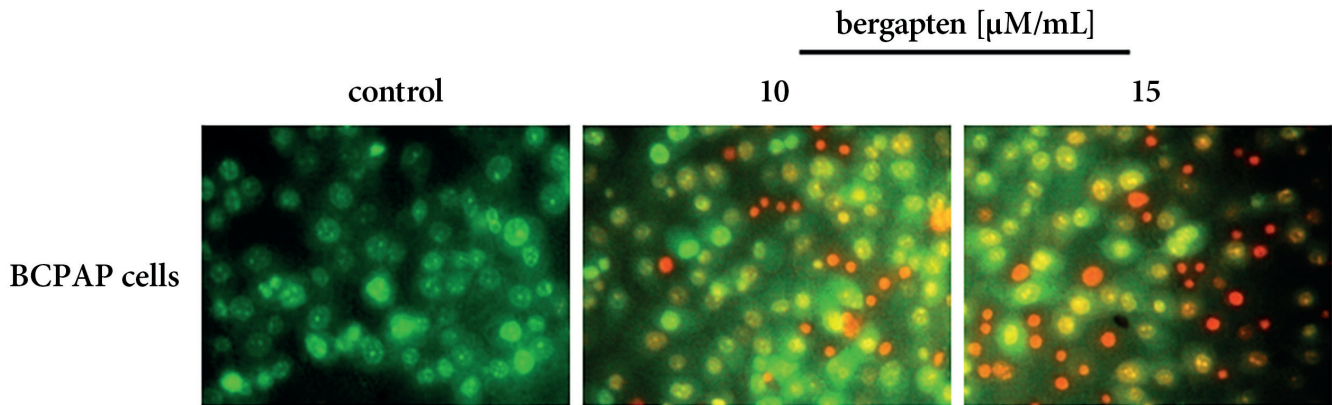
bergapten [μM/mL]

| control | 10 | 15 |

Fig. 2. Assessment of bergapten (BG) on human papillary thyroid carcinoma (PTC) cell apoptosis using acridine orange/ethidium bromide (AO/EB) staining. BCPAP cancer cells were treated with BG (0 μM/mL (n = 6), 10 μM/mL (n = 6) or 15 μM/mL (n = 6)) for 1 day. Human PTC cell apoptosis was studied using AO/EB dual staining and was observed under a fluorescence microscope (Nikon Eclipse TS100; Nikon Corp., Tokyo, Japan)

bergapten [μM/mL]

| control | 10 | 15 |
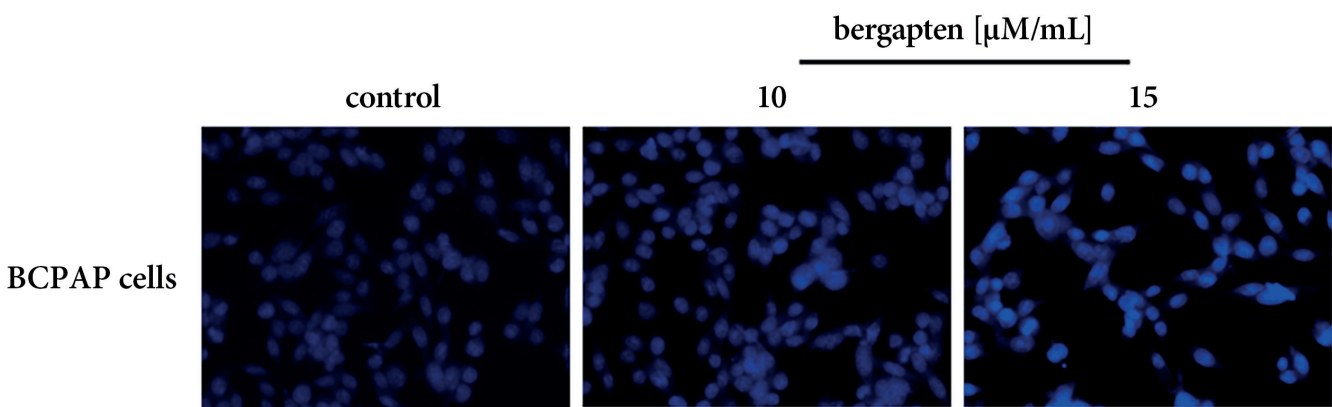
Fig. 3. Evaluation of bergapten (BG) on human papillary thyroid carcinoma (PTC) cells apoptosis using 4′,6-diamidino-2-phenylindole (DAPI) staining. The BCPAP cancer cells were treated with BG (0 μM/mL (n = 6), 10 μM/mL (n = 6) or 15 μM/mL (n = 6)) for 1 day. Human PTC cell apoptosis was evaluated using DAPI staining and observed under a fluorescence microscope (Nikon Eclipse TS100; Nikon Corp., Tokyo, Japan)

bergapten [μM/mL]

| control | 10 | 15 |
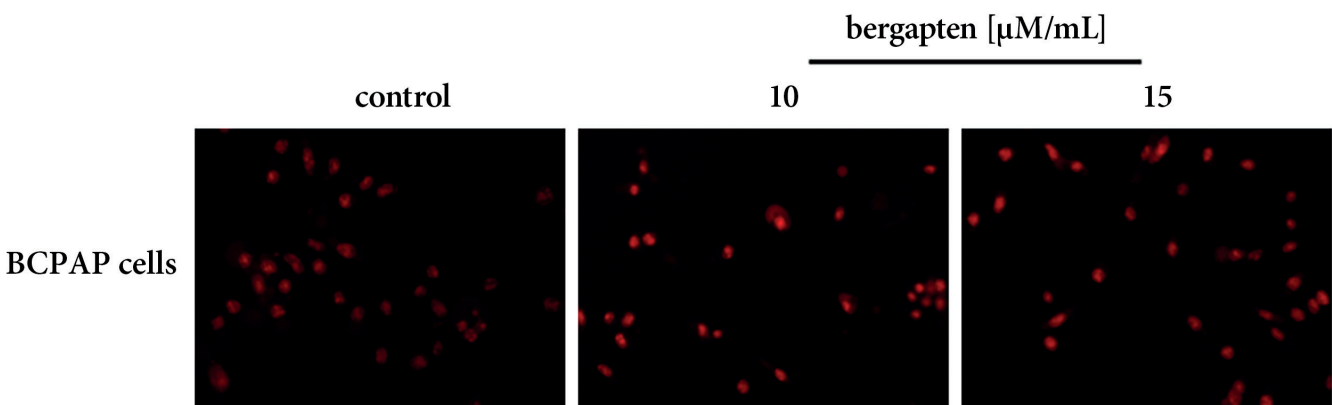
Fig. 4. Effects of bergapten (BG) on human papillary thyroid carcinoma (PTC) cells apoptosis confirmed using propidium iodide (PI) staining. Human PTC cells BCPAP were treated with 0 μM/mL (n = 6), 10 μM/mL (n = 6) or 15 μM/mL (n = 6) BG for 24 h. The BCPAP cancer cell apoptotic activity was assessed with PI staining

boosted apoptotic activity. The apoptotic nuclei of PTC cancer cells were identified using PI labeling. The cells were labeled with PI after the membrane's integrity was compromised, which is related to the loss of membrane polarity and leads to apoptosis. As a result, BG-induced apoptosis inhibited the growth of human PTC cells (Fig. 4).

BG enhanced caspase-8 and caspase-9 levels, as measured using ELISA

Human PTC cells treated with BG had higher caspase-8 and caspase-9 levels than the control. Caspase-8 and caspase-9 levels increased considerably ($p < 0.05$) after 15 μM BG treatment, and the increase was greater than after

Fig. 5. Measurement of caspase-8 and caspase-9 in bergapten (BG)-treated BCPAP cells. Human papillary thyroid carcinoma (PTC) BCPAP cells were treated with 0 µM/mL (n = 6), 10 µM/mL (n = 6) or 15 µM/mL (n = 6) BG for 24 h. Caspase-8 and caspase-9 levels were measured using enzyme-linked immunosorbent assay (ELISA). This figure presents data (black dots) and the medians (horizontal lines)

*p < 0.001 compared to the control group (Table 3).

10 µM BG treatment. Bergapten increased caspase activity in a dose-dependent manner (Table 1,3, Fig. 5).

Effects of BG on BCPAP human PTC cell mRNA expression
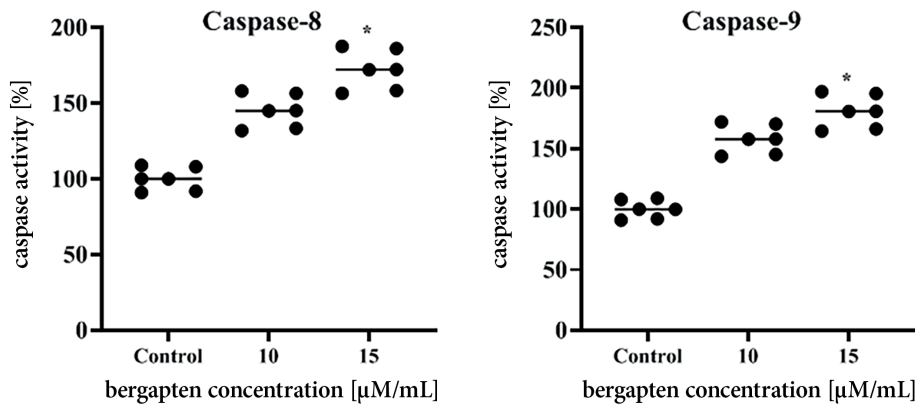
BCPAP cells were treated with BG (10 µM/mL and 15 µM/mL) to determine mRNA expression due to apoptosis. Cyclin-D1, Bcl-2, c-Myc, and survivin showed higher mRNA levels in untreated BCPAP cancer cells, although Bax and caspase-3 levels were lower. Bergapten significantly lowered the expression of cyclin-D1, Bcl-2, c-Myc, and survivin mRNA while raising Bax and caspase-3 in a concentration-dependent manner (Table 1,3, Fig. 6).

BG suppressed the P13K/AKT/GSK-3β pathway, as analyzed with western blot

The P13K/AKT/GSK-3β pathway is involved in the genesis and spread of cancer. Accordingly, P13K, AKT and GSK-3β protein levels are increased in human PTC cells. P13K/Akt/GSK-3β levels were lower in both PTC cells after exposure to BG (10 µM/mL and 15 µM/mL). In human PTC cells, BG inhibited the expression of these proteins

in a concentration-dependent way. The results showed that BG inhibited PTC cell proliferation and induced caspase-mediated apoptosis by decreasing PI3K/AKT/GSK-3β signaling (Table 1,3, Fig. 7).

Discussion

Globally, TC primarily affects women, with PTC exhibiting a significant negative impact.[2,3] There are currently no effective treatments for PTC, though TC can be surgically treated if detected early. However, there are no viable treatments available for those with iodine-resistant or incurable malignancies,[5,6] which emphasizes the significance of our research on BG's potential anti-cancer benefits to these patients.

The use of compounds produced from natural sources is gaining popularity for elucidating the basic processes of new drugs. According to our findings, BG stimulates a caspase-mediated process in PTC cells that changes multiple cellular pathways and eventually induces apoptosis. This study is the first to establish how BG inhibits PTC cell viability, causes cell cycle arrest, and ultimately triggers apoptosis.

Table 3. Comparison of the studied groups

Variables	Control (n = 6)	10 µM (n = 6)	15 µM (n = 6)	p-value*
Caspase-9	100.05 (91–109)	157.89 (143.61–172.01)	180.84 (164.48–197.02)	0.001
Caspase-8	100.05 (91–109)	145.05 (133.93–158.03)	172.18 (156.61–187.59)	0.001
Cyclin-D1	1 (0.91–1.09)	0.74 (0.67–0.81)	0.56 (0.51–0.61)	<0.001
Bcl-2	1 (0.91–1.09)	0.74 (0.64–0.76)	0.56 (0.45–0.53)	<0.001
Bax	1 (0.91–1.09)	2.10 (1.91–2.29)	3.30 (3–3.60)	<0.001
Caspase-3	1 (0.91–1.09)	1.92 (1.75–2.09)	2.70 (2.46–2.94)	<0.001
C-Myc	1 (0.91–1.09)	0.60 (0.55–0.65)	0.47 (0.43–0.51)	<0.001
Survivin	1 (0.91–1.09)	0.55 (0.50–0.60)	0.39 (0.35–0.43)	<0.001
PI3K	1 (0.91–1.09)	0.73 (0.66–0.80)	0.43 (0.39–0.47)	<0.001
AKT	1 (0.91–1.09)	0.70 (0.64–0.76)	0.41 (0.37–0.45)	<0.001
GSK-3β	1 (0.91–1.08)	0.80 (0.73–0.86)	0.56 (0.51–0.61)	0.001

10 µM – 10 µM bergapten group; 15 µM – 15 µM bergapten group. Data were presented as median (min and max); *p-value was generated from Kruskal–Wallis test. There was a significant difference among all groups in the Dunn's test.
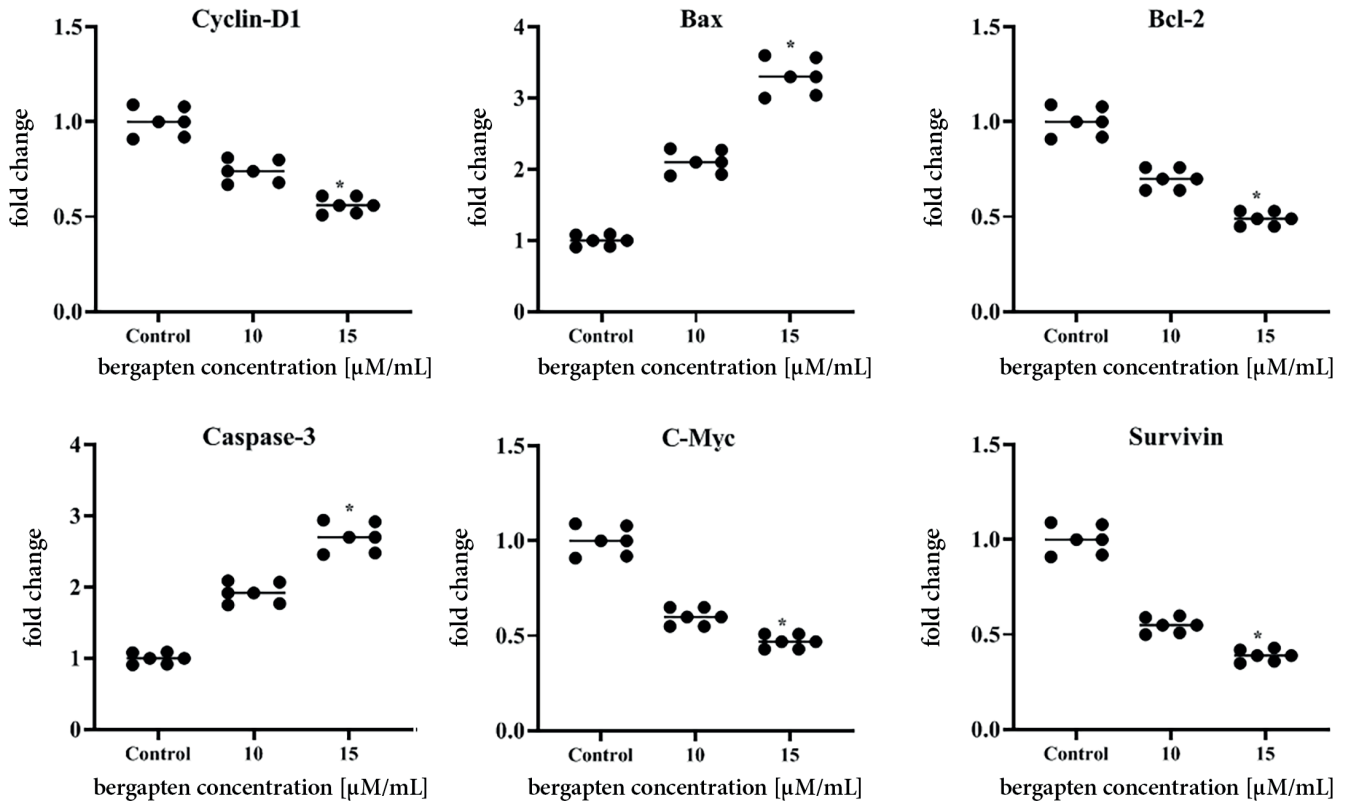
Fig. 6. Influence of bergapten (BG) on the messenger ribonucleic acid (mRNA) expression of human thyroid cancer (TC) BCPAP cells. BCPAP cancer cells were treated with 0 μM/mL (n = 6), 10 μM/mL (n = 6) or 15 μM/mL (n = 6) BG for 24 h. The mRNA levels of cyclin-D1, Bcl-2, Bax, caspase-3, c-Myc, and survivin were determined using reverse transcriptase polymerase chain reaction (RT-PCR) analysis. This figure presents data (black dots) and the medians (horizontal lines)

*p < 0.001 compared to the control group (Table 3)
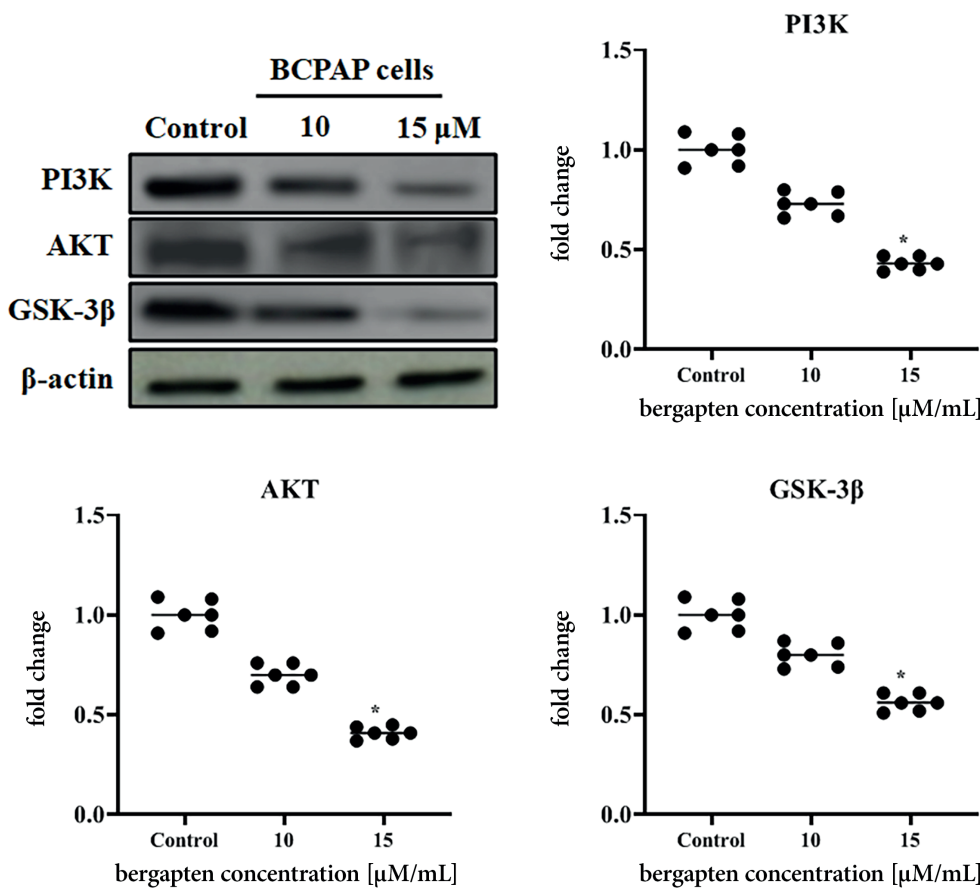
Fig. 7. Effects of BG-treated human papillary thyroid carcinoma (PTC) BCPAP cells on the P13K/AKT/GSK-3β pathway. Human PTC BCPAP cells were treated with 0 μM/mL (n = 6), 10 μM/mL (n = 6) or 15 μM/mL (n = 6) BG for 24 h. P13K, AKT, GSK-3β, and β-actin protein levels were measured using western blot. This figure presents data (black dots) and the medians (horizontal lines)

*p < 0.001 compared to the control group (Table 3)

120

J. Li et al. Bergapten suppressed thyroid cancer cells

Our experiments investigated the anti-cancer effects of BG on human PTC cells (BCPAP), and we discovered that BG can decrease the growth of both cells, which may lead to the stimulation of cell cycle arrest and cell death. Since uncontrolled cell growth and proliferation are the fundamental goals of tumor pathogenesis, highlighting the linked unregulated pathways may reduce tumorigenesis.[13] The research found that BG improved the cytotoxic and anti-proliferative properties of BCPAP cancer cells in a dose-dependent manner, showing that BG has anti-cancer activity by inhibiting PTC cell proliferation when caspase-mediated death and cell-cycle arrest are activated. The cell cycle and apoptosis are 2 critical elements influencing the cytotoxicity rate, with cell cycle checkpoints being an essential component for ensuring high-fidelity cell partition. Apoptosis, a type of cell death, permits other cells to reuse organelles and proteins.[14] We found that BG can successfully stop the cell cycle and trigger apoptosis in PTC cells. Previous research has shown that BG can inhibit the proliferation of certain types of malignant cells, and recent findings suggest that BG can reduce PTC cell viability, including human NSCLC cell lines A549 and NCIH460,[19,15,24,25] and MEC1,[26] as well as hepatocellular carcinoma and bladder cell lines, implying that BG could be used to treat PTC.

Bergapten significantly decreased BCPAP cell growth by triggering apoptotic cell death via the modulation of several apoptosis-related proteins and the production of caspases. Human PTC cells treated with 10 μM BG showed early apoptotic cells, compacted chromatin and vivid greenish-yellow areas caused by membrane blebbing. After 15 μM BG treatment, BCPAP cells exhibited late apoptotic changes such as chromatin condensation, fragmented nuclei and membrane blebbing. Furthermore, BCPAP cells were orange-red and had lost membrane integrity. In contrast to untreated PTC cells, BG-treated BCPAP cancer cells displayed improved nuclear morphology and nuclear body disintegration, leading to apoptosis. The apoptotic nuclei of PTC cancer cells were identified using PI labeling after the membrane's integrity was compromised, which is related to the loss of membrane polarity and leads to apoptosis. Using AO/EB, DAPI and PI labeling, the current findings indicate that the anti-tumor effects of BG were achieved through apoptotic induction.

Our findings also revealed that BG reduced the expression of Bcl-2, cyclin-D1, c-Myc, survivin, and Bax. Furthermore, caspase-3, caspase-8 and caspase-9 concentrations were considerably greater in PTC cells. The elevated levels of caspase-8 and caspase-9 revealed that both intrinsic and extrinsic mechanisms were involved in triggering apoptosis.[15,16] Many anti-cancer medications are thought to induce apoptosis by targeting Bcl-2 family proteins (Bax/Bcl-2), which are critical in determining whether or not cells die. Finally, the Bax protein reduced the potential of the mitochondrial membrane, allowing cytochrome-c to be released and the formation of the homodimer.[27–29]

According to the gene expression analysis, BG improved cell viability by inducing apoptosis.

Apoptosis may facilitate cell cycle arrest. Cyclins are cell cycle proteins that govern CDK activity, which controls the flipping of cell cycle checkpoint transitions. Ceramide analogs have been shown to trigger apoptosis and G0/G1 cell cycle arrest in PTC cells.[30] Similarly, we found that BG-induced cell cycle arrest occurred in BCPAP cells during the G0/G1 phase. Tumor initiation and progression are linked to cell cycle disruption.[31] As a result, it appears that the cell cycle is one of the primary therapeutic goals for the treatment of neoplasms. The cell cycle's transition from the G1 to the S stage is dependent on one of the cyclins, cyclin-D1, and many carcinomas have been found to have cyclin-D1 hyperactivity.[32,33] In the course of our investigation, BCPAP cells showed highly expressed cyclin-D1, C-Myc and survivin. Furthermore, BG therapy significantly reduced cyclin-D1, C-Myc and survivin mRNA expression, with previous work showing that BG was capable of restoring normal Bax, caspases, Bcl-2, and cyclin-D1 protein levels in human lung cancer cells A549 and NCIH460.[19] In summary, these findings indicate that BG was cytotoxic, caused BCPAP cell death and restricted their ability to multiply.

The PI3K/AKT/GSK-3 pathway promotes cell survival and apoptosis. AKT is essential for tumor growth and progression by promoting cell proliferation and inhibiting apoptosis.[34] AKT phosphorylates GSK-3, which is then involved in the regulation of cell viability, cell cycle progression and anti-apoptotic pathways.[35] Bergapten has been recently shown to downregulate the PI3K/Akt/GSK3 pathway in human breast cancer cells.[7,36] The current study found that BG lowered PI3K, AKT and GSK-3β phosphorylation, showing that BG affects the PI3K/AKT/GSK-3β pathway.

Limitations

In this research, we could not perform clinical PTC experiments. Further clinical studies are required on the therapeutic anti-cancer use of BG.

Conclusions

This study evaluated the anti-cancer and apoptotic effects of BG on PTC cells. Our findings revealed that BG inhibits the proliferation of BCPAP human PTC cells and promotes apoptosis via the PI3K/AKT/GSK-3β pathway by increasing the levels of Bax and caspases while decreasing the levels of Bcl-2, cyclin-D1, c-Myc, and survivin. Our findings show that BG has powerful anti-proliferative and apoptotic properties, making it a promising natural anti-cancer treatment for PTC. In vitro findings demonstrated that BG has anti-tumor effects on PTC cells. However, more research into BG's anti-cancer properties in vivo is needed.

Supplementary data

The supplementary materials are available at https://doi.org/10.5281/zenodo.10602882. The package contains the following files:

Supplementary Table 1. Results of the Kruskal–Wallis test as presented in Fig. 5.

Supplementary Table 2. Results of the Kruskal–Wallis test as presented in Fig. 6.

Supplementary Table 3. Results of the Kruskal–Wallis test as presented in Fig. 7.

Data availability

The datasets generated and/or analyzed during the current study are available from the corresponding author on reasonable request.

Consent for publication

Not applicable.

ORCID iDs

Jingjing Li ⓘ https://orcid.org/0009-0006-3316-1873
Shaik A. Hussain ⓘ https://orcid.org/0000-0001-6389-9146
Jayasimha R. Daddam ⓘ https://orcid.org/0000-0002-0666-8517
Mengjie Sun ⓘ https://orcid.org/0009-0000-7330-4003

References

1. Lee K, Anastasopoulou C, Chandran C, Cassaro S. Thyroid cancer. In: *StatPearls*. Treasure Island, USA: StatPearls Publishing; 2024:Bookshelf ID NBK459299. http://www.ncbi.nlm.nih.gov/books/NBK459299. Accessed February 13, 2024.
2. Limaiem F, Rehman A, Anastasopoulou C, Mazzoni T. Papillary thyroid carcinoma. In: *StatPearls*. Treasure Island, USA: StatPearls Publishing; 2024:Bookshelf ID NBK536943. http://www.ncbi.nlm.nih.gov/books/NBK536943. Accessed February 13, 2024.
3. Li Y, Che W, Yu Z, et al. The incidence trend of papillary thyroid carcinoma in the United States during 2003–2017. *Cancer Control*. 2022;29:107327482211354. doi:10.1177/10732748221135447
4. Zhao L, Wang L, Jia X, et al. The coexistence of genetic mutations in thyroid carcinoma predicts histopathological factors associated with a poor prognosis: A systematic review and network meta-analysis. *Front Oncol*. 2020;10:540238. doi:10.3389/fonc.2020.540238
5. Cheng F, Xiao J, Shao C, et al. Burden of thyroid cancer from 1990 to 2019 and projections of incidence and mortality until 2039 in China: Findings from global burden of disease study. *Front Endocrinol (Lausanne)*. 2021;12:738213. doi:10.3389/fendo.2021.738213
6. Mumtaz M, Lin LS, Hui KC, Mohd Khir AS. Radioiodine I-131 for the therapy of Graves' disease. *Malays J Med Sci*. 2009;16(1):25–33. PMID:22589645. PMCID:PMC3336179.
7. Nicolis E, Lampronti I, Dechecchi MC, et al. Modulation of expression of IL-8 gene in bronchial epithelial cells by 5-methoxypsoralen. *Int Immunopharmacol*. 2009;9(12):1411–1422. doi:10.1016/j.intimp.2009.08.013
8. Liang Y, Xie L, Liu K, et al. Bergapten: A review of its pharmacology, pharmacokinetics, and toxicity. *Phytother Res*. 2021;35(11):6131–6147. doi:10.1002/ptr.7221
9. Panno ML, Giordano F. Effects of psoralens as anti-tumoral agents in breast cancer cells. *World J Clin Oncol*. 2014;5(3):348. doi:10.5306/wjco.v5.i3.348
10. Guerrini A, Lampronti I, Bianchi N, et al. Bergamot (*Citrus bergamia* Risso) fruit extracts as γ-globin gene expression inducers: Phytochemical and functional perspectives. *J Agric Food Chem*. 2009;57(10):4103–4111. doi:10.1021/jf803489p
11. Yoo SW, Kim JS, Kang SS, et al. Constituents of the fruits and leaves of *Euodia daniellii*. *Arch Pharm Res*. 2002;25(6):824–830. doi:10.1007/BF02976999
12. Diwan R, Malpathak N. Furanocoumarins: Novel topoisomerase I inhibitors from *Ruta graveolens* L. *Bioorg Med Chem*. 2009;17(19):7052–7055. doi:10.1016/j.bmc.2009.04.023
13. Shaha AR. Implications of prognostic factors and risk groups in the management of differentiated thyroid cancer. *Laryngoscope*. 2004;114(3):393–402. doi:10.1097/00005537-200403000-00001
14. Kroemer G, El-Deiry WS, Golstein P, et al. Classification of cell death: Recommendations of the Nomenclature Committee on Cell Death. *Cell Death Differ*. 2005;12(Suppl 2):1463–1467. doi:10.1038/sj.cdd.4401724
15. Indran IR, Tufo G, Pervaiz S, Brenner C. Recent advances in apoptosis, mitochondria and drug resistance in cancer cells. *Biochim Biophys Acta*. 2011;1807(6):735–745. doi:10.1016/j.bbabio.2011.03.010
16. Li J, Yuan J. Caspases in apoptosis and beyond. *Oncogene*. 2008;27(48):6194–6206. doi:10.1038/onc.2008.297
17. Bellacosa A, De Feo D, Godwin AK, et al. Molecular alterations of the *AKT* 2 oncogene in ovarian and breast carcinomas. *Int J Cancer*. 1995;64(4):280–285. doi:10.1002/ijc.2910640412
18. Richardson JSM, Sethi G, Lee GS, Malek SNA. Chalepin: Isolated from *Ruta angustifolia* L. Pers induces mitochondrial mediated apoptosis in lung carcinoma cells. *BMC Complement Altern Med*. 2016;16(1):389. doi:10.1186/s12906-016-1368-6
19. Chiang S, Lin C, Lin H, Shieh P, Kao S. Bergapten induces G1 arrest of non-small cell lung cancer cells, associated with the p53-mediated cascade. *Mol Med Rep*. 2019;19(3):1972–1978. doi:10.3892/mmr.2019.9810
20. Mosmann T. Rapid colorimetric assay for cellular growth and survival: Application to proliferation and cytotoxicity assays. *J Immunol Methods*. 1983;65(1–2):55–63. doi:10.1016/0022-1759(83)90303-4
21. Kasibhatla S, Amarante-Mendes GP, Finucane D, Brunner T, Bossy-Wetzel E, Green DR. Acridine orange/ethidium bromide (AO/EB) staining to detect apoptosis. *Cold Spring Harb Protoc*. 2006;2006(3):pdb.prot4493. doi:10.1101/pdb.prot4493
22. Grimm D, Bauer J, Kossmehl P, et al. Simulated microgravity alters differentiation and increases apoptosis in human follicular thyroid carcinoma cells. *FASEB J*. 2002;16(6):604–606. doi:10.1096/fj.01-0673fje
23. Unuma K, Aki T, Funakoshi T, Hashimoto K, Uemura K. Extrusion of mitochondrial contents from lipopolysaccharide-stimulated cells: Involvement of autophagy. *Autophagy*. 2015;11(9):1520–1536. doi:10.1080/15548627.2015.1063765
24. Lee YM, Wu TH, Chen SF, Chung JG. Effect of 5-methoxypsoralen (5-MOP) on cell apoptosis and cell cycle in human hepatocellular carcinoma cell line. *Toxicol In Vitro*. 2003;17(3):279–287. doi:10.1016/S0887-2333(03)00014-6
25. Keane TE, Petros JA, Velimirovich B, Yue KT, Graham SD. Methoxypsoralen phototherapy of transitional cell carcinoma. *Urology*. 1994;44(6):842–846. doi:10.1016/S0090-4295(94)80168-1
26. Wu JZ, Situ ZQ, Wang W, Chen JY, Liu B. Antitumor activity of psoralen on mucoepidermoid carcinoma cell line MEC-1. *Chin Med J (Engl)*. 1992;105(11):913–917. PMID:1304460.
27. Gupta S, Afaq F, Mukhtar H. Involvement of nuclear factor-kappa B, Bax and Bcl-2 in induction of cell cycle arrest and apoptosis by apigenin in human prostate carcinoma cells. *Oncogene*. 2002;21(23):3727–3738. doi:10.1038/sj.onc.1205474
28. Emi M, Kim R, Tanabe K, Uchida Y, Toge T. Targeted therapy against Bcl-2-related proteins in breast cancer cells. *Breast Cancer Res*. 2005;7(6):R940–R952. doi:10.1186/bcr1323
29. Xu X, Zhang Y, Qu D, Jiang T, Li S. Osthole induces G2/M arrest and apoptosis in lung cancer A549 cells by modulating PI3K/Akt pathway. *J Exp Clin Cancer Res*. 2011;30(1):33. doi:10.1186/1756-9966-30-33
30. Rossi MJ, Sundararaj K, Koybasi S, et al. Inhibition of growth and telomerase activity by novel cationic ceramide analogs with high solubility in human head and neck squamous cell carcinoma cells. *Otolaryngol Head Neck Surg*. 2005;132(1):55–62. doi:10.1016/j.otohns.2004.08.015
31. Drexler H. Review of alterations of the cyclin-dependent kinase inhibitor *INK4* family genes p15, p16, p18 and p19 in human leukemia–lymphoma cells. *Leukemia*. 1998;12(6):845–859. doi:10.1038/sj.leu.2401043

32. Xiao-Ping H, Tie-Hua R, Peng L, et al. Cyclin D1 overexpression in esophageal cancer from southern China and its clinical significance. *Cancer Lett*. 2006;231(1):94–101. doi:10.1016/j.canlet.2005.01.040

33. Li W, Wen C, Bai H, et al. JNK signaling pathway is involved in piper-longumine-mediated apoptosis in human colorectal cancer HCT116 cells. *Oncol Lett*. 2015;10(2):709–715. doi:10.3892/ol.2015.3371

34. Choi MJ, Park EJ, Oh JH, et al. Cafestol, a coffee-specific diterpene, induces apoptosis in renal carcinoma Caki cells through down-regulation of anti-apoptotic proteins and Akt phosphorylation. *Chem Biol Interact*. 2011;190(2–3):102–108. doi:10.1016/j.cbi.2011.02.013

35. Arafa ESA, Zhu Q, Barakat BM, et al. Tangeretin sensitizes cisplat-in-resistant human ovarian cancer cells through downregulation of phosphoinositide 3-kinase/Akt signaling pathway. *Cancer Res*. 2009;69(23):8910–8917. doi:10.1158/0008-5472.CAN-09-1543

36. Santoro M, Guido C, De Amicis F, et al. Bergapten induces meta-bolic reprogramming in breast cancer cells. *Oncol Rep*. 2016;35(1): 568–576. doi:10.3892/or.2015.4327

Recombinant Klotho protein protects pulmonary alveolar epithelial cells against sepsis-induced apoptosis by inhibiting the Bcl-2/Bax/caspase-3 pathway

Xiao Bo Li[1,2,A–C,E,F], Jia Li Liu[1,2,B,C], Shuang Zhao[1,2,C], Jing Li[1,2,B,D], Guang-Yan Zhang[1,2,C,D], Qing Tang[1,2,B], Wei Yong Chen[1,2,A,C]

[1] Respiratory Department, Chengdu Seventh People's Hospital, China

[2] Respiratory Department, Tumor Hospital Affiliated to Chengdu Medical College, China

A – research concept and design; B – collection and/or assembly of data; C – data analysis and interpretation;
D – writing the article; E – critical revision of the article; F – final approval of the article

Address for correspondence
Xiao Bo Li
E-mail: xiaoboli2023@163.com

Abstract

Background. Inflammation-induced apoptosis of alveolar type II epithelial cells is a primary contributor to sepsis-induced acute respiratory distress syndrome (ARDS). Klotho is a single-pass transmembrane protein with anti-inflammatory and anti-apoptotic effects. However, the role and mechanism of Klotho in the development of ARDS remains unknown.

Objectives. This study aimed to investigate the effect of Klotho on sepsis-induced apoptosis in human pulmonary alveolar epithelial cells (HPAEpiCs) together with the potential mechanism.

Materials and methods. Cecal ligation and puncture (CLP) were performed to generate an in vivo sepsis model, and HPAEpiCs were treated with lipopolysaccharide (LPS) to mimic sepsis in vitro. Both models were administered recombinant Klotho protein. The morphology of the lung tissue was observed, and apoptotic cells and cell viability were detected. Interleukin (IL)-1β, IL-6, and tumor necrosis factor alpha (TNF-α) levels were detected using enzyme-linked immunosorbent assay (ELISA), while the expression of Bcl-2, Bax and cleaved caspase-3 was detected with western blotting.

Results. Klotho reversed the CLP-induced decrease in mouse survival in vivo (p < 0.001) and increased inflammatory cell infiltration and inflammatory substance exudation in the lung tissue of mice with sepsis (both p < 0.001). Klotho also suppressed apoptosis (p < 0.001) as demonstrated by IL-1β, IL-6 and TNF-α expression (all p < 0.001), and Bcl-2/Bax/caspase-3 pathway activation (p < 0.001). Klotho pretreatment significantly prevented LPS-induced apoptosis in vitro (p < 0.001), as demonstrated by IL-1β, IL-6 and TNF-α upregulation (all p < 0.001); and Bcl-2/Bax/caspase-3 pathway activation in HPAEpiCs (p < 0.001).

Conclusions. This study demonstrated that Klotho can ameliorate acute lung injury (ALI) induced by sepsis by inhibiting inflammatory responses and exerting anti-apoptotic effects by suppressing Bcl-2/Bax/caspase-3 pathway activation.

Key words: sepsis, ARDS, apoptosis, Klotho, HPAEpiC

124

X. Li et al. Klotho against LPS induced HPAEpiC apoptosis

Background

Sepsis is a life-threatening inflammatory response, with approx. 30% mortality rate.[1] The lungs are the most vulnerable organ attacked by inflammatory factors during sepsis, and sepsis progresses to acute respiratory distress syndrome (ARDS) in approx. 50% of patients.[2] Although great progress has been made recently in the treatment of ARDS, its morbidity and mortality remain high.[3] Therefore, understanding the complex pathogenesis of ARDS is of great significance. Acute respiratory distress syndrome is a complex clinical syndrome with a heterogeneous clinical phenotype, and it is characterized by pulmonary edema in the interstitium and air spaces of the lungs. The accumulation of fluid increases the work of breathing and impairs gas exchange, resulting in hypoxemia, reduced CO_2 excretion and, ultimately, acute respiratory failure.[4] Acute respiratory failure ultimately leads to hypoxia, which has a poor prognosis.[5,6] Furthermore, acute respiratory failure is among the sequela of complications that can develop in response to sepsis, which can induce severe inflammatory responses.[7]

Sepsis is facilitated by bacterial infections inducing the excessive release of inflammatory cytokines, such as tumor necrosis factor alpha (TNF-α), interleukin (IL)-1 and IL-6, causing cellular injury and multiple organ dysfunction syndrome.[8] Lipopolysaccharide (LPS) is a bacterial endotoxin that can induce a severe inflammatory response.[9] Lipopolysaccharide is commonly used to establish murine lung injury models to mimic sepsis-induced ARDS in humans, and such models help investigate the pathogenesis of ARDS.[10] Alveolar epithelial cell apoptosis complicates the pathogenesis of ARDS.[11] Apoptosis can be activated by 2 pathways, namely, the mitochondrial pathway and the external death receptor pathway. When cells encounter direct or indirect DNA damage, reactive oxygen species (ROS), hypoxia, or inflammation, the mitochondrial apoptosis pathway is activated.[12,13] These stimuli ultimately disrupt mitochondrial function by inducing the expression of proapoptotic Bcl-2 family members, such as Bcl-2, Bax and Bak.[14] The imbalance of Bax and Bcl-2 can induce the activation of caspase-3,[15] thereby promoting apoptosis.[16] Many studies have revealed that LPS induces apoptosis in HPAEpiCs.[17,18] However, the mechanism of LPS-induced HPAEpiCs apoptosis has not yet been fully elucidated.

It has been reported that acute inflammation/sepsis suppresses the activation of α-Klotho, and α-Klotho upregulation during acute sepsis may participate in the counterregulatory response to severe inflammation in patients with sepsis.[19] Klotho deficiency aggravates sepsis-related multiple organ dysfunction.[20] Klotho has been recognized as a gene involved in the aging process in mammals for more than 30 years,[21] and this single-pass transmembrane protein counteracts oxidative stress[22] and cell senescence[23] and promotes autophagy.[24] In addition, Klotho has anti-apoptotic effects.[25] Klotho suppresses diabetes-induced podocyte apoptosis[26] and inhibits H_2O_2-induced apoptosis in periodontal ligament stem cells.[27] Normal lungs do not express Klotho protein, but they can obtain cell protection from soluble circulating Klotho.[28] However, the effect of Klotho on sepsis-induced apoptosis in alveolar epithelial cells has not been reported. Chen et al. revealed that Klotho can inhibit proliferation and increase apoptosis in A549 cells by regulating the expression of the apoptosis-related genes Bcl-2 and Bax.[29] Therefore, we hypothesized that Klotho protects alveolar epithelial cells against sepsis or LPS-induced apoptosis by inhibiting the Bcl-2/Bax/caspase-3 pathway.

Objectives

The objective of this study was to explore the effects of Klotho on sepsis-induced inflammatory cytokine release and LPS-induced HPAEpiC apoptosis and demonstrate the potential mechanism of Klotho protects HPAEpiC against sepsis or LPS-induced apoptosis.

Materials and methods

Cecal ligation and puncture (CLP) were performed to generate a mouse sepsis model, and HPAEpiCs were treated with LPS to create an in vitro model of sepsis-induced ARDS. Both models were treated with recombinant Klotho protein to explore its effects on sepsis-induced alveolar type II epithelial cells and its potential mechanism.

Cell culture

The HPAEpiC was brought from the American Type Culture Collection (ATCC, Manassas, USA). The cells were cultured in a high glucose Dulbecco's modified Eagle's medium (DMEM) containing 10% fetal bovine serum (FBS) and incubated at 37°C under 5% CO_2 and 95% humidity; then, cells were passaged when confluence reached 90%. The use of HPAEpiC was approved by the Human Ethics Committee of Chengdu Seventh People's Hospital on January 26, 2022 (Human Experimental Inspection Form of Chengdu Seventh People's Hospital No. 2200647).

Animals and treatment

The C57BL/6 mice (male, 8 weeks old, weight = 20–25 g) were purchased from ENSIWEIER Biotechnology Co., LTD (Chongqing, China). The mice were supplied sterile water and food and kept in a specific pathogen-free environment (temperature: 22°C ±2°C; humidity: 40–60%). The animal experiment was approved by the Animal Ethics Committee of Chengdu Seventh People's Hospital on January 13, 2022 (Animal Experimental Ethical

Inspection Form of Chengdu Seventh People's Hospital No. 2200638). The mice were randomly divided into 4 groups, namely, the sham, Klotho, CLP, and CLP+Klotho groups (n = 10/group). Mice in the sham group underwent sham operation without CLP, whereas mice in the Klotho group were intraperitoneally injected with recombinant mouse Klotho protein (10 μg/kg; R&D Systems, Minneapolis, USA). Mice in the CLP group underwent CLP, and those in the CLP+Klotho group underwent CLP, followed by intraperitoneal treatment with recombinant mouse Klotho protein. Them, 24 h after CLP, 2% isoflurane was used to anesthetize the mice, which were euthanized via cervical dislocation, and their lungs were collected for hematoxylin and eosin (H&E) staining, terminal deoxynucleotidyl transferase-mediated biotinylated UTP labeling (TUNEL) assay and western blotting.

Cecal ligation and puncture mouse model

Cecal ligation and puncture mouse model was created as described previously.[30] In brief, after anesthesia was induced with 2% isoflurane, the cecum of each mouse was completely exposed through an abdominal surface incision. Then, 70% of the total length of the cecum was ligated with a 4-0 silk suture and a penetrating puncture was performed with a No. 22 needle (BD Biosciences, Franklin Lakes, USA). Sham-operated mice underwent the same procedure without ligation and puncture of the cecum.

Humane endpoints of surgery/treatment in mice

Several evaluation items are often used as the endpoints of animal experiments. First, experiments may cause pain and discomfort to animals. If drugs or other methods cannot be used to relieve their pain and distress, euthanasia is performed. Second, animals should be euthanized in response to the rapid weight loss of 15–20% or cachexia and long-term muscle catabolism. Third, animals should be euthanized if they do not eat for 24–48 h or if they ingest only a small amount of food for 3 days. Lastly, animals should be euthanized when they cannot drink or eat by themselves.

Survival studies

Survival rates were assessed as described by Alves et al.[31] To evaluate the effect of Klotho on the survival of mice with sepsis, 80 mice were randomly divided into the sham, Klotho, CLP, and CLP+Klotho groups (n = 20/group). The mice in the CLP+Klotho and Klotho groups received intraperitoneal injections of 10 μg/kg Klotho once daily. Survival curves were plotted every 6–12 h for 7 consecutive days. After 7 days, 2% isoflurane was used to anesthetize the surviving mice, which were euthanized via cervical dislocation.

Collection of bronchoalveolar lavage fluid and cell culture medium for IL-1β, IL-6 and TNF-α detection

Bronchoalveolar lavage fluid (BALF) was collected as previously described.[32] In brief, all mice were anesthetized with 2% isoflurane and immediately subjected to thoracotomy, and the right great bronchus below the tracheal bifurcation was ligated. Then, the left bronchial tube was intubated and rinsed 3 times with ice-cold phosphate-buffered saline (PBS) (0.5 mL). The mice were sacrificed via cervical dislocation under anesthesia. We also collected the culture medium of HPAEpiCs. In brief, the cells were treated with 0.1 mg/L, 1 mg/L or 10 mg/L LPS or 10 mg/L LPS combined with 50 mg/L recombinant Klotho for 24 h; then, the conditioned culture media was collected. The collected BALF and cell culture medium were centrifuged at 1000 × g and 4°C for 10 min. The supernatant was stored at −80°C for further analysis. The total protein level was detected using the bicinchoninic acid (BCA) assay kit (Beyotime Biotechnology, Shanghai, China), and the protein concentration was standardized before enzyme-linked immunosorbent assay (ELISA) detection (Beyotime Biotechnology) of IL-1β, IL-6 and TNF-α in BALF and cell culture medium according to the manufacturer's protocol.

Hematoxylin and eosin staining

Morphological changes in the lungs of mice were evaluated with H&E staining.[33] In brief, paraffin sections of lung tissue were soaked in xylene I and xylene II for 10 min. Then, the sections were successively incubated in 100% (I, II), 90%, 80%, and 70% alcohol for 5 min each and rinsed 3 times with running water for 5 min each. Finally, the sections were stained with hematoxylin for 5 min and eosin (1%) staining for 2 min, then rinsed with water. Images of the lung tissues were captured (magnification: ×400) using an optical microscope (Leica DFC550 DM4 B; Leica Camera AG, Wetzlar, Germany).

TUNEL assay

To detect apoptosis in lung tissue in situ, we used a TUNEL kit.[34] In brief, 5-μm-thick paraffin sections of lung tissue were dewaxed, rehydrated, and treated with protease K working solution for 30 min. The slides were then incubated in the TUNEL reaction mixture at 37°C for 1 h. The slides were stained with 4′,6-diamidino-2-phenylindole (DAPI) for 5 min, and the tissue was mounted in an Anti-Fade Mounting Medium. Images of the lung tissues were captured using an optical microscope (magnification ×200; Leica DFC550 DM4 B).

Cell Counting Kit-8 cell viability assay

Changes in cell viability were determined using the Cell Counting Kit-8 (CCK-8) assay.[35] In brief, HPAEpiCs (5×10^3/well) were plated in 96-well plates. The cells were exposed to LPS (0.1 mg/L, 1 mg/L or 10 mg/L) for 24 h or 10 mg/L LPS for 12 h, 24 h or 48 h. Then, 10 μL of CCK-8 was added to each well. The absorption of each well was read at 450 nm using a microplate reader (Bio-Rad 680; Bio-Rad Hercules, USA). In addition, cells were pretreated with 10 mg/L LPS for 1 h and then incubated with various concentrations (0 mg/L, 50 mg/L and 100 mg/L) of recombinant Klotho protein for 24 h or 50 mg/L recombinant Klotho protein for 12 h, 24 h or 48 h. Cell Counting Kit-8 was added to each well as previously described, and the plate was incubated at 37°C for 1 h. The absorption of each well was read at 450 nm using a microplate reader (Bio-Rad 680; Bio-Rad).

Annexin/propidium iodide (PI) staining

Annexin V/propidium iodide (PI) staining was used to investigate cell apoptosis.[36] In brief, cells were exposed to 0.1 mg/L, 1 mg/L or 10 mg/L LPS or 10 mg/L LPS combined with 50 mg/L recombinant Klotho for 24 h. Untreated cells served as the control group. The cells were then harvested and washed with PBS to remove the medium. At least 1×10^5 cells were resuspended in 100 μL of binding buffer containing Annexin V–FITC and PI and incubated for another 15 min at room temperature in the dark. Fluorescence from 1×10^4 cells in the Annexin V–FITC and PI binding channels FL-1 (Annexin V–FITC) and FL-3 (PI) was quantified using FACScan and analyzed using Cellquest Pro (BD Biosciences, Franklin Lakes, USA).

Western blotting

Protein expression was detected with western blotting as previously described.[37] The cells and lung tissue of mice were lysed using radioimmunoprecipitation assay (RIPA) lysis buffer containing protease and phosphatase inhibitors and centrifuged for 15 min at $12,700 \times g$ and 4°C. The supernatant was collected, the protein concentration was measured, and the samples were boiled for 5 min. Then, 30 μg of protein was electrophoresed on an 8% sodium dodecyl sulfate-polyacrylamide gel electrophoresis (SDS-PAGE) gel, transferred to a polyvinylidene difluoride (PVDF) membrane, and blocked with 5% skim milk at room temperature for 2 h. The membrane was incubated overnight with primary antibodies against GAPDH (ab8245; 1:5000), Bcl-2 (ab182858; 1:1000), Bax (ab32503; 1:1000), pro-caspase-3 (ab32499; 1:1000), and cleaved caspase-3 (ab214430; ab2302; 1:1000; all from: Abcam, Cambridge, UK) at 4°C, then washed 3 times with Tris-buffered saline containing 0.1% Tween-20, then incubated with HRP Anti-Rabbit IgG antibody (ab288151; 1:10000; Abcam) for 2 h. The protein bands were visualized using

chemiluminescence and analyzed using Quantity One software v. 6.0 (Bio-Rad).

Statistical analyses

All experiments were repeated at least 3 times, and data were expressed as the mean ± standard deviation (M ± SD). All the data were analyzed using GraphPad Prism 8.0 (GraphPad Software, San Diego, USA). Statistical significance was indicated by $p < 0.05$. Quantitative data were presented as dots and medians. The survival analysis between groups used the log-rank (Mantel–Cox) method, and due to the limited sample size, other data were assessed with non-parametric tests. The Kruskal–Wallis test was used for a comparison of 3 or more groups, followed by Dunn's post hoc test. The medians and quartiles were presented in supplement tables. The test levels of α = 0.05 and $p < 0.05$ were considered significant.

Results

Klotho increased mouse survival and decreased IL-1β, IL-6 and TNF-α levels

To determine the effects of Klotho on mice with sepsis, mice that underwent CLP were intraperitoneally injected with recombinant Klotho protein. All mice in the CLP group died on day 4, whereas 40% of those in the CLP+Klotho group survived ($p < 0.002$, Fig. 1A). Hematoxylin and eosin staining of mouse lung tissue in the CLP group revealed swelling, cell edema, inflammatory cell infiltration, and inflammatory mediator exudation, and these effects were ameliorated by Klotho treatment (Fig. 1B). We also detected IL-1β, IL-6 and TNF-α in the BALF of mice. The results showed that IL-1β ($p < 0.001$), IL-6 ($p < 0.001$) and TNF-α ($p < 0.001$) levels were significantly higher in the CLP group compared to the sham group, and these increases were significantly reduced by Klotho treatment (all $p < 0.05$; Fig. 1C–E).

Effects of Klotho on alveolar epithelial cell apoptosis and Bcl-2/Bax/caspase-3 signaling in mice with sepsis

To detect the effect of Klotho on alveolar epithelial cell apoptosis in mice with sepsis, apoptotic cells were detected using TUNEL staining. The number of TUNEL-positive cells was significantly higher in the CLP group compared to sham mice ($p < 0.001$) and CLP+Klotho groups ($p < 0.05$; Fig. 2A,B). We also detected the protein levels of Bcl-2, Bax and caspase-3 in the lung tissue of mice, finding that CLP decreased the Bcl-2/GAPDH ratio ($p < 0.001$) and increased the Bax/GAPDH ($p < 0.001$) and cleaved caspase-3/caspase-3 ratios ($p < 0.001$); and these effects were reversed by Klotho treatment (all $p < 0.05$; Fig. 2C,D).
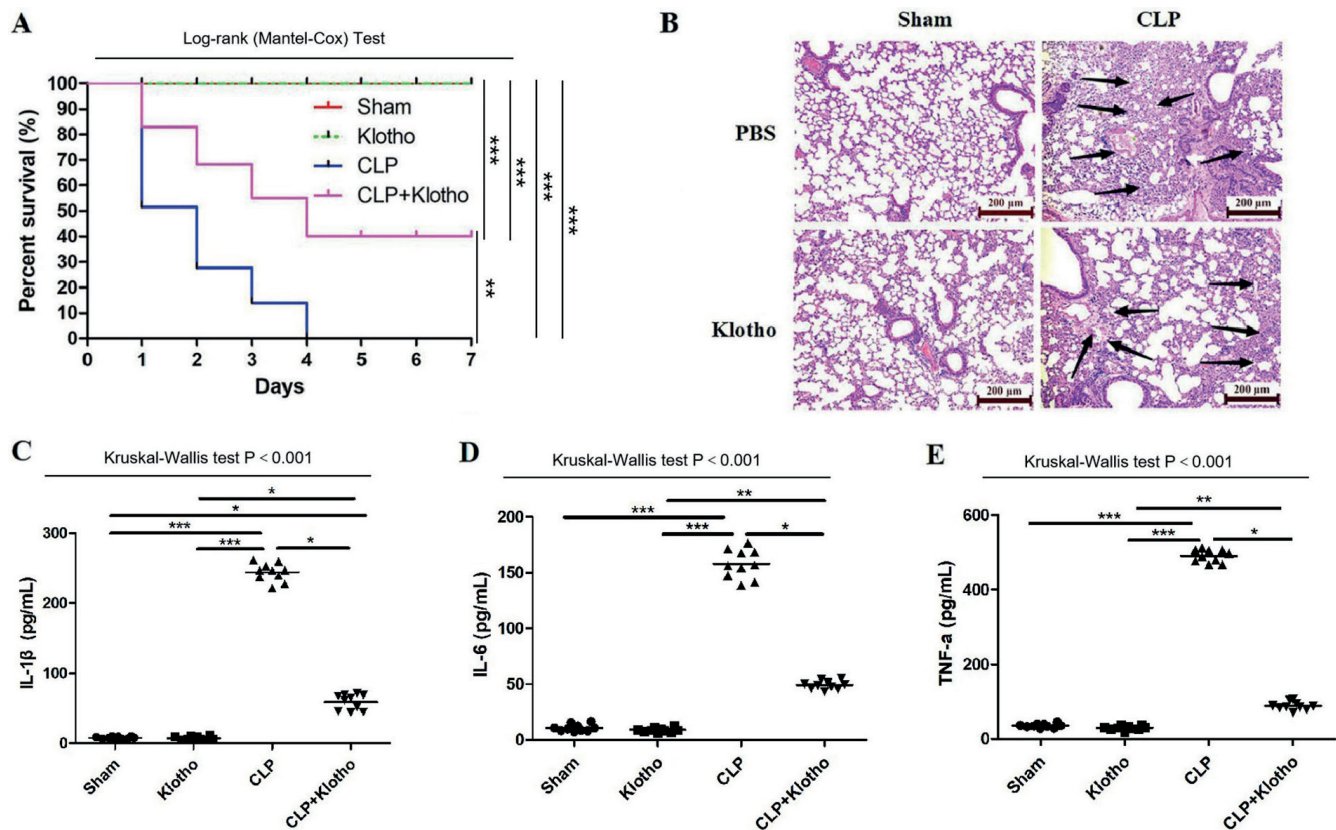
Fig. 1. Klotho increased the survival of mice with sepsis and decreased the release of interleukin (IL)-1β, IL-6 and tumor necrosis factor alpha (TNF-α).
A. The survival rates of mice in the sham, Klotho, cecal ligation and puncture (CLP), and Klotho+CLP groups (n = 20/group) were analyzed. Data were analyzed with the log-rank (Mantel–Cox) test; **p < 0.002 compared with the CLP group; ***p < 0.001 compared with the CLP group or CLP+Klotho group.
B. Hematoxylin and eosin (H&E) staining was performed to detect the morphological structure of the lung tissue of mice in the 4 groups (n = 10/group).
C–E. IL-1β, IL-6, and TNF-α levels were measured (n = 10/group). The graph presents the results of data dots and medians. Data were analyzed with the Kruskal–Wallis test, and then Dunn's multiple comparison test was used for post hoc analysis; ***p < 0.001 compared with the CLP group; *p < 0.05 and **p < 0.01 compared with the CLP+Klotho group

Lipopolysaccharide-induced apoptosis, inflammatory factor release and Bcl-2/Bax/caspase-3 pathway activation in HPAEpiCs

Human pulmonary alveolar epithelial cells were exposed to 0.1 mg/L, 1 mg/L or 10 mg/L LPS for 24 h or 10 mg/L LPS for 12 h, 24 h and 48 h, followed by cell viability assessment. The results showed that LPS reduced cell viability in a concentration- (p < 0.05; Fig. 3A) and time-dependent manner (p < 0.05; Fig. 3B). The apoptotic rate of HPAEpiCs was tested using Annexin/PI staining. Lipopolysaccharide significantly increased the percentage of apoptotic cells compared with that in the control group (p < 0.05; Fig. 3C–D). In addition, 10 mg/L LPS significantly increased the release of IL-1β (p < 0.05), IL-6 (p < 0.05) and TNF-α (p < 0.05; Fig. 3E–G).

Because LPS induced HPAEpiC apoptosis, we detected the protein expression of Bcl-2, Bax and cleaved caspase-3 in LPS-treated cells. The results illustrated that LPS decreased the Bcl-2/GAPDH ratio (p < 0.01) and increased the Bax/GAPDH and cleaved caspase-3/pro-caspase-3 ratios (both p < 0.05; Fig. 3H–K). These results indicated that LPS induced apoptosis and Bcl-2/Bax/caspase-3 pathway activation in HPAEpiCs.

Effect of recombinant Klotho protein on viability, apoptosis and inflammatory factor release in LPS-exposed HPAEpiCs

To explore the effect of Klotho protein on the viability of LPS-exposed HPAEpiCs, we treated HPAEpiCs with LPS (10 mg/L) for 1 h followed by incubation with 10 mg/L, 50 mg/L or 100 mg/L recombinant Klotho for 24 h or 50 mg/L recombinant Klotho protein for 12 h, 24 h or 48 h. The results indicated that recombinant Klotho protein reversed the LPS-induced decrease in cell viability in a concentration- (p < 0.05; Fig. 4A) and time-dependent manner (p < 0.001; Fig. 4B). The apoptotic rate of HPAEpiCs was tested using Annexin/PI staining (Fig. 4C). As previously observed, 10 mg/L LPS induced significant apoptosis in HPAEpiCs (p < 0.01), and this effect was reversed by 50 mg/L recombinant Klotho protein treatment (p < 0.05; Fig. 4D). In addition, recombinant Klotho protein treatment reversed the LPS-induced release of IL-1β, IL-6 and TNF-α (all p < 0.05; Fig. 4E–G).
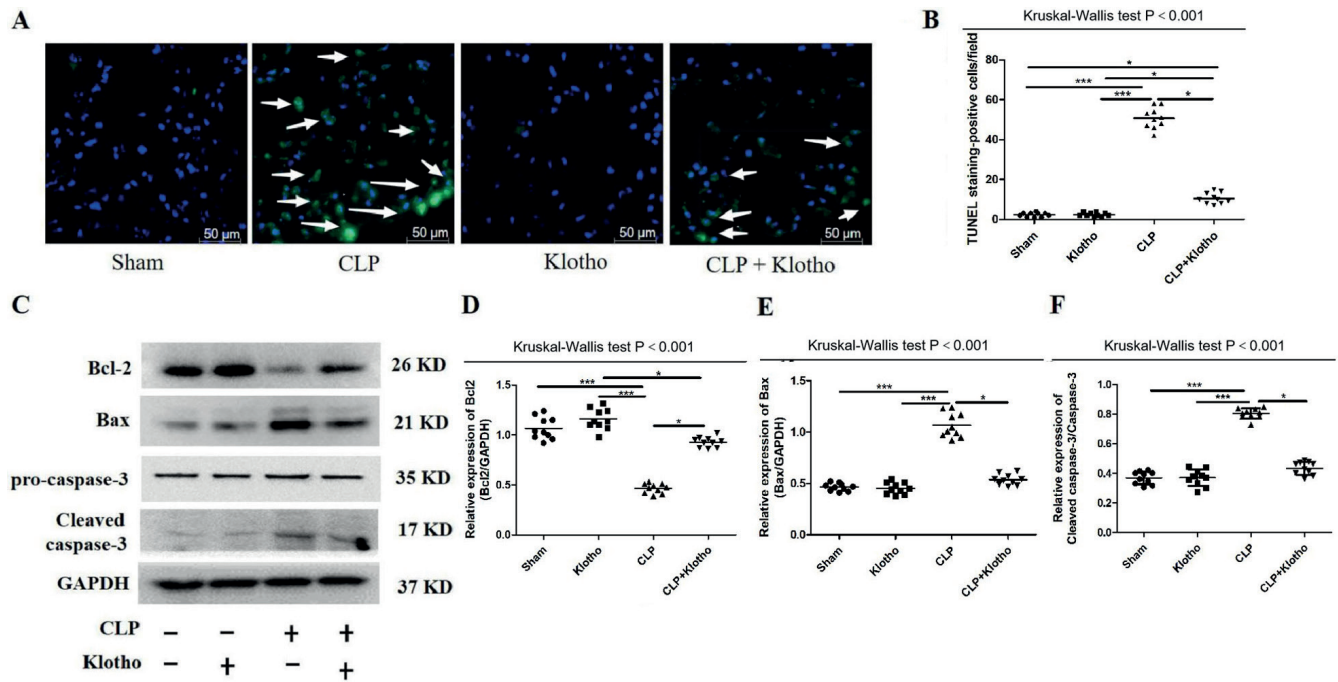
Fig. 2. Effects of Klotho on alveolar epithelial cell apoptosis and Bcl-2/Bax/caspase-3 signaling in mice with sepsis. A,B. The terminal deoxynucleotidyl transferase-mediated biotinylated UTP labeling (TUNEL) assay was performed to detect apoptotic cells in the lung tissues of mice in the sham, cecal ligation and puncture (CLP), Klotho, and CLP+Klotho groups (n = 10/group). TUNEL-positive cells were counted and compared among the groups. The graph presents the results of data dots and medians. The data were analyzed with the Kruskal–Wallis test, and then Dunn's multiple comparison test was used for post hoc analysis; *p < 0.05 and ***p < 0.001 compared with the CLP group. C–F. Western blotting was performed to detect the expression of Bcl-2, Bax, pro-caspase-3, and cleaved caspase-3. The graph presents the results of data dots and medians. The data were analyzed with the Kruskal–Wallis test, and then the Dunn's multiple comparison test was used for post hoc analysis; *p < 0.05 and ***p < 0.001 compared with the CLP group

Recombinant Klotho protein blocked Bcl-2/Bax/caspase-3 signaling in LPS-exposed HPAEpiCs

The cells were treated with LPS (10 mg/L) for 1 h and then incubated with 50 mg/L recombinant Klotho protein, after which we detected the protein expression of Bcl-2, Bax, pro-caspase-3, and cleaved caspase-3. The results demonstrated that LPS decreased the Bcl-2/GAPDH ratio and increased the Bax/GAPDH and cleaved caspase-3/pro-caspase-3 ratios (all p < 0.01), and these effects were partially reversed by recombinant Klotho protein administration (all p < 0.05; Fig. 5A–D).

Discussion

In vivo, we found that recombinant Klotho protein significantly reduced the inflammatory response and percentage of apoptotic cells in lung tissue, increased the survival rate of mice with sepsis and prevented the activation of BCL-2/Bax/caspase-3 signaling. Moreover, we observed that Klotho increased the viability and decreased the apoptosis of HPAEpiCs exposed to LPS in vitro. Finally, we demonstrated that LPS activated the Bcl-2/Bax/caspase-3 pathway, which was inhibited by Klotho.

The lungs represent the initial organ affected by inflammation in sepsis.[38] Sepsis causes severe systemic inflammatory response syndrome, leading to ARDS/

Fig. 3. Lipopolysaccharide induced apoptosis and activated the Bcl-2/Bax/caspase-3 pathway in human pulmonary alveolar epithelial cells (HPAEpiCs). A. Human pulmonary alveolar epithelial cells were exposed to 0.1 mg/L, 1 mg/L or 10 mg/L LPS for 24 h, and then the Cell Counting Kit-8 (CCK-8) assay was performed to detect cell viability. The graph presents the results of data dots and medians. Data were analyzed with the Kruskal–Wallis test. The Dunn's multiple comparison test was used for post hoc analysis; *p < 0.05 compared with the control group. B. Human pulmonary alveolar epithelial cells were exposed to 10 mg/L LPS, and the CCK-8 assay was performed to detect cell viability after 12 h, 24 h and 48 h. The graph presents the results of data dots and medians. Data were analyzed with the Kruskal–Wallis test. A Dunn's multiple comparison test was used for post hoc analysis; *p < 0.05 compared with the control (0 h) group. C–D. Human pulmonary alveolar epithelial cells were treated with LPS (0.1 mg/L, 1 mg/L or 10 mg/L) for 24 h, and the apoptosis rate was determined with flow cytometry. The graph presents the results of data dots and medians. Data were analyzed with the Kruskal–Wallis test. The Dunn's multiple comparison test was used for post hoc analysis; *p < 0.05 compared with the control group. E–G. Interleukin (IL)-1β, IL-6, and tumor necrosis factor alpha (TNF-α) levels were detected using enzyme-linked immunosorbent assay (ELISA). The graph presents the results of data dots and medians. Data were analyzed with the Kruskal–Wallis test. The Dunn's multiple comparison test was used for post hoc analysis; *p < 0.05 compared with the control group. H. Human pulmonary alveolar epithelial cells were treated with 0.1 mg/L, 1 mg/L or 10 mg/L LPS for 24 h, and the expression of Bcl-2, Bax, pro-caspase-3, and cleaved caspase-3 was detected with western blotting. I–K. The graph presents the results of data dots and medians. Data were analyzed with the Kruskal–Wallis test. The Dunn's multiple comparison test was used for post hoc analysis; *p < 0.05 and **p < 0.01 compared with the control group
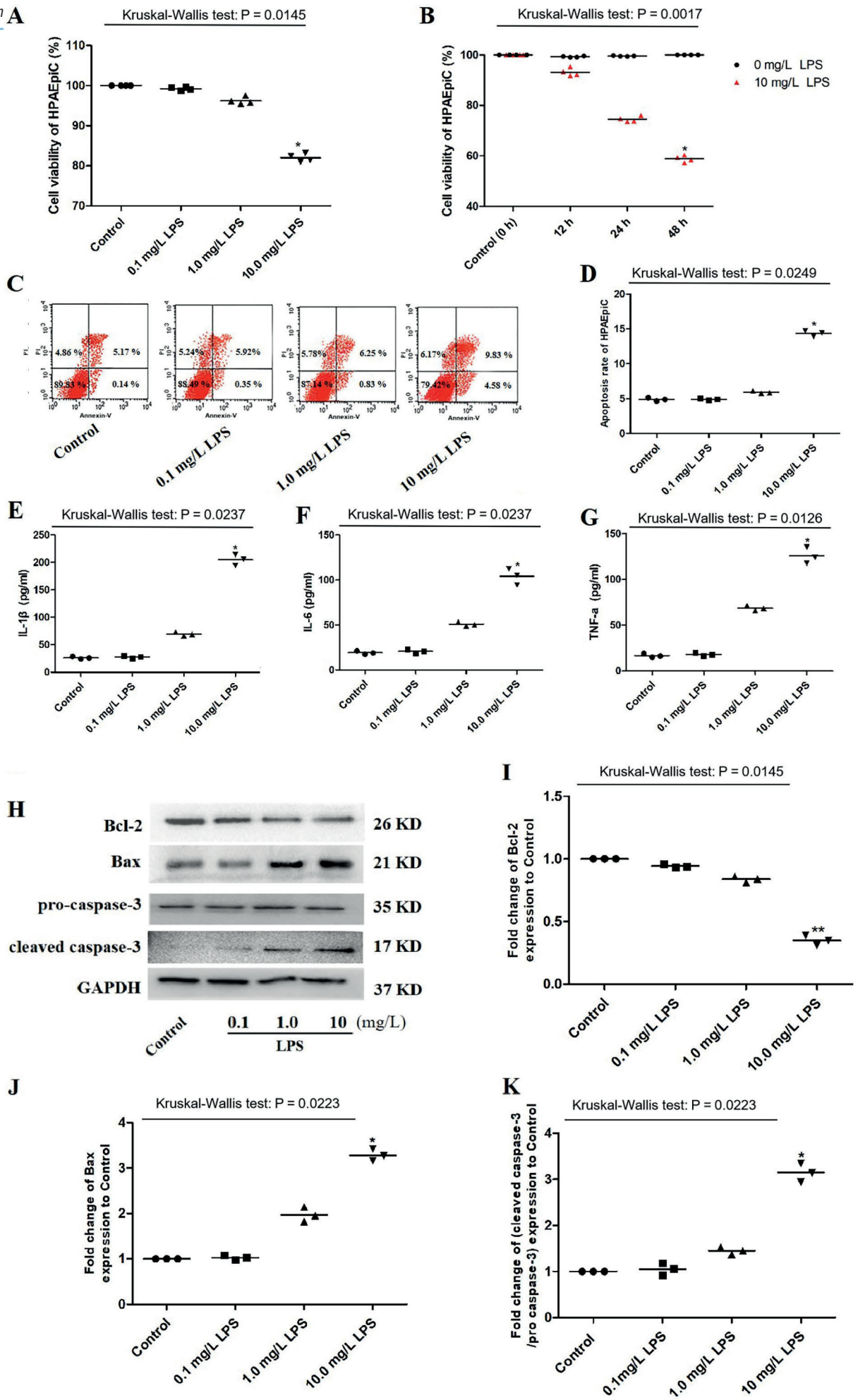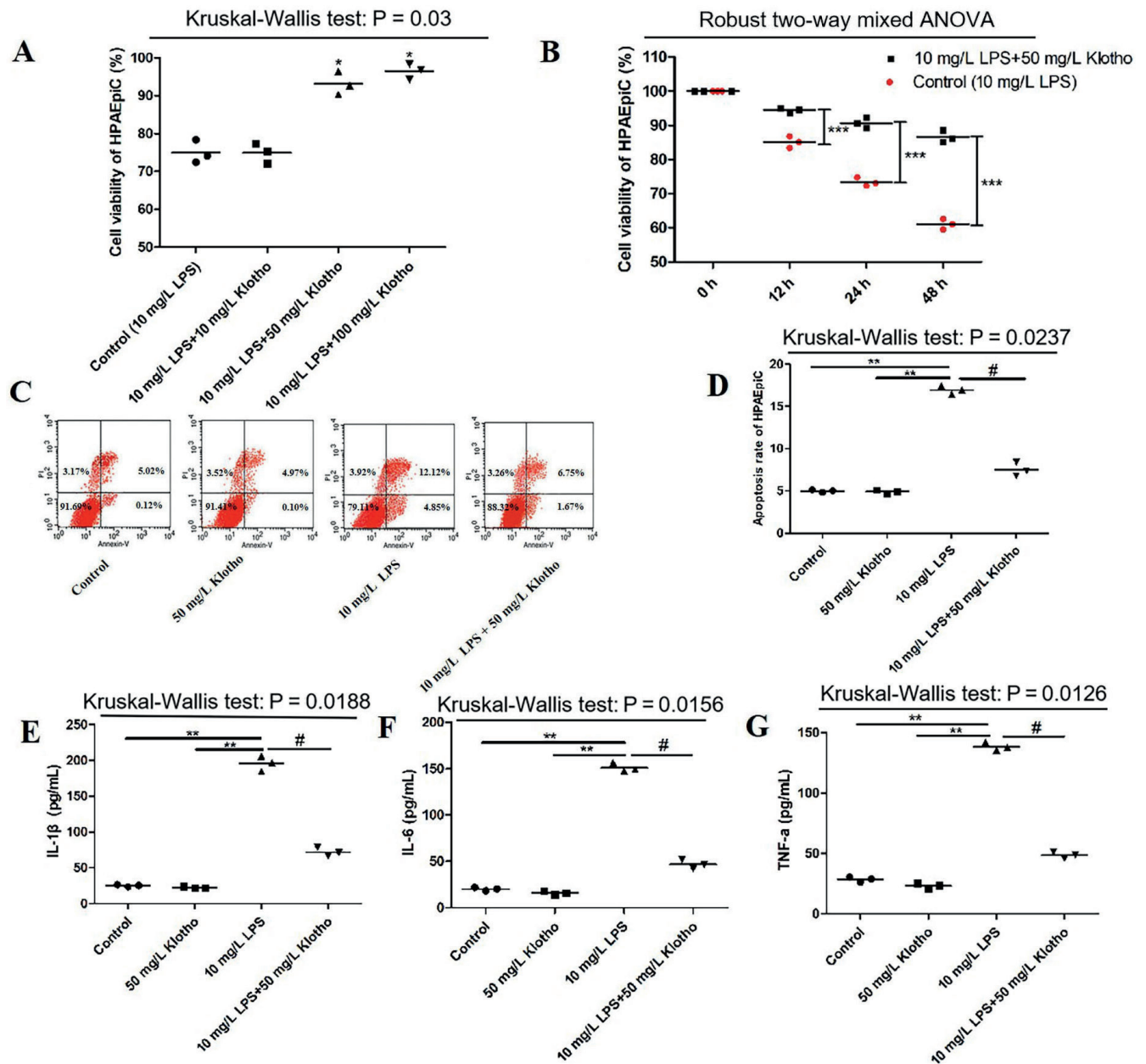
Fig. 4. Effects of recombinant Klotho protein on cell viability, apoptosis and inflammatory factor expression in lipopolysaccharide-treated human pulmonary alveolar epithelial cells. A. Human pulmonary alveolar epithelial cells were pretreated with 10 mg/L lipopolysaccharide (LPS) for 1 h and then incubated with various concentrations of recombinant Klotho (10 mg/L. 50 mg/L and and 100 mg/L) for 24 h. The Cell Counting Kit-8 (CCK-8) assay was performed to detect cell viability. The graph presents the results of data dots and medians. Data were analyzed with the Kruskal–Wallis test. The Dunn's multiple comparison test was used for post hoc analysis; *p < 0.05 compared with the control group; B. Human pulmonary alveolar epithelial cells were pretreated with 10 mg/L LPS for 1 h, followed by treatment with 50 mg/L recombinant Klotho protein for different periods (12 h, 24 h and 48 h). Cell viability was assessed using the CCK-8 assay. The graph presents the results of data dots and medians. Data were analyzed with Robust 2-way mixed analysis of variance (ANOVA) using WRS2 package; ***p < 0.001 compared with the control group. C,D. Cells were pretreated with 10 mg/L LPS for 1 h followed by incubation with 50 mg/L recombinant Klotho protein for 24 h. The apoptosis rate was determined with flow cytometry. The graph presents the results of data dots and medians. Data were analyzed with the Kruskal–Wallis test. The Dunn's multiple comparison test was used for post hoc analysis; **p < 0.01 compared with the 10 mg/L LPS group; #p < 0.05 compared with the 10 mg/L LPS+50 mg/L Klotho group; E–G. Interleukin (IL)-1β, IL-6, and tumor necrosis factor alpha (TNF-α) levels in the cell culture medium were detected using enzyme-linked immunosorbent assay (ELISA). The graph presents the results of data dots and medians. Data were analyzed with the Kruskal–Wallis test. Dunn's multiple comparison test was used for post hoc analysis; **p < 0.01 compared with the 10 mg/L LPS group; #p < 0.05 compared with the 10 mg/L LPS + 50 mg/L Klotho group

acute lung injury (ALI) and high mortality and morbidity rates.[39] In ARDS, severe inflammation caused by bacterial infection disrupts the endothelial barrier, increasing the permeability of the pulmonary vasculature to circulating fluids, macromolecules and leukocytes, and resulting in alveolar flooding and neutrophil influx,

which is responsible for the high mortality rate.[40] One of the pathophysiological characteristics of sepsis and subsequent ARDS/ALI are hyperactive and dysregulated endogenous inflammatory cytokines, such as IL-6, IL-1β and TNF-α.[41–44] In our study, we observed that CLP-induced sepsis decreased survival in mice and increased alveolar
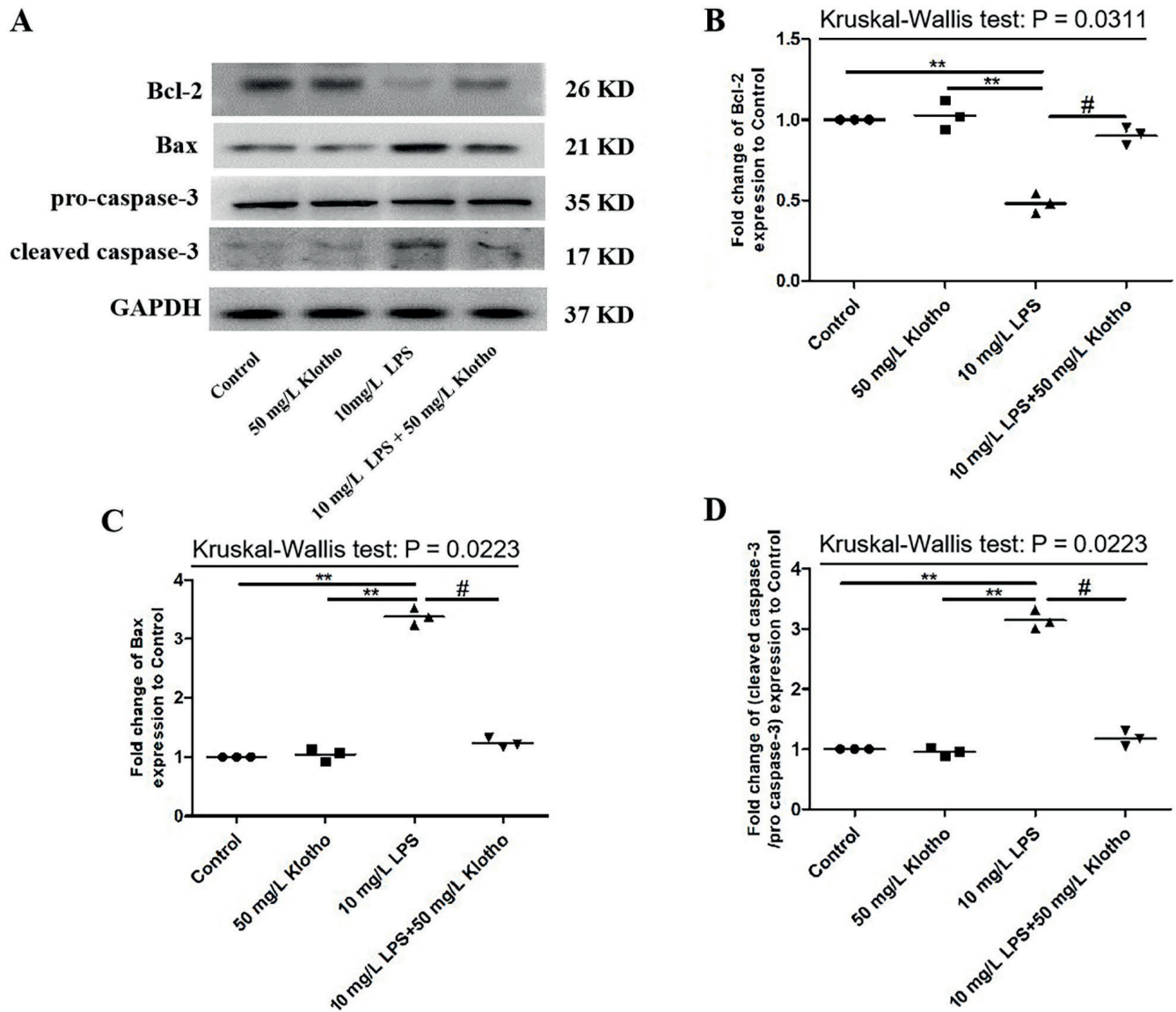
Fig. 5. Recombinant Klotho protein blocked the lipopolysaccharide (LPS)-induced activation of the Bcl-2/Bax/caspase-3 pathway in human pulmonary alveolar epithelial cells. A–D. Human pulmonary alveolar epithelial cells were pretreated with 10 mg/L LPS for 1 h and then incubated with 50 mg/L recombinant Klotho protein for 24 h. Bcl-2, Bax, pro-caspase-3, and cleaved caspase-3 expression were detected with western blotting. The graph presents the results of data dots and medians. Data were analyzed with the Kruskal–Wallis test. The Dunn's multiple comparison test was used for post hoc analysis; **p < 0.01 compared with the 10 mg/L LPS group; #p < 0.05 compared with the 10 mg/L LPS + 50 mg/L Klotho group

flooding, neutrophil influx and inflammatory factor release in the lungs. Human pulmonary alveolar epithelial cells apoptosis contributes to the pathogenesis of ALI and ARDS, which are common complications of sepsis.[45,46] Upon apoptosis in alveolar epithelial cells, DNA breaks are induced, and the cell decreases in size, resulting in its destruction by nearby phagocytes. These events lead to the destruction of the alveolar epithelium and serious damage to the alveolar–capillary barrier, which in turn promotes the pathogenesis of ALI and ARDS.[47] Our study found that CLP induced apoptosis in alveolar epithelial cells in mouse lung tissue.

Sepsis is mostly caused by endotoxin, which is released from Gram-negative bacteria.[48] Lipopolysaccharide is an important component of endotoxin that can cause a cascade of immune stimulation and toxic pathophysiological activities in the body, including ALI induced by sepsis.[49] Lipopolysaccharide is often used to generate animal models of diseases involving dysregulated inflammatory responses, such as ALI.[50,51] Accumulating evidence indicates that inflammation is involved in apoptosis,[52] and it has been reported that LPS can induce apoptosis in neurons,[53] cardiomyocytes,[54] renal tubular cells,[55] macrophages,[56] and HPAEpiCs.[57] Our research also found that LPS decreased the viability and increased the apoptosis rate in HPAEpiCs.

An imbalance between Bax and Bcl-2 plays an important role in the mitochondria-mediated caspase cascade, which was confirmed by an increased Bax/Bcl-2 ratio, release of cytochrome C from the mitochondria to the cytoplasm, cleavage of caspase-3, and subsequent induction of apoptosis.[58,59] Yang et al. reported that LPS induced apoptosis

132

X. Li et al. Klotho against LPS induced HPAEpiC apoptosis

in alveolar macrophage cells by increasing the Bax/Bcl-2 ratio,[60] while Chopra et al. demonstrated that CLP-induced sepsis resulted in myocardial apoptosis through upregulation of the ratio of Bax/Bcl-2.[61] Herein, we demonstrated that CLP and LPS treatment resulted in decreased Bcl-2 expression and increased Bax and cleaved caspase-3 expression.

Klotho is expressed primarily in renal cells, and it has anti-sepsis properties.[20] It has been reported that renal Klotho expression was significantly reduced in patients with sepsis-induced acute kidney injury (AKI) and in mice with sepsis.[62] Recombinant Klotho ameliorates sepsis-induced multiple organ dysfunction,[63–65] whereas Klotho deficiency has been reported to increase the production of TNF-α, IL-1β and IL-6, which aggravate sepsis-induced multiple organ dysfunction syndrome.[20] In a CLP model, Klotho knockout mice exhibited significantly higher mortality, higher bacterial loads, and higher TNF-α, IL-6 and IL-10 concentrations.[66] In our study, Klotho increased the survival of mice with sepsis and decreased alveolar flooding, neutrophil influx and inflammatory factor release in the lungs of mice.

Accumulating evidence indicates that Klotho exerts anti-apoptotic effects; it has been shown to suppress endothelial apoptosis via a mitogen-activated kinase pathway.[67] Genetic Klotho deficiency increases cardiomyocyte apoptotic activity, whereas Klotho supplementation can reverse changes in apoptotic activity caused by D-galactose.[68] Klotho pretreatment inhibited apoptosis in retinal pigment epithelial cells by increasing Bcl-2 levels and decreasing Bax and cleaved caspase-3 levels. Moreover, it has been reported that Klotho protects lung epithelial cells from hyperoxia-induced apoptosis.[69] However, the effect of Klotho on CLP- or LPS-induced apoptosis in alveolar type II epithelial cells has never been explored. Our study has provided the first evidence that recombinant Klotho protein inhibited CLP- and LPS-induced apoptosis in HPAEpiCs. We also found that recombinant Klotho protein blocked the CLP- and LPS-induced activation of the Bcl-2/Bax/caspase-3 pathway in HPAEpiCs.

Limitations

We did not perform gene intervention in mouse lung tissue and HPAEpiCs. We also did not further explore the effect of Klotho on the Bcl-2/Bax/caspase-3 pathway, which are future research goals.

Conclusions

Our research indicated that recombinant Klotho protein protected alveolar type II epithelial cells against sepsis-induced apoptosis and increased their survival by blocking the Bcl-2/Bax/caspase-3 pathway. Considering the protective effect of Klotho on sepsis-induced apoptosis in alveolar type II epithelial cells, it could represent a promising agent for treating sepsis-induced ALI.

Supplementary data

The Supplementary materials are available at https://doi.org/10.5281/zenodo.10975284.The package includes the following files:

Supplementary Table 1. Statistical methods, results and sample size for Fig. 1.

Supplementary Table 2. Statistical methods, results and sample size for Fig. 2.

Supplementary Table 3. Statistical methods, results and sample size for Fig. 3.

Supplementary Table 4. Statistical methods, results and sample size for Fig. 4.

Supplementary Table 5. Statistical methods, results and sample size for Fig. 5.

Data availability

The datasets generated and/or analyzed during the current study are available from the corresponding author on reasonable request.
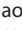
Consent for publication

Not applicable.

ORCID iDs

Xiao Bo Li ⓘ https://orcid.org/0009-0009-1279-8842
Jia Li Liu ⓘ https://orcid.org/0009-0004-0386-4282
Shuang Zhao ⓘ https://orcid.org/0009-0006-7118-8364
Jing Li ⓘ https://orcid.org/0009-0002-5640-6651
Guang-Yan Zhang ⓘ https://orcid.org/0009-0002-2730-5800
Qing Tang ⓘ https://orcid.org/0009-0006-1684-6555
Wei Yong Chen ⓘ https://orcid.org/0009-0009-7296-3950

References

1. Bringué J, Guillamat-Prats R, Martinez M, et al. Methotrexate ameliorates systemic inflammation and septic associated-lung damage in a cecal ligation and puncture septic rat model. *Int J Mol Sci*. 2021; 22(17):9612. doi:10.3390/ijms22179612
2. Dushianthan A, Grocott MPW, Postle AD, Cusack R. Acute respiratory distress syndrome and acute lung injury. *Postgrad Med J*. 2011; 87(1031):612–622. doi:10.1136/pgmj.2011.118398
3. Beitler JR, Thompson BT, Baron RM, et al. Advancing precision medicine for acute respiratory distress syndrome. *Lancer Respir Med*. 2022; 10(1):107–120. doi:10.1016/S2213-2600(21)00157-0
4. Huppert L, Matthay M, Ware L. Pathogenesis of acute respiratory distress syndrome. *Semin Respir Crit Care Med*. 2019;40(1):031–039. doi:10.1055/s-0039-1683996
5. Ervin JN, Rentes VC, Dibble ER, et al. Evidence-based practices for acute respiratory failure and acute respiratory distress syndrome. *Chest*. 2020;158(6):2381–2393. doi:10.1016/j.chest.2020.06.080
6. Chesley CF, Anesi GL, Chowdhury M, et al. Characterizing equity of intensive care unit admissions for sepsis and acute respiratory failure. *Ann Am Thorac Soc*. 2022;19(12):2044–2052. doi:10.1513/Annals ATS.202202-115OC
7. Drescher GS, Al-Ahmad MM. Analysis of noninvasive ventilation in subjects with sepsis and acute respiratory failure. *Respir Care*. 2021; 66(7):1063–1073. doi:10.4187/respcare.08599

8. Remick DG. Pathophysiology of sepsis. *Am J Pathol*. 2007;170(5): 1435–1444. doi:10.2353/ajpath.2007.060872

9. Erlanson-Albertsson C, Stenkula KG. The importance of food for endotoxemia and an inflammatory response. *Int J Mol Sci*. 2021;22(17):9562. doi:10.3390/ijms22179562

10. Tirunavalli SK, Gourishetti K, Kotipalli RSS, et al. Dehydrozingerone ameliorates lipopolysaccharide induced acute respiratory distress syndrome by inhibiting cytokine storm, oxidative stress via modulating the MAPK/NF-κB pathway. *Phytomedicine*. 2021;92:153729. doi:10.1016/j.phymed.2021.153729

11. Carnino JM, Lee H, He X, Groot M, Jin Y. Extracellular vesicle-cargo miR-185-5p reflects type II alveolar cell death after oxidative stress. *Cell Death Discov*. 2020;6(1):82. doi:10.1038/s41420-020-00317-8

12. Tompkins KD, Thorburn A. Regulation of apoptosis by autophagy to enhance cancer therapy. *Yale J Biol Med*. 2019;92(4):707–718. PMID:31866785. PMCID:PMC6913805.

13. El Hayek MS, Ernande L, Benitah JP, Gomez AM, Pereira L. The role of hyperglycaemia in the development of diabetic cardiomyopathy. *Arch Cardiovasc Dis*. 2021;114(11):748–760. doi:10.1016/j.acvd.2021.08.004

14. Hoshyar R, Mollaei H. A comprehensive review on anticancer mechanisms of the main carotenoid of saffron, crocin. *J Pharm Pharmacol*. 2017;69(11):1419–1427. doi:10.1111/jphp.12776

15. Han JH, Park MH, Myung CS. *Garcinia cambogia* ameliorates nonalcoholic fatty liver disease by inhibiting oxidative stress-mediated steatosis and apoptosis through NRF2-ARE activation. *Antioxidants*. 2021;10(8):1226. doi:10.3390/antiox10081226

16. Du J, Song D, Cao T, et al. Saikosaponin-A induces apoptosis of cervical cancer through mitochondria- and endoplasmic reticulum stress-dependent pathway in vitro and in vivo: Involvement of PI3K/AKT signaling pathway. *Cell Cycle*. 2021;20(21):2221–2232. doi:10.1080/15384101.2021.1974791

17. Zhao S, Gao J, Li J, Wang S, Yuan C, Liu Q. PD-L1 regulates inflammation in LPS-induced lung epithelial cells and vascular endothelial cells by interacting with the HIF-1α signaling pathway. *Inflammation*. 2021;44(5):1969–1981. doi:10.1007/s10753-021-01474-3

18. Hou L, Zhang J, Liu Y, et al. MitoQ alleviates LPS-mediated acute lung injury through regulating Nrf2/Drp1 pathway. *Free Radic Biol Med*. 2021;165:219–228. doi:10.1016/j.freeradbiomed.2021.01.045

19. Dounousi E, Torino C, Pizzini P, et al. Intact FGF23 and α-Klotho during acute inflammation/sepsis in CKD patients. *Eur J Clin Invest*. 2016; 46(3):234–241. doi:10.1111/eci.12588

20. Jorge LB, Coelho FO, Sanches TR, et al. Klotho deficiency aggravates sepsis-related multiple organ dysfunction. *Am J Physiol Renal Physiol*. 2019;316(3):F438–F448. doi:10.1152/ajprenal.00625.2017

21. Buchanan S, Combet E, Stenvinkel P, Shiels PG. Klotho, aging, and the failing kidney. *Front Endocrinol (Lausanne)*. 2020;11:560. doi:10.3389/fendo.2020.00560

22. Lian WY, Lu ZP, Zhao W, et al. The role of Klotho protein against sevoflurane-induced neuronal injury. *Neurochem Res*. 2022;47(2):315–326. doi:10.1007/s11064-021-03444-5

23. Marquez-Exposito L, Tejedor-Santamaria L, Santos-Sanchez L, et al. Acute kidney injury is aggravated in aged mice by the exacerbation of proinflammatory processes. *Front Pharmacol*. 2021;12:662020. doi:10.3389/fphar.2021.662020

24. Xue M, Yang F, Le Y, et al. Klotho protects against diabetic kidney disease via AMPK- and ERK-mediated autophagy. *Acta Diabetol*. 2021; 58(10):1413–1423. doi:10.1007/s00592-021-01736-4

25. Zhuang X, Sun X, Zhou H, et al. Klotho attenuated doxorubicin-induced cardiomyopathy by alleviating dynamin-related protein 1-mediated mitochondrial dysfunction. *Mech Ageing Dev*. 2021;195:111442. doi:10.1016/j.mad.2021.111442

26. Xing L, Guo H, Meng S, et al. Klotho ameliorates diabetic nephropathy by activating Nrf2 signaling pathway in podocytes. *Biochem Biophys Res Commun*. 2021;534:450–456. doi:10.1016/j.bbrc.2020.11.061

27. Xu Z, Zheng S, Feng X, Cai C, Ye X, Liu P. Klotho gene improves oxidative stress injury after myocardial infarction. *Exp Ther Med*. 2020; 21(1):52. doi:10.3892/etm.2020.9484

28. Gagan JM, Cao K, Zhang YA, et al. Constitutive transgenic α-Klotho overexpression enhances resilience to and recovery from murine acute lung injury. *Am J Physiol Lung Cell Mol Physiol*. 2021;321(4):L736–L749. doi:10.1152/ajplung.00629.2020

29. Chen B, Wang X, Zhao W, Wu J. Klotho inhibits growth and promotes apoptosis in human lung cancer cell line A549. *J Exp Clin Cancer Res*. 2010;29(1):99. doi:10.1186/1756-9966-29-99

30. Xie J, Zhao ZZ, Li P, et al. Senkyunolide I protects against sepsis-associated encephalopathy by attenuating sleep deprivation in a murine model of cecal ligation and puncture. *Oxid Med Cell Longev*. 2021;2021:6647258. doi:10.1155/2021/6647258

31. Alves GF, Aimaretti E, Einaudi G, et al. Pharmacological inhibition of FAK-Pyk2 pathway protects against organ damage and prolongs the survival of septic mice. *Front Immunol*. 2022;13:837180. doi:10.3389/fimmu.2022.837180

32. Zhang W, Li L, Zheng Y, et al. *Schistosoma japonicum* peptide SJMHE1 suppresses airway inflammation of allergic asthma in mice. *J Cell Mol Med*. 2019;23(11):7819–7829. doi:10.1111/jcmm.14661

33. Yang H, Lv H, Li H, Ci X, Peng L. Oridonin protects LPS-induced acute lung injury by modulating Nrf2-mediated oxidative stress and Nrf2-independent NLRP3 and NF-κB pathways. *Cell Commun Signal*. 2019; 17(1):62. doi:10.1186/s12964-019-0366-y

34. Resnick-Silverman L. Using TUNEL assay to quantitate p53-induced apoptosis in mouse tissues. *Methods Mol Biol*. 2021;2267:181–190. doi:10.1007/978-1-0716-1217-0_12

35. Wang L, Li S, Luo H, Lu Q, Yu S. PCSK9 promotes the progression and metastasis of colon cancer cells through regulation of EMT and PI3K/AKT signaling in tumor cells and phenotypic polarization of macrophages. *J Exp Clin Cancer Res*. 2022;41(1):303. doi:10.1186/s13046-022-02477-0

36. Zheng JY, Wang SC, Tang SC, et al. Sodium acetate ameliorates cisplatin-induced kidney injury in vitro and in vivo. *Chem Biol Interact*. 2023;369:110258. doi:10.1016/j.cbi.2022.110258

37. Di Silverio F, Gallucci M, Alpi G, et al. Indications and limits of percutaneous nephrolithotripsy and extracorporeal shock wave lithotripsy combined treatment. *Contrib Nephrol*. 1987;58:262–265. doi:10.1159/000414530

38. Sun R, Zhao N, Wang Y, et al. High concentration of hydrogen gas alleviates lipopolysaccharide-induced lung injury via activating Nrf2 signaling pathway in mice. *Int Immunopharmacol*. 2021;101:108198. doi:10.1016/j.intimp.2021.108198

39. Chen DQ, Shen MJ, Wang H, et al. Sirt3 maintains microvascular endothelial adherens junction integrity to alleviate sepsis-induced lung inflammation by modulating the interaction of VE-cadherin and β-catenin. *Oxid Med Cell Longev*. 2021;2021:8978795. doi:10.1155/2021/8978795

40. Matthay MA, Ware LB, Zimmerman GA. The acute respiratory distress syndrome. *J Clin Invest*. 2012;122(8):2731–2740. doi:10.1172/JCI60331

41. Bateman RM, Sharpe MD, Jagger JE, et al; South Yorkshire Hospitals Research Collaboration. 36ᵗʰ International Symposium on Intensive Care and Emergency Medicine: Brussels, Belgium. 15–18 March 2016. *Crit Care*. 2016;20(Suppl 2):94. doi:10.1186/s13054-016-1208-6

42. Montoya-Ruiz C, Jaimes FA, Rugeles MT, López JÁ, Bedoya G, Velilla PA. Variants in LTA, TNF, IL1B and IL10 genes associated with the clinical course of sepsis. *Immunol Res*. 2016;64(5–6):1168–1178. doi:10.1007/s12026-016-8860-4

43. Edelman DA, Jiang Y, Tyburski JG, Wilson RF, Steffes CP. Cytokine production in lipopolysaccharide-exposed rat lung pericytes. *J Trauma*. 2007;62(1):89–93. doi:10.1097/TA.0b013e31802dd712

44. Wang F, Fang B, Qiang X, Shao J, Zhou L. The efficacy of mesenchymal stromal cell-derived therapies for acute respiratory distress syndrome: A meta-analysis of preclinical trials. *Respir Res*. 2020;21(1):307. doi:10.1186/s12931-020-01574-y

45. Gong Y, Lan H, Yu Z, et al. Blockage of glycolysis by targeting PFKFB3 alleviates sepsis-related acute lung injury via suppressing inflammation and apoptosis of alveolar epithelial cells. *Biochem Biophys Res Commun*. 2017;491(2):522–529. doi:10.1016/j.bbrc.2017.05.173

46. Kimura H, Suzuki M, Konno S, et al. Orchestrating role of apoptosis inhibitor of macrophage in the resolution of acute lung injury. *J Immunol*. 2017;199(11):3870–3882. doi:10.4049/jimmunol.1601798

47. Gu LZ, Sun H. Lonicerin prevents inflammation and apoptosis in LPS-induced acute lung injury. *Front Biosci*. 2020;25(3):480–497. doi:10.2741/4815

48. Wohlfart S, Kilian M, Storck P, Gutsmann T, Brandenburg K, Mier W. Mass spectrometric quantification of the antimicrobial peptide Pep19-2.5 with stable isotope labeling and acidic hydrolysis. *Pharmaceutics*. 2021;13(9):1342. doi:10.3390/pharmaceutics13091342

134

X. Li et al. Klotho against LPS induced HPAEpiC apoptosis

49. Wann S, Chi P, Huang W, Cheng C, Chang Y. Combination therapy of iPSC-derived conditioned medium with ceftriaxone alleviates bacteria-induced lung injury by targeting the NLRP3 inflammasome. *J Cell Physiol*. 2022;237(2):1299–1314. doi:10.1002/jcp.30596

50. Su VYF, Chen WC, Yu WK, Wu HH, Chen H, Yang KY. Nintedanib regulates GRK2 and CXCR2 to reduce neutrophil recruitment in endotoxin-induced lung injury. *Int J Mol Sci*. 2021;22(18):9898. doi:10.3390/ijms22189898

51. Hong J, Mo S, Gong F, et al. lncRNA-SNHG14 plays a role in acute lung injury induced by lipopolysaccharide through regulating autophagy via miR-223-3p/Foxo3a. *Mediators Inflamm*. 2021;2021:7890288. doi:10.1155/2021/7890288

52. Wu X, Liu Y, Guo X, et al. Prolactin inhibits the progression of intervertebral disc degeneration through inactivation of the NF-κB pathway in rats. *Cell Death Dis*. 2018;9(2):98. doi:10.1038/s41419-017-0151-z

53. Liu J, Lin M, Qiao F, Zhang C. Exosomes derived from lncRNA TCTN2-modified mesenchymal stem cells improve spinal cord injury by miR-329-3p/IGF1R axis. *J Mol Neurosci*. 2022;72(3):482–495. doi:10.1007/s12031-021-01914-7

54. Luo Y, Tu H, Yang Z, et al. Long non-coding RNA MALAT1 silencing elevates microRNA-26a-5p to ameliorate myocardial injury in sepsis by reducing regulator of calcineurin 2. *Arch Biochem Biophys*. 2022;715:109047. doi:10.1016/j.abb.2021.109047

55. Gao Z, Lu L, Chen X. Release of HMGB1 in podocytes exacerbates lipopolysaccharide-induced acute kidney injury. *Mediators Inflamm*. 2021;2021:5220226. doi:10.1155/2021/5220226

56. Zhang S, Fu B, Xiong Y, et al. Tgm2 alleviates LPS-induced apoptosis by inhibiting JNK/BCL-2 signaling pathway through interacting with Aga in macrophages. *Int Immunopharmacol*. 2021;101:108178. doi:10.1016/j.intimp.2021.108178

57. Nan CC, Zhang N, Cheung KCP, et al. Knockdown of lncRNA MALAT1 alleviates LPS-induced acute lung injury via inhibiting apoptosis through the miR-194-5p/FOXP2 axis. *Front Cell Dev Biol*. 2020;8:586869. doi:10.3389/fcell.2020.586869

58. Li J, Liu F, Jiang S, et al. Berberine hydrochloride inhibits cell proliferation and promotes apoptosis of non-small cell lung cancer via the suppression of the MMP2 and Bcl-2/Bax signaling pathways. *Oncol Lett*. 2018;15(5):7409–7414. doi:10.3892/ol.2018.8249

59. Strasser A, O'Connor L, Dixit VM. Apoptosis signaling. *Annu Rev Biochem*. 2000;69(1):217–245. doi:10.1146/annurev.biochem.69.1.217

60. Yang L, Zhang Z, Zhuo Y, et al. Resveratrol alleviates sepsis-induced acute lung injury by suppressing inflammation and apoptosis of alveolar macrophage cells. *Am J Transl Res*. 2018;10(7):1961–1975. PMID:30093935. PMCID:PMC6079135.

61. Chopra M, Sharma AC. Distinct cardiodynamic and molecular characteristics during early and late stages of sepsis-induced myocardial dysfunction. *Life Sci*. 2007;81(4):306–316. doi:10.1016/j.lfs.2007.05.021

62. Jou-Valencia D, Molema G, Popa E, et al. Renal Klotho is reduced in septic patients and pretreatment with recombinant Klotho attenuates organ injury in lipopolysaccharide-challenged mice. *Crit Care Med*. 2018;46(12):e1196–e1203. doi:10.1097/CCM.0000000000003427

63. Liu X, Niu Y, Zhang X, et al. Recombinant α-Klotho protein alleviated acute cardiorenal injury in a mouse model of lipopolysaccharide-induced septic cardiorenal syndrome type 5. *Anal Cell Pathol (Amst)*. 2019;2019:5853426. doi:10.1155/2019/5853426

64. Chen X, Tong H, Chen Y, et al. Klotho ameliorates sepsis-induced acute kidney injury but is irrelevant to autophagy. *Onco Targets Ther*. 2018;11:867–881. doi:10.2147/OTT.S156891

65. Cóndor JM, Rodrigues CE, De Sousa Moreira R, et al. Treatment with human Wharton's jelly-derived mesenchymal stem cells attenuates sepsis-induced kidney injury, liver injury, and endothelial dysfunction. *Stem Cell Transl Med*. 2016;5(8):1048–1057. doi:10.5966/sctm.2015-0138

66. Abdelmalik PA, Stevens RD, Singh S, et al. Anti-aging factor, serum alpha-Klotho, as a marker of acute physiological stress, and a predictor of ICU mortality, in patients with septic shock. *J Crit Care*. 2018;44:323–330. doi:10.1016/j.jcrc.2017.11.023

67. Maekawa Y, Ohishi M, Ikushima M, et al. Klotho protein diminishes endothelial apoptosis and senescence via a mitogen-activated kinase pathway. *Geriatr Gerontol Int*. 2011;11(4):510–516. doi:10.1111/j.1447-0594.2011.00699.x

68. Li-Zhen L, Chen Z, Wang SS, Liu W, Zhuang X. Klotho deficiency causes cardiac ageing by impairing autophagic and activating apoptotic activity. *Eur J Pharmacol*. 2021;911:174559. doi:10.1016/j.ejphar.2021.174559

69. Kim SJ, Cheresh P, Eren M, et al. Klotho, an antiaging molecule, attenuates oxidant-induced alveolar epithelial cell mtDNA damage and apoptosis. *Am J Physiol Lung Cell Mol Physiol*. 2017;313(1):L16–L26. doi:10.1152/ajplung.00063.2017